

# Spectroscopic and Theoretical Studies of Transition Metal Oxides and Dioxygen Complexes

Yu Gong and Mingfei Zhou\*

Department of Chemistry, Shanghai Key Laboratory of Molecular Catalysts and Innovative Materials, Advanced Materials Laboratory, Fudan University, Shanghai 200433, China

Lester Andrews†

Department of Chemistry, University of Virginia, Charlottesville, Virginia 22901

Received May 9, 2009

## Contents

1. Introduction	6765	5.3. V Group	6793
2. Spectroscopic and Theoretical Methods	6767	5.4. Cr Group	6797
2.1. Spectroscopic Methods	6767	5.5. Mn Group	6798
2.1.1. Matrix Isolation Infrared Absorption Spectroscopy	6767	5.6. Fe Group	6798
2.1.2. Photoelectron Spectroscopy (PES)	6768	5.7. Co Group	6798
2.1.3. Electron Spin Resonance Spectroscopy (ESR)	6768	5.8. Ni Group	6798
2.1.4. Infrared Photon Dissociation Spectroscopy (IR-PD)	6768	5.9. Cu Group	6799
2.1.5. Laser-Induced Fluorescence (LIF)	6769	6. Summary	6800
2.1.6. Other Spectroscopic Methods	6769	7. Acknowledgments	6800
2.2. Theoretical Methods	6769	8. References	6800
3. Neutral Mononuclear Transition Metal Oxides and Dioxygen Complexes	6769		
3.1. Sc Group	6772		
3.2. Ti Group	6773		
3.3. V Group	6775		
3.4. Cr Group	6776		
3.5. Mn Group	6777		
3.6. Fe Group	6779		
3.7. Co Group	6780		
3.8. Ni Group	6782		
3.9. Cu Group	6782		
3.10. Zn Group	6784		
3.11. Lanthanide Group	6784		
3.12. Actinide Group	6785		
3.13. Periodic Trends on Bonding and Reactivity	6785		
4. Ionic Mononuclear Transition Metal Oxide Species	6787		
4.1. Cations	6788		
4.2. Anions	6790		
4.2.1. Monoxide Anions	6790		
4.2.2. Dioxide Anions	6791		
4.2.3. Oxygen-Rich Anions	6792		
5. Multinuclear Transition Metal Oxide Clusters	6792		
5.1. Sc Group	6793		
5.2. Ti Group	6793		

## 1. Introduction

Dioxygen binding and activation at metal centers are of major importance in a wide range of catalytic and biological processes. Metal oxides and dioxygen complexes are potential intermediates or products during oxidation of metal atoms or clusters. Consequently, great effort has been devoted to the preparation and characterization of various metal oxides and dioxygen complexes. The structures, physicochemical properties, and reactivity of these species have been the subject of intensive experimental and theoretical studies, which have been described in numerous reviews.<sup>1–5</sup> As the initially formed species in most metal oxidation processes, metal dioxygen complexes are of particular interest in light of their postulated involvement in oxygen carrier systems in biology. Dioxygen reacts with biological molecules at isolated metallic active sites in forming metal–dioxygen adducts. Due to the intrinsic chemical interest in understanding metal–dioxygen interactions, a host of transition metal–dioxygen complexes that are structural and functional analogues of biological dioxygen carriers have been synthesized and are spectroscopically and structurally characterized. Progress on the characterization of such transition metal–dioxygen complexes stabilized by bulky ligands has been the subject of a series of recent reviews,<sup>2–5</sup> which is beyond the scope of this review.

Transition metal oxide materials are widely used as catalyst systems. As has been pointed out in a recent review,<sup>6</sup> gas-phase studies of neutral and ionic metal oxide clusters aid in the identification of the reactive sites in heterogeneous catalysis.<sup>7</sup> Many investigations including oxide cluster reactions in the gas phase have shown a direct similarity between reaction mechanisms involving clusters and similar ones effected by industrial catalysts.<sup>8</sup> The reactivity on size-

\* To whom correspondence should be addressed. E-mail: mzfzhou@fudan.edu.cn.

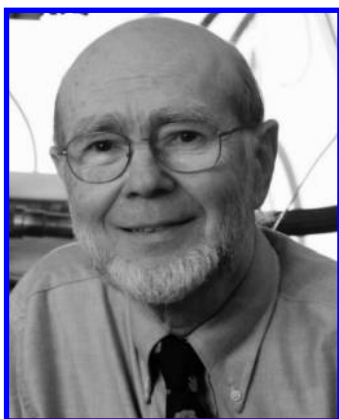
† E-mail: lsa@virginia.edu.



Yu Gong was born in Shanghai, People's Republic of China, in 1982. He received his B.S. degree in chemistry at Fudan University in 2005. He is now a Ph.D. student in the group of Mingfei Zhou at Fudan University. His research interest mainly focuses on the reactions between transition metals and small molecules in solid matrix.



Mingfei Zhou was born in Zhejiang province of China in 1968. He received his B.S. and Ph.D. degrees in chemistry from Fudan University in 1990 and 1995, respectively. After a postdoctoral stay at the University of Virginia with Professor Lester Andrews, he joined the chemistry faculty at Fudan University in 1999. His research interests include experimental and theoretical studies of reactive intermediates and free radicals.



Lester Andrews was born in Lincolnton, NC, on January 31, 1942. He earned a B.S. degree in Chemical Engineering from Mississippi State University in 1963 and a Ph.D. degree in Physical Chemistry from the University of California, Berkeley, in 1966. Dr. Andrews joined the faculty of the University of Virginia in 1966 where he has been active in matrix-isolation spectroscopy, publishing over 750 research papers on novel chemical species. He is now Professor Emeritus. In addition, he enjoys playing the E-flat soprano clarinet.

selected transition metal oxide molecules and clusters has been widely studied in the gas phase in order to gain insight

into the relationship between geometric structure and observed reactivity patterns. Investigations on such a topic have been intensively discussed<sup>9–12</sup> and will not be included in this review.

Here we will review spectroscopic and theoretical studies on the geometric and electronic structures of transition metal–oxygen molecules and small clusters. We mainly focus on binary transition metal–oxygen molecular species with several metal and oxygen atoms, which may exist in several structural forms and involve different chemical bonding. Molecular oxygen can bond either side-on or end-on to a metal center in forming dioxygen complexes, which are intermediate states for the complete cleavage of the O–O bond to form metal oxides. These species can be considered as the simplest model for oxygen binding to metal centers. Such model systems can be studied under well-defined conditions at the molecular level that are free of effects from ligands, solvents, surface active sites, and the crystal lattice.

Much of our knowledge about the geometric and electronic structures of transition metal oxides and dioxygen complexes comes from molecular spectroscopic studies. Although mass spectrometry excels at determining the composition and reactivity of molecular ions, these gas-phase mass spectrometric studies are blind to neutral species and thus are unable to provide detailed structural information. Laser-based spectroscopic techniques including laser-induced fluorescence spectroscopy (LIF), resonantly enhanced multiphoton ionization spectroscopy (REMPI), zero kinetic energy spectroscopy (ZEKE), and infrared photon dissociation spectroscopy (IRPD) offer precise and detailed measurements of vibrational or rotational transitions of some simple transition metal oxide molecules as well as oxide clusters. Detailed analysis of rotational structures in the gas-phase spectrum may even yield a quantitative determination of the molecular structure. Negative ion photoelectron spectroscopic studies in the gas phase are able to provide valuable information on the vibrational and electronic structure of mass-selected transition metal oxides and dioxygen complexes. This technique can provide spectroscopic information on both neutral and anionic species. Different from the other LIF, ZEKE, and rotational gas-phase spectroscopic methods, which mainly focused on metal monoxides and dioxides, photoelectron spectroscopy can handle large species including metal oxide clusters and oxygen-rich molecules. Besides photoelectron and electronic spectroscopy, infrared absorption spectroscopy is another commonly used technique for probing the molecular properties of metal oxides and dioxygen complexes. All metal oxide molecules and metal–dioxygen complexes have infrared absorptions. Analysis of the vibrational transitions in characteristic spectral regions permits the identification of different structural isomers and provides detailed information about specific types of bonding. Due to its low sensitivity, conventional infrared absorption spectroscopy is mainly used in conjunction with the matrix isolation technique. It is very difficult to carry out a straightforward infrared absorption study in the gas phase. However, with advances in free electron lasers and tunable IR lasers, vibrational spectroscopic investigations in the gas phase have become possible. Recently developed infrared photon dissociation experiments with tunable IR lasers have allowed for detailed gas-phase vibrational spectroscopic studies of a number of transition metal oxide ions.

Spectroscopic studies of binary metal–oxygen species face strong challenges, because most of them are highly chemi-

cally reactive and are transient species at normal experimental conditions. Spectroscopic detection of such species formed in the gas phase requires sensitive and time-resolved techniques. Laser-based molecular spectroscopy, which is not only highly sensitive but also time specific in a wide range of time scales, is well-suited for such studies. Matrix isolation has proven to be a powerful technique in trapping transient reactive intermediates for spectroscopic studies.<sup>13–20</sup> Noble gases, such as Ne and Ar, are commonly used as matrices, which are sufficiently rigid to effectively isolate the reactive species at low temperatures (4–10 K). The chemically inert noble gas matrix that confines the reactive species is generally electronically innocent, that is, the species trapped in the solid matrix are normally regarded as isolated “gas-phase” molecules. The molecular properties measured in solid noble gas matrices are slightly different from those measured in the gas phase in most cases, as has been addressed by Jacox in a series of reviews.<sup>21</sup>

Matrix isolation is suited for trapping not only neutral molecules but also charged species including cations as well as anions.<sup>15,22</sup> Since noble gas matrices are transparent in the infrared spectral range, the structure-specific infrared absorption spectroscopy is most commonly employed to study the target species trapped in solid matrices. Unlike spectra recorded in solution or the solid state, it is straightforward to obtain well-resolved infrared spectra of species trapped in solid matrices, and most of the time, a diagnostic identification and vibrational assignment can be made. Such conditions are very suitable for the study of isotopic shifts and splittings, which are extremely important for product identification and structure determination. In addition to the spectroscopic assignment, isotopic substitution also provides information for the interpretation of reaction mechanisms.

Besides experimental investigations, a number of theoretical studies have been devoted to transition metal oxides and dioxygen complexes. Due to the existence of *d* electrons, transition metal systems require more sophisticated computational approaches. Various quantum chemical methods including *ab initio* as well as density functional theory (DFT) are now feasible that allow quantitative computations of vibrational frequencies and thermochemical properties with high accuracy. Theoretical studies have successfully reproduced experimental results, and disagreement between experiment and theory often initiates more accurate experimental as well as theoretical studies. In addition, theoretical calculations are especially valuable in predicting properties such as bonding, charge, and spin distribution, which often cannot be directly obtained from experiment.

In this review, we will describe advances in the spectroscopic and theoretical studies of binary transition metal–oxygen molecular and small cluster species. Both neutral and singly charged species will be included. We will emphasize spectroscopic and theoretical investigations of vibrational frequencies and structures of mononuclear transition metal oxides and dioxygen complexes. Besides the well-studied monoxide and dioxide species that have previously been reviewed,<sup>23–29</sup> we will also include oxygen-rich ( $\text{MO}_x$ ,  $x \geq 3$ ) species, which reveal diverse structural and bonding properties. The periodic trends on reaction mechanisms of transition metal atoms and dioxygen will be discussed. Numerous matrix isolation as well as gas-phase spectroscopic results will be included. Studies on large metal oxide clusters and bulk metal oxide materials go beyond the scope of this review and will not be included. However, some small metal

oxide clusters with their spectral and structural information being clearly determined will be discussed, in particular, dinuclear oxide species. These small clusters are fundamental building blocks for the formation of large metal oxide clusters. There are a large number of gas-phase studies on metal oxide cations using various mass spectrometric methods, which have provided valuable thermodynamic properties of metal oxide cations. These methods do not give detailed spectroscopic and structural information and will not be discussed in detail in this review.

## 2. Spectroscopic and Theoretical Methods

### 2.1. Spectroscopic Methods

#### 2.1.1. Matrix Isolation Infrared Absorption Spectroscopy

Infrared absorption spectroscopy is commonly employed in conjunction with the matrix isolation technique to characterize transition metal–oxygen species. Vibrational spectroscopy is bond specific and can identify new species particularly when isotopic substitution is employed. Matrix isolated transition metal oxides and dioxygen complexes are mainly prepared via reactions of metal atoms with dioxygen in solid matrices. Thermal evaporation has been successfully employed in the preparation of matrix samples for spectroscopic studies.<sup>17,30</sup> The ground-state metal atoms are generated either from a continuously heated tantalum or boron nitride Knudsen cell or from a heated tungsten filament wetted with target metals. Thermally evaporated metal atoms react with co-deposited dioxygen to form transition metal oxides or dioxygen complexes on sample annealing or on irradiation. Metal oxide molecules can also be produced via direct evaporation of bulk metal oxide target materials.

Laser ablation is another convenient technique that is used in our laboratories to prepare matrix-isolated transition metal oxides and dioxygen complexes. This method has been widely used to produce novel species for spectroscopic studies.<sup>15,16,26,31</sup> In contrast to conventional thermal evaporation techniques, with laser ablation only a small amount of the material is directly heated, thus minimizing the heat load and the introduction of impurities into the sample, particularly for transition metals, which have a very high melting point temperature. Simple transition metal oxide molecules, such as monoxides and dioxides, can also be prepared via laser evaporation of bulk metal oxide targets under controlled experimental conditions. With relatively low evaporation laser energy, matrix reactions are dominated by mononuclear species. However, multinuclear products may also be formed when relatively high evaporation laser energy is employed. The experimental apparatus for pulsed laser-evaporation matrix isolation infrared spectroscopy has been described in detail previously.<sup>15,16</sup> In general, the matrix sample is maintained at 6–10 K for argon matrix studies or at 4 K for neon matrix investigations. Because of the very low temperature of the deposit, the laser-evaporated species are quenched to their ground state in solid matrices. The as-deposited samples are annealed to higher temperatures to allow trapped reactants to diffuse and to react. The reaction can be very effectively quenched after the primary reaction, and the energy-rich intermediates, which fragment readily in the gas phase can be stabilized in solid matrices. Different wavelength range photolysis experiments are frequently performed to initiate further photoinduced isomerization or dissociation reactions.

As a structure-specific spectroscopic technique, infrared absorption spectroscopy is sensitive in detecting transition metal oxides and dioxygen complexes in solid matrices. Under low-temperature matrix isolation conditions, the fine structures derived from rotational transitions are suppressed. Well-resolved infrared absorptions with typical half width of less than  $1\text{ cm}^{-1}$  are obtained. Transition metal dioxygen complexes often exhibit strong O–O stretching absorptions, which are quite structurally sensitive. Metal dioxygen complexes are generally defined as superoxides and peroxides depending on the extent of charge transfer from metal center to dioxygen. It is often quite difficult to determine the amount of charge transferred experimentally; hence, the classification is regularly based on the experimentally observed or theoretically predicted O–O stretching vibrational frequencies. Complexes with O–O stretching frequencies in the range of  $1050\text{--}1200\text{ cm}^{-1}$  are assigned as superoxides, whereas those with O–O stretching frequencies in the range of  $800\text{--}930\text{ cm}^{-1}$  are designated as peroxides.<sup>32–36</sup> Metal oxide molecules also exhibit strong absorptions in the terminal M=O and bridged M–O–M stretching vibrational regions. The terminal M=O stretching vibrations are commonly located in the  $1050\text{--}800\text{ cm}^{-1}$  range, whereas the bridged oxide species absorb at a much lower frequency region.

Isotopic substitution experiments are extremely important for product identifications and structural determination. Isotopically labeled  $^{18}\text{O}_2$  samples are always used in the transition metal and dioxygen reaction experiments. The experimentally observed oxygen isotopic shifts give information on the extent of oxygen atom(s) participation in the observed vibrational modes. The use of isotopic  $^{16}\text{O}_2 + ^{18}\text{O}_2$  and  $^{16}\text{O}_2 + ^{16}\text{O}^{18}\text{O} + ^{18}\text{O}_2$  mixtures results in multiple absorptions for different isotopomers, which is a major factor for determining the number of oxygen atoms involved in the observed vibrational modes.

Transition metal-containing species such as simple transition metal oxides and dioxygen complexes are polar species. The metal center in these species is positively charged and electrophilic and, hence, is able to interact with noble gas atoms in many cases. Some transition metal-containing species trapped in solid noble gas matrices are chemically coordinated by one or multiple noble gas atoms and cannot be regarded as completely isolated species.<sup>37,38</sup> Noble gas coordination may change the spectra and geometric and electronic structure, as well as reactivity, of the species trapped in solid matrices.<sup>39</sup> In order to determine whether the transition metal oxides and dioxygen complexes trapped in solid noble gas matrices are coordinated by noble gas atoms and to determine the number of coordinated noble gas atoms experimentally, one can use mixtures of a lighter noble gas host doped with heavier noble gas atoms as matrix. If the trapped species are coordinated by noble gas atoms, the coordinated lighter noble gas atoms can be successively substituted by heavier noble gas atoms when the solid matrix sample is annealed, which will induce vibrational frequency shifts on the infrared spectrum. The coordination number can be determined by the number of new absorption bands formed.

### 2.1.2. Photoelectron Spectroscopy (PES)

Photoelectron spectroscopy is one of the most important techniques in spectroscopic investigation of mass-selected transition metal oxide species in the gas phase. Since the pioneering work by Lineberger's group on the photodetach-

ment PES study of transition metal species including several transition metal oxides,<sup>40,41</sup> systematic investigations on transition metal oxide species using anion photoelectron spectroscopy have been conducted by Wang's group, which have been summarized in a recent review.<sup>26</sup> The difficulty in studying transition metal oxide species in the gas phase is how to generate them with sufficient number density. Pulsed laser evaporation coupled with supersonic expansion is the most frequently used source in producing transition metal oxide anions for PES study. The details of PES experiment have been described in detail in previous publications.<sup>26,42</sup> Briefly, a focused pulsed laser beam is used to vaporize metal species. A short and intense helium carrier gas beam doped with a small amount of  $\text{O}_2$  mixes with the laser-evaporated metal species and undergoes a supersonic expansion to form a cluster beam. Negatively charged species are extracted from the beam and are subjected to a time-of-flight mass analysis. The anions of interest are mass selected and are interacted with a pulsed detachment laser beam. Pulsed lasers including the harmonics of Nd:YAG laser (532, 355, and 266 nm) and excimer lasers (248, 193, and 157 nm) are used for detachment. Low photon energies allow optimum spectral resolution, while high photon energies can reveal more highly excited states. The kinetic energy of detached electrons is detected by a magnetic-bottle time-of-flight photoelectron analyzer.

PES studies on transition metal oxide species can provide direct information on their electron affinities, low-lying electronic states, and vibrational frequencies. Although the vibrational assignment is less accurate due to limited resolution compared with other spectroscopic methods, PES is a versatile and convenient method in gas-phase studies, which complements the extensively used matrix isolation infrared spectroscopic investigations. Since the selection rules for vibrational transitions are determined by the Franck–Condon factors, it is often possible to observe vibrational states that are forbidden or weak in infrared spectroscopy. For example, the symmetric stretching vibration for a linear transition metal dioxide molecule is IR inactive and cannot be observed with infrared absorption spectroscopy. However, the vibrational frequency of this mode can be determined from the resolved vibrational structures of PES of metal dioxide anion.

### 2.1.3. Electron Spin Resonance Spectroscopy (ESR)

Electron spin resonance spectroscopy is of great importance in understanding the neutral and charged radicals with unpaired electrons.<sup>43,44</sup> **A**- and **g**-tensors are the most useful parameters obtained from ESR experiments, from which direct information on singly occupied orbitals can be derived. No ESR signals can be obtained if target molecules possess a closed-shell singlet ground state with all the electrons involved being paired. In addition, molecules with degenerate ground states ( $\Pi$ ,  $\Delta$ , etc.) are not suitable for ESR investigations due to the broadening of the absorption lines caused from anisotropy of **g**-tensor. ESR spectroscopy in conjunction with the matrix isolation technique has been extensively employed in the electronic characterization of some transition metal oxide species.<sup>44</sup>

### 2.1.4. Infrared Photon Dissociation Spectroscopy (IR-PD)

With the development of tunable infrared lasers, infrared photon dissociation spectroscopy has become a very powerful

method for studying mass-selected molecular and cluster ions in the gas phase, as has been reviewed.<sup>45,46</sup> The vibrations of transition metal oxides and dioxygen complexes are roughly located in the range of 1600–400  $\text{cm}^{-1}$ . Free electron laser can generate intense and continuously tunable IR irradiation in this wavelength range. More recently, intense and tunable middle IR laboratory lasers have become available. Gas-phase ions are produced via the laser evaporation–supersonic expansion technique as used in anion PES studies. The ion beam from the source is mass-selected. The selected ions are interacted with a pulsed IR dissociation laser beam. Infrared photodissociation spectra are obtained by monitoring the fragment ion signal. For weakly bound complexes, one absorbed IR photon can be sufficient to bring the complex above the dissociation barrier such that it can undergo vibrational predissociation. For strongly bound clusters, many IR photons need to be absorbed in order to induce fragmentation. The IR spectrum from multiple photon processes may not be the same as a regular linear absorption spectrum. A useful method to avoid multiple photon excitation and measure IR photodissociation spectra in the linear regime is the messenger atom technique. Generally, noble gas atoms are chosen as messenger atoms. By formation of ion–noble gas atom complexes, the dissociation threshold of the system is lowered. If the binding energy of the cluster ion–noble gas complex is below the photon energy, absorption of a single photon will be followed by vibrational predissociation. In general, the perturbation of the geometric and electronic structures of cluster ions by the messenger atom is negligible; hence, the IR spectrum of the cluster ion–noble gas atom complex reflects the IR spectrum of the free cluster ion.

### 2.1.5. Laser-Induced Fluorescence (LIF)

With widespread application of lasers especially tunable lasers, laser-induced fluorescence has become a valuable spectroscopic method in studying metal atoms, clusters, radicals, and molecular ions both in the gas phase and in the condensed phases.<sup>13,31</sup> The LIF studies benefit from the rather high sensitivity over other spectroscopic techniques. Pulsed laser vaporization or discharge is commonly combined with the supersonic jet technique for producing target species in the gas phase for LIF studies. High-resolution gas-phase studies can provide well-resolved vibrational and rotational structures of target species. Both the ground state and excited states accessible by allowed transition from ground state can be studied. LIF study of matrix-isolated species was first introduced by Bondybey and co-workers.<sup>31</sup> In solid matrices, the selection rules are often relaxed, and hence, some rigorously forbidden transitions in the gas phase can be studied in the matrices. However, the rotational structure that is important in determining the geometric parameters is lost in solid matrices. LIF studies on transition metal–oxygen species are mainly focused on monoxides and some dioxide molecules due to the complex transitions involved in polyatomic systems.

### 2.1.6. Other Spectroscopic Methods

Besides the above-mentioned spectroscopic methods, other techniques, such as rotational spectroscopy,<sup>47</sup> infrared emission spectroscopy,<sup>48</sup> resonance-enhanced multiple photon ionization/dissociation spectroscopy (REMPI/D),<sup>49</sup> and pulsed-field ionization zero kinetic energy (PFI-ZEKE) photoelec-

tron spectroscopy,<sup>50</sup> have also been used for spectroscopic studies. These techniques are helpful in understanding the electronic and geometric structures of simple transition metal–oxygen species.

## 2.2. Theoretical Methods

Dramatically increased computational power allows the application of various quantum chemical methods to predict molecular properties including equilibrium geometries, energies, and vibrational frequencies of transition metal-containing species. In order to give accurate predictions, electron correlation must be included. Single-reference post-Hartree–Fock ab initio methods such as Møller–Plesset perturbation theory<sup>51</sup> and coupled-cluster approaches<sup>52</sup> have been used to calculate equilibrium geometries, relative stabilities, and vibrational frequencies for some simple metal–oxygen species. However, high-level ab initio calculations such as CCSD(T) with reasonably large basis sets are very computationally demanding and are not practical methods for larger systems such as multinuclear transition metal oxides and mononuclear oxygen-rich species. Density functional theory (DFT), which also incorporates electron correlation effects, is more commonly used in the calculation of transition metal–oxygen species. DFT has the advantage of predicting equilibrium geometries and vibrational frequencies that are comparable in quality to those obtained with more highly correlated methods. Several well-calibrated DFT methods such as BLYP, BPW91, B3LYP, BH and HLYP, and BP86, which have proven to give good results for transition metal-containing compounds, are frequently employed.<sup>53</sup> In addition, some new methods have also been developed for transition metal systems in recent years.<sup>54</sup> For some species that show strong multireference character, calculations using single-reference based methods may give unreliable results. In such cases, multireference methods such as CASSCF<sup>55</sup> and internally contracted MRCI<sup>56</sup> methods should be used to give a reliable prediction. Taking  $\text{FeO}_2^-$  anion as an example, the  $\text{FeO}_2^-$  anion is experimentally determined to be linear. However, single-reference based methods including MP2–4, CCSD(T), and various DFT methods all gave unreliable predictions due to the strong multireference character of the  $\text{FeO}_2^-$  anion and the symmetry-breaking problems in the single-reference wave functions. Only the state-averaged multireference MRCI methods, which incorporate both dynamical and nondynamical correlation effects, predict that the anion has a linear doublet ground state, consistent with the experimental observations.<sup>57</sup>

Relativistic effects should be taken into consideration when calculating transition metal oxides and dioxygen complexes, particularly for heavy transition metals.<sup>58,59</sup> Upon geometric optimization and vibrational frequency calculations, the scalar relativistic effects can be included by use of suitably parametrized relativistic pseudopotentials. Spin–orbital coupling effect should also be taken into consideration, particularly for open-shell species. Although spin–orbital effects are found not to be important in many cases, they may be important for f-element metal-containing species in order to obtain reliable energy predictions.

## 3. Neutral Mononuclear Transition Metal Oxides and Dioxygen Complexes

Neutral  $\text{MO}_x$  series spectroscopically characterized both in the gas phase and in solid matrices will be summarized

**Table 1. Ground Spin States and Vibrational Frequencies (cm<sup>-1</sup>) for Transition Metal Monoxides in the Gas Phase and in Solid Neon and Argon Matrices<sup>a</sup>**

molecule	ground state	vibrational frequency			refs
		gas phase	Ne	Ar	
ScO	<sup>2</sup> Σ <sup>+</sup>	965.0	962.1 <sup>b</sup>	954.8	24, 105
TiO	<sup>3</sup> Δ	1000.0	997.7 <sup>b</sup>	987.8	24, 27, 132
VO	<sup>4</sup> Σ <sup>-</sup>	1001.8	998.3 <sup>b</sup>	983.6	24, 27, 182
CrO	<sup>5</sup> Π	885.0	880.2	846.3	24, 201, 202
MnO	<sup>6</sup> Σ <sup>+</sup>	832.4	830.9 <sup>b</sup>	833.1	24, 246
FeO	<sup>5</sup> Δ	871.2	869.8 <sup>b</sup>	872.8	24, 270
CoO	<sup>4</sup> Δ	851.7	851.2	846.2	24, 27, 318, 320
NiO	<sup>3</sup> Σ <sup>-</sup>	828.3	831.4 <sup>b</sup>	825.7	24, 27, 347
CuO	<sup>2</sup> Π	631.3 <sup>c</sup>		627.7	24, 383
ZnO	<sup>1</sup> Σ <sup>+</sup>	738 <sup>d</sup>		769.2	456, 464, 465
YO	<sup>2</sup> Σ <sup>+</sup>	855.2	852.2 <sup>b</sup>	843.1	25, 109
ZrO	<sup>1</sup> Σ <sup>+</sup>	969.8	966.9 <sup>b</sup>	958.6	25, 70, 95, 132
NbO	<sup>4</sup> Σ <sup>-</sup>	981.4	978.5 <sup>b</sup>	970.6	25, 183
MoO	<sup>5</sup> Π			893.5	70, 71, 157, 208
TcO	<sup>6</sup> Σ <sup>+</sup>				70, 71, 207
RuO	<sup>5</sup> Δ	863.5	849.7	834.2	261, 314
RhO	<sup>4</sup> Σ <sup>-</sup>	805	799.8	799.0	332, 334, 337
PdO	<sup>3</sup> Σ <sup>-</sup> ( <sup>3</sup> Π) <sup>e</sup>				356
AgO	<sup>2</sup> Π	485		499.2	71, 430, 434
CdO	<sup>1</sup> Σ <sup>+</sup>			645.1	464, 466, 468
LaO	<sup>2</sup> Σ <sup>+</sup>	808.3	808.5 <sup>b</sup>	796.7	25, 109
HfO	<sup>1</sup> Σ <sup>+</sup>	974.1	965.8 <sup>b</sup>	958.3	73, 129, 132
TaO	<sup>2</sup> Δ	1028.9	1020.0 <sup>b</sup>	1014.2	73, 175, 183
WO	<sup>3</sup> Σ <sup>-</sup> ( <sup>5</sup> Π) <sup>e</sup>	1053.7	1056.1	1051.3	25, 201, 210
ReO	<sup>4</sup> Φ( <sup>2</sup> Δ, <sup>6</sup> Σ <sup>+</sup> ) <sup>e</sup>	979.1		73, 259–261	
OsO	<sup>5</sup> Σ <sup>+</sup> ( <sup>3</sup> Φ) <sup>e</sup>			73, 261	
IrO	<sup>4</sup> Σ <sup>-</sup>		827.2	822.1	340, 341
PtO	<sup>3</sup> Σ <sup>-</sup>	841.1	837.7 <sup>b</sup>	828.0	357, 366, 367
AuO	<sup>2</sup> Π	624.6		619.2	430, 443
HgO	<sup>3</sup> Π			676	475, 477
CeO	<sup>3</sup> Φ	824.3	819.9 <sup>b</sup>	808.3	74, 480, 504
PrO			828.0	816.9	504
NdO			825.1	814.2	504
PmO	<sup>6</sup> Σ <sup>+</sup>			74	
SmO			819	807.4	503, 504
EuO	<sup>8</sup> Σ <sup>-</sup>			667.8	74, 504
GdO	<sup>9</sup> Σ <sup>-</sup>	790 ± 40	824	812.7	74, 489, 503, 504
TbO			833.5 <sup>b</sup>	823.9	505
DyO			839.0	829.0	505
HoO		841.4	838.1	828.1	497, 505
ErO				828.5	505
TmO				832.0	505
YbO	<sup>1</sup> Σ <sup>+</sup>	683.1		660.0	74, 501, 505
LuO	<sup>2</sup> Σ <sup>+</sup>		811	829.3	74, 503, 505
ThO	<sup>1</sup> Σ <sup>+</sup>	895.8 <sup>d</sup>	887.1	876.4	521, 533, 534, 538, 580
UO	quintet	882.4	889.5	819.8	532, 546, 549
PuO	<sup>7</sup> Π			822.3	563, 564

<sup>a</sup> Only the values for the most abundant metal isotope and major site are listed. <sup>b</sup> Unpublished results. <sup>c</sup> 631.3 cm<sup>-1</sup> for <sup>2</sup>Π<sub>3/2</sub> and 627.5 cm<sup>-1</sup> for <sup>2</sup>Π<sub>1/2</sub>. <sup>d</sup> Harmonic frequency. <sup>e</sup> Ground state undetermined.

in this section. We will focus on the structures and vibrational frequencies of the MO<sub>x</sub> species in their electronic ground states. Since various experimental studies have been performed using different methods for producing and characterization transition metal–oxygen species, controversy assignments on measured vibrational fundamentals have been reported in many cases. Assignments from earlier reports now known to be incorrect will not be mentioned here, but these are discussed in the recent literature where the new assignments are given.

For the simplest member in this series, transition metal monoxides are among the most studied species. The spectra, electronic structures, and bonding of transition metal monoxides have been systematically reported.<sup>24–29,60–75</sup> The ground spin states and vibrational frequencies of all transition metal monoxides in the gas phase and in solid argon and neon matrices are summarized in Table 1. In general, the

**Table 2. Ground Spin States, Symmetry Point Groups, and Vibrational Frequencies (cm<sup>-1</sup>) for M(O<sub>2</sub>) Species in Solid Argon<sup>a</sup>**

molecule	ground state	point group	vibrational frequency	ref
Rh(η <sup>2</sup> -O <sub>2</sub> )	<sup>2</sup> A <sub>2</sub>	C <sub>2v</sub>	959.5	336
Ni(η <sup>2</sup> -O <sub>2</sub> )	<sup>1</sup> A <sub>1</sub> ( <sup>3</sup> B <sub>1</sub> ) <sup>b</sup>	C <sub>2v</sub>	967.1, 538.3, 511.7	76, 239, 347, 371, 372, 375–379
Pd(η <sup>2</sup> -O <sub>2</sub> )	<sup>1</sup> A <sub>1</sub>	C <sub>2v</sub>	1023.0	357, 380
Pt(η <sup>2</sup> -O <sub>2</sub> )	<sup>1</sup> A <sub>1</sub>	C <sub>2v</sub>	928.1, 512.3, 551.2	372
Cu(η <sup>1</sup> -O <sub>2</sub> )	<sup>2</sup> A''	C <sub>s</sub>	1089.0	383
Ag(η <sup>1</sup> -O <sub>2</sub> )	<sup>2</sup> A''	C <sub>s</sub>	1075.7	430
Au(η <sup>1</sup> -O <sub>2</sub> )	<sup>2</sup> A''	C <sub>s</sub>	1093.8	430

<sup>a</sup> Only the values for the most abundant metal isotope are listed.

<sup>b</sup> These two states are close in energy, and the vibrational frequencies for the <sup>1</sup>A<sub>1</sub> state are in better agreement with the experimental values.

matrix frequencies are usually slightly red-shifted from the gas-phase values with the argon matrix shift being larger than that of neon.

There are three structural isomers for triatomic MO<sub>2</sub> species, namely, the side-on and end-on bonded metal dioxygen complexes and the inserted metal dioxide molecule. The electronic structure and bonding of first and second row transition metal dioxygen complexes and dioxide species have been systematically investigated theoretically.<sup>76–78</sup> Experimentally, the dioxide form has been observed for all transition metals except technetium, silver, and mercury, while the dioxygen complex isomers are only reported for some late transition metals. The geometric structures and vibrational frequencies of transition metal dioxygen complexes are summarized in Table 2. Both the side-on and end-on bonded metal–dioxygen complexes usually show strong O–O stretching vibrations. The coordination fashion (side-on versus end-on) can be sorted out from the spectrum with mixed isotopic samples. In the experiment with a 1:2:1 molar mixture of <sup>16</sup>O<sub>2</sub>/<sup>16</sup>O<sup>18</sup>O/<sup>18</sup>O<sub>2</sub>, the O–O stretching mode of side-on bonded M(O<sub>2</sub>) complex will split into a triplet with approximately 1:2:1 relative intensities; but the O–O stretching mode of the end-on bonded complex will consist of a quartet with two closely spaced mixed isotopic absorptions for the M<sup>16</sup>O<sup>18</sup>O and M<sup>18</sup>O<sup>16</sup>O isotopic molecules. The geometric structures and vibrational frequencies of all transition metal dioxides in gas phase and in solid noble gas matrices are organized in Table 3. The inserted dioxide structure may be either bent or linear. The symmetric stretching mode (ν<sub>1</sub>) of linear OMO is IR inactive. However, the ν<sub>1</sub> fundamental of <sup>16</sup>OM<sup>18</sup>O is IR activated because of the reduced symmetry. Along with the observation of the ν<sub>1</sub> + ν<sub>3</sub> combination, the crossed anharmonic term, X<sub>13</sub> can be obtained. Hence, the band position of the ν<sub>1</sub> fundamental can be predicted. Both the symmetric (ν<sub>1</sub>) and antisymmetric (ν<sub>3</sub>) stretching modes of bent insertion molecules are IR active. The observed isotopic frequency ratio of the antisymmetric stretching mode provides a route to estimate the bond angle of a bent metal dioxide molecule.<sup>79</sup> The upper limit of bond angle can be determined from the oxygen isotopic frequency ratio, while the lower limit can be deduced from the metal isotopic frequency ratio if the metal isotopic shift can be resolved. The average of upper and lower limits is very close to the true bond angle, as has been demonstrated earlier for SO<sub>2</sub> and more recently for S<sub>3</sub>.<sup>80,81</sup>

Three structures have been observed for species with MO<sub>3</sub> stoichiometry: metal trioxide with planar D<sub>3h</sub> or nonplanar C<sub>3v</sub> symmetry, metal ozonide complex, and metal monox-

**Table 3. Ground Spin States, Experimental Bond Angles (Degree) and Vibrational Frequencies (cm<sup>-1</sup>) for Transition Metal Dioxides in the Gas Phase and in Solid Neon and Argon Matrices<sup>a</sup>**

molecule	ground state	bond angle <sup>b</sup>	gas phase frequency	Ne		Ar		ref
				$\nu_1$	$\nu_3$	$\nu_1$	$\nu_3$	
ScO <sub>2</sub>	<sup>2</sup> B <sub>2</sub>	bent	740 ± 80 ( $\nu_1$ )					89, 108, 109
TiO <sub>2</sub>	<sup>1</sup> A <sub>1</sub>	113 ± 5	960 ± 40 ( $\nu_1$ )	962.7 <sup>c</sup>	936.5 <sup>c</sup>	946.9	917.1	115, 132, 139
VO <sub>2</sub>	<sup>2</sup> A <sub>1</sub>	118 ± 3	970 ± 40 ( $\nu_1$ )	958.0 <sup>c</sup>	947.4 <sup>c</sup>	946.3	935.9	77, 165, 182
CrO <sub>2</sub>	<sup>3</sup> B <sub>1</sub>	128 ± 4	895 ± 20 ( $\nu_1$ ) 220 ± 20 ( $\nu_2$ )	920.8	974.9	914.4	965.4	201, 202, 217
MnO <sub>2</sub>	<sup>4</sup> B <sub>1</sub>	135 ± 5	800 ± 40 ( $\nu_1$ )	834.0 <sup>c</sup>	962.8 <sup>c</sup>	816.4	948.0	240, 246
FeO <sub>2</sub>	<sup>3</sup> B <sub>1</sub>	150 ± 10		811.1 <sup>c</sup>	957.7 <sup>c</sup>	797.1	945.8	270, 286
CoO <sub>2</sub>	<sup>2</sup> $\Sigma_g^+$	180		796.2 <sup>d</sup>	954.7	783.7 <sup>d</sup>	945.4	320, 326
NiO <sub>2</sub>	<sup>1</sup> $\Sigma_g^+$	180	750 ± 30 ( $\nu_1$ )		967.7		954.9	344, 347, 371, 372
CuO <sub>2</sub>	<sup>2</sup> $\Pi_g^-$	180			836.7 <sup>c</sup>		823.0	382, 383
ZnO <sub>2</sub>	<sup>3</sup> $\Sigma_g^-$	180			762.9		748.2	464, 612
YO <sub>2</sub>	<sup>2</sup> B <sub>2</sub>	bent	640 ± 80 ( $\nu_1$ )			708.2		89, 109
ZrO <sub>2</sub>	<sup>1</sup> A <sub>1</sub>	113 ± 5	887 ± 40 ( $\nu_1$ )	903.4 <sup>c</sup>	838.7 <sup>c</sup>	884.3	818.0	132, 137, 146
NbO <sub>2</sub>	<sup>2</sup> A <sub>1</sub>	108 ± 5		957.2 <sup>c</sup>	907.8 <sup>c</sup>	933.5	875.9	183
MoO <sub>2</sub>	<sup>3</sup> B <sub>1</sub>	118 ± 4		950.7	901.3	939.3	885.5	201, 210
TcO <sub>2</sub>	<sup>4</sup> B <sub>1</sub> ( <sup>4</sup> B <sub>2</sub> ) <sup>e</sup>	bent						78, 258
RuO <sub>2</sub>	<sup>1</sup> A <sub>1</sub>	151 ± 5			911.9		902.1	261
RhO <sub>2</sub>	<sup>2</sup> $\Sigma_g^{+f}$	180			908.6	845 <sup>d</sup>	899.9	325, 334, 337
PdO <sub>2</sub>	<i>e</i>		680 ± 30 ( $\nu_1$ )					342
AgO <sub>2</sub>	<sup>4</sup> $\Sigma_g^+$	180						355
CdO <sub>2</sub>	<sup>3</sup> $\Sigma_g^-$	180			638.8		625.4	464, 612
LaO <sub>2</sub>	<sup>2</sup> B <sub>2</sub>	bent				569.8		109
HfO <sub>2</sub>	<sup>1</sup> A <sub>1</sub>	113 ± 5	887 ± 40 ( $\nu_1$ )	901.9 <sup>c</sup>	831.9 <sup>c</sup>	883.4	814.0	132, 137, 146
TaO <sub>2</sub>	<sup>2</sup> A <sub>1</sub>	106 ± 5	968	979.2 <sup>c</sup>	920.9 <sup>c</sup>	965.3	912.2	174, 183
WO <sub>2</sub>	<sup>1</sup> A <sub>1</sub>	108 ± 5	325 ± 15 ( $\nu_2$ )	1030.3	983.9	978.3	938.0	201, 210, 225
ReO <sub>2</sub>	<sup>4</sup> B <sub>1</sub>	127 ± 4		989.1	941.0	981.9	931.7	261
OsO <sub>2</sub>	<sup>3</sup> B <sub>1</sub>	135 ± 5			957.3		949.9	261
IrO <sub>2</sub>	<sup>2</sup> $\Sigma_g^+$	180			938.2	960 <sup>d</sup>	929.0	340, 341
PtO <sub>2</sub>	<sup>1</sup> $\Sigma_g^+$	180	895 ± 30 ( $\nu_1$ )		958.7		961.8	342, 355, 357, 372
AuO <sub>2</sub>	<sup>2</sup> $\Pi_g^-$	180	740 ± 60 ( $\nu_1$ )		824.2		817.9	355, 357, 440
CeO <sub>2</sub>	<sup>1</sup> A <sub>1</sub>	139		780.3 <sup>c</sup>	755.6 <sup>c</sup>	757.3	736.7	504, 510
PrO <sub>2</sub>		180			752.5		730.1	504
NdO <sub>2</sub>		180			737.6		716.9	504
SmO <sub>2</sub>		180					643.2	504
EuO <sub>2</sub>		90					622.8	504
GdO <sub>2</sub>		97					635.5	504
TbO <sub>2</sub>		125		769.5 <sup>c</sup>	730.4 <sup>c</sup>	758.6	718.6	505
DyO <sub>2</sub>		180			599.2		580.5	505
HoO <sub>2</sub>		125		668.2		649.2	549	505
TmO <sub>2</sub>		128				706.6	615.7	505
YbO <sub>2</sub>		180					627.7	505
ThO <sub>2</sub>	<sup>1</sup> A <sub>1</sub>	122 ± 2		808.4	756.8	787.1	735.1	521, 533, 538
UO <sub>2</sub>	<sup>3</sup> $\Phi_u$	180			914.8		775.7	546, 549
PuO <sub>2</sub>	<sup>5</sup> $\Sigma_g^+$	180					794.2	563–565

<sup>a</sup> Only the values for the most abundant metal isotope and major site are listed. <sup>b</sup> Angles are estimated from oxygen 16/18 isotopic ratio and metal isotopic ratio (if available) for the  $\nu_3$  mode. For HoO<sub>2</sub>, the angle is estimated from oxygen 16/18 isotopic ratio for the  $\nu_1$  mode. <sup>c</sup> Unpublished results. <sup>d</sup> Calculated by  $(\nu_1 + \nu_3)_{\text{exp}} - (\nu_3)_{\text{exp}}$  with the anharmonic term corrected. <sup>e</sup> Ground state undetermined. <sup>f</sup> A linear geometry is proposed from matrix ESR experiments (ref 325) but a slightly bent geometry is obtained from theoretical calculations (ref 334 and 336).

ide–dioxygen complex. For early transition metals (Sc group and Ti group), only the metal monoxide–dioxygen complex structure has been observed due to limited valence electrons available for bonding, while both the trioxide and monoxide–dioxygen complex structures have been reported for some late transition metals. The metal ozonide structure is rare, only very few ozonide complexes have been experimentally reported. The experimentally characterized structures of MO<sub>3</sub> species are listed in Table 4.

For oxygen-rich MO<sub>x</sub> species with  $x \geq 4$ , the number of possible structures is much larger than that of the simple MO<sub>2</sub> and MO<sub>3</sub> species. However, only some of them have been experimentally characterized, which will be discussed in detail in this section. The geometric structures and vibrational frequencies of oxygen-rich MO<sub>x</sub> species with  $x \geq 4$  are organized in Tables 5 and 6. In the matrix isolation studies, each structural isomer exhibits charac-

teristic infrared absorptions in different spectral regions. The isotopic shifts and splitting in mixed isotopic spectra provide detailed information about the number of dioxygen units or oxygen atoms involved in a transition metal–oxygen species. Theoretical calculations at various levels have been intensively performed to predict the ground-state structure and vibrational frequencies of transition metal–oxygen species for comparison with the experimental values to support the experimental identification of new species. Due to problems such as near-degeneracy effects and s–d energy separation, the unambiguous assignment of the ground state of transition metal oxides and dioxygen complexes based solely on theoretical predictions is often quite complicated, particularly for late transition metal systems. Contradictory results are frequently obtained using different theoretical methods. Nevertheless, the experimentally determined spectroscopic properties pro-

**Table 4. Ground Spin States, Symmetry Point Groups, and Vibrational Frequencies (cm<sup>-1</sup>) for the MO<sub>3</sub> Species in Solid Argon<sup>a</sup>**

molecule	ground state	point group	vibrational frequency <sup>b</sup>	ref
( $\eta^2$ -O <sub>2</sub> )ScO	<sup>2</sup> A'	C <sub>s</sub>	1109.5, 922.0, 466.3	85, 105
( $\eta^2$ -O <sub>2</sub> )YO	<sup>2</sup> A''	C <sub>s</sub>	1111.1, 798.7	109
( $\eta^2$ -O <sub>2</sub> )LaO	<sup>2</sup> A''	C <sub>s</sub>	1123.4, 757.8	109
( $\eta^2$ -O <sub>2</sub> )TiO	<sup>1</sup> A'	C <sub>s</sub>	863.3, 971.9, 624.8, 611.1	147
( $\eta^2$ -O <sub>2</sub> )ZrO	<sup>1</sup> A'	C <sub>s</sub>	808.8, 885.7, 590.8, 580.2	148
( $\eta^2$ -O <sub>2</sub> )HfO	<sup>1</sup> A'	C <sub>s</sub>	782.8, 879.4, 614.9, 557.3	148
( $\eta^2$ -O <sub>2</sub> )FeO	<sup>5</sup> B <sub>2</sub>	C <sub>2v</sub>	1002.3	295
( $\eta^2$ -O <sub>2</sub> )NiO	triplet	C <sub>2v</sub>	1095.5	347
( $\eta^2$ -O <sub>2</sub> )PtO	<sup>3</sup> B <sub>2</sub>	C <sub>2v</sub>	1174.2	357
( $\eta^1$ -O <sub>2</sub> )NiO	singlet	C <sub>s</sub>	1393.7	347
( $\eta^1$ -O <sub>2</sub> )PtO	<sup>5</sup> A'	C <sub>s</sub>	1402.1	357
Cu( $\eta^2$ -O <sub>3</sub> )	<sup>2</sup> B <sub>1</sub>	C <sub>2v</sub>	802.7	383, 391
Ag( $\eta^2$ -O <sub>3</sub> )	<sup>2</sup> B <sub>1</sub>	C <sub>2v</sub>	791.8	430, 431
CrO <sub>3</sub>	<sup>1</sup> A <sub>1</sub>	C <sub>3v</sub>	968.4	201, 202
MoO <sub>3</sub>	<sup>1</sup> A <sub>1</sub>	C <sub>3v</sub>	915.8	201, 210
WO <sub>3</sub>	<sup>1</sup> A <sub>1</sub>	C <sub>3v</sub>	922.5	201, 210
ReO <sub>3</sub>	<sup>2</sup> A <sub>1</sub>	C <sub>3v</sub>	953.4	261
FeO <sub>3</sub>	<sup>1</sup> A <sub>1</sub> '	D <sub>3h</sub>	948.6	295
RuO <sub>3</sub>	<sup>1</sup> A <sub>1</sub> '	D <sub>3h</sub>	893.3	261
OsO <sub>3</sub>	<sup>1</sup> A <sub>1</sub> '	D <sub>3h</sub>	959.1	261
UO <sub>3</sub>	<sup>1</sup> A <sub>1</sub>	C <sub>2v</sub>	852.5, 843.5, 745.5, 211.6, 186.2, 151.5	367, 368, 549

<sup>a</sup> Only the values for the most abundant metal isotope are listed.

<sup>b</sup> The mode assignments are discussed in the cited literature.

vide a criterion to compare with the calculated values, which aids in determining the true ground state.

### 3.1. Sc Group

As the starting point for transition metals, scandium possesses the simplest electronic structure with only three valence electrons. The ground state of ScO is found to be <sup>2</sup>Σ from matrix isolation ESR as well as gas-phase experiments,<sup>24,82,83</sup> which is further confirmed by a series of theoretical calculations at different levels.<sup>27–29,61–69,76,84–88</sup> The Sc 4s<sub>σ</sub> and 3d<sub>π</sub> orbitals can interact with O 2p orbitals in forming σ and π bonds, respectively. The lone pair electrons on oxygen can be donated to the vacant 3d orbital of Sc with the formation of a dative bond. Hence ScO can be formally described as a diatomic molecule with a Sc≡O triple bond. The remaining electron of Sc is located on an σ orbital, which is mainly metal-based 4s orbital in character. Both experiments and theoretical calculations reveal that yttrium and lanthanum monoxide molecules possess the same <sup>2</sup>Σ ground state as ScO, and the spectroscopic properties of these two diatomic molecules have been well studied.<sup>71,72,74,75,82,83,89–102</sup>

Scandium dioxide is the only molecule that has not been identified in solid matrices among the first row transition metal dioxides. Mass spectrometric study on the reaction of scandium dioxide cation and nitrogen dioxide provides evidence for the existence of scandium dioxide molecule in the gas phase.<sup>103</sup> The symmetric stretching mode ( $\nu_1$ ) for ScO<sub>2</sub> is determined to be 740 ± 80 cm<sup>-1</sup> by photoelectron spectroscopy.<sup>89</sup> An infrared absorption at 722.5 cm<sup>-1</sup> has been assigned to the antisymmetric stretching mode ( $\nu_3$ ) of scandium dioxide in solid argon,<sup>104</sup> but late study reassigns this absorption to the OSco<sup>-</sup> anion instead of the neutral dioxide molecule.<sup>105</sup> According to the DFT and high-level ab initio calculations, both the C<sub>2v</sub> and symmetry-broken C<sub>s</sub> structures are stable minima. However, the relative stability depends strongly on the theoretical levels used.<sup>76,77,84,85,105–107</sup> A recent benchmark study by Kim and Crawford<sup>108</sup> using

**Table 5. Ground Spin States, Symmetry Point Groups, and Vibrational Frequencies (cm<sup>-1</sup>) for the MO<sub>4</sub> Species in Solid Argon<sup>a</sup>**

molecule	ground state	point group	vibrational frequency <sup>b</sup>	ref
( $\eta^2$ -O <sub>2</sub> )LaO <sub>2</sub>	<sup>2</sup> A <sub>2</sub>	C <sub>2v</sub>	1111.1, 602.9	109, 112
( $\eta^2$ -O <sub>2</sub> )VO <sub>2</sub>	<sup>2</sup> A <sub>2</sub>	C <sub>2v</sub>	1121.9, 974.1, 975.3, 506.9, 555.6	183
( $\eta^2$ -O <sub>2</sub> )NbO <sub>2</sub>	<sup>2</sup> A <sub>2</sub>	C <sub>2v</sub>	1109.3, 903.6, 945.9, 511.3	183
( $\eta^2$ -O <sub>2</sub> )TaO <sub>2</sub>	<sup>2</sup> A <sub>2</sub>	C <sub>2v</sub>	1095.7, 894.5, 950.5, 524.2	183
( $\eta^2$ -O <sub>2</sub> )MnO <sub>2</sub>	<sup>2</sup> A <sub>1</sub>	C <sub>2v</sub>	974.8, 951.3	247
( $\eta^2$ -O <sub>2</sub> )ReO <sub>2</sub>	<sup>2</sup> A <sub>1</sub>	C <sub>2v</sub>	992.4, 964.6, 882.4	261
( $\eta^2$ -O <sub>2</sub> )FeO <sub>2</sub>	<sup>1</sup> A <sub>1</sub>	C <sub>2v</sub>	968.8, 955.8, 558.1, 548.3	288
( $\eta^2$ -O <sub>2</sub> )RuO <sub>2</sub>	<sup>1</sup> A <sub>1</sub>	C <sub>2v</sub>	921.8, 920.7, 940.2, 579.8, 558.4	261
( $\eta^2$ -O <sub>2</sub> )OsO <sub>2</sub>	<sup>1</sup> A <sub>1</sub>	C <sub>2v</sub>	898.1, 970.0, 1004.8	261
( $\eta^2$ -O <sub>2</sub> )CoO <sub>2</sub>	<sup>2</sup> A <sub>2</sub>	C <sub>2v</sub>	950.6, 898.2, 842.8, 405.7, 419.6	327
( $\eta^2$ -O <sub>2</sub> )RhO <sub>2</sub>	<sup>2</sup> A <sub>2</sub>	C <sub>2v</sub>	928.6, 831.1, 865.0, 473.5	334, 337
( $\eta^2$ -O <sub>2</sub> )IrO <sub>2</sub>	<sup>2</sup> A <sub>2</sub>	C <sub>2v</sub>	894.8, 874.9, 937.7, 547.9, 517.8	340
( $\eta^2$ -O <sub>2</sub> )NiO <sub>2</sub>	triplet	C <sub>2v</sub>	1135.8, 851.0	347
( $\eta^1$ -O <sub>2</sub> )FeO <sub>2</sub>	<sup>3</sup> A''	C <sub>s</sub>	1204.5, 975.3, 871.6	288
( $\eta^1$ -O <sub>2</sub> )CoO <sub>2</sub>	<sup>4</sup> A'	C <sub>s</sub>	1286.2, 953.1, 805.8	327
( $\eta^1$ -O <sub>2</sub> )RhO <sub>2</sub>	<sup>2</sup> A'	C <sub>s</sub>	1116.5, 890.6, 837.7	334, 337
( $\eta^1$ -O <sub>2</sub> )IrO <sub>2</sub>	<sup>2</sup> A''	C <sub>s</sub>	1022.6, 947.4, 946.6	340
Sc( $\eta^2$ -O <sub>2</sub> ) <sub>2</sub>	<sup>2</sup> A <sub>2</sub>	C <sub>2v</sub>	1102.4, 836.0, 631.7, 612.7	111
Y( $\eta^2$ -O <sub>2</sub> ) <sub>2</sub>	<sup>2</sup> A <sub>2</sub>	C <sub>2v</sub>	1104.5, 773.6, 565.8	112
Rh( $\eta^2$ -O <sub>2</sub> ) <sub>2</sub>	<sup>4</sup> B <sub>1u</sub>	D <sub>2h</sub>	1048.4	336
Ni( $\eta^2$ -O <sub>2</sub> ) <sub>2</sub>	triplet	D <sub>2h</sub>	1063.9	347
Pd( $\eta^2$ -O <sub>2</sub> ) <sub>2</sub>	<sup>1</sup> A <sub>g</sub>	D <sub>2h</sub>	1110.1	380
Pt( $\eta^2$ -O <sub>2</sub> ) <sub>2</sub>	<sup>1</sup> A <sub>g</sub>	D <sub>2h</sub>	1051.3	357
Cu( $\eta^2$ -O <sub>2</sub> ) <sub>2</sub>	<sup>4</sup> B <sub>2u</sub>	D <sub>2h</sub>	1110.1	424, 425
Ag( $\eta^1$ -O <sub>2</sub> ) <sub>2</sub>	<sup>4</sup> B <sub>1</sub>	C <sub>2v</sub>	1299.2, 1053.9 <sup>c</sup>	355
OSc( $\eta^2$ -O <sub>3</sub> )	<sup>2</sup> A'	C <sub>s</sub>	921.7, 801.8	111
OY( $\eta^2$ -O <sub>3</sub> )	<sup>2</sup> A'	C <sub>s</sub>	805.6, 795.7	112
OLa( $\eta^2$ -O <sub>3</sub> )	<sup>2</sup> A'	C <sub>s</sub>	763.9, 792.0	112
RuO <sub>4</sub>	<sup>1</sup> A <sub>1</sub>	T <sub>d</sub>	916.6	261
OsO <sub>4</sub>	<sup>1</sup> A <sub>1</sub>	T <sub>d</sub>	956.2	261
IrO <sub>4</sub>	<sup>2</sup> A <sub>1</sub>	D <sub>2d</sub>	870.5, 859.5	340

<sup>a</sup> Only the values for the most abundant metal isotope are listed.

<sup>b</sup> The mode assignments are discussed in the cited literature. <sup>c</sup> Neon matrix values, unpublished results.

high-level coupled cluster methods up to full CCSD(T) indicates that the scandium dioxide molecule lies in a flat symmetry-breaking potential with indefinite sign and the zero-point vibrational energy lies above the barrier for the interconversion between the C<sub>s</sub> and C<sub>2v</sub> isomers. Although the symmetry-broken C<sub>s</sub> structure is predicted to be lower in energy than the C<sub>2v</sub> isomer, it is unlikely for the C<sub>s</sub> structure to be experimentally detected due to an overall dynamical C<sub>2v</sub> symmetry for this unusual molecule. Although the scandium dioxide molecule is not observed in solid matrices, the yttrium and lanthanum dioxide molecules have been formed via the reactions of metal atoms with dioxygen in solid argon, which are characterized to have a bent C<sub>2v</sub> structure<sup>109,110</sup> A recent CASPT2 calculation predicts a <sup>2</sup>B<sub>1</sub> ground state for LaO<sub>2</sub>.<sup>100</sup> The 708.2 cm<sup>-1</sup> symmetric stretching frequency ( $\nu_1$ ) observed in solid argon is in good agreement with the gas-phase value derived from the photoelectron spectroscopic study of YO<sub>2</sub>.<sup>89</sup>

The experimentally observed structure for the MO<sub>3</sub> (M = Sc, Y, and La) species in solid matrices is the metal monoxide–dioxygen complex structure, which is characterized to have a doublet ground state with nonplanar C<sub>s</sub> symmetry.<sup>104,105,109</sup> All three complexes are due to superoxide species with the metal centers in their formal +3 oxidation state. The previously assigned ozonide complexes in solid argon<sup>104,105,109</sup> are due to oxygen-rich species.<sup>111,112</sup> The (O<sub>2</sub>)ScO and (O<sub>2</sub>)LaO complexes are proposed to be the photodetachment products of the ScO<sub>3</sub><sup>-</sup> and LaO<sub>3</sub><sup>-</sup> anions



**Table 6. Ground Spin States, Symmetry Point Groups, and Vibrational Frequencies (cm<sup>-1</sup>) for the Oxygen-Rich MO<sub>x</sub> (x ≥ 5) Species in Solid Argon**

molecule	ground state	point group	vibrational frequency <sup>a</sup>	ref
(η <sup>2</sup> -O <sub>2</sub> ) <sub>2</sub> TiO	<sup>3</sup> A''	C <sub>s</sub>	1124.1, 1116.6, 996.8, 596.4	147
(η <sup>2</sup> -O <sub>2</sub> ) <sub>2</sub> CrO <sub>2</sub>	<sup>3</sup> B <sub>2</sub>	C <sub>2v</sub>	1153.9, 1134.2, 971.5, 939.6, 632.0	238
(η <sup>2</sup> -O <sub>2</sub> ) <sub>2</sub> MoO <sub>2</sub>		C <sub>2v</sub>	1119.3, 1111.2, 944.2, 966.4, 522.8	201
(η <sup>2</sup> -O <sub>2</sub> ) <sub>2</sub> WO <sub>2</sub>		C <sub>2v</sub>	1105.5, 1098.1, 951.2, 990.3, 497.7	201
OTi(η <sup>2</sup> -O <sub>2</sub> )(η <sup>2</sup> -O <sub>3</sub> )	<sup>3</sup> A	C <sub>1</sub>	1131.8, 1022.4, 999.8, 806.3, 686.8, 561.4	152
OZr(η <sup>2</sup> -O <sub>2</sub> )(η <sup>2</sup> -O <sub>3</sub> )	<sup>3</sup> A	C <sub>1</sub>	1117.8, 1015.2, 912.9, 796.4, 668.3, 472.2	148
OHf(η <sup>2</sup> -O <sub>2</sub> )(η <sup>2</sup> -O <sub>3</sub> )	<sup>3</sup> A	C <sub>1</sub>	1105.6, 1014.3, 902.3, 801.3, 680.2, 451.0	153
OTi(η <sup>2</sup> -O <sub>2</sub> )(η <sup>1</sup> -O <sub>3</sub> )	<sup>3</sup> A'	C <sub>s</sub>	1341.2, 1117.6, 993.4, 679.8, 554.2, 516.7	152
(η <sup>2</sup> -O <sub>2</sub> )MnO <sub>4</sub>	<sup>2</sup> A <sub>2</sub>	C <sub>2v</sub>	1511.7, 959.2, 929.8	247
Cu(η <sup>2</sup> -O <sub>2</sub> )(η <sup>2</sup> -O <sub>3</sub> )	<sup>4</sup> A <sub>1</sub>	C <sub>2v</sub>	1109.6, 796.4, 733.4	425
Cu(η <sup>2</sup> -O <sub>2</sub> )(η <sup>1</sup> -O <sub>2</sub> ) <sub>2</sub>	<sup>4</sup> B <sub>1</sub>	C <sub>2v</sub>	1299.8, 1135.2, 1060.7	428
Rh(η <sup>2</sup> -O <sub>2</sub> ) <sub>2</sub> (η <sup>1</sup> -O <sub>2</sub> )	<sup>2</sup> A'	C <sub>s</sub>	1280.1, 1127.6, 1076.7	336
Sc(η <sup>2</sup> -O <sub>2</sub> ) <sub>3</sub>	<sup>4</sup> A <sub>1</sub> ''	D <sub>3h</sub>	1106.7, 551.7	111
Hf(η <sup>2</sup> -O <sub>2</sub> ) <sub>3</sub>	<sup>3</sup> B	C <sub>2</sub>	1092.1, 1090.2, 804.4, 563.2, 438.5	153
(η <sup>2</sup> -O <sub>2</sub> )Sc(η <sup>2</sup> -O <sub>3</sub> ) <sub>2</sub>	<sup>4</sup> B	C <sub>2</sub>	818.7, 681.2, 678.7, 544.6	111
(η <sup>2</sup> -O <sub>2</sub> )Y(η <sup>2</sup> -O <sub>3</sub> ) <sub>2</sub>	<sup>4</sup> B	C <sub>2</sub>	1107.9, 1014.9, 811.6, 656.9, 447.0	112
Hf(η <sup>2</sup> -O <sub>2</sub> ) <sub>4</sub>	<sup>5</sup> B <sub>2</sub>	D <sub>2d</sub>	1102.4, 476.6, 423.3	153

<sup>a</sup> The mode assignments are discussed in the cited literature.

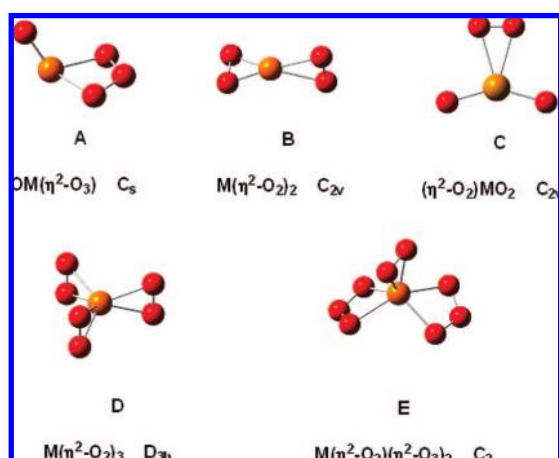


**Figure 1.** Optimized structures for oxygen-rich group III metal–oxygen species.

in the photoelectron spectroscopic studies,<sup>89,93</sup> while an ozonide complex is identified in the PES study of YO<sub>3</sub>.<sup>89</sup>

Although scandium dioxide molecule is not produced in solid matrices, our recent experiments on the Sc + O<sub>2</sub> reaction have shown that the ground-state scandium atoms react spontaneously with two dioxygen molecules to form OSc(η<sup>2</sup>-O<sub>3</sub>), which is predicted to have a <sup>2</sup>A' ground state with nonplanar C<sub>s</sub> symmetry (Figure 1A).<sup>111</sup> The OSc(η<sup>2</sup>-O<sub>3</sub>) complex can be regarded as [(ScO)<sup>+</sup>(O<sub>3</sub>)<sup>-</sup>], a scandium monoxide cation coordinated by a side-on bonded O<sub>3</sub><sup>-</sup> anion. The OSc(η<sup>2</sup>-O<sub>3</sub>) complex isomerizes to the Sc(η<sup>2</sup>-O<sub>2</sub>)<sub>2</sub> complex upon visible light (400 < λ < 580 nm) irradiation, which is characterized to be a superoxo scandium peroxide complex, that is, a scandium trication coordinated by an O<sub>2</sub><sup>-</sup> anion and an O<sub>2</sub><sup>2-</sup> anion. The Sc(η<sup>2</sup>-O<sub>2</sub>)<sub>2</sub> complex has a doublet ground state (<sup>2</sup>A<sub>2</sub>) with C<sub>2v</sub> symmetry, in which the superoxo ScO<sub>2</sub> plane is perpendicular to the peroxo ScO<sub>2</sub> plane (Figure 1 B).<sup>111</sup> The OY(η<sup>2</sup>-O<sub>3</sub>) and Y(η<sup>2</sup>-O<sub>2</sub>)<sub>2</sub> complexes are formed in the Y + O<sub>2</sub> reaction, which exhibit similar spectral, structural, and bonding properties to the scandium analogs.<sup>112</sup> In the lanthanum and dioxygen reaction, a (η<sup>2</sup>-O<sub>2</sub>)LaO<sub>2</sub> complex is also observed, which is the precursor for the formation of the OLa(η<sup>2</sup>-O<sub>3</sub>) complex under near-infrared excitation. The (η<sup>2</sup>-O<sub>2</sub>)LaO<sub>2</sub> complex possesses a planar C<sub>2v</sub> symmetry with a strong O–O stretching vibration in the superoxide region (Figure 1C).<sup>112</sup>

The MO<sub>5</sub> species (M = Y, La) have been reported only in gas-phase photoelectron spectroscopic studies. The PES spectra are quite broad and featureless.<sup>89,93</sup> The floppy (O<sub>2</sub>)<sub>2</sub>YO complex is tentatively assigned as the major isomer from the PES spectrum of YO<sub>5</sub><sup>-</sup>. The geometry of the neutral may be significantly changed upon detachment of the electron from the anion.<sup>89</sup> No structural information can be derived from the PES spectrum of LaO<sub>5</sub><sup>-</sup>.<sup>93</sup>

The Sc(η<sup>2</sup>-O<sub>2</sub>)<sub>3</sub> complex, which possesses a strong Sc–O<sub>2</sub> vibration and a weak doubly degenerate O–O vibration, is the only example experimentally known with MO<sub>6</sub> stoichiometry in this group.<sup>111</sup> It is characterized to have a <sup>4</sup>A<sub>1</sub>'' ground state with D<sub>3h</sub> symmetry having three side-on bonded O<sub>2</sub> ligands around the scandium atom, which thus presents a 6-fold coordination (Figure 1D). This complex can be described as [Sc<sup>3+</sup>(O<sub>2</sub><sup>-</sup>)<sub>3</sub>], a side-on bonded homoleptic scandium trisuperoxide complex. Population analysis indicates that the three unpaired electrons are mainly distributed on the three equivalent O<sub>2</sub><sup>-</sup> fragments. The Sc(η<sup>2</sup>-O<sub>2</sub>)<sub>3</sub> complex is quite similar to the recently characterized 6-fold coordinated trisuperoxo Al(η<sup>2</sup>-O<sub>2</sub>)<sub>3</sub> complex.<sup>113</sup> Scandium is isoivalent with aluminum, and both metals have three valence electrons with the highest oxidation state of +3.

The highest MO<sub>x</sub> species reported in this group is MO<sub>8</sub> (M = Sc, Y), which is determined to be a 6-fold coordinated superoxo scandium (yttrium) bisozonide complex.<sup>111,112</sup> The complex is predicted to have a <sup>4</sup>B ground state with C<sub>2</sub> symmetry, in which the O<sub>2</sub> and O<sub>3</sub> ligands are side-on bonded to the metal center (Figure 1E). The observation of the MO<sub>8</sub> complex provides not only a rare example that up to eight oxygen atoms can be bound to the same metal center but also a new model complex bearing two molecular ozonide ligands in one molecule. Similar ozonide complexes of early transition metals have been theoretically proposed.<sup>114</sup>

### 3.2. Ti Group

The spectroscopic properties of ground-state TiO have been the subject of a number of experimental investigations due to its importance in catalysis and astrophysics.<sup>24–26,115–121</sup> Theoretical calculations confirm that the diatomic TiO molecule possesses a <sup>3</sup>Δ ground state, in which the two unpaired electrons occupy the 1δ and 9σ orbitals that are largely derived from the Ti 3d orbitals.<sup>27–29,61–69,122–124</sup> For the next two members in this group, the ground state of

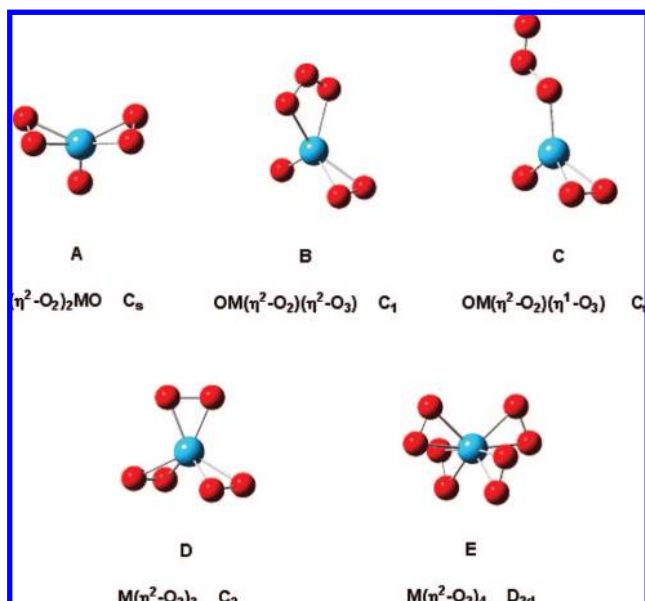


**Figure 2.** Optimized structures for oxygen-rich group IV metal–oxygen species.

both ZrO and HfO molecules is a closed-shell singlet ( $^1\Sigma^+$ ),<sup>70,73,95,116,125–129</sup> but the energy separation between the  $^3\Delta$  and  $^1\Sigma^+$  states of ZrO is rather small ( $1099\text{ cm}^{-1}$ ).<sup>130</sup> Due to lanthanide contraction, the vibrational fundamentals of ZrO and HfO, which lie lower than that of TiO, are quite close to each other.<sup>131,132</sup> The geometric and electronic structures of group IV metal dioxide molecules have been well established.<sup>26,76–78,107,115,122,132–146</sup> All of the three molecules possess a  $^1A_1$  ground state with bent structure. The valence angle for TiO<sub>2</sub> is determined to be  $113^\circ \pm 5^\circ$ .<sup>132</sup> The HfO<sub>2</sub> stretching frequencies are about the same as those of ZrO<sub>2</sub> due to a combination of lanthanide contraction and relativistic effects for hafnium.<sup>132</sup>

The only experimentally observed MO<sub>3</sub> species in this group is the  $(\eta^2\text{-O}_2)\text{MO}$  complex structure.<sup>115,147,148</sup> All three MO<sub>3</sub> complexes possess a closed-shell singlet ground state and nonplanar C<sub>s</sub> geometry with the O<sub>2</sub> ligand side-on bonded to the metal center.<sup>122,147–150</sup> These complexes are predicted to have rather long O–O bond lengths around 1.5 Å, which fall into the peroxide category. DFT/B3LYP calculations reveal that the O–O bond length increases from titanium (1.471 Å) to zirconium (1.493 Å) and hafnium (1.523 Å), which implies that the metal center tends to donate more electrons to the dioxygen ligand going down the series. As a result, the HfO<sub>3</sub> molecule has the longest O–O bond length and lowest O–O stretching vibrational frequency ( $782.8\text{ cm}^{-1}$ ).<sup>148</sup> A similar periodic trend has been observed in group IV metal monocarbonyls.<sup>151</sup> The  $(\eta^2\text{-O}_2)\text{TiO}$  complex can further coordinate another dioxygen to form the TiO<sub>5</sub> molecule, which is characterized to be a disuperoxo titanium monoxide complex,  $(\eta^2\text{-O}_2)_2\text{TiO}$ . The complex is predicted to have a  $^3A''$  ground state with nonplanar C<sub>s</sub> geometry, in which the two superoxo ligands are equivalent and are side-on bonded (Figure 2A).<sup>147</sup>

No stable species with MO<sub>4</sub> stoichiometry in this group are experimentally known, due to the high stability of the closed-shell metal dioxide molecules. However, our recent studies show that the metal dioxide molecules are able to react with two dioxygen molecules to form the  $\text{OM}(\eta^2\text{-O}_2)(\eta^2\text{-O}_3)$  complexes (M = Ti, Zr, Hf) in solid argon, featuring characteristic O–O stretching, antisymmetric O<sub>3</sub>

stretching, and M=O stretching vibrations in the infrared spectra.<sup>152,153</sup> The geometric and electronic structures of these complexes are very similar. Taking the  $\text{OTi}(\eta^2\text{-O}_2)(\eta^2\text{-O}_3)$  complex as an example, the complex is predicted to be slightly distorted from the C<sub>s</sub> symmetry in which the O<sub>3</sub> subunit and the central Ti atom lie in the same plane that is perpendicular to the molecular plane, as shown in Figure 2B.<sup>152</sup> The side-on-bonded O<sub>2</sub> fragment is due to a superoxide ligand based on the observed O–O stretching frequency.<sup>32–36</sup> The O<sub>3</sub> fragment also bound in an  $\eta^2$  side-on fashion with two nearly equivalent Ti–O bonds. The experimentally observed antisymmetric O–O stretching vibration of the O<sub>3</sub> subunit ( $806.3\text{ cm}^{-1}$ ) is very close to that of the O<sub>3</sub><sup>−</sup> anion isolated in solid argon.<sup>154</sup> While the O<sub>2</sub> and O<sub>3</sub> subunits coordinate with the Ti atom by forming weak Ti–O bonds with bond order of 0.5, the terminal Ti–O bond is strongly covalent bonded with a bond order close to 3. Therefore, the complex can be regarded as a side-on-bonded oxo–superoxo titanium ozonide complex,  $[(\text{TiO})^{2+}(\text{O}_2^-)(\text{O}_3^-)]$ , that is, a TiO<sup>2+</sup> dication coordinated by one O<sub>2</sub><sup>−</sup> anion and one O<sub>3</sub><sup>−</sup> anion.<sup>152</sup>

The  $\text{OTi}(\eta^2\text{-O}_2)(\eta^2\text{-O}_3)$  complex rearranges to a less stable  $\text{OTi}(\eta^2\text{-O}_2)(\eta^1\text{-O}_3)$  isomer under 532 nm laser irradiation, in which the O<sub>3</sub> unit is end-on bonded to Ti.<sup>152</sup> The  $\text{OTi}(\eta^2\text{-O}_2)(\eta^1\text{-O}_3)$  complex is predicted to have a  $^3A'$  ground state with C<sub>s</sub> symmetry (Figure 2C). The geometric features of the  $\text{OTi}(\eta^2\text{-O}_2)(\eta^1\text{-O}_3)$  structural unit in  $\text{OTi}(\eta^2\text{-O}_2)(\eta^1\text{-O}_3)$  are about the same as those in the  $\text{OTi}(\eta^2\text{-O}_2)(\eta^2\text{-O}_3)$  isomer. The O<sub>3</sub> fragment lies in the molecular plane and binds in an  $\eta^1$  end-on fashion with two different O–O bonds. The complex can also be described as  $[(\text{TiO})^{2+}(\text{O}_2^-)(\text{O}_3^-)]$ , an end-on bonded oxo–superoxo titanium ozonide complex. It is found that these two structural isomers are interconvertible, that is, formation of the end-on-bonded isomer is accompanied by demise of the side-on-bonded complex under 532 nm laser irradiation and vice versa upon sample annealing. Theoretical calculations predict that the side-on bonded complex is 7.3 kcal/mol more stable than the end-on bonded isomer at the B3LYP/6-311+G(d) level of theory. The reaction from side-on to end-on is endothermic and is computed to have a barrier height of 10.5 kcal/mol at the triplet potential energy surface. Figure 3 clearly shows the formation and interconversion of the two TiO<sub>6</sub> isomers.

The photoinduced isomerization reaction feature of  $\text{OHf}(\eta^2\text{-O}_2)(\eta^2\text{-O}_3)$  is different from that of  $\text{OTi}(\eta^2\text{-O}_2)(\eta^2\text{-O}_3)$ . The  $\text{OHf}(\eta^2\text{-O}_2)(\eta^2\text{-O}_3)$  complex rearranges to a  $\text{Hf}(\eta^2\text{-O}_2)_3$  isomer under visible light irradiation and the rearrangement is reversed upon UV irradiation (266 nm).<sup>153</sup> Unlike the trisuperoxo complexes of scandium and aluminum, which have D<sub>3h</sub> and D<sub>3</sub> symmetry with three equivalent superoxo ligands,<sup>111,113</sup> the  $\text{Hf}(\eta^2\text{-O}_2)_3$  complex is characterized to have a  $^3B$  ground state with C<sub>2</sub> symmetry (Figure 2D).<sup>153</sup> According to DFT calculations, the  $\text{Hf}(\eta^2\text{-O}_2)_3$  complex is 6.1 kcal/mol more stable than the  $\text{OHf}(\eta^2\text{-O}_2)(\eta^2\text{-O}_3)$  isomer. At the optimized geometry of  $\text{Hf}(\eta^2\text{-O}_2)_3$ , two O<sub>2</sub> subunits are side-on bonded and are equivalent with an O–O bond length of 1.338 Å, which falls into the range of superoxide. The third O<sub>2</sub> subunit is also side-on bonded with a much longer O–O bond length than that of the other two O<sub>2</sub> subunits. The predicted O–O bond length of 1.512 Å is appropriate for a peroxide complex. Accordingly, the  $\text{Hf}(\eta^2\text{-O}_2)_3$  molecule can be considered as  $[\text{Hf}^{4+}(\text{O}_2^-)_2(\text{O}_2^{2-})]$ , a side-on bonded disuperoxo hafnium peroxide complex.

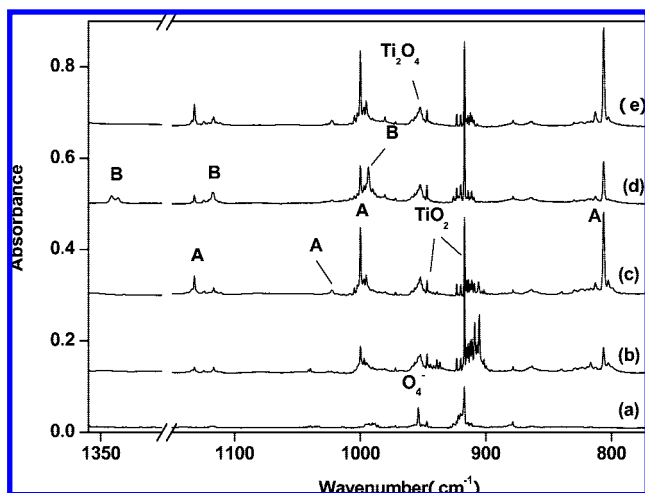


**Figure 3.** Infrared spectra in the 1360–1300 and 1150–770  $\text{cm}^{-1}$  regions from co-deposition of laser-evaporated titanium atoms with 0.5%  $\text{O}_2$  in argon: (a) 1 h of sample deposition at 6 K; (b) after 35 K annealing; (c) after 40 K annealing; (d) after 15 min 532 nm irradiation; (e) after 35 K annealing (A and B denote absorptions of  $\text{OTi}(\eta^2\text{-O}_2)(\eta^2\text{-O}_3)$  and  $\text{OTi}(\eta^2\text{-O}_2)(\eta^1\text{-O}_3)$ ). Reproduced from ref 152. Copyright 2007 American Chemical Society.

According to our recent studies on the reaction of hafnium atoms and  $\text{O}_2$ , the hafnium center can be coordinated by up to four  $\text{O}_2$  molecules in forming a homoleptic tetrasuperoxo hafnium complex,  $\text{Hf}(\eta^2\text{-O}_2)_4$ .<sup>153</sup> DFT/B3LYP calculations predict a  $^5\text{B}_2$  ground state with  $D_{2d}$  symmetry, in which the four  $\text{O}_2$  ligands are side-on bonded with the two oxygen atoms in each  $\text{O}_2$  subunit being slightly inequivalent (Figure 2E). Similar structure has been observed previously in group V and VI tetraperoxometallate anions.<sup>4g,155</sup> The  $^5\text{B}_2$  ground state of  $\text{Hf}(\eta^2\text{-O}_2)_4$  has an electronic configuration of (core)  $(a_2)^1(b_1)^1(e)^2$  with two unpaired electrons occupying the nonbonding  $a_2$  and  $b_1$  molecular orbitals, which are the combinations of four  $\text{O}_2^- \pi^*$  orbitals. The remaining two unpaired electrons occupy the doubly degenerate  $e$  molecular orbitals, which are also combinations of four  $\text{O}_2^- \pi^*$  orbitals but comprise significant  $\text{O}_2^- \pi^*$  to  $\text{Hf}^{4+}$  bonding. The  $\text{Hf}(\eta^2\text{-O}_2)_4$  complex is the only example of a binary neutral transition metal complex with four side-on bonded superoxide ligands.

### 3.3. V Group

Both the VO and NbO diatomic molecules are determined to have a  $4\Sigma^-$  ground state.<sup>24–29,61–72,88,156–171</sup> In contrast, the ground state of TaO is a  $2\Delta$  state.<sup>73,168,172–178</sup> The metal dioxides of this group are bent molecules.<sup>26,76–78,160–165,172,174,179–181</sup> Both the symmetric ( $\nu_1$ ) and antisymmetric ( $\nu_3$ ) stretching modes have been observed in solid matrices.<sup>182–187</sup> Recent experiments indicate that the dioxide molecules trapped in solid argon are coordinated by two argon atoms and should be regarded as the  $\text{MO}_2(\text{Ar})_2$  complexes.<sup>188,189</sup> However, argon atom coordination only slightly changes the spectral and structural properties of the dioxide molecules. Based on the observed isotopic frequency ratios of the  $\nu_3$  mode, the valence bond angle is estimated to be  $118^\circ \pm 3^\circ$  for  $\text{VO}_2$ ,  $108^\circ \pm 5^\circ$  for  $\text{NbO}_2$ , and  $106^\circ \pm 5^\circ$  for  $\text{TaO}_2$ .<sup>182,183</sup> Due to the anharmonicity in the  $\nu_3$  mode, the true angles of these dioxide molecules will be on the order of  $4^\circ$  lower than the estimated upper limits. While the stretching frequencies for  $\text{VO}_2$  and  $\text{TiO}_2$  are similar,<sup>132,182</sup> the stretching frequencies for  $\text{NbO}_2$  and  $\text{TaO}_2$  are some 50–100  $\text{cm}^{-1}$  higher than their neighboring  $\text{ZrO}_2$  and

$\text{HfO}_2$  molecules, which are estimated to have similar valence angle upper limits around  $115^\circ \pm 5^\circ$ .<sup>132</sup> The frequencies for  $\text{TaO}_2$  are some 30  $\text{cm}^{-1}$  higher than those for the lighter  $\text{NbO}_2$  molecule.<sup>183</sup> This suggests greater lanthanide contraction and relativistic effect for Ta relative to Nb than that for Hf relative to Zr. All three dioxide molecules are predicted to have a  $^2\text{A}_1$  ground state.<sup>76–78,160–164,172,179,183</sup>

The infrared spectrum of the neutral  $\text{VO}_3$  molecule has not been reported in solid matrices. DFT/B3LYP and BP86 calculations suggest a pyramidal structure with  $C_s$  symmetry to be the most stable structure for  $\text{VO}_3$ .<sup>160,161</sup> However, a nonplanar trigonal geometry with  $C_{3v}$  symmetry is predicted to be the ground state at the BPW91 level of theory,<sup>162</sup> which is consistent with the result given by diffusion quantum Monte Carlo calculations using BP86 and B3LYP methods.<sup>163</sup> In a matrix ESR spectroscopic investigation on the  $\text{VO}_x$  ( $x = 1–3$ ) system, an anisotropic octet absorption ( $g = 2.022$ ) with a relatively small  $^{51}\text{V } A_{\perp}$  value of  $\pm 62$  MHz is tentatively assigned to the  $\text{VO}_3$  radical.<sup>164</sup> Although the CASSCF calculations suggest that the minimum energy structure is pyramidal with  $C_s$  symmetry, a planar isomer with  $C_{2v}$  symmetry is calculated to be about 31 kcal/mol lower in energy than the  $C_s$  structure using MR-SDCI method. This planar  $C_{2v}$  structure is proposed to be the origin of the observed matrix ESR signal. A gas-phase PES study indicates that the  $\text{VO}_3$  molecule has a large adiabatic electron affinity of 4.36(5) eV due to the closed-shell nature of the  $\text{VO}_3^-$  anion.<sup>165</sup> The first detachment feature of the  $\text{VO}_3^-$  anion in the PES spectrum is associated with the bending mode involving two oxygen atoms, and no VO stretching vibrational progression has been observed. No detailed structural information on the neutral  $\text{TaO}_3$  molecule can be derived from the photoelectron spectrum of  $\text{TaO}_3^-$  except for a broad featureless band beginning at around 2 eV.<sup>161</sup> Both the  $\text{NbO}_3$  and  $\text{TaO}_3$  molecules are theoretically predicted to have three-dimensional pyramidal structures.<sup>172,180</sup>

The metal dioxide–dioxygen complex structure is the only structure experimentally characterized with  $\text{MO}_4$  stoichiometry ( $M = \text{V}, \text{Nb}, \text{Ta}$ ).<sup>182,183</sup> In an early report on photoinduced oxidation of  $\text{V}(\text{CO})_6$  in the presence of  $\text{O}_2$  in solid argon, a group of absorptions are attributed to an end-on bonded  $\text{OOVO}_2$  complex.<sup>190</sup> In the following study on the reaction of laser-ablated vanadium atoms with  $\text{O}_2$ , similar absorptions are assigned to the end-on coordinated  $\text{OOVO}_2$  complex.<sup>182</sup> The assignment of the end-on bonded structure is based on the observation of 1.8  $\text{cm}^{-1}$  split for the intermediate absorption of the O–O stretching vibration in the spectrum using a  $^{16}\text{O}_2 + ^{16}\text{O}^{18}\text{O} + ^{18}\text{O}_2$  sample. However, the side-on bonded  $(\eta^2\text{-O}_2)\text{VO}_2$  isomer is theoretically predicted to be more stable than the end-on bonded isomer.<sup>160–163,183</sup> Recent matrix isolation infrared spectroscopic work in this laboratory shows that the experimentally observed absorptions should be reassigned to the side-on bonded complex, which is coordinated by one argon atom to form the  $\text{VO}_4(\text{Ar})$  complex in a solid argon matrix.<sup>188</sup> The  $\text{VO}_4(\text{Ar})$  complex has a  $^2\text{A}''$  ground state with  $C_s$  symmetry (Figure 4). The Ar atom and the coordinated  $\text{O}_2$  subunits are in the same plane, which is perpendicular to the  $\text{VO}_2$  plane. The two oxygen atoms in the coordinated  $\text{O}_2$  subunit are slightly inequivalent due to argon atom coordination. As a result, the intermediate absorption of the O–O stretching vibration should split into two closely spaced absorptions in the spectrum with the  $^{16}\text{O}_2 + ^{16}\text{O}^{18}\text{O} + ^{18}\text{O}_2$  sample. The  $\text{NbO}_4$  and  $\text{TaO}_4$  complexes have the same structure as the

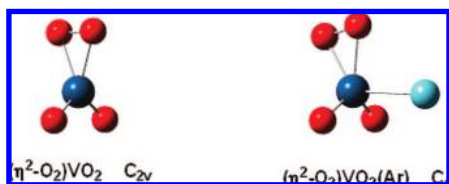


**Figure 4.** Optimized structures for  $\text{VO}_4$  and  $\text{VO}_4(\text{Ar})$ .

vanadium analog.<sup>189</sup> The metal–Ar binding energies for these noble gas atom complexes are predicted to be within several kcalories per mole, which are comparable with those of previously reported transition metal–noble gas complexes.<sup>191</sup>

The  $(\text{O}_2)_2\text{VO}$  complex is the only example in this group with  $\text{MO}_5$  stoichiometry that has been theoretically reported. The geometry of this complex is similar to that of the  $(\text{O}_2)_2\text{TiO}$  complex, which is determined to have nonplanar  $C_s$  symmetry. The  $(\text{O}_2)_2\text{VO}$  complex has a  $^2A''$  ground state with quite long O–O bonds (1.45 Å predicted at the BPW91/LANL2DZ level of theory).<sup>162</sup> It is found that the  $(\eta^2\text{-O}_2)\text{MO}_2$  complexes are able to coordinate another dioxygen molecule to form the very weakly bonded  $(\eta^2\text{-O}_2)\text{MO}_2\text{-O}_2$  complexes.<sup>188,189</sup> No other structures have been reported.

### 3.4. Cr Group

Chromium monoxide possesses a  $^5\Pi$  ground state with a  $(\text{core})(9\sigma)^1(1\delta)^2(4\pi)^1$  electronic configuration, in which the last electron occupies the  $4\pi$  antibonding orbital derived from the Cr  $3d_{\pi}$  and O  $2p_{\pi}$  orbitals due to the large  $3d\text{--}3d$  exchanged energy.<sup>24–29,61–69,192–200</sup> The population in the antibonding orbital suggests the decrease in the Cr–O bond order. The Cr–O fundamental observed at  $885\text{ cm}^{-1}$  in the gas phase is about  $100\text{ cm}^{-1}$  red-shifted from that of its neighboring vanadium monoxide.<sup>24</sup> The CrO fundamental in neon ( $880.2\text{ cm}^{-1}$ ) is slightly red-shifted from the gas-phase value,<sup>201</sup> but a large shift about  $35\text{ cm}^{-1}$  is observed for the corresponding argon matrix value ( $846.3\text{ cm}^{-1}$ ).<sup>202</sup> Recent study shows that the CrO molecule trapped in solid argon is coordinated by an argon atom. The absorption at  $846.3\text{ cm}^{-1}$  in solid argon should be assigned to  $\text{ArCrO}$  instead of the isolated diatomic molecule.<sup>38</sup>

Similar to the chromium congener, molybdenum monoxide also has a  $^5\Pi$  ground state,<sup>70,71,116,157,192,196,203–207</sup> whose infrared absorption is observed at  $893.5\text{ cm}^{-1}$  in solid argon.<sup>208</sup> The ground electronic state of the diatomic WO molecule remains unclear. A  $^3\Sigma^-$  spin state has been considered as the ground state in most experimental and theoretical studies.<sup>192,203,209–212</sup> However, a  $^5\Pi$  state was predicted to be the lowest state from the SCF and CASSCF calculations,<sup>213</sup> on the basis of which several low-lying electronic states in the near-infrared region are identified.<sup>214</sup> In a more recent theoretical investigation, a closed-shell singlet state was calculated to be lowest in energy using a series of DFT methods.<sup>73</sup> The vibrational fundamentals of WO were experimentally determined to be around  $1050\text{ cm}^{-1}$  both in the gas phase and in different noble gas matrices.<sup>25,201,210</sup>

The chromium dioxide molecule has been produced either via the reaction of chromium atom with  $\text{O}_2$  or from photo-oxidation of  $\text{Cr}(\text{CO})_6$  in  $\text{O}_2$ -doped matrices.<sup>215,216</sup> According to the most recent matrix investigations, the symmetric and antisymmetric stretching vibrations are observed at  $914.4$  and  $965.4\text{ cm}^{-1}$  in argon and  $920.8$  and  $971.9\text{ cm}^{-1}$  in neon.<sup>201,202</sup> The symmetric stretching and bending vibrations are deter-

mined to be  $895 \pm 20$  and  $220 \pm 20\text{ cm}^{-1}$  from photoelectron spectroscopy in the gas phase.<sup>217</sup> Theoretical calculations at different levels reveal that  $\text{CrO}_2$  has a  $^3B_1$  ground state with bent geometry.<sup>76,77,197,201,202,218–221</sup> The bond angle is determined to be  $128^\circ \pm 4^\circ$  based on the observed chromium and oxygen isotopic shifts of the  $\nu_3$  mode.<sup>202</sup> Besides the dioxide structure, the chromium dioxygen complex isomer has also been reported from photoelectron spectroscopic study of the  $\text{CrO}_2^-$  anion in the gas phase. A weak signal observed around  $1.5\text{ eV}$  is assigned to the photodetachment band of the  $\text{Cr}(\text{O}_2)^-$  anion, which results in the formation of the chromium peroxide complex,  $\text{Cr}(\text{O}_2)$ .<sup>197</sup>

The molybdenum dioxide molecule has also been characterized to have a triplet ground state with bent geometry.<sup>71,201,216,219,222–224</sup> The bond angle is estimated to be around  $118^\circ \pm 4^\circ$  from the observed Mo and O isotopic frequencies in solid argon and neon.<sup>201,202</sup> The last member in this group, the tungsten dioxide molecule, has a singlet ground state.<sup>201,219</sup> The singlet–triplet separation was experimentally determined to be  $0.327(6)\text{ eV}$  from photoelectron spectroscopy.<sup>225</sup> The vibrational frequencies of ground state  $\text{WO}_2$  are measured at  $1030\text{ cm}^{-1}$  ( $\nu_1$ ) and  $983\text{ cm}^{-1}$  ( $\nu_3$ ) in solid neon,<sup>201,214</sup> about  $50\text{ cm}^{-1}$  higher than those observed in solid argon and krypton.<sup>201,210,226</sup> The large neon-to-argon shifts suggest the existence of strong interactions between tungsten dioxide and matrix noble gas atoms.

The trioxide molecules of group VI metals are the only experimentally observed isomers with  $\text{MO}_3$  stoichiometry.<sup>197,201,202,210,212,216,224,226–231</sup> Gas-phase PES studies reveal that all three trioxide molecules in this group possess large HOMO–LUMO gaps, suggesting that these oxides are highly stable species and can serve as building blocks for large clusters and bulk materials.<sup>197,227–229</sup> All three trioxide molecules have been identified in matrix infrared studies from their characteristic doubly degenerate  $\text{M}=\text{O}$  stretching vibrations.<sup>201,202,210,212,224,226</sup> Calculations at various levels predict that these trioxide molecules all have a closed-shell  $^1A_1$  ground state with pyramidal  $C_{3v}$  symmetry.<sup>78,197,201,210,223,227,228,232–235</sup> All the metal valence electrons are involved in bonding with oxygen, and the metal centers are in their highest +6 oxidation state.

The information on group VI  $\text{MO}_4$  species is mainly obtained from gas-phase PES investigations, as well as theoretical calculations. The vibrational assignments of  $\text{MO}_4$  species remain unclear in solid matrices although some assignments have been proposed.<sup>202,210,216</sup> A PES study on the  $\text{CrO}_n$  ( $n = 1\text{--}5$ ) system suggests that  $\text{CrO}_4$  is a chromium dioxide–dioxygen complex,  $(\text{O}_2)\text{CrO}_2$ , which is predicted to have a closed-shell singlet ground state with  $C_2$  symmetry (DFT/BPW91).<sup>197</sup> The vertical electron detachment energy for the ground state of  $(\text{O}_2)\text{CrO}_2^-$  anion is predicted to be  $4.95\text{ eV}$ , in good agreement with the experimental value of  $5.07\text{ eV}$ . Recent density functional calculations at B3LYP level on the  $\text{WO}_4$  isomers reveal that the spectroscopic character of an end-on bonded tungsten dioxide–dioxygen complex structure is identical to the results from a vibrationally resolved PES study despite its metastable character.<sup>236,237</sup> However, a more recent PES investigation indicates that tungsten prefers tetrahedral coordination with oxygen without an O–O bond.<sup>228</sup>  $\text{WO}_4$ , as well as  $\text{MoO}_4$ , possesses extremely high electron affinities; thus, they belong to the category of strong oxidizers called superhalogens. The calculation of the ground state of neutral  $\text{WO}_4$  is particularly difficult due to symmetry-breaking issues. At the CCSD(T)/aug-cc-pVDZ level of theory, the ground state of  $\text{WO}_4$  is predicted to be

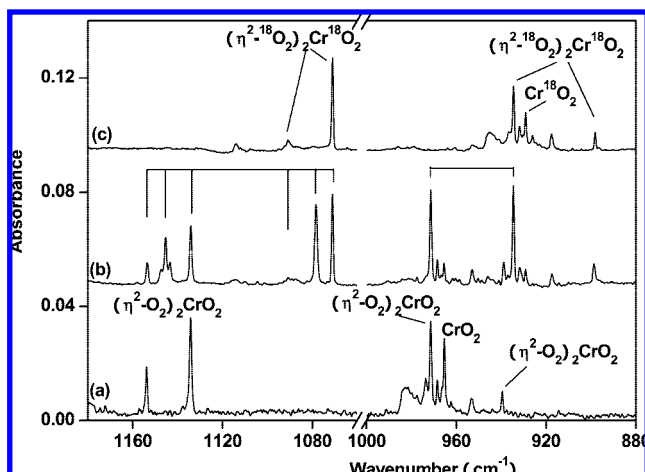


**Figure 5.** Infrared spectra in the 1180–1060 and 1000–880  $\text{cm}^{-1}$  regions from co-deposition of laser-ablated chromium atoms with isotopically substituted  $\text{O}_2$  in excess argon at 12 K. Spectra are taken after 1 h of sample deposition followed by 45 K annealing: (a) 2.0%  $^{16}\text{O}_2$ ; (b) 1.5%  $^{16}\text{O}_2$  + 1.5%  $^{18}\text{O}_2$ ; and (c) 2.0%  $^{18}\text{O}_2$ . Reproduced from ref 238. Copyright 2008 American Chemical Society.

a triplet  $^3\text{A}_2$  state with  $D_{2d}$  symmetry with a W–O distance of 1.828 Å and a  $\angle\text{OWO}$  bond angle of  $102.2^\circ$ , significantly distorted from the ideal  $T_d$  geometry. The W–O bond distance is not that of an oxo O but is more like that of an oxyl ( $-\text{O}^\bullet$ ).<sup>228</sup> The metal dioxide–dioxygen complex isomer, which is proposed to exist in solid noble gas matrices, is predicted to be higher in energy than the  $D_{2d}$  structure.

Structural information on the ground-state  $\text{MO}_5$  species has been obtained only from photoelectron spectroscopy, as well as theoretical predictions.<sup>197,228</sup> The most stable structure for all three  $\text{MO}_5$  species is found to be a dioxygen complex of metal trioxide,  $(\text{O}_2)\text{MO}_3$ . On the basis of experimental electron detachment energies and theoretical calculations, the  $(\text{O}_2)\text{CrO}_3$  complex is determined to have a  $^3\text{A}''$  ground state with an end-on bonded  $\text{O}_2$  moiety. The O–O bond distance is predicted to be 1.22 Å at the BPW91 level of theory, only slightly longer than that of free  $\text{O}_2$ , suggesting a weak interaction between  $\text{O}_2$  and  $\text{CrO}_3$ .<sup>197</sup> The  $\text{O}_2$  ligand is much more activated upon coordination to tungsten trioxide.<sup>228</sup> The O–O bond length of the  $(\text{O}_2)\text{WO}_3$  complex is predicted to be 1.312 Å at the B3LYP level; thus,  $\text{WO}_5$  can be described as an  $\text{O}_2^-$  interacting with  $\text{WO}_3^+$ . In the ground state of  $\text{WO}_5$ , one unpaired electron is localized on the  $\text{O}_2$  fragment as in the case of the anion, and the other unpaired electron is localized on one of the O atoms of  $\text{WO}_3$ , giving rise to the unusual charge-transfer complex,  $(\text{O}_2^-)\text{WO}_3^+$ . The energy for addition of  $\text{O}_2$  to  $\text{WO}_3$  to form  $\text{WO}_5$  is estimated to be exothermic by only 13.7 kcal/mol at the CCSD(T)/aug-cc-pVTZ level. This exothermicity is 3 eV less than that of  $\text{WO}_2$  plus  $\text{O}_2$  and shows that only a weak complex of  $\text{O}_2$  with  $\text{WO}_3$  is formed because the three oxo bonds in  $\text{WO}_3$  have consumed all the available valency of W.<sup>228</sup>

The metal dioxide–bisdioxygen complex structure is the only structural isomer experimentally characterized with  $\text{MO}_6$  stoichiometry. A group of absorptions at 1153.9, 1134.2, 971.5, 939.6, and 532.0  $\text{cm}^{-1}$  from the reaction of chromium atom with dioxygen in solid argon have been assigned to  $\text{CrO}_6$  based upon the observed mixed isotopic spectral features (Figure 5).<sup>201,238</sup> The assignment of the 1153.9, 1134.2, and 971.5  $\text{cm}^{-1}$  absorptions to  $\text{CrOO}$ ,  $\text{OOCrOO}$ , and  $\text{OOCrO}_2$  species in early matrix isolation studies is incor-

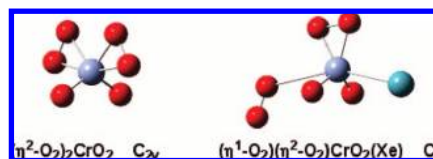


**Figure 6.** Optimized structures for  $\text{CrO}_6$  and  $\text{CrO}_6(\text{Xe})$ .

rect.<sup>202</sup> The  $(\eta^2\text{-O}_2)_2\text{CrO}_2$  complex is predicted to have a  $^3\text{B}_2$  ground state with a tetrahedral skeleton of  $C_{2v}$  symmetry, in which the two  $\text{O}_2$  fragments lie in the same plane, which is perpendicular to the  $\text{OCrO}$  plane.<sup>238</sup> The two  $\eta^2\text{-O}_2$  fragments are equivalent and bound in an asymmetric, side-on fashion, with two slightly inequivalent Cr–O bonds (Figure 6). The  $(\eta^2\text{-O}_2)_2\text{CrO}_2$  complex can be regarded as a side-on bonded disuperoxo chromium dioxide complex,  $[(\text{O}_2^-)_2(\text{CrO}_2)^{2+}]$ , where two  $\text{O}_2^-$  anions are bound to a  $\text{CrO}_2^{2+}$  dication.<sup>238</sup> The  $\text{MoO}_6$  and  $\text{WO}_6$  complexes are characterized to have similar structures as  $\text{CrO}_6$ .<sup>201</sup>

Our recent matrix experiments reveal that the  $(\eta^2\text{-O}_2)_2\text{CrO}_2$  complex can undergo a xenon-atom-induced disproportionation reaction to give a xenon atom coordinated  $(\eta^1\text{-OO})(\eta^2\text{-O}_2)\text{CrO}_2(\text{Xe})$  complex.<sup>238</sup> The  $(\eta^1\text{-OO})(\eta^2\text{-O}_2)\text{CrO}_2(\text{Xe})$  complex is predicted to have a  $C_s$  symmetry and  $^3\text{A}''$  ground state with the two  $\text{O}_2$  fragments and xenon atom in the same plane, which is perpendicular to the  $\text{OCrO}$  plane (Figure 6). The end-on bonded  $\eta^1\text{-OO}$  fragment is predicted to have an O–O bond length of 1.206 Å, which is about the same as that of free  $\text{O}_2$ , while the Cr–OO distance is calculated to be rather long (3.903 Å) at the B3LYP level. Therefore, the complex is regarded as a triplet  $\text{O}_2$  molecule adsorbed on a closed-shell  $(\eta^2\text{-O}_2)\text{CrO}_2(\text{Xe})$  complex. The conversion from the disuperoxo chromium dioxide complex to the peroxo–chromium dioxide–xenon complex reaction provides a model system in demonstrating  $\text{O}_2$  activation through electron transfer from metal oxides to form the superoxo complex and further convert to dioxygen and peroxide complex.

### 3.5. Mn Group

Due to the occupation of another doubly degenerate antibonding  $4\pi$  orbital, the diatomic  $\text{MnO}$  molecule has a  $^6\Sigma^+$  ground state with a  $(\text{core})(9\sigma)^1(1\delta)^2(4\pi)^2$  electronic configuration. The ground-state  $\text{MnO}$  molecule has the highest magnetic moment among the first row transition metal monoxide molecules.<sup>27–29,61–69,239–243</sup> The  $\text{MnO}$  bond is even weaker than that of its neighboring  $\text{CrO}$ . Therefore, the vibrational fundamental of  $\text{MnO}$  observed in the gas phase and in solid matrices is slightly lower than that of  $\text{CrO}$ .<sup>24,244–246</sup> An early ESR investigation suggested that the inserted manganese dioxide molecule is linear in the noble gas matrix.<sup>243</sup> However, subsequent matrix isolation infrared absorption spectroscopic investigation provided solid evidence that manganese dioxide is bent. Both the symmetric and antisymmetric stretching vibrations are observed in solid matrices.<sup>246</sup> The upper limit of valence angle is estimated to be  $140^\circ \pm 5^\circ$  from the  $\nu_3$  isotopic frequency ratio. The symmetric stretching mode is determined to be  $800 \pm 40 \text{ cm}^{-1}$  from PES study in the gas phase,<sup>240</sup> which is in good agreement with the  $816.4 \text{ cm}^{-1}$  value in solid argon.<sup>246</sup> Theoretical calculations at different levels reveal that the inserted  $\text{MnO}_2$  molecule has a  $^4\text{B}_1$  ground state with a bent structure.<sup>76,77,239,240,246</sup> The end-on bonded superoxide complex  $\text{MnOO}$  and the side-on bonded peroxide complex  $\text{Mn}(\text{O}_2)$  were suggested to exist in solid matrices from early matrix isolation studies.<sup>246</sup> However, recent investigation in

our laboratory indicates that the absorptions previously assigned to the  $\text{Mn}(\text{O}_2)$  complexes are due to larger clusters.<sup>247</sup> Theoretical calculations indicate that both the side-on and end-on bonded  $\text{Mn}(\text{O}_2)$  complexes are much higher in energy than the inserted dioxide isomer.<sup>76,77,239</sup> Gas-phase studies suggest that the ground-state manganese atoms are unreactive toward  $\text{O}_2$ .<sup>248</sup> It is very unlikely that these high-energy manganese dioxygen complexes can be formed and trapped in noble gas matrices.

Two structural isomers have been reported for  $\text{MnO}_3$ . A matrix-isolation ESR study indicated that  $\text{MnO}_3$  exhibits very large manganese hyperfine coupling, which suggests that the unpaired spin is best described as occupying an  $\text{sd}_{z^2}$  hybrid orbital, resulting in a molecule of planar  $D_{3h}$  symmetry and  ${}^2\text{A}_1$  ground state.<sup>243</sup> Theoretical calculations predict that the ground state of  $\text{MnO}_3$  is  ${}^2\text{A}_1$ , which possesses a pyramidal  $\text{C}_{3v}$  geometry.<sup>240</sup> The photoelectron spectrum of  $\text{MnO}_3^-$  at 266 nm reveals a single vibrationally resolved band with an  $840\text{ cm}^{-1}$  vibrational spacing and an adiabatic binding energy of 3.335 eV. The observed features are assigned to detachment transitions from the ground state of  $\text{MnO}_3^-$  to that of  $\text{MnO}_3$ . The observed vibrational progression is attributed to the symmetric  $\text{Mn}=\text{O}$  stretching vibration.<sup>240</sup> Matrix-isolation infrared absorption spectroscopic investigation of the reactions of laser-ablated manganese atoms with dioxygen failed to produce the manganese trioxide molecule. In contrast, a  $(\eta^2\text{-O}_2)\text{MnO}$  complex was tentatively identified with the  $\text{Mn}=\text{O}$  stretching vibration observed at  $886.9\text{ cm}^{-1}$  in solid argon.<sup>246</sup>

Two structural isomers have been reported experimentally for  $\text{MnO}_4$ . In a photoelectron spectroscopic study of  $\text{MnO}_4^-$  in gas phase, the observed spectral features were attributed to transitions from the ground state of the tetrahedral  $\text{MnO}_4^-$  anion to the ground and excited states of the  $\text{MnO}_4$  neutral, which is proposed to be a distorted tetrahedron with all four oxygen atoms bonded to the Mn center dissociatively.<sup>249</sup> This  $\text{MnO}_4$  structure was determined to have an electron affinity of 5 eV, which is significantly larger than that of atomic chlorine, the most electronegative element in the periodic table. In our recent matrix isolation study, a manganese dioxide–dioxygen complex,  $(\eta^2\text{-O}_2)\text{MnO}_2$ , is formed via the reaction of  $\text{MnO}_2$  and  $\text{O}_2$  in solid argon. The complex is characterized to be a side-on bonded peroxy manganese dioxide complex.<sup>247</sup> Theoretical calculations on  $\text{MnO}_4$  present contradictory results. The side-on bonded  $(\eta^2\text{-O}_2)\text{MnO}_2$  complex structure and the distorted tetrahedral isomer without O–O bonding are predicted to be close in energy with the complex structure being slightly (0.18 eV) less stable than the distorted tetrahedral isomer according to the BPW91 calculations.<sup>249,250</sup> In contrast, the complex structure is predicted to be about 4.4 kcal/mol more stable than the distorted tetrahedral isomer from our newly performed B3LYP calculations.<sup>247</sup> Single point energy calculations at the CCSD(T) level with the B3LYP optimized geometries give an even larger energy separation of 12.5 kcal/mol.<sup>247</sup>

The only experimentally characterized species with  $\text{MnO}_6$  stoichiometry is  $(\eta^2\text{-O}_2)\text{MnO}_4$ , a dioxygen complex of manganese tetroxide, which is produced from the reaction of  $\text{O}_2$  and the  $(\eta^2\text{-O}_2)\text{MnO}_2$  complex in solid argon.<sup>247</sup> This complex features an unusually intense O–O stretching vibration at  $1511.7\text{ cm}^{-1}$ . Theoretical calculations predict that the  $(\eta^2\text{-O}_2)\text{MnO}_4$  complex has a  ${}^2\text{A}_2$  ground state with  $\text{C}_{2v}$  symmetry, in which the  $\text{O}_2$  fragment is coordinated to two oxygen atoms of the  $\text{MnO}_4$  fragment, as shown in Figure 7.

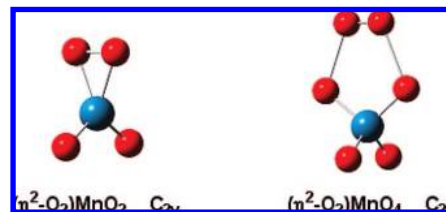


Figure 7. Optimized structures for  $\text{MnO}_4$  and  $\text{MnO}_6$ .

The O–O bond length of the  $\text{O}_2$  fragment in the  ${}^2\text{A}_2$  ground state  $(\eta^2\text{-O}_2)\text{MnO}_4$  complex is predicted to be  $1.184\text{ \AA}$  at the B3LYP/6-311+G(d) level, slightly shorter than the value of free molecular oxygen, whereas the O–O distance between the  $\text{O}_2$  and  $\text{MnO}_4$  fragments is computed to be  $2.226\text{ \AA}$ ,<sup>247</sup> significantly longer than that of typical O–O single bond and even longer than that of the  $\text{H}_2\text{OOO}^+$  cation, which is characterized to be a 3c–1e bond.<sup>251</sup> Unlike a number of transition metal dioxygen complexes, in which the  $\text{O}_2$  fragment is negatively charged, natural charge population analysis shows that the  $\text{O}_2$  ligand in  $(\eta^2\text{-O}_2)\text{MnO}_4$  is positively charged by about +0.21 e. However, the  $(\eta^2\text{-O}_2)\text{MnO}_4$  complex cannot be regarded as a pure ionic  $[\text{O}_2^+][\text{MnO}_4^-]$  charge-transfer complex. Generally, the O–O stretching vibrational modes of dioxygenyl fluorometallate salts, which are regarded as pure ionic compounds, lie around  $1850\text{ cm}^{-1}$ .<sup>252</sup> The O–O stretching frequency of  $(\eta^2\text{-O}_2)\text{MnO}_4$  is very close to that of the  $\text{XeOO}^+$  cation ( $1507.9\text{ cm}^{-1}$ ) in solid argon, which is characterized to involve a ( $p-\pi^*$ )  $\sigma$  bonding between Xe and  $\text{O}_2$ .<sup>253</sup> The interaction between  $\text{O}_2$  and  $\text{MnO}_4$  in  $(\eta^2\text{-O}_2)\text{MnO}_4$  is similar to that in the dioxygen complex of  $\text{FSO}_3$  radical.<sup>254</sup> The experimental electron affinity of  $\text{MnO}_4$  is determined to be  $4.80 \pm 0.10\text{ eV}$ ,<sup>249</sup> about the same as that of the  $\text{FSO}_3$  radical,<sup>255</sup> but is much smaller than that of  $\text{PtF}_6$  ( $7.00 \pm 0.35\text{ eV}$ ).<sup>256</sup>  $\text{PtF}_6$  is well-known to be able to oxidize the  $\text{O}_2$  molecule to form the  $[\text{O}_2^+][\text{PtF}_6^-]$  charge-transfer complex.<sup>257</sup>

Experimental reports on simple oxide and dioxygen complexes of Tc are rare due to the radioactive character of Tc. Much of the information on Tc system comes from theoretical calculations. Technetium monoxide is predicted to have a  ${}^6\Sigma^+$  ground state using both density functional and modified coupled pair functional (MCPF) methods.<sup>70,71,207</sup> These calculations yield an equilibrium bond length around  $1.76\text{ \AA}$  and a vibrational fundamental in the range of  $840\text{--}910\text{ cm}^{-1}$ . All three structural isomers with  $\text{TcO}_2$  stoichiometry have been calculated.<sup>78</sup> For the inserted technetium dioxide molecule with bent  $\text{C}_{2v}$  symmetry, a  ${}^4\text{B}_2$  state is predicted to be the ground state using the MCPF method.<sup>78</sup> However, calculations at the DFT/B3LYP level find a  ${}^4\text{B}_1$  state to be the ground state, which is about 12 kcal/mol lower in energy than the  ${}^4\text{B}_2$  state.<sup>258</sup> Both the end-on superoxo ( ${}^8\text{A}''$ ) and side-on peroxy ( ${}^4\text{B}_2$ ) complexes are predicted to be about 90 kcal/mol less stable than the inserted dioxide isomer at the MCPF level of theory.<sup>78</sup> The technetium trioxide molecule is computed to have a  ${}^2\text{A}_1'$  ground state with planar  $\text{D}_{3h}$  symmetry.<sup>78</sup>

The ground state of rhenium monoxide remains unclear. The vibrational frequency of  $\text{ReO}$  is determined to be  $979.1\text{ cm}^{-1}$  from the emission spectrum in the gas phase.<sup>259</sup> In a recent intermodulated fluorescence spectroscopic study, a  ${}^2\Delta$  state with (core) $1\sigma^2 2\sigma^2 1\pi^4 1\delta^3 3\sigma^2$  electronic configuration is found to be consistent with the experimentally observed magnetic hyperfine constant.<sup>260</sup> However, a  ${}^4\Phi$  state is predicted to be the ground state by BP86 and B3LYP

calculations with the  ${}^2\Delta$  and  ${}^6\Sigma^+$  states lying slightly higher in energy;<sup>261</sup> the  ${}^6\Sigma^+$  state is suggested to be the ground state in a recent theoretical study using various DFT methods.<sup>73</sup>

Both rhenium dioxide and trioxide molecules have been reported in solid matrix-isolation infrared spectroscopic and gas-phase PES studies.<sup>261,262</sup> The inserted  $\text{ReO}_2$  molecule is determined to have a  ${}^4B_1$  ground state with bent  $C_{2v}$  symmetry.<sup>258,261</sup> The rhenium trioxide molecule is found to have a  ${}^2A_1$  state with pyramidal  $C_{3v}$  geometry.<sup>261</sup> The electron affinities of  $\text{ReO}_2$  and  $\text{ReO}_3$  are measured to be  $2.5 \pm 0.1$  and  $3.6 \pm 0.1$  eV, respectively.<sup>262</sup> For the oxygen-rich  $\text{ReO}_4$  species, a peroxy rhenium dioxide complex,  $(\eta^2\text{-O}_2)\text{ReO}_2$ , has been identified in solid matrices. Theoretical calculations at the BP86 and B3LYP levels reveal that the  $(\eta^2\text{-O}_2)\text{ReO}_2$  complex has a closed-shell singlet ground state with non-planar  $C_{2v}$  symmetry.<sup>261</sup>

### 3.6. Fe Group

The diatomic  $\text{FeO}$  molecule is one of the most studied metal oxide species. Its molecular constants have been obtained by matrix infrared, photoelectron, photoluminescent, microwave, and electronic spectroscopy.<sup>24–26,40,263–275</sup> It has also been the subject of a number of theoretical studies.<sup>27–29,61–69,123,239,276–282</sup> It is well established that  $\text{FeO}$  has a  ${}^5\Delta$  ground state with five closely spaced spin orbital components (about  $200\text{ cm}^{-1}$ ). The vibrational fundamental is experimentally determined to be around  $870\text{ cm}^{-1}$  in the gas phase as well as in solid noble gas matrices.<sup>24,266,270,272,274</sup>

The  $\text{FeO}_2$  species have been the subject of a number of gas-phase and matrix experimental studies. Anion photoelectron spectroscopic investigation on  $\text{FeO}_2^-$  indicates that only the inserted  $\text{FeO}_2$  neutral structure is observed in the gas phase.<sup>268,269</sup> The photoelectron spectra of  $\text{FeO}_x^-$  ( $x = 1–4$ ) are shown in Figure 8. However, spectral assignments on the  $\text{FeO}_2$  species in solid matrices are not straightforward, and many disagreements are found in the literature. In an early matrix-isolation infrared spectroscopic study on the reaction of thermally evaporated iron atoms with dioxygen, absorptions at  $945.9$  and  $517.1\text{ cm}^{-1}$  are assigned to vibrations of the cyclic  $\text{Fe}(\text{O}_2)$  molecule in solid argon.<sup>283</sup> In the next work, three  $\text{FeO}_2$  isomers were proposed to be formed from the reactions of hollow-cathode sputtered iron atoms with dioxygen in argon. A band at  $956\text{ cm}^{-1}$  was assigned to the O–O stretching mode of the cyclic  $\text{Fe}(\text{O}_2)$  structure, while the bands at  $969$  and  $946\text{ cm}^{-1}$  were attributed to the linear and bent  $\text{OFeO}$  isomers.<sup>284</sup> In the photooxidation of matrix-isolated iron pentacarbonyl in the presence of oxygen, a  $956\text{ cm}^{-1}$  absorption was also assigned to the cyclic  $\text{Fe}(\text{O}_2)$  molecule, but a  $945\text{ cm}^{-1}$  absorption was attributed to  $\text{FeO}_3$  instead of  $\text{OFeO}$ .<sup>285</sup> More recent investigations employed the reactions of laser-ablated iron atoms with dioxygen; the absorption at  $956.0\text{ cm}^{-1}$  was retained for cyclic  $\text{Fe}(\text{O}_2)$ , but the absorptions at  $945.8$  and  $797.1\text{ cm}^{-1}$  were assigned to the antisymmetric and symmetric stretching modes of the inserted  $\text{FeO}_2$  molecule, while an absorption at  $1204.5\text{ cm}^{-1}$  was characterized as the O–O stretching mode of a  $\text{FeOO}$  isomer.<sup>270,286</sup> The assignment of the bent inserted  $\text{FeO}_2$  molecule was further supported by a matrix-isolation Mössbauer spectroscopic study.<sup>287</sup> The bond angle was determined to be  $150^\circ \pm 10^\circ$  based upon the observed oxygen and iron isotopic  $\nu_3$  frequencies.<sup>270,286</sup> Recently, we reinvestigated the reaction of iron atoms and dioxygen using matrix-isolation infrared absorption spectroscopy.<sup>288</sup> We found that the inserted iron dioxide molecule

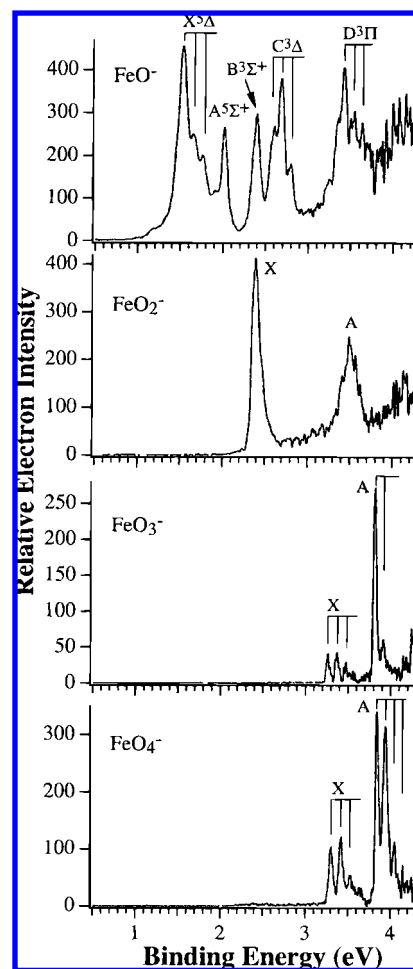


**Figure 8.** Photoelectron spectra of  $\text{FeO}_x^-$  ( $x = 1–4$ ) at 266 nm. The vertical lines indicate the resolved vibrational structures. X represents the ground state of the neutrals, and the other letters represent the excited states. Reproduced from ref 268a. Copyright 1996 American Chemical Society.

was the only isomer with  $\text{FeO}_2$  stoichiometry formed in solid argon. The absorptions previously assigned to  $\text{FeOO}$  ( $1204.5\text{ cm}^{-1}$ ) and cyclic  $\text{Fe}(\text{O}_2)$  ( $956.0\text{ cm}^{-1}$ ) are due to the end-on and side-on bonded dioxygen–iron dioxide complexes formed by the reactions of inserted  $\text{FeO}_2$  molecule with dioxygen in the matrix.<sup>288</sup> It was not possible to determine the ground state of iron dioxide from the theoretical point of view since the relative stability of different spin states depends strongly on the theoretical levels employed.<sup>76,77,239,270,286,289–294</sup> The ground state of iron dioxide was determined to be  ${}^3B_1$  based on comparison between the calculated and experimentally observed vibrational frequencies and isotopic frequency ratios.<sup>270,286</sup> Both the side-on bonded  $\text{Fe}(\text{O}_2)$  and end-on bonded  $\text{FeOO}$  complexes were predicted to lie much higher in energy than the inserted  $\text{FeO}_2$  isomer according to most theoretical predictions.<sup>76,77,270,286</sup>

Two structural isomers with  $\text{FeO}_3$  stoichiometry have been reported. A vibrationally resolved photoelectron spectroscopic study indicates that the observed  $\text{FeO}_3$  species is due to the  $D_{3h}$  iron trioxide molecule with three  $\text{Fe}=\text{O}$  bonds. The symmetric  $\text{Fe}=\text{O}$  stretching vibrational frequency was determined to be  $850 \pm 50\text{ cm}^{-1}$ .<sup>268</sup> Both the trioxide structure and an iron monoxide–dioxygen complex structure,  $(\text{O}_2)\text{FeO}$ , were suggested to be formed in previous matrix-isolation studies.<sup>270</sup> However, the spectral assignments were proven to be incorrect. Recently, both the  $(\text{O}_2)\text{FeO}$  complex

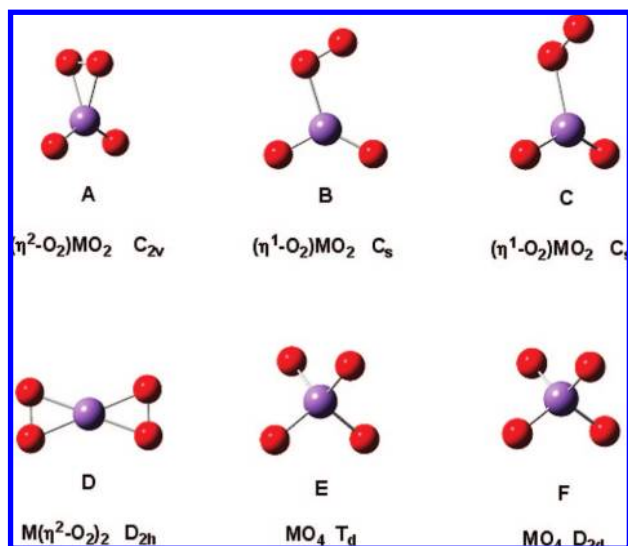


**Figure 9.** Optimized structures for  $\text{MO}_4$  isomers of group VIII metals.

and the trioxide molecule were prepared via the reactions of iron monoxide with dioxygen in solid argon.<sup>295</sup> The  $(\eta^2\text{-O}_2)\text{FeO}$  complex was predicted to have a  ${}^5\text{B}_2$  ground state with a planar  $\text{C}_{2v}$  structure, in which the  $\text{O}_2$  fragment is side-on bonded to the iron center. The predicted bond length of the  $(\eta^2\text{-O}_2)\text{FeO}$  complex lies on the boundary between typical superoxo anion and peroxo dianion. Hence, it is more reasonable to consider the  $(\eta^2\text{-O}_2)\text{FeO}$  complex as an intermediate between superoxide and peroxide. The complex isomerizes to the more stable iron trioxide molecule upon visible light excitation. The trioxide molecule was predicted to have a  ${}^1\text{A}_1'$  ground state with  $\text{D}_{3h}$  symmetry, in which iron possesses the +VI oxidation state.<sup>270,287,291,295,296</sup> It should be noted that the bond length and vibrational frequencies of  $\text{FeO}_3$  are about the same as those of  $\text{CrO}_3$ .<sup>202</sup>

As for the  $\text{FeO}_4$  species, an anion photoelectron spectroscopic study suggests that the observed  $\text{FeO}_4$  species is due to  $(\eta^2\text{-O}_2)\text{FeO}_2$ .<sup>268</sup> Our recent matrix isolation infrared spectroscopic study on the reaction of Fe and  $\text{O}_2$  provides evidence for the existence of two structural isomers of  $\text{FeO}_4$ , namely, the end-on bonded dioxygen–iron dioxide complex and the side-on bonded dioxygen–iron dioxide complex (Figure 9A,B).<sup>288</sup> These two  $\text{FeO}_4$  isomers are interconvertible; that is, the side-on bonded complex converts to the end-on bonded isomer under near-infrared light ( $\lambda > 850$  nm) excitation and vice versa with red light irradiation ( $\lambda > 600$  nm), as shown in Figure 10. The end-on bonded isomer is characterized to be a superoxide complex with a planar  ${}^3\text{A}''$  ground state, while the side-on bonded structure is a peroxide complex having a singlet ground state with a nonplanar  $\text{C}_{2v}$  symmetry. Although most pure DFT calculations predict that the tetroxide structure ( $T_d$  symmetry) without O–O bonding is more stable than the side-on bonded  $(\eta^2\text{-O}_2)\text{FeO}_2$  structure,<sup>278,297,298</sup> ab initio and hybrid DFT calculations indicate that the tetroxide structure is less stable than the side-on structure.<sup>299</sup>

There is no experimental report on the  $\text{FeO}_5$  and  $\text{FeO}_6$  species. A bisuperoxo iron monoxide complex,  $(\text{O}_2)_2\text{FeO}$ , is predicted to have a singlet ground state with  $\text{C}_2$  symmetry.<sup>297</sup> In a recent first-principles molecular dynamics based theoretical study, both the  $\text{FeO}_5$  and  $\text{FeO}_6$  species were proposed to be dioxygen adducts of iron trioxide and tetroxide.<sup>277</sup>

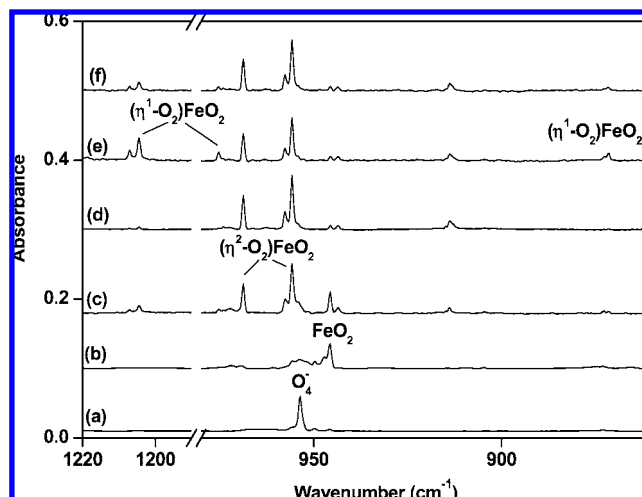


**Figure 10.** Infrared spectra in the 1220–1190 and 980–860  $\text{cm}^{-1}$  regions from co-deposition of laser-evaporated Fe atoms with 1.0%  $\text{O}_2$  in argon: (a) 1 h of sample deposition at 6 K; (b) after 15 min of broadband irradiation ( $250 < \lambda < 580$  nm); (c) after annealing to 25 K; (d) after annealing to 35 K; (e) after 15 min of  $\lambda > 850$  nm irradiation; (f) after 15 min of  $\lambda > 600$  nm irradiation. Spectra c, e, and f are taken with six scans. Reproduced from ref 288. Copyright 2007 American Chemical Society.

Compared with the rich studies on the  $\text{FeO}_x$  system, the Ru and Os analogs have received much less attention, except for the well-known tetroxides.<sup>300–312</sup> The RuO molecule has been studied spectroscopically in the gas phase and in solid matrices.<sup>261,313–315</sup> The ground state was determined to be a  ${}^5\Delta$  state.<sup>70–72,261,280</sup> No spectroscopic data is available for the osmium monoxide. DFT calculations predict that a  ${}^5\Sigma^+$  state and a  ${}^3\Phi$  state are very close in energy.<sup>73,261</sup> Both the ruthenium and osmium dioxide and trioxide molecules have been observed in solid matrices.<sup>261,313</sup> The RuO<sub>2</sub> molecule was predicted to have a  ${}^1\text{A}_1$  ground state with a bond angle close to  $150^\circ$ .<sup>78,261</sup> From the isotopic frequencies for the  $\nu_3$  mode in solid neon, the upper and low limits of the RuO<sub>2</sub> bond angle were estimated to be  $169^\circ$  and  $151^\circ$ .<sup>261</sup> A  ${}^3\text{B}_1$  state was predicted to be the ground state for OsO<sub>2</sub>. The upper limit of the bond angle was estimated to be  $144^\circ$  in neon and  $140^\circ$  in argon using the most abundant <sup>192</sup>Os isotope; hence, the true angle should be around  $135^\circ$ .<sup>261</sup> The RuO<sub>3</sub> and OsO<sub>3</sub> molecules were characterized to exhibit a trioxide structure with  $\text{D}_{3h}$  symmetry.<sup>78,261</sup>

Two structural isomers have been observed for RuO<sub>4</sub> and OsO<sub>4</sub>. It was found that the metal dioxide molecules reacted with dioxygen in solid matrices to form the dioxygen–dioxide complexes, which were characterized to have a singlet ground state with  $\text{C}_{2v}$  symmetry (Figure 9 A).<sup>261</sup> The complexes rearrange to the more stable tetroxide isomers upon visible light excitation.<sup>261</sup> The RuO<sub>4</sub> and OsO<sub>4</sub> molecules, which are the only two stable transition metal tetroxides in bulk form with the metal centers in the highest +8 oxidation state, are well-known tetrahedral molecules (Figure 9E).<sup>316</sup>

### 3.7. Co Group

Most experimental and theoretical studies suggest that cobalt monoxide has a  ${}^4\Delta$  ground state,<sup>24,27,28,61–65,67,69,239,317–322</sup> while a  ${}^4\Sigma^-$  state is predicted to be lowest in energy in a few cases.<sup>66,68,274,323,324</sup> An early ESR study on the reaction of cobalt atom toward dioxygen showed that the cobalt dioxide molecule is linear with a  ${}^2\Sigma^+$  ground state.<sup>325</sup> No other chemically bound forms of CoO<sub>2</sub> than the linear dioxide



structure are stabilized in solid argon. All three forms of  $\text{CoO}_2$  (linear dioxide and side-on bonded and end-on bonded complexes) were claimed to have been observed in a matrix infrared spectroscopic study on the reaction of laser-ablated cobalt atom with dioxygen.<sup>320</sup> More recently, the reactivity of atomic cobalt toward dioxygen in solid noble gas matrices has been reinvestigated using infrared spectroscopy. The results showed that only the dioxide form is stabilized in the matrix and that the IR absorptions previously assigned to the end-on and side-on bonded complexes are due to other larger species.<sup>326</sup> The IR data of cobalt dioxide also support the linear geometry in solid matrices. Similar to the isoelectronic  $\text{FeO}_2^-$  anion,<sup>57</sup> theoretical calculations on cobalt dioxide require sophisticated treatment. Calculations using DFT-based methods such as BPW91 and BP86 predict a bent structure with a  ${}^2\text{A}_1$  ground state;<sup>77,320</sup> B1LYP calculations give a near-linear  ${}^6\text{A}_1$  ground state;<sup>76,239,322</sup> ab initio CASSCF calculations predict a linear structure with a  ${}^2\Delta_g$  state, which is  $1487\text{ cm}^{-1}$  below the  ${}^2\Sigma_g^+$  state.<sup>320</sup> Recent CCSD(T) calculations predict a linear ground-state structure with the  ${}^2\Sigma_g^+$  state lying lower than the  ${}^2\Delta_g$  state, which are in good agreement with the experimental results.<sup>326</sup> The trioxide  $\text{CoO}_3$  molecule is found to be thermodynamically unstable with respect to  $\text{CoO} + \text{O}_2$  dissociation, but the monoxide–dioxygen complex structure,  $(\text{O}_2)\text{CoO}$ , is calculated to be stable with respect to dissociation.<sup>322</sup> It is predicted to have a  ${}^6\text{A}_1$  ground state with  $\text{C}_{2v}$  symmetry. Two absorptions at  $1090.0$  and  $783.0\text{ cm}^{-1}$  are tentatively assigned to the  $(\text{O}_2)\text{CoO}$  complex.<sup>320</sup>

A recent investigation indicated that  $\text{CoO}_4$  is formed following molecular diffusion by complexation of ground-state  $\text{CoO}_2$  by dioxygen in solid matrices.<sup>327</sup> The  $\text{CoO}_4$  complex is first formed in a metal-stable excited state and then spontaneously relaxes to the ground state after remaining in the dark. The ground state of  $\text{CoO}_4$  was determined to be a  ${}^2\text{A}_2$  state with nonplanar  $\text{C}_{2v}$  symmetry (Figure 9 A). The observed excited-state  $\text{CoO}_4$  was characterized to have nonplanar  $\text{C}_s$  symmetry with an end-on coordinated dioxygen ligand (Figure 9C). DFT calculations suggested that the observed metal-stable state correlates to a  ${}^4\text{A}'$  first excited state lying  $0.37\text{ eV}$  above the ground state of  $\text{CoO}_4$ . The excited-state lifetime is estimated to be around  $23 \pm 2$  min in argon and  $15 \pm 2$  min in neon, indicative of a slow, spin-forbidden process.<sup>327</sup> Theoretical calculations at the B1LYP level of theory reveal a cobalt bisdioxygen complex structure with a  ${}^6\text{B}_2$  ground state and nonplanar  $\text{D}_{2d}$  symmetry to be the most stable structure of  $\text{CoO}_4$ .<sup>322</sup> No such species has been observed experimentally.<sup>327</sup>

Both spectroscopic and theoretical studies suggested that the rhodium monoxide molecule has a  ${}^4\Sigma^-$  ground state.<sup>70,71,328–334</sup> Experimental information on the  $\text{RhO}_x$  ( $x \geq 2$ ) species is mainly from matrix-isolation studies.<sup>334–336</sup> Two structural isomers with  $\text{RhO}_2$  stoichiometry have been identified experimentally. Matrix infrared and ESR studies indicated that the inserted rhodium dioxide molecule formed via the reaction of rhodium atom and dioxygen is linear or near linear with a doublet ground state.<sup>325,334</sup> Recent studies in our laboratory indicated that the side-on bonded  $\text{Rh}(\text{O}_2)$  complex is the precursor for the formation of inserted dioxide molecule. The  $\text{Rh}(\text{O}_2)$  complex was characterized to have a  ${}^2\text{A}_2$  ground state with  $\text{C}_{2v}$  symmetry.<sup>336</sup>

Three structural isomers have been experimentally reported for  $\text{RhO}_4$ . A rhodium dioxide–dioxygen complex,  $(\eta^2\text{-O}_2)\text{RhO}_2$ , is formed via the reaction of rhodium dioxide with



Figure 11. Optimized structures for  $\text{RhO}_6$ ,  $\text{CuO}_5$ , and  $\text{CuO}_6$ .

dioxygen, which is characterized by a side-on bonded peroxide complex with  $\text{C}_{2v}$  symmetry (Figure 9A). Upon dioxygen coordination, the  $\text{ORhO}$  fragment is bent with an estimated bond angle of  $110^\circ$ .<sup>334</sup> Besides the side-on bonded  $\text{RhO}_4$  complex, the end-on bonded  $(\eta^1\text{-O}_2)\text{RhO}_2$  complex has also been observed in our recent experiments (Figure 9C).<sup>337</sup> Both complexes are predicted to have a doublet ground state. Similar to the  $\text{FeO}_4$  system, the side-on and end-on bonded isomers are found to be interconvertible. The end-on bonded complex converts to the side-on bonded isomer under infrared light irradiation and back with near-infrared light ( $\lambda > 850\text{ nm}$ ).<sup>337</sup> The third isomer, a bisdioxygen complex,  $\text{Rh}(\eta^2\text{-O}_2)_2$ , is also produced from the reaction of rhodium and dioxygen in solid argon. This complex structure is predicted to have a  ${}^4\text{B}_{1u}$  ground state with planar  $\text{D}_{2h}$  symmetry (Figure 9 D).<sup>336</sup> Based on the observed O–O stretching frequency,  $\text{Rh}(\eta^2\text{-O}_2)_2$  belongs to a disuperoxide complex. It is found that the  $\text{Rh}(\eta^2\text{-O}_2)_2$  complex is able to weakly coordinate a third dioxygen in forming the oxygen-rich  $\text{Rh}(\eta^2\text{-O}_2)_2(\eta^1\text{-O}_2)$  complex.<sup>336</sup> Geometric optimizations at the DFT/B3LYP level give a stable doublet  $\text{Rh}(\eta^2\text{-O}_2)_2(\eta^1\text{-O}_2)$  structure with  $\text{C}_s$  symmetry (Figure 11), in which two  $\text{O}_2$  subunits are side-on bonded and are equivalent; the third  $\text{O}_2$  subunit is end-on bonded with the  $\text{RhOO}$  plane perpendicular to the  $(\text{O}_2)_2$  plane. A stable quartet with very similar geometry is predicted to be only  $0.8\text{ kcal/mol}$  less stable than the doublet. Xenon-doped experiments in our laboratory indicate that the  $\text{Rh}(\text{O}_2)$ ,  $\text{Rh}(\eta^2\text{-O}_2)_2$ , and  $\text{Rh}(\eta^2\text{-O}_2)_2(\eta^1\text{-O}_2)$  complexes are coordinated by one or two argon atoms in solid argon matrix.<sup>336</sup>

Investigations on the  $\text{IrO}_x$  system in the literature are quite limited. Gas-phase spectroscopic investigation failed to determine the ground state of  $\text{IrO}$ .<sup>338</sup> The  $\text{IrO}$  product was not observed in a gas-phase kinetic study on the reaction between Ir and  $\text{O}_2$ .<sup>339</sup> The vibrational fundamental of  $\text{IrO}$  is observed at  $822.1\text{ cm}^{-1}$  in solid argon,<sup>340</sup> consistent with the frequency of the  ${}^4\Sigma^-$  ground state from DFT calculations.<sup>73,341</sup> Matrix infrared and ESR studies imply that the iridium dioxide molecule is linear, the same as the cobalt and rhodium dioxide molecules.<sup>325</sup> The linear structure with a  ${}^2\Sigma_g^+$  ground state can be reproduced by DFT/BPW91 calculations with larger 6-311+G(3d) basis set on oxygen.<sup>341</sup> It was found that the ground-state iridium atom reacted with  $\text{O}_2$  to form the inserted  $\text{IrO}_2$  spontaneously on annealing; hence, the iridium dioxygen complex is not expected to be formed.<sup>340</sup> The IR absorptions previously assigned to the iridium dioxygen complex<sup>341</sup> are due to larger iridium–oxygen species.<sup>340</sup>

Similar to rhodium, both the side-on and end-on bonded dioxygen–iridium dioxide complexes have been observed experimentally.<sup>340</sup> These  $\text{IrO}_4$  isomers are also interconvertible. Note that the end-on bonded  $(\eta^1\text{-O}_2)\text{MO}_2$  complexes with  $\text{M} = \text{Fe}, \text{Rh},$  or  $\text{Ir}$  are characterized to have similar structure to that of the excited-state  $\text{CoO}_4$  complex. However, these complexes are attributed to be a stable structural isomer

of  $\text{MO}_4$  instead of excited-state species. The end-on bonded complexes in the iron, rhodium, and iridium systems are found to be stable species in the dark; they rearrange to the more stable side-on bonded isomer only under photon excitation. Besides the two dioxygen metal dioxide complex structures, a third isomer with  $\text{IrO}_4$  stoichiometry, namely, the iridium tetroxide molecule, is formed when the side-on and end-on bonded  $\text{IrO}_4$  complexes are subjected to visible light ( $\lambda > 500$  nm) irradiation. The iridium tetroxide molecule is characterized to have a doublet ground state with  $D_{2d}$  symmetry (Figure 9F), in which the iridium center is in an unusual +8 oxidation state.<sup>340</sup> Note that such a high oxidation state has only been observed in the Ru and Os cases.<sup>261</sup> So far, the highest experimentally well-established stable oxidation state of iridium is +6.<sup>316</sup>

### 3.8. Ni Group

It is now well-established that nickel monoxide possesses a  $^3\Sigma^-$  ground state.<sup>24,27–29,61–69,159,196,239,274,342–353</sup> For PdO, a  $^3\Sigma^-$  state and a  $^3\Pi$  state were found to be almost isoenergetic. The relative stability of these two states strongly depends on the theoretical levels employed.<sup>70–72,159,196,350,354–359</sup> Anion photoelectron spectroscopic studies suggested the  $^3\Sigma^-$  state to be the ground state.<sup>342,360</sup> Both experimental and theoretical studies confirm that the  $^3\Sigma^-$  state is the ground state for  $\text{PtO}$ .<sup>73,350,356,361–370</sup>

Both the side-on bonded superoxide and inserted dioxide structures of  $\text{NiO}_2$  have been characterized experimentally. The superoxide complex can be formed from the reaction of ground-state metal atom with dioxygen in solid matrices.<sup>347,355,357,371–374</sup> Theoretical calculations on  $\text{Ni}(\eta^2\text{-O}_2)$  provide contradictory results. Calculations at the CCSD(T) and CASSCF levels of theory predict a singlet ground state,<sup>375–378</sup> whereas DFT calculations using several functionals predict that the triplet state is more stable than the singlet state.<sup>76,77,239,347,375,376,379</sup> More recent DFT calculations at the PW91PW91/6-311G(3df) level with the addition of scalar relativistic effects indicate that the singlet state is slightly more stable than the triplet state by 0.1 kcal/mol.<sup>371</sup> The vibrational frequencies calculated for the singlet state are in much better agreement with those measured in solid argon and neon. The nickel dioxide molecule is determined to be linear with a singlet  $^1\Sigma_g^+$  ground state.<sup>77,347,371,378</sup> The palladium dioxygen complex is the only  $\text{PdO}_2$  isomer observed in solid matrix,<sup>355,357,374,380</sup> which is predicted to have a singlet ground state with  $C_{2v}$  symmetry.<sup>355,357,380</sup> The inserted palladium dioxide molecule has not been observed in solid matrices. However, it has been suggested to be the photodetachment product of the  $\text{PdO}_2^-$  anion from gas-phase photoelectron spectroscopic study.<sup>342</sup> The symmetric OPdO vibration was determined to be  $680 \pm 30$   $\text{cm}^{-1}$ . The ground state of palladium dioxide remains unclear. Both the linear  $^3\Pi_g$  or  $^3\Sigma_g^-$  states and the bent  $^5A_1$  or  $^3A_2$  states have been suggested as the ground state depending on the theoretical levels employed.<sup>78,355,357,381</sup> The PES results support a  $^3\Sigma_g^+$  state for the inserted  $\text{PdO}_2$  molecule.<sup>342</sup> The  $\text{PtO}$  molecule is predicted to have the same spin state and geometry as  $\text{ONiO}$ .<sup>355,357,368</sup> The singlet  $\text{Pt}(\eta^2\text{-O}_2)$  complex with  $C_{2v}$  symmetry has been observed in a solid matrix.<sup>355,357,372</sup> Although the end-on bonded  $\text{PtOO}$  isomer is predicted to have a triplet ground state and is more stable than the side-on bonded complex, it is not formed in solid matrices.<sup>357</sup>

Both the  $\text{NiO}_3$  and  $\text{PtO}_3$  species, which are characterized to be metal monoxide–dioxygen complexes, have been

identified in solid matrices.<sup>347,357</sup> It has been found that the  $\text{O}_2$  fragment can be bound to the metal centers in either the side-on or end-on fashion. The O–O vibrational frequency for the end-on bonded complex is about  $300$   $\text{cm}^{-1}$  higher than that of the side-on bonded isomer. DFT calculations indicate that the  $(\eta^1\text{-O}_2)\text{NiO}$  complex has a singlet ground state with planar  $C_s$  symmetry, while the side-on bonded  $(\eta^2\text{-O}_2)\text{NiO}$  complex has a triplet state with  $C_{2v}$  symmetry.<sup>347</sup> The side-on bonded  $(\eta^2\text{-O}_2)\text{PtO}$  complex has similar geometry and triplet ground state to those of the nickel analogs, while a  $^5A'$  state is predicted to be the ground state for the end-on bonded  $(\eta^1\text{-O}_2)\text{PtO}$  complex.<sup>357</sup>

The metal disuperoxide complexes  $\text{M}(\text{O}_2)_2$  with  $\text{M} = \text{Ni}$ , Pd, or Pt have also been observed from the reactions between metal atoms and dioxygen in solid matrices.<sup>347,355,357,373,374,380</sup> All three disuperoxide complexes exhibit strong O–O stretching vibrations around  $1080 \pm 30$   $\text{cm}^{-1}$ . DFT calculations indicate that these complexes have planar  $D_{2h}$  geometry (Figure 9D). The  $\text{Ni}(\text{O}_2)_2$  complex was characterized to have a triplet ground state,<sup>347</sup> while the  $\text{Pt}(\text{O}_2)_2$  complex has a singlet  $^1A_g$  ground state.<sup>355,357</sup> Our recent DFT/BPW91 calculations yielded a triplet ground state for the  $\text{Pd}(\text{O}_2)_2$  complex, but single-point CCSD(T) calculations at the DFT-optimized geometries indicated that the singlet state is slightly more stable than the triplet state.<sup>380</sup> Besides the disuperoxide complex, a nickel dioxide–dioxygen complex,  $(\eta^2\text{-O}_2)\text{NiO}_2$ , which is predicted to have a singlet ground state with almost nonplanar  $C_{2v}$  symmetry, is also produced via the association reaction of nickel dioxide and  $\text{O}_2$  in solid argon.<sup>347</sup>

### 3.9. Cu Group

The  $\text{CuO}$  molecule has a  $^2\Pi$  ground state as demonstrated by numerous experimental and theoretical studies.<sup>24,26–28,61–69,76,382–402</sup> Due to the antibonding nature of the singly occupied  $4\pi$  orbital, the Cu–O bond is significantly weakened relative to that of  $\text{NiO}$ , which results in a long CuO bond length as well as a quite low CuO vibrational fundamental.<sup>24,383,391</sup>

As for the  $\text{CuO}_2$  species, two structural isomers have been observed both in the gas phase and in solid matrices.<sup>382,383,403–408</sup> In solid matrices, the ground-state copper atoms tend to react with  $\text{O}_2$  to form the  $\text{Cu}(\text{O}_2)$  complex, while excited copper atoms are required for the formation of the inserted copper dioxide molecule.<sup>383</sup> An earlier matrix-isolation ESR experiment suggested a bent geometry for the  $\text{Cu}(\text{O}_2)$  complex with an end-on bonded  $\text{O}_2$  ligand,<sup>405,406</sup> but a late theoretical interpretation indicated that the magnetic inequivalency derived from the ESR spectra may not be large enough to distinguish the coordination fashion of the  $\text{O}_2$  molecule.<sup>409</sup> Although the doublet end-on bonded structure is favored at various DFT calculations, high-level ab initio calculations predict that the side-on bonded isomer is slightly more stable.<sup>76,77,377,383,410–414</sup> The dipole moment of the end-on bonded complex is larger than that of the side-on bonded isomer. Therefore, the end-on bonded structure is expected to be stabilized via interaction with solid argon, as also supported by high-level ab initio calculations.<sup>414</sup> The inserted  $\text{OCuO}$  molecule was determined to be linear based on the experimental observations.<sup>382,383,403,404</sup> Most theoretical calculations suggested a doublet ground state for this linear molecule.<sup>415–417</sup> The  $\nu_3$  mode is about  $130$   $\text{cm}^{-1}$  lower than that of  $\text{NiO}_2$ , suggesting a weak bonding interaction between the copper center and two terminal oxygen atoms. Note that the inserted dioxide structure is the most stable  $\text{MO}_2$

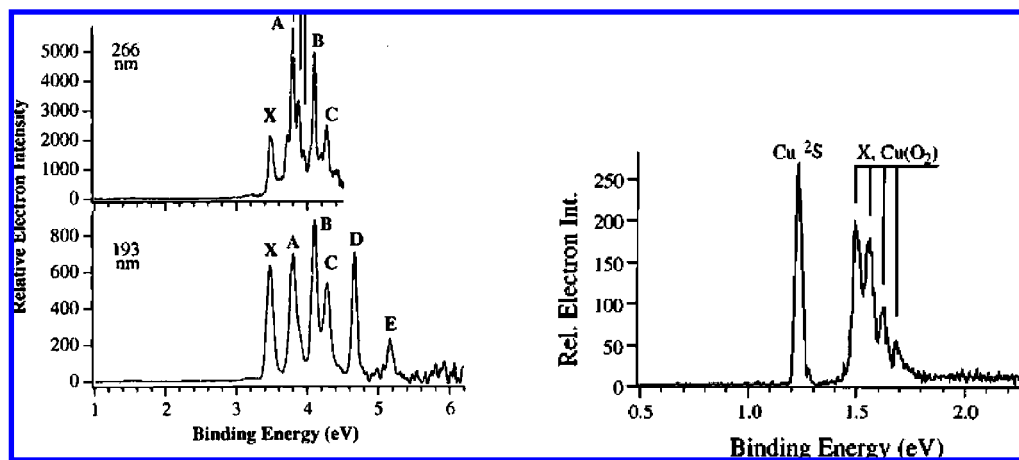


**Figure 12.** Photoelectron spectra of  $\text{OCuO}^-$  at 266 and 193 nm (left) and  $\text{Cu}(\text{O}_2)^-$  at 532 nm (right). Reproduced from refs 382 (Copyright 1997 American Chemical Society) and 403 (Copyright 1995 American Institute of Physics).

configuration for all first row transition metals except copper, which prefers a dioxygen complex structure.<sup>77,78</sup> The PES spectra of  $\text{CuO}_2^-$  taken at 532, 266, and 193 nm shown in Figure 12 also demonstrate the coexist of two isomers in the gas phase.<sup>26</sup> One isomer, constituting a very small portion of the  $\text{CuO}_2^-$  anion beam and dissociating at 532 nm, has a low electron affinity of about 1.5 eV. The second isomer, with dominating abundance, has a very high electron affinity of about 3.46 eV. These two isomers correspond to the copper dioxygen complex and the inserted copper dioxide molecule observed in matrix studies.

Two structural isomers with  $\text{CuO}_3$  stoichiometry have been experimentally characterized.<sup>382,383,391</sup> An anion photoelectron spectroscopic study suggested that the observed  $\text{CuO}_3$  species in the gas phase is due to a  $(\text{O}_2)\text{CuO}$  complex.<sup>382</sup> A copper ozonide complex, which is the only definitive example of binary ozonide complex of the first row transition metals, was assigned in solid matrices.<sup>383,391</sup> Due to the extraordinary oxidizing capability of ozone, binary metal ozonide complexes known so far are limited to the alkali and alkaline earth metal ozonide complexes, which have been prepared and characterized by infrared and Raman spectroscopy.<sup>418,419</sup> The stable structures of the  $\text{CuO}_3$  species have been the subject of several theoretical studies.<sup>383,420–423</sup> The planar  $(\text{O}_2)\text{CuO}$  complex structure with a side-on bonded  $\text{O}_2$  is predicted to be more stable than the copper ozonide complex structure. The  $\text{Cu}(\eta^2\text{-O}_3)$  complex is calculated to possess a doublet ground state with planar  $C_{2v}$  symmetry, which can be described as  $\text{Cu}^+(\text{O}_3)^-$ . The successful isolation of the  $\text{Cu}(\eta^2\text{-O}_3)$  complex may be attributed to the relative stability of the +1 oxidation state for copper and the higher energy barrier that prevents its further isomerization.

Photoelectron spectroscopic results indicate that two  $\text{CuO}_4$  isomers coexist in the gas phase, that is, a bisdioxygen  $\text{Cu}(\eta^2\text{-O}_2)_2$  complex and a copper dioxide–dioxygen complex.<sup>382</sup> The  $\text{Cu}(\eta^2\text{-O}_2)_2$  complex was also observed in several matrix-isolation studies. Early matrix infrared studies assigned a  $1110\text{ cm}^{-1}$  absorption in solid argon to the  $\text{Cu}(\eta^2\text{-O}_2)_2$  complex with two equivalent  $\text{O}_2$  fragments.<sup>391,424</sup> However this absorption was proposed to originate from the  $(\text{CuOO})(\text{O}_2)_2$  complex in a late matrix-isolation study.<sup>383</sup> According to our recent experimental results on the  $\text{CuO}_x$  system, the spectroscopic character of the absorption at  $1110\text{ cm}^{-1}$  is similar to that in earlier matrix-isolation experiments, and we assert that the  $1110\text{ cm}^{-1}$  band is due to the  $\text{Cu}(\eta^2\text{-O}_2)_2$  complex.<sup>425</sup> Theoretical calculations suggest that the

most stable configuration for the  $\text{Cu}(\eta^2\text{-O}_2)_2$  complex possesses planar  $D_{2h}$  symmetry with a  $^4\text{B}_{2u}$  ground state.<sup>425</sup> The absorption previously attributed to  $(\text{CuOO})(\text{O}_2)_2$  was reassigned to a  $\text{CuO}_5$  complex.<sup>425</sup>

The  $\text{CuO}_5$  complex has been produced via the reaction of copper atoms with  $\text{O}_2$  or  $\text{O}_3$  in solid argon.<sup>425</sup> The complex is characterized to have an  $(\eta^2\text{-O}_2)\text{Cu}(\eta^2\text{-O}_3)$  structure, in which the copper center is coordinated by a  $\text{O}_2$  ligand and an  $\text{O}_3$  ligand. The complex is predicted to have a  $^4\text{A}_1$  ground state with planar  $C_{2v}$  symmetry (Figure 11),<sup>425</sup> in agreement with that calculated using the spin-polarized GGA method with plane-wave basis sets.<sup>426</sup> However, an anion photoelectron spectroscopic study suggested that the observed  $\text{CuO}_5$  species in the gas phase is due to an  $\text{O}_2$  solvated  $(\text{O}_2)\text{CuO}$  complex.<sup>382</sup>

In the case of  $\text{CuO}_6$ , an anion photoelectron spectroscopic study suggested that two isomers: a copper dioxide dioxygen complex,  $\text{OCuO}(\text{O}_2)_2$  and a copper dioxide complex,  $\text{Cu}(\text{O}_2)_3$ , coexist in the gas phase.<sup>382</sup> However, both structures are theoretically predicted not to be the global minima on the potential energy surfaces of  $\text{CuO}_6$ .<sup>421,427</sup> A bisozonide structure is predicted as the ground state for the  $\text{CuO}_6$  complex using the spin-polarized GGA method with plane-wave basis sets, but isomers containing  $\text{Cu}(\text{O}_2)$  building blocks are very close in energy to the bisozonide structure. Among the isomers based on the  $\text{Cu}(\text{O}_2)$  unit, the structure containing one side-on and two end-on bonded  $\text{O}_2$  units with  $C_{2v}$  symmetry lies lowest in energy.<sup>427</sup> Density functional calculations using the PBE functional indicate that several competitive structures exist with structures containing ozonide units being higher in energy than those with  $\text{O}_2$  units. The structure with one side-on and two end-on bonded  $\text{O}_2$  units ( $C_{2v}$ ) is predicted to be lowest in energy.<sup>421</sup> Recently, an oxygen-rich  $\text{CuO}_6$  complex bearing both side-on and end-on bonded ligands was synthesized via the reaction of Cu and  $\text{O}_2$  in solid argon.<sup>428</sup> The complex was characterized to have a  $^4\text{B}_1$  ground state with planar  $C_{2v}$  symmetry involving one side-on and two end-on bonded  $\text{O}_2$  units (Figure 11), which can be formally described as a trisuperoxide  $\text{Cu}^{3+}(\text{O}_2^-)_3$  complex with the copper center in its unusual +3 oxidation state. Compounds with copper in its +3 oxidation state are rare; only some copper peroxide complexes have been reported to exhibit Cu(III) character.<sup>429</sup>

Both the silver and gold monoxide molecules are found to have a  $^2\Pi$  ground state.<sup>71–73,196,388,400,430–446</sup> The  $\text{Ag}(\text{O}_2)$  complex is the only structure with  $\text{AgO}_2$  stoichiometry

observed in solid matrices, however, whether the O<sub>2</sub> ligand is side-on bonded or end-on bonded cannot be clearly identified.<sup>405,406,430,447,448</sup> According to the recent theoretical calculations, the end-on isomer in doublet spin state is lowest in energy for the Ag(O<sub>2</sub>) complex.<sup>355,430,449</sup> Earlier matrix infrared and ESR studies indicated that the Au(O<sub>2</sub>) complex is side-on bonded, but the end-on bonded isomer is predicted to be more stable.<sup>355,430,450–453</sup> Note that the O–O vibrational frequency of Au(O<sub>2</sub>) is sensitive to the matrix, which exhibits a large neon to argon matrix shift.<sup>355</sup> Besides the Au(O<sub>2</sub>) complex, the inserted AuO<sub>2</sub> molecule was also observed to be the reaction product of laser-ablated gold atoms and O<sub>2</sub>.<sup>355,430</sup> The gold dioxide molecule is determined to have a <sup>2</sup>Π<sub>g</sub> ground state with linear geometry.<sup>355,430,440</sup> Gold dioxide was the only AuO<sub>2</sub> isomer observed in the gas-phase photoelectron spectroscopic study.<sup>440</sup>

A silver ozonide complex, Ag(η<sup>2</sup>-O<sub>3</sub>) was reported to be formed in the reactions between silver atoms and O<sub>2</sub> or O<sub>3</sub>.<sup>355,430,431</sup> Based on the isotopic substitution experiments, an infrared absorption around 790 cm<sup>-1</sup> was assigned to the ozonide complex, in which O<sub>3</sub> is bound to the silver center in a side-on fashion. DFT calculations suggest a doublet ground state with planar C<sub>2v</sub> symmetry for this ozonide complex.<sup>355,430</sup> A similar ozonide complex is not formed for gold. Note that +1 is a stable oxidation state for silver but not for gold.

The AgO<sub>4</sub> complex is formed in solid matrices and was initially supposed to be Ag<sup>+</sup>(O<sub>2</sub>)<sub>2</sub><sup>-</sup>, which involves a five-membered puckered ring,<sup>448</sup> similar to that of the CsO<sub>4</sub> complex.<sup>454</sup> However, recent DFT/B3LYP calculations suggested that the most stable configuration for AgO<sub>4</sub> is the bisdioxygen Ag(O<sub>2</sub>)<sub>2</sub> complex with C<sub>2v</sub> symmetry having a <sup>4</sup>B<sub>1</sub> ground state. Both O<sub>2</sub> ligands are bound to the silver center in an end-on fashion.<sup>355</sup> Frequency analysis also supported reassignment of the previously observed absorptions to the bisdioxygen complex structure, which is due to a disuperoxide complex with the silver center in its +2 oxidation state. The analogous AuO<sub>4</sub> complex has not been observed experimentally. Theoretical calculations predict that the most stable structure is a bisdioxygen complex with planar C<sub>2h</sub> symmetry having a quartet ground state.<sup>452</sup>

### 3.10. Zn Group

Group 12 of the periodic table, consisting of zinc, cadmium, and mercury, is usually considered as a post-transition metal group because the outmost shell of d orbitals is filled and does not participate significantly in chemical bonding. With the recent experimental observation of HgF<sub>4</sub>, in which the 5d orbitals of mercury are strongly involved in bonding, mercury should be viewed as a genuine transition metal element.<sup>455</sup> The electronic structure of ZnO is quite similar to that of group IIA metal monoxides. The diatomic ZnO molecule has been spectroscopically studied in the gas phase as well as in solid matrices.<sup>456–464</sup> Theoretical calculations confirm that the ground state for zinc monoxide is <sup>1</sup>Σ<sup>+</sup> with a (core)9σ<sup>2</sup>4π<sup>4</sup> configuration, in which the 9σ orbital is the bonding combination of Zn 4s and O 2p<sub>σ</sub> orbitals, while the 4π orbital is largely O 2p<sub>π</sub> orbital in character.<sup>61–69,465–474</sup> Spectroscopic information on cadmium monoxide is mainly from the matrix isolation studies.<sup>463,464</sup> An infrared absorption at 719 cm<sup>-1</sup> in solid nitrogen is initially assigned to the CdO molecule,<sup>463</sup> but this absorption is suggested to be due to a dioxygen complex.<sup>464</sup> Infrared absorptions at 645.1 cm<sup>-1</sup> in argon and 654.4 cm<sup>-1</sup> in nitrogen are reassigned to the CdO fundamental.<sup>464</sup> A <sup>3</sup>Π state is found to be the most stable

spin state using most density functionals,<sup>71</sup> but a <sup>1</sup>Σ<sup>+</sup> state is predicted to be the ground state using high-level ab initio methods.<sup>466,468</sup>

The zinc and cadmium dioxide molecules have been produced in solid argon and nitrogen from the reactions of laser-ablated metal atoms with O<sub>2</sub>.<sup>464</sup> Note that neither dioxide was formed in previous thermal evaporation experiments, suggesting that the laser-ablated excited-state metal atoms are responsible for the formation of these inserted products.<sup>463</sup> Both of the two dioxide molecules were determined to have a <sup>3</sup>Σ<sub>g</sub><sup>-</sup> ground state with linear geometry.<sup>76,77,464</sup> Resolved natural zinc isotopic splittings assist in the characterization of the ZnO<sub>2</sub> molecule. The ZnO<sub>2</sub> molecule is calculated to be thermodynamically unstable; its decay with the evolution of molecular oxygen is exothermic by about 0.6 eV. Hence, its observation in solid argon suggests a barrier to decomposition. Besides the inserted dioxide molecule, a Cd(η<sup>1</sup>-O<sub>2</sub>) complex with an end-on bonded O<sub>2</sub> ligand has also been tentatively identified in solid matrices, but DFT calculations predict that the side-on bonded isomer with a <sup>3</sup>B<sub>2</sub> ground state is more stable than the end-on bonded complex.<sup>464</sup>

No gas-phase spectroscopic studies are available on mercury oxide species. A 676 cm<sup>-1</sup> absorption has tentatively been assigned to the vibrational fundamental of HgO in an early matrix-isolation study.<sup>475</sup> However, theoretical calculations at different levels suggest that HgO has a <sup>3</sup>Π ground state with a vibrational fundamental around 300 cm<sup>-1</sup>.<sup>73,466,468,476–478</sup> No spectroscopic identification of mercury dioxide has been reported, but a mercury superoxide complex was suggested to have been observed in a solid matrix.<sup>475</sup>

### 3.11. Lanthanide Group

Lanthanide metals can be classified into two groups: typical lanthanides and atypical lanthanides. Typical lanthanides exhibit a formal oxidation state of +3 and possess characteristic properties associated with rare earth metals. Due to the presence of the half-filled and filled 4f orbitals, the atypical lanthanides, Eu and Yb, exhibit a formal oxidation state of +2 and have physical properties more nearly like the alkaline earth metals. Most of the lanthanide metal monoxide molecules have been spectroscopically studied.<sup>479–502</sup> The vibrational fundamentals of typical lanthanide metal monoxides increase slightly along the series from Ce to Lu due to the effect of lanthanide contraction, and all are located in the narrow range of 800–830 cm<sup>-1</sup> in solid argon (Table 1).<sup>503–505</sup> The vibrational fundamentals of atypical lanthanide metal monoxides are observed around 660 cm<sup>-1</sup>,<sup>504,505</sup> identical to the predictions given by ligand field theory.<sup>506</sup> From the theoretical point of view, most studies have focused on CeO, EuO, GdO, YbO and LuO,<sup>96–99,507–515</sup> while the other lanthanide monoxide molecules have been less investigated.<sup>74,75,516–519</sup> Since the bonding ability of d orbitals is larger than that of s orbitals, the 5d orbitals of lanthanide atoms are the major component in the metal–oxygen bonding for the diatomic LnO molecules; while the 4f electrons are less active due to the localized character of the 4f orbitals. Lanthanide atoms with f<sup>n-1</sup>d<sup>1</sup> configurations can form relatively strong metal–oxygen bonds, and those with f<sup>n</sup> configuration can also afford strong Ln–O bonds via f to d promotions if the energy separation is not too large. Due to the extra stability of half-filled f<sup>7</sup> and filled f<sup>14</sup> configurations for atypical lanthanide metals, no d electrons are available for participating the Ln–O

bonding, which results in the lower vibrational frequencies for EuO and YbO.<sup>504,505</sup> Note that these two diatomic molecules have the lowest binding energies among the lanthanide metal monoxides.<sup>520</sup> Following this trend, the experimentally unknown PmO molecule should absorb around 810 cm<sup>-1</sup>, which is in accord with the calculated value of the <sup>6</sup>Σ<sup>+</sup> ground-state PmO.<sup>74</sup>

Spectroscopic information on the inserted metal dioxide molecules are mainly from matrix-isolation infrared spectroscopic studies. Earlier thermal evaporation investigations have identified the dioxide molecules of Ce, Pr, and Tb,<sup>503,521</sup> while dioxide molecules of the remaining lanthanides except for Pm, Er, and Lu have been produced from the reactions of laser-ablated lanthanide atoms and O<sub>2</sub>.<sup>504,505</sup> The dioxide molecules for Pr, Nd, Sm, Dy, and Yb were suggested to have linear geometries due to their similar oxygen isotopic ratios (about 1.049) for the antisymmetric stretching vibration ( $\nu_3$ ). It can be found from Table 3 that the  $\nu_3$  vibrational frequencies decrease from Ce to Ho except for Gd and Tb. Note that the infrared fundamentals of the bent CeO<sub>2</sub> and TbO<sub>2</sub> molecules are quite close to each other, suggesting a similar bonding interaction between the metal center and the oxygen atoms. Both Ce and Tb are known to form compounds with the metal centers in the +4 oxidation state.<sup>522</sup> Hence these two lanthanide metals can afford two Ln=O double bonds in forming the strongly bound OCeO and OTbO molecules.

### 3.12. Actinide Group

Due to experimental challenges faced in handling actinide metals, most spectroscopic studies are focused on thorium and uranium oxide species.<sup>523–531</sup> Spectroscopic and theoretical studies of the oxides of thorium and uranium have been reviewed recently.<sup>532</sup> The results regarding the structures and vibrational fundamentals of ground spin state thorium and uranium oxides are briefly outlined here. Thorium monoxide absorbs around 876 cm<sup>-1</sup> in solid argon.<sup>521,533</sup> It was calculated to have a closed-shell singlet ground state.<sup>534–537</sup> The thorium dioxide molecule was characterized to be bent based on the matrix infrared spectra and theoretical calculations.<sup>521,533,538–543</sup>

Uranium monoxide was observed around 820 cm<sup>-1</sup> in solid argon and 890 cm<sup>-1</sup> in solid neon.<sup>544–547</sup> Both ab initio and DFT calculations predicted a quintet ground state for uranium monoxide,<sup>517,548,549</sup> whereas a triplet state was proposed to be the ground state based on group theory and atomic and molecular reactive statics.<sup>550</sup> The inserted uranium dioxide molecule was characterized to be a linear molecule with the antisymmetric stretching mode ( $\nu_3$ ) observed at 776 cm<sup>-1</sup> in solid argon<sup>544–547</sup> and 915 cm<sup>-1</sup> in solid neon.<sup>549</sup> The large shift in frequency from argon to neon (139 cm<sup>-1</sup>) is not due to typical polarizability-based matrix effects, and a strong interaction between UO<sub>2</sub> and the noble gas matrix should be considered. Both DFT and high-level ab initio calculations confirm that the linear UO<sub>2</sub> molecule has a <sup>3</sup>Φ<sub>u</sub> ground state arising from a 5f<sup>1</sup>7s<sup>1</sup> configuration with a <sup>3</sup>H<sub>g</sub> state derived from the 5f<sup>2</sup> configuration slightly higher in energy.<sup>549,551–556</sup> Scalar relativistic DFT and CCSD(T) calculations suggest that the uranium dioxide molecule in the <sup>3</sup>H<sub>g</sub> state can be coordinated by five Ar atoms in forming the UO<sub>2</sub>(Ar)<sub>5</sub> complex.<sup>556</sup> The argon–uranium interactions are far less attractive for the <sup>3</sup>Φ<sub>u</sub> state UO<sub>2</sub>, largely because of repulsive interactions between the Ar atoms and the 7s-localized electron. A comparison of the calculated DFT vibrational frequencies to those observed in neon and argon matrices

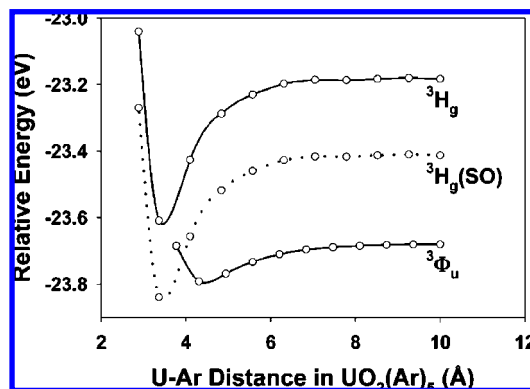


**Figure 13.** Calculated linear-transit potential energy curves for  $D_{5h}$  UO<sub>2</sub>(Ar)<sub>5</sub> for the <sup>3</sup>Φ<sub>u</sub> and <sup>3</sup>H<sub>g</sub> electronic states of UO<sub>2</sub>. The dotted line represents a lowering of the curve for the <sup>3</sup>H<sub>g</sub> state by a constant 0.23 eV to account for differential spin–orbit stabilization of the <sup>3</sup>H<sub>g</sub> state. Reproduced from ref 556. Copyright 2004 American Chemical Society.

suggests that the large frequency change is very likely due to a change in electronic state. The calculated  $\nu_3$  mode for isolated <sup>3</sup>Φ<sub>u</sub> state, 919 cm<sup>-1</sup>, is in excellent agreement with that observed in solid neon. The  $\nu_3$  mode for the <sup>3</sup>H<sub>g</sub> state is red-shifted by 95 cm<sup>-1</sup> relative to the <sup>3</sup>Φ<sub>u</sub> state, and the coordination of five argon atoms leads to an additional 19 cm<sup>-1</sup> red shift. The energy separation between the <sup>3</sup>H<sub>g</sub> and <sup>3</sup>Φ<sub>u</sub> states are lowered upon argon coordination, and the <sup>3</sup>H<sub>g</sub> state is found to be lowest in energy if spin orbital coupling is taken into consideration (Figure 13). Hence the ground state for UO<sub>2</sub> molecule seems to be changed from argon to neon, in which the slightly less stable configuration can be stabilized upon argon coordination.<sup>556</sup> Such noble-gas-induced ground-state reversal has been observed in the CUO molecule.<sup>39,557</sup> However, a recent dispersed fluorescence spectroscopic study on molecular UO<sub>2</sub> suggested that UO<sub>2</sub> exists in the <sup>3</sup>Φ<sub>u</sub> state in solid argon, the same as that in gas phase.<sup>529</sup> The electronic spectra observed in solid argon were found to be identical to the recent gas-phase calculations although it cannot be determined whether the ground state of uranium dioxide is changed upon argon coordination.<sup>558</sup>

The uranium trioxide molecule has been observed in solid matrix.<sup>544–547,549,559,560</sup> Earlier thermal-evaporated uranium reactions propose a T-shaped structure for uranium trioxide.<sup>559,560</sup> However, theoretical calculations predict that uranium trioxide has a closed-shell singlet ground state with a planar Y-shaped  $C_{2v}$  structure.<sup>549,561,562</sup>

The radioactive plutonium monoxide and dioxide molecules have also been studied in a solid matrix. An infrared absorption around 820 cm<sup>-1</sup> was assigned to PuO,<sup>563</sup> which is predicted to have a <sup>7</sup>Π ground state.<sup>564</sup> Plutonium dioxide absorbs at 794.3 and 786.8 cm<sup>-1</sup> in solid argon and krypton.<sup>563</sup> Both DFT and high-level ab initio calculations suggested that plutonium dioxide has a <sup>5</sup>Σ<sub>g</sub><sup>+</sup> ground state with a linear geometry.<sup>564,565</sup>

### 3.13. Periodic Trends on Bonding and Reactivity

Some periodic trends on the reaction mechanism can be drawn from matrix spectroscopic investigations on the reactions between transition metal atoms and dioxygen. Since only the ground-state metal atoms are trapped in solid matrices, the species observed on annealing are produced from the ground-state metal atom reactions. It is found that the ground state transition metal atoms are able to react with

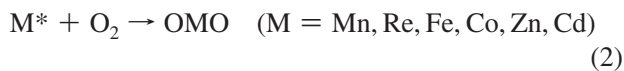
dioxygen to form the inserted dioxide molecules or the side-on or end-on bonded dioxygen complexes. The ground-state early transition metal atoms from the Sc group to the Cr group are found to be able to insert directly into the O–O bond of dioxygen to form metal dioxide molecules without activation energy (reaction 1; the ScO<sub>2</sub> molecule is not observed in solid matrices).<sup>109,132,182,183,201,202,210</sup>



The kinetics of the reactions of ground-state transition metal atoms with dioxygen have been studied in the gas phase. It has been found that most early transition metal atoms react with dioxygen via a bimolecular abstraction mechanism to form the metal monoxides.<sup>566–568</sup> A mechanism involving electron transfer from the neutral reactant potential energy surface to an ion pair product surface is proposed for these reactions. The oxidation reaction of the ground-state Ti(<sup>3</sup>F) with the O<sub>2</sub> molecule has been studied theoretically.<sup>569</sup> An inserted fast dissociation mechanism is proposed. The reaction is predicted to proceed with the initial formation of a side-on bonded Ti( $\eta^2$ -O<sub>2</sub>) complex followed by the O–O bond breaking in forming an inserted dioxide intermediate, which dissociates readily to give TiO and O. The reaction is predicted to have a very small entrance activation barrier. In solid matrices, the internal energy of the inserted intermediate can be very effectively quenched, and therefore, the inserted dioxide molecule is trapped as the primary reaction product.

Among the late transition metal atoms, only the Ru, Os, and Ir atoms are found to be able to react with dioxygen to form the inserted dioxide molecules without activation energy.<sup>261,313,340</sup> Gas-phase kinetic studies also showed that the ground-state iridium atom reacted with dioxygen to form the inserted IrO<sub>2</sub> molecule via a termolecular reaction mechanism.<sup>339</sup> The relatively larger reactivity of iridium is attributed to a surface crossing with the low-lying 5d<sup>8</sup>6s<sup>1</sup> electronic state. The larger reactivity of Ru with respect to iron is understandable because Ru has a 4d<sup>7</sup>5s<sup>1</sup> ground-state configuration.<sup>570</sup> The energy separation for the 5d<sup>7</sup>6s<sup>1</sup> and 5d<sup>6</sup>6s<sup>2</sup> states of osmium is comparable to those of early transition metals, which makes it possible to undergo a spontaneous bimolecular abstraction reaction with O<sub>2</sub> in the gas phase.<sup>571</sup>

The other late transition metal atoms, Mn, Re, Fe, Co, Zn, and Cd, are unreactive toward dioxygen in solid matrices, and the inserted dioxide molecules are formed under UV–visible excitation or excitation under laser ablation conditions (reaction 2).<sup>246,247,261,286,288,320,326,464</sup> Gas-phase kinetic studies also indicate that the ground states of these metal atoms are less reactive or unreactive toward dioxygen at room temperature.<sup>248,572–575</sup>



The remaining late transition metal atoms interact with dioxygen to form the side-on or end-on bonded metal dioxygen complexes spontaneously on annealing, which rearrange to the inserted isomers upon UV–visible excitation (reaction 3) except Pd and Ag.<sup>336,347,355,357,383,430</sup> The inserted silver and palladium dioxide molecules have not been produced in solid matrices.<sup>355,357,430,447,448,451</sup>



Note that all the metals that are able to form dioxygen complexes exhibit d<sup>n–1</sup>s<sup>1</sup> (Rh, Pt, Cu–Au) or d<sup>n</sup>s<sup>0</sup> (Pd) ground-state electronic configurations except Ni. Although Ni has a 3d<sup>8</sup>4s<sup>2</sup> ground-state configuration, the first excited state with 3d<sup>9</sup>4s<sup>1</sup> configuration lies only about 250 cm<sup>–1</sup> higher in energy than the ground state. At the annealing temperatures (25–40 K) in solid argon, the first excited state is also populated. Gas-phase kinetic investigations also indicate that the transition metals with d<sup>n–1</sup>s<sup>1</sup> configurations are more reactive than their d<sup>n–1</sup>s<sup>2</sup> counterparts. Efficient depletion of the atoms of d<sup>n–1</sup>s<sup>1</sup> configuration by O<sub>2</sub> is interpreted by an attractive interaction correlated to a stable intermediate.<sup>574</sup>

The reaction of ground-state nickel atoms with dioxygen to form the nickel dioxide molecule has been theoretically studied.<sup>371</sup> The potential energy profiles calculated at the PW91PW91/6-311G(3df) level are shown in Figure 14. The reaction starting from triplet state Ni(<sup>3</sup>D) + O<sub>2</sub>(<sup>3</sup>Σ<sub>g</sub><sup>–</sup>) proceeds first on the quintet surface toward the formation of a superoxo complex (<sup>5</sup>B<sub>1</sub>). The complex, however, evolves rapidly to the <sup>3</sup>B<sub>1</sub> state due to a favorable crossing of the two related states (denoted as P1). Since the <sup>3</sup>B<sub>1</sub> and <sup>1</sup>A<sub>1</sub> states are nearly isoenergetic, one can conclude that the Ni + O<sub>2</sub> reaction results in the superoxo cyclic complexes (<sup>1</sup>A<sub>1</sub> and <sup>3</sup>B<sub>1</sub>) with a high exothermicity at these thermal conditions. If the internal energy is not quenched by the matrix solid, the superoxide complex can overcome a barrier height of 14 kcal/mol to reach the second minimum at the <sup>3</sup>B<sub>1</sub> curve corresponding to a dioxide state. Intersystem crossing between the <sup>3</sup>B<sub>1</sub> state and the second <sup>1</sup>A<sub>1</sub> state (correlates to the <sup>1</sup>Σ<sub>g</sub><sup>+</sup> state of dioxide) allows the system to relax toward the final product, namely, the <sup>1</sup>Σ<sub>g</sub><sup>+</sup> dioxide. Consequently, the formation of the superoxide intermediate and dioxide product can be envisaged from the Ni(<sup>3</sup>D) + O<sub>2</sub>(<sup>3</sup>Σ<sub>g</sub><sup>–</sup>) entry channel. The photochemical conversion of side-on bonded nickel superoxide complex to the nickel dioxide molecule is more complicated, which may involve some excited states. Two formation pathways of the nickel dioxide, starting from the cyclic superoxide singlet state (<sup>1</sup>A<sub>1</sub>) have been proposed based on theoretical calculations.<sup>371</sup>

As can be seen in Table 3, the metal dioxide molecules from the Sc group to the Fe group are bent, while those of the Co, Ni and Cu groups are linear. Among the first row transition metal dioxide molecules, the ν<sub>3</sub> vibrational frequencies are quite close, and all are located in the range of 1000–900 cm<sup>–1</sup> characteristic of stable molecules with strong metal–oxide bonds except for ScO<sub>2</sub>, CuO<sub>2</sub>, and ZnO<sub>2</sub>. Due to limited metal valence electrons available for bonding with oxygen, the ScO<sub>2</sub> molecule is not able to be stabilized in solid matrices, while the CuO<sub>2</sub> molecule is characterized to be weakly bonded with the Cu–O bonds more like that of an oxyl (–O•). The ν<sub>1</sub> frequencies decrease monotonically along the series from Ti to Ni. The same relationship can be found in the second row transition metal dioxides. But the ν<sub>3</sub> vibrational frequencies of second row metal dioxides are lower than those of the corresponding first row metal dioxides due to shell expansions. The third row transition metal dioxide ν<sub>3</sub> frequencies for TaO<sub>2</sub>, WO<sub>2</sub>, OsO<sub>2</sub>, and IrO<sub>2</sub> exceed the corresponding second row fundamentals as a consequence of relativistic contraction. But the ZrO<sub>2</sub> and HfO<sub>2</sub> molecules have about the same ν<sub>3</sub> vibrational fundamentals due to a

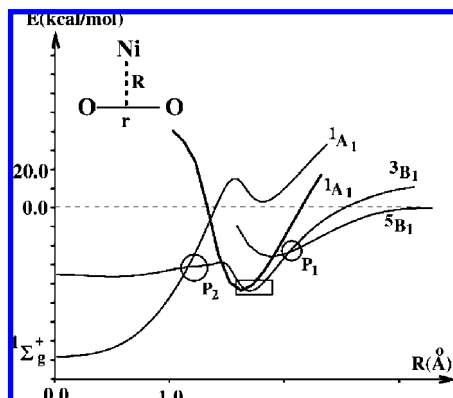
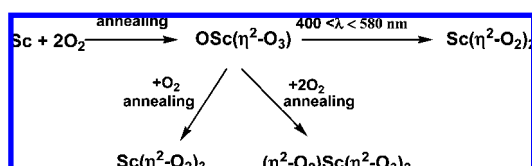


**Figure 14.** Potential energy profiles from the reactants ( $\text{Ni}(^3\text{D}) + \text{O}_2(^3\Sigma_g^+)$ ) to the ONiO dioxide ( $^3\Sigma_g^+$ ).  $\text{P}_1$  and  $\text{P}_2$  represent intersystem crossing points. Two nearly degenerate  $^3\text{B}_1$  and  $^1\text{A}_1$  minima corresponding to the cyclic intermediate are shown by a rectangle. Reprinted with permission from ref 371. Copyright 2006 Royal Society of Chemistry.

### Scheme 1



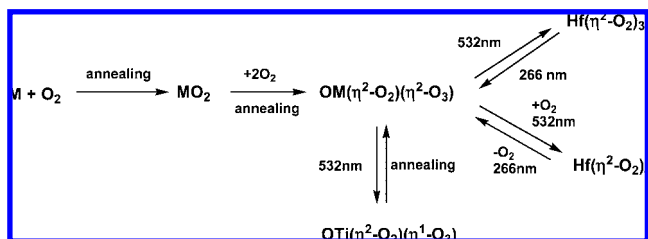
combination of lanthanide contraction and relativistic effects for hafnium.

It is found that the primary formed metal dioxide molecules or dioxygen complexes are able to react with additional dioxygen to form oxygen-rich metal dioxygen complexes in solid matrices on sample annealing, which exhibit characteristic photochemical reaction properties.

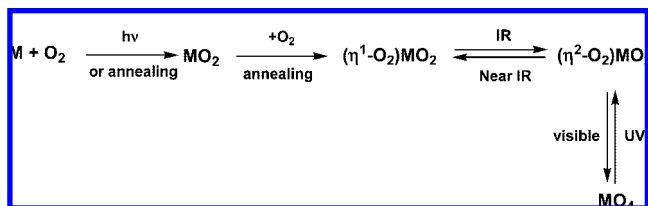
Due to limited valence electrons available for bonding, the metal dioxides of Sc and Ti groups prefer to interact with dioxygen to form high-valent dioxygen or ozonide complexes. The reactions between the Sc metal atom and dioxygen are summarized in Scheme 1. Although the scandium dioxide molecule is not produced, the experiments on the  $\text{Sc} + \text{O}_2$  reaction in solid argon show that the ground-state scandium atoms react spontaneously with two dioxygen molecules to form the  $\text{OSc}(\eta^2\text{-O}_3)$  complex.<sup>111</sup> In the lanthanum and dioxygen reaction, an  $(\eta^2\text{-O}_2)\text{LaO}_2$  complex is observed to be the precursor for the formation of the  $\text{OLa}(\eta^2\text{-O}_3)$  complex under near-infrared excitation.<sup>112</sup> The  $\text{OSc}(\eta^2\text{-O}_3)$  complex either isomerizes to the more stable  $\text{Sc}(\eta^2\text{-O}_2)_2$  isomer under visible light excitation or interacts with additional dioxygen to give the even oxygen-rich  $\text{Sc}(\eta^2\text{-O}_2)_3$  and  $(\eta^2\text{-O}_2)\text{Sc}(\eta^2\text{-O}_3)_2$  clusters.<sup>111</sup>

The oxidation of Ti group atoms with dioxygen proceeds with the initial formation of the metal dioxide molecules, which further react with dioxygen to form the  $\text{OM}(\eta^2\text{-O}_2)(\eta^2\text{-O}_3)$  complexes.<sup>152,153</sup> In the case of hafnium, the  $\text{OHf}(\eta^2\text{-O}_2)(\eta^2\text{-O}_3)$  complex can be converted to the homoleptic  $\text{Hf}(\eta^2\text{-O}_2)_3$  and  $\text{Hf}(\eta^2\text{-O}_2)_4$  complexes, as shown in Scheme 2. The  $\text{HfO}_2$ ,  $\text{OHf}(\eta^2\text{-O}_2)(\eta^2\text{-O}_3)$ ,  $\text{Hf}(\eta^2\text{-O}_2)_3$  and  $\text{Hf}(\eta^2\text{-O}_2)_4$  species all are high-valent compounds with the metal center in its formal +4 oxidation state. The results also demonstrate that the reactions from 2-fold coordinated metal dioxide to 5-fold coordinated  $\text{OHf}(\eta^2\text{-O}_2)(\eta^2\text{-O}_3)$ , and to 6-fold coordinated  $\text{Hf}(\eta^2\text{-O}_2)_3$ , and finally to 8-fold coordinated  $\text{Hf}(\eta^2\text{-O}_2)_4$  are energetically favored with increasing coordination numbers at the same oxidation state for the metal center.<sup>153</sup>

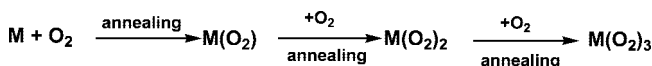
### Scheme 2



### Scheme 3



### Scheme 4



The results on Sc and Ti groups indicate that the metal oxide structures can be converted to the dioxygen complex structures via an ozonide structure intermediate.

All the metal dioxide molecules from the V group to the Co group and Ni are found to react with dioxygen spontaneously to form the metal dioxide–dioxygen complexes in solid matrices.<sup>182,183,201,238,247,261,288,334,337,340,341</sup> For the Cr group metals, the metal dioxide molecules prefer to coordinate two dioxygen molecules to form the disuperoxide complexes.<sup>201,238</sup> In selected systems (Fe, Co, Rh, Ir), both the side-on and end-on bonded complexes are formed, which are photochemically interconvertible.<sup>288,327,337,340</sup> In general, infrared light induces the conversion of the end-on bonded  $(\eta^1\text{-O}_2)\text{MO}_2$  complex to the side-on bonded  $(\eta^2\text{-O}_2)\text{MO}_2$  isomer, and vice versa with near-infrared light irradiation (Scheme 3). The metal dioxide–dioxygen complexes of Ru, Os, and Ir are also able to be rearranged to the metal tetroxide isomers.<sup>261,340</sup> In the case of manganese, the manganese tetroxide  $\text{MnO}_4$  is predicted to be less stable than the  $(\eta^2\text{-O}_2)\text{MnO}_2$  isomer and is not able to be stabilized in solid argon matrix.<sup>247</sup> However, it is found that the  $(\eta^2\text{-O}_2)\text{MnO}_2$  complex interacts with another weakly coordinated dioxygen to give the  $(\eta^2\text{-O}_2)\text{MnO}_4$  complex via visible light excitation, in which the manganese tetroxide is coordinated and stabilized by a side-on bonded  $\text{O}_2$  molecule.

The primary formed side-on or end-on bonded 1:1 metal dioxygen complexes of Rh, Ni group metals, Cu, and Ag are also able to bind an additional one (Ni group, Ag) or two (Rh and Cu) dioxygen molecules to form binary oxygen-rich complexes, as illustrated in Scheme 4.<sup>336,347,355,357,380,425,428</sup>

## 4. Ionic Mononuclear Transition Metal Oxide Species

Spectroscopic investigation of molecular ions is generally more difficult than that of neutrals, because charged species are often quite reactive. Both the production and spectroscopic detection face great challenges. Laser-ablation serves as the most commonly used technique in producing charged species for gas-phase spectroscopic studies.<sup>26</sup> The number density of ions that are available for spectroscopic study is

often low because of space charge effects or because the ions may be difficult to make in significant abundance. Thus, gas-phase investigation requires sensitive spectroscopic techniques, and conventional absorption spectroscopies are often not suitable.

Anion photon electron spectroscopy is widely used for studying molecular anions, but this technique provides spectroscopic information mainly on the neutral molecules. Only if hot bands (transitions originating from excited vibrational levels of the anion) are observed, can their energy spacings be used to determine the vibrational levels of the anions.<sup>26</sup> Laser-based spectroscopic techniques such as LIF, REMPI, and ZEKE, which often rely on access to a bound excited electronic state, are not suited for detecting anions, because most anions do not possess any significantly bound excited electronic states.<sup>576</sup> Laser ablation in conjunction with matrix isolation is a valuable tool in preparing charged species for conventional spectroscopic studies.<sup>15</sup> As has been discussed, laser ablation produces neutral species as well as electrons and cations, and as a result, anions can be formed by electron capture of the neutral molecules and cations can be produced by cation–molecule reactions or via photoionization by radiation in the ablation plume. Most anions bind their outmost electron less tightly than do most neutrals and cations, and therefore, they are more photosensitive. Photolysis of the initial deposited sample with filtered radiation can provide useful information in identifying the anionic species. In addition, adding a supplementary electron trapping molecule such as CCl<sub>4</sub> may reduce the concentration of anions and enhance the concentration of cations.<sup>15</sup> Knight et al. have observed that any attempts to isolate cations are unsuccessful when there is less than a 5 eV difference between the ionization energy of the matrix substrate atom and the electron affinity of the cation in question.<sup>577</sup> Utilizing the observed 5 eV difference, ions with an electron affinity greater than 10.8 eV (ionization energy of Ar is 15.76 eV) are not expected to be observed in an argon matrix. Neon has much higher ionization energy (21.56 eV) than argon,<sup>578</sup> hence, the neon matrix is the best choice for cationic species. For cationic transition metal–oxygen species, one should pay special attention, because some transition metal cationic species may interact strongly with the matrix substrate atoms, even with the lighter noble gases. Only a few transition metal oxide/dioxygen cations have been reported in solid noble gas matrices, most of which are characterized to be coordinated by one or multiple noble gas atoms. Recently developed infrared dissociation spectroscopy provides a powerful tool in studying the vibrational spectrum of free cation species in the gas phase, and some results on simple transition metal oxide cations will be discussed here.

#### 4.1. Cations

The electronic structures of mononuclear oxide cations have been the subject of many experimental studies and theoretical calculations.<sup>27,29,71,73,102,156,158,160,195,281,292,395,453,510,548,579–596</sup> The vibrational frequencies of mononuclear cations are listed in Table 7. Recently, the thermochemical properties of a series of transition metal oxide cations have been summarized.<sup>597</sup>

In solid matrices, the singly charged monoxide cations have been reported for Sc group metals as well as lanthanide metals.<sup>105,109,504,505</sup> These metal monoxide cations are closed-shell species with the metal center in the most stable +3 oxidation state. An infrared absorption at 976.3 cm<sup>-1</sup>, which was initially attributed to the ScO neutral<sup>104</sup> was reassigned

**Table 7. Ground Spin States and Vibrational Frequencies (cm<sup>-1</sup>) for Mononuclear Transition Metal Oxide Cations in the Gas Phase and in Solid Argon Matrix**

molecule	ground state	vibrational frequency <sup>a</sup>	experimental method <sup>b</sup>	ref
ScO <sup>+</sup>	<sup>1</sup> Σ <sup>+</sup>	976.3 (1006.2 <sup>c</sup> )	MI-IR <sup>c</sup>	105
Sc(O <sub>2</sub> ) <sup>+</sup>	<sup>1</sup> A <sub>1</sub>	892.9 (ν <sub>1</sub> ), 641.1 (ν <sub>2</sub> ), 624.8 (ν <sub>3</sub> )	MI-IR	85, 105
YO <sup>+</sup>	<sup>1</sup> Σ <sup>+</sup>	872.0 (899.8 <sup>c</sup> )	MI-IR	109
Y(O <sub>2</sub> ) <sup>+</sup>	<sup>1</sup> A <sub>1</sub>	816.3 (ν <sub>1</sub> ), 595.3 (ν <sub>2</sub> ), 587.5 (ν <sub>3</sub> )	MI-IR	109
LaO <sup>+</sup>	<sup>1</sup> Σ <sup>+</sup>	838.2 (864.0 <sup>c</sup> )	MI-IR	109
La(O <sub>2</sub> ) <sup>+</sup>	<sup>1</sup> A <sub>1</sub>	804.0 (ν <sub>1</sub> )	MI-IR	109
LaO <sub>2</sub> <sup>+</sup>	<sup>1</sup> Σ <sub>g</sub> <sup>+</sup>	689.3	MI-IR	109
CeO <sup>+</sup>	<sup>2</sup> Φ	849.4 (874.8 <sup>c</sup> )	MI-IR	74, 504
PrO <sup>+</sup>	<sup>3</sup> Σ <sup>-</sup>	857.4 (882.3)	MI-IR	74, 504
NdO <sup>+</sup>	<sup>4</sup> Φ	848.3 (878.4)	MI-IR	74, 504
SmO <sup>+</sup>	<sup>6</sup> Φ	840.0	MI-IR	74, 504
EuO <sup>+</sup>	<sup>7</sup> Σ <sup>-</sup>	756.9	MI-IR	74, 504
GdO <sup>+</sup>	<sup>8</sup> Σ <sup>-</sup>	844.8	MI-IR	74, 504
TbO <sup>+</sup>	<sup>9</sup> Σ <sup>-</sup>	856.5 (883.7 <sup>c</sup> )	MI-IR	74, 505
DyO <sup>+</sup>	<sup>8</sup> Σ <sup>-</sup>	861.2 (888.6)	MI-IR	74, 505
HoO <sup>+</sup>	<sup>5</sup> Σ <sup>+</sup>	860.5 (887.9)	MI-IR	74, 505
ErO <sup>+</sup>	<sup>4</sup> Σ <sup>-</sup>	861.8	MI-IR	74, 505
TmO <sup>+</sup>	<sup>3</sup> Σ <sup>-</sup>	864.2	MI-IR	74, 505
YbO <sup>+</sup>	<sup>2</sup> Σ <sup>+</sup>	788.7	MI-IR	74, 505
LuO <sup>+</sup>	<sup>1</sup> Σ <sup>+</sup>	864.9	MI-IR	74, 505
HfO <sup>+</sup>	<sup>4</sup> Σ <sup>-</sup>	1017.7 <sup>d</sup>	ZEKE	579, 599
VO <sup>+</sup>	<sup>3</sup> Σ <sup>-</sup>	1060 ± 40	PES	166
		1053 ± 5	IR-PD	606, 630
VO <sub>2</sub> <sup>+</sup>	<sup>1</sup> A <sub>1</sub>	1017 (ν <sub>1</sub> ), 990 (ν <sub>3</sub> )	IR-PD	606, 630
VO <sub>3</sub> <sup>+</sup>	<sup>3</sup> A <sup>′</sup>	1069, 1037	IR-PD	606, 630
NbO <sub>2</sub> <sup>+</sup>	<sup>1</sup> A <sub>1</sub>	988.0 (ν <sub>1</sub> ), 937.1 (ν <sub>3</sub> )	MI-IR	183
TaO <sub>2</sub> <sup>+</sup>	<sup>1</sup> A <sub>1</sub>	993.1 (ν <sub>1</sub> ), 938.8 (ν <sub>3</sub> )	MI-IR	183
CrO <sup>+</sup>	<sup>4</sup> Σ <sup>-</sup>	640 ± 30	PES	589, 592
ThO <sup>+</sup>	<sup>2</sup> Σ <sup>+</sup>	955.0 <sup>d</sup>	ZEKE	580
UO <sup>+</sup>		911.9 <sup>d</sup>	ZEKE	581
UO <sub>2</sub> <sup>+</sup>	<sup>2</sup> Φ	921 <sup>d</sup> (ν <sub>1</sub> ), 145.5 <sup>d</sup> (ν <sub>2</sub> ) 952.3 (980.1) (ν <sub>3</sub> )	ZEKE MI-IR	602 549

<sup>a</sup> The vibrational frequencies in parentheses are neon matrix values.

<sup>b</sup> Abbreviations: MI-IR, matrix-isolation infrared spectroscopy; PES, photoelectron spectroscopy; IR-PD, infrared photon dissociation spectroscopy; ZEKE, zero-electron kinetic energy photoelectron spectroscopy. <sup>c</sup> Unpublished results. <sup>d</sup> Harmonic frequency.

to the ScO<sup>+</sup> cation in solid argon.<sup>105</sup> Note that the ground-state configuration for ScO is 8σ<sup>2</sup>3π<sup>4</sup>9σ<sup>1</sup>, in which the unpaired electron is mainly distributed in the scandium-based 3d orbital. Although the covalent interaction between scandium and oxygen is barely changed upon removal of the 9σ electron in forming the cation, the scandium and oxygen atoms are more strongly bound due to the increase in electrostatic interaction. Hence, it is expected that the Sc=O bond length will be shortened in the ScO<sup>+</sup> cation with the vibrational frequency blue-shifted from that of the neutral molecule.<sup>105</sup> This trend is followed by the YO<sup>+</sup> and LaO<sup>+</sup> cations, but with a larger cation-to-neutral shift.<sup>109</sup> Recent studies in this laboratory indicate that both the ScO<sup>+</sup> and YO<sup>+</sup> cations are coordinated by multiple argon atoms in solid argon matrix in forming noble gas complexes.<sup>598</sup> The doping experimental results show that ScO<sup>+</sup> coordinates up to five argon atoms, and YO<sup>+</sup> coordinates six argon atoms. Therefore, the ScO<sup>+</sup> and YO<sup>+</sup> cations trapped in solid argon should be regarded as the [ScO(Ar)<sub>5</sub>]<sup>+</sup> and [YO(Ar)<sub>6</sub>]<sup>+</sup> complexes (Figure 15). The bonding in these complexes involves the Lewis acid–base interactions, in which electron density in the Ng lone pairs is donated into the vacant orbitals of the metal center (Figure 15). The binding energies per Ar atom are computed to be several kcalories per mole, lower than that of the formal covalent bonds but are significantly higher than that of the van der Waals interactions.<sup>598</sup>

The niobium and tantalum monoxide cations have been characterized in solid argon and neon by Weltner and co-



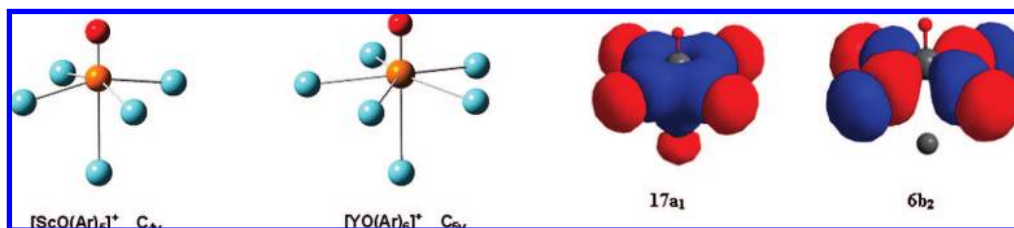


**Figure 15.** Optimized structures for the  $[\text{ScO}(\text{Ar})_5]^+$  and  $[\text{YO}(\text{Ar})_6]^+$  complexes and the bonding molecular orbital pictures of  $[\text{ScO}(\text{Ar})_5]^+$ . Adapted from ref 598. Copyright 2005 American Chemical Society.

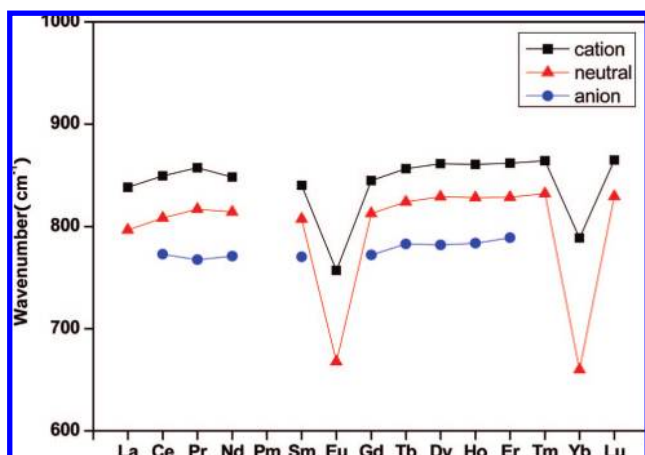


**Figure 16.** Plot of the vibrational fundamentals for lanthanide metal monoxide cations, neutrals, and anions in solid argon. From refs 109, 504, and 505.

workers using electron spin resonance spectroscopy. Both cations are suggested to have a  $^2\Sigma$  ground state from the characteristic metal hyperfine splittings in the X band of the ESR spectra.<sup>599</sup>

Figure 16 presents the vibrational fundamentals of the lanthanide metal monoxide cations and neutrals in solid argon. Due to the lanthanide contraction effect, the vibrational frequencies for most lanthanide monoxide cations increase slightly from Ce to Lu with the cation-to-neutral shifts around  $30\text{--}40\text{ cm}^{-1}$ . As found in the neutral case, the monoxide cations for Eu and Yb exhibit rather lower vibrational frequencies than those of others. Note that the frequency shifts for the  $\text{EuO}^+$  and  $\text{YbO}^+$  cations are about three times as large as those of the other monoxide cations. The peculiarities for these two cationic species may be related to the  $f^7$  and  $f^{14}$  configurations of the neutral monoxide molecules, which leads to the increase in metal–oxygen interactions due to the loss of half-filled and filled shell structures upon ionization. Theoretical studies on the lanthanide monoxide cations are fewer than those of the neutrals.<sup>102,510,518</sup> Recently, the electronic structures and molecular properties of the complete lanthanide monoxide species have been studied using DFT methods.<sup>74</sup> It is found that the ground spin multiplicity for the cationic species can be obtained by  $-1$  or  $+1$  from that of the neutral molecules.

Several monoxide cations have been studied in the gas phase using the PFI-ZEKE and resonance-enhanced photodissociation spectroscopic methods. Rotationally or vibrationally resolved spectra were recorded for the ground states and some low-lying electronically excited states. Vibrational frequencies and anharmonicity constants for low-lying energy levels were reported. Accurate ionization energies for the neutrals were determined.<sup>579–587</sup>

Cationic species with more than one oxygen atom are mainly limited to those with  $\text{MO}_2$  stoichiometry. For the Sc

group metals, the cationic  $\text{M}(\text{O}_2)^+$  species are formed in solid matrices, which can be regarded as peroxide cations with the metal center in the  $+3$  oxidation state. All three cations are predicted to have a  $^1A_1$  ground state with  $C_{2v}$  symmetry.<sup>105,109</sup> Besides the peroxide cation, a linear lanthanum dioxide cation is also formed in the reaction between La and  $\text{O}_2$ . This dioxide cation is predicted to have a  $^1\Sigma_g^+$  ground state, which is about  $40\text{ kcal/mol}$  less stable than the peroxide isomer.<sup>109</sup> In addition to the lanthanum dioxide cation, transition metal dioxide cations have also been reported for Nb, Ta, Pr, Nd, and U. The  $\text{NbO}_2^+$  and  $\text{TaO}_2^+$  cations are isovalent with the  $\text{ZrO}_2$  and  $\text{HfO}_2$  neutrals. Both cations are calculated to have a closed-shell singlet ground state with bent  $C_{2v}$  symmetry.<sup>183</sup> Their stretching vibrational frequencies are about  $30\text{ cm}^{-1}$  higher than those of the neutrals. The two lanthanide dioxide cations, which exhibit similar O-18 isotopic ratios as the corresponding linear neutral molecules, are suggested to have linear geometry.<sup>504</sup> These two cations are found to undergo a larger cation-to-neutral shift than that of the  $\text{NbO}_2^+$  and  $\text{TaO}_2^+$  cations.

Uranium is known to form an important cationic species, namely, uranyl,  $\text{UO}_2^{2+}$ , which has been the subject of many investigations.<sup>600</sup> The monocharged  $\text{UO}_2^+$  cation is observed as the cationic counterpart in the  $(\text{UO}_2)^+(\text{NO}_2)^-$  and  $(\text{UO}_2)^+(\text{NO})^-$  complexes in earlier thermal reactions between neutral  $\text{UO}_2$  and  $\text{NO}_2/\text{NO}$ .<sup>601</sup> In a laser ablation experiment, the uranium dioxide molecule was able to react with  $\text{O}_2$  to give the  $(\text{UO}_2)^+(\text{O}_2)^-$  complex, in which the  $\text{UO}_2^+$  cation exhibits a similar vibrational frequency as in the  $(\text{UO}_2)^+(\text{NO}_2)^-$  case.<sup>546</sup> The infrared absorptions at  $980.1$  and  $952.3\text{ cm}^{-1}$  are assigned to the isolated  $\text{UO}_2^+$  cation in solid neon and argon.<sup>549</sup> The IR inactive symmetric stretching vibration and the bending fundamental are determined to be  $919$  and  $145\text{ cm}^{-1}$  from recent gas-phase PFI-ZEKE spectroscopic study.<sup>602</sup> Consistent with the experimental identification, the  $\text{UO}_2^+$  cation is predicted to have a linear geometry with a  $^2\Phi_u$  ground state. Recent investigations indicate that  $\text{UO}_2^+$  coordinates up to five heavy noble gas atoms in forming complexes in solid noble gas matrices.<sup>603</sup> The calculated binding energies are much larger than those for the neutral  $\text{UO}_2(\text{Ng})_n$  complexes due to the combination of electron-donation and ion-induced dipole interactions. As for the bare  $\text{UO}_2^{2+}$  dication, frequency analysis reveals that it absorbs about  $100\text{ cm}^{-1}$  higher than the singly charged cation,<sup>549,551,604</sup> which is much higher than that of uranyl dication observed in condensed phase.<sup>605</sup> Apparently, solute or anion interactions are responsible for the lower  $\sigma_u$  vibrations of linear  $\text{UO}_2^{2+}$  dication observed in condensed phases, and only in the gas phase can  $\text{UO}_2^{2+}$  be considered as a true dication.

The vibrational spectra of some mononuclear vanadium oxide cations have been obtained via infrared predissociation of the corresponding ion–messenger atom complexes in gas phase.<sup>606</sup> The vibrational frequency of the  $\text{VO}^+$  cation is

**Table 8. Ground Spin States and Vibrational Frequencies (cm<sup>-1</sup>) for Transition Metal Monoxide Anions in the Gas Phase**

molecule	ground state	vibrational frequency	ref
ScO <sup>-</sup>	<sup>1</sup> Σ <sup>+</sup>	840 ± 60 <sup>a</sup>	84, 89
TiO <sup>-</sup>	<sup>2</sup> Δ	800 ± 60	115, 122
VO <sup>-</sup>	<sup>3</sup> Σ <sup>-</sup>	900 ± 50	156, 165
CrO <sup>-</sup>	<sup>4</sup> Π <sup>b</sup>	885 ± 80	193, 198
MnO <sup>-</sup>	<sup>5</sup> Σ <sup>+</sup>	760 ± 50	240
FeO <sup>-</sup>	<sup>4</sup> Δ	740 ± 60	40, 63, 65, 76, 276
CoO <sup>-</sup>	<sup>3</sup> Δ( <sup>3</sup> Σ <sup>-</sup> ) <sup>c</sup>		63, 65, 76
NiO <sup>-</sup>	<sup>2</sup> Π <sup>d</sup>	660 ± 40 <sup>e</sup>	63, 343
CuO <sup>-</sup>	<sup>1</sup> Σ <sup>+</sup>	739 ± 25	384
ZnO <sup>-</sup>	<sup>2</sup> Σ <sup>+</sup>	625 ± 40	441, 443
YO <sup>-</sup>	<sup>1</sup> Σ <sup>+</sup>	740 ± 60	71, 89
ZrO <sup>-</sup>	<sup>2</sup> Δ		71
NbO <sup>-</sup>	<sup>3</sup> Σ <sup>-</sup>		71
MoO <sup>-</sup>	<sup>4</sup> Π	810 ± 40	71, 204
TcO <sup>-</sup>	<sup>5</sup> Σ <sup>+</sup>		71
RuO <sup>-</sup>	<sup>4</sup> Δ		71
RhO <sup>-</sup>	<sup>3</sup> Σ <sup>-</sup>	730 ± 80	71, 333
PdO <sup>-</sup>	<sup>2</sup> Π		71, 342, 360
AgO <sup>-</sup>	<sup>1</sup> Σ <sup>+</sup>	497 ± 20	71, 432
CdO <sup>-</sup>	<sup>2</sup> Σ <sup>+</sup>		71
LaO <sup>-</sup>	<sup>1</sup> Σ <sup>+</sup>		74, 93
HfO <sup>-</sup>	<sup>4</sup> Σ <sup>-</sup>		73
TaO <sup>-</sup>	<sup>3</sup> Σ <sup>-</sup>		73, 174
WO <sup>-</sup>	<sup>6</sup> Σ <sup>-</sup>		73
ReO <sup>-</sup>	<sup>5</sup> Σ <sup>-</sup>		73
OsO <sup>-</sup>	<sup>4</sup> Δ		73
IrO <sup>-</sup>	<sup>3</sup> Σ <sup>-</sup>		73
PtO <sup>-</sup>	<sup>2</sup> Π	770 ± 30	73, 342
AuO <sup>-</sup>	<sup>1</sup> Σ <sup>+</sup>		73, 440, 441
HgO <sup>-</sup>	<sup>2</sup> Σ <sup>+</sup>		73

<sup>a</sup> The vibrational frequency for the ScO<sup>-</sup> anion is observed at 889.2 cm<sup>-1</sup> in solid argon (ref 608). <sup>b</sup> A slightly more stable <sup>6</sup>Σ<sup>+</sup> state was predicted in refs 65 and 76, and it was assigned to the ground state of the CrO<sup>-</sup> anion in a recent photoelectron spectroscopic study (ref 197). High-level ab initio calculations suggested that the <sup>4</sup>Π state is lowest in energy (ref 193), in agreement with earlier photoelectron spectroscopic study (ref 198). <sup>c</sup> Ground state undetermined. <sup>d</sup> A <sup>4</sup>Σ<sup>-</sup> ground state is predicted in refs 65 and 76. <sup>e</sup> A different value of 810 ± 50 cm<sup>-1</sup> is reported in another experiment (ref 344).

observed around 1053 cm<sup>-1</sup>, identical with the earlier value from photoelectron spectroscopy,<sup>166</sup> and a <sup>3</sup>Σ<sup>-</sup> ground state is obtained from theoretical calculations.<sup>156,158,160,163,607</sup> Two infrared absorptions around 1000 cm<sup>-1</sup> are observed for the vanadium dioxide cation, which is predicted to have a <sup>1</sup>A<sub>1</sub> ground state with bent C<sub>2v</sub> geometry.<sup>160,163,606</sup> The VO<sub>3</sub><sup>+</sup> cation is found to absorb at 1037 and 1069 cm<sup>-1</sup>. The nonplanar C<sub>s</sub> oxovanadium superoxide structure with a <sup>3</sup>A'' ground state is found to have similar vibrational frequencies with the experimentally observed values,<sup>163,607</sup> although the corresponding singlet state is predicted to be more stable in some theoretical calculations.<sup>160</sup>

## 4.2. Anions

### 4.2.1. Monoxide Anions

The electronic structures and vibrational frequencies of most transition metal monoxide anions have been obtained from anion photoelectron spectroscopy, while matrix-isolation infrared spectroscopy has provided direct spectroscopic information on the lanthanide monoxide anions. The ground states and vibrational frequencies of transition metal monoxide anions and lanthanide metal and actinide metal monoxide anions are listed in Tables 8 and 9, respectively. Due to limited resolution, vibrational frequencies deduced from photoelectron spectra show large uncertainties. The vibrational fundamental of scandium monoxide anion is determined to be around 840 cm<sup>-1</sup>

**Table 9. Ground Spin States and Vibrational Frequencies (cm<sup>-1</sup>) for Lanthanide Monoxide Anions in Solid Neon and Argon Matrices**

molecule	ground state	vibrational frequency		ref
		Ne	Ar	
CeO <sup>-</sup>	<sup>2</sup> Φ		772.8	74, 504
PrO <sup>-</sup>	<sup>3</sup> Σ <sup>-</sup>	792.6	767.4	74, 504
NdO <sup>-</sup>	<sup>4</sup> Φ	789.9	771.0	74, 504
PmO <sup>-</sup>	<sup>5</sup> Σ <sup>+</sup>			74
SmO <sup>-</sup>	<sup>6</sup> Φ		770.2	74, 504
EuO <sup>-</sup>	<sup>7</sup> Σ <sup>-</sup>			74
GdO <sup>-</sup>	<sup>8</sup> Σ	<sup>a</sup>	772.2	74, 504
TbO <sup>-</sup>	<sup>7</sup> Σ <sup>-</sup>		782.9	74, 505
DyO <sup>-</sup>	<sup>6</sup> Σ <sup>+</sup>		782.0	74, 505
HoO <sup>-</sup>	<sup>5</sup> Σ <sup>+</sup>		783.6	74, 505
ErO <sup>-</sup>	<sup>4</sup> Δ		788.8	74, 505
TmO <sup>-</sup>	<sup>3</sup> Σ <sup>-</sup>			74
YbO <sup>-</sup>	<sup>2</sup> Σ <sup>+</sup>			74
LuO <sup>-</sup>	<sup>1</sup> Σ <sup>+</sup>			74

<sup>a</sup> The gas-phase vibrational frequency for the GdO<sup>-</sup> anion was determined to be 702 ± 40 cm<sup>-1</sup> from anion photoelectron spectroscopy (ref 489).

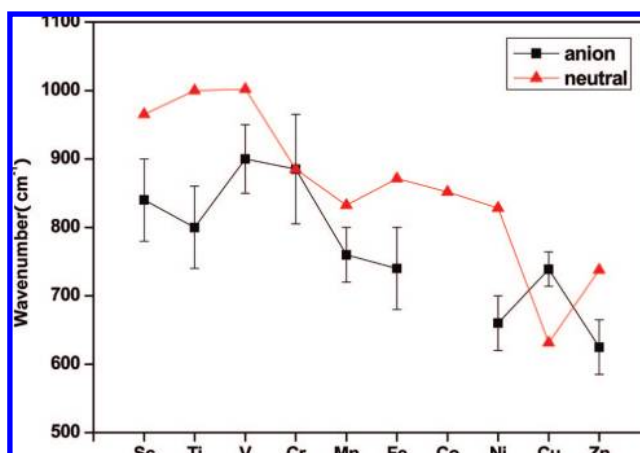


**Figure 17.** Plot of the vibrational fundamentals for the first row transition metal monoxide neutrals and anions. The vibrational frequencies from ScO to CuO are taken from ref 24, and the frequency for ZnO is taken from ref 456. All the vibrational frequencies for the anions are taken from Table 8.

from the hot band transitions in the photoelectron spectrum, and a <sup>3</sup>Δ state is suggested to be lowest in energy for this anion.<sup>89</sup> The ScO<sup>-</sup> anion has also been observed in solid argon with the vibrational fundamental at 889.2 cm<sup>-1</sup>, which is predicted to have a <sup>1</sup>Σ<sup>+</sup> ground state.<sup>608</sup> Figure 17 shows the vibrational fundamentals of the first row transition metal monoxide neutrals and anions. The vibrational frequencies for the ScO<sup>-</sup>, TiO<sup>-</sup>, VO<sup>-</sup>, FeO<sup>-</sup>, NiO<sup>-</sup>, and ZnO<sup>-</sup> anions are much lower than those of the corresponding neutral molecules.<sup>40,115,165,343,460–462</sup> Unlike other first row transition metal monoxide anions, the chromium and manganese monoxide anions exhibit less change in the vibrational frequencies upon electron attachment to the neutral molecules.<sup>198,240</sup> The additional electrons tend to occupy the nonbonding σ orbitals of both neutral CrO and MnO molecules in forming the <sup>4</sup>Π and <sup>5</sup>Σ<sup>+</sup> state anions, which results in the similarities in vibrational frequencies between the neutral and anionic monoxide molecules. Copper monoxide anion is another special example whose vibrational fundamental lies higher than that of the neutral CuO.<sup>384</sup> The vibrational frequency of CuO<sup>-</sup> anion is around 739 cm<sup>-1</sup>, comparable with the value of the isoelectronic ZnO molecule.<sup>460,461</sup> The blue-shift in vibrational frequency

**Table 10. Ground Spin States, Geometry, and Vibrational Frequencies (cm<sup>-1</sup>) for Transition Metal Dioxide Anions in Solid Neon and Argon Matrices<sup>a</sup>**

molecule	ground state	geometry	Ne		Ar		ref
			$\nu_1$	$\nu_3$	$\nu_1$	$\nu_3$	
ScO <sub>2</sub> <sup>-</sup>	<sup>1</sup> A <sub>1</sub>	bent		722.2 <sup>b</sup>		722.5	105, 106
TiO <sub>2</sub> <sup>-</sup>	<sup>2</sup> A <sub>1</sub>	bent		892.2 <sup>b</sup>		878.4	122, 132
VO <sub>2</sub> <sup>-</sup>	<sup>3</sup> A <sub>1</sub> ( <sup>3</sup> B <sub>1</sub> , <sup>3</sup> B <sub>2</sub> )	bent	894.8 <sup>b</sup>	907.8 <sup>b</sup>	886.5	896.9	76, 77, 161, 182, 183
CrO <sub>2</sub> <sup>-</sup>	<sup>4</sup> B <sub>1</sub>	bent	847.1	918.7		906.9 <sup>b</sup>	201
MnO <sub>2</sub> <sup>-</sup>	<sup>5</sup> B <sub>2</sub>	bent	781.3 <sup>b</sup>	870.5 <sup>b</sup>		858.3	609
FeO <sub>2</sub> <sup>-</sup>	<sup>2</sup> Δ <sub>g</sub>	linear				870.6	57
CoO <sub>2</sub> <sup>-</sup>	<sup>1</sup> Σ <sub>g</sub> <sup>+</sup>	linear		974.7		972.5	77, 610
NiO <sub>2</sub> <sup>-</sup>	<sup>4</sup> B <sub>1</sub> ( <sup>2</sup> A <sub>2</sub> )	linear <sup>c</sup>		893.9 <sup>b</sup>	<sup>d</sup>	886.8	76, 77, 347
CuO <sub>2</sub> <sup>-</sup>	<sup>3</sup> Σ <sub>g</sub> <sup>-</sup> ( <sup>3</sup> Σ <sub>g</sub> <sup>+</sup> )	linear			<sup>d</sup>		76, 77, 383
ZnO <sub>2</sub> <sup>-</sup>	<sup>2</sup> Π <sub>g</sub>	linear		624.1		626	612
YO <sub>2</sub> <sup>-</sup>	<sup>1</sup> A <sub>1</sub>	bent		616.6 <sup>b</sup>	702.0	618.0	109
ZrO <sub>2</sub> <sup>-</sup>	<sup>2</sup> A <sub>1</sub>	bent		785.8 <sup>b</sup>		761.4	132, 146
NbO <sub>2</sub> <sup>-</sup>	<sup>1</sup> A <sub>1</sub>	bent	931.4 <sup>b</sup>	878.0 <sup>b</sup>		854.1	183
MoO <sub>2</sub> <sup>-</sup>	<sup>4</sup> B <sub>1</sub>	bent	883.1	837.3			201
RuO <sub>2</sub> <sup>-</sup>	<sup>2</sup> A <sub>1</sub>	near linear		860.6		851.8	261
RhO <sub>2</sub> <sup>-</sup>	<sup>1</sup> A <sub>1</sub>	near linear		898.6		893.6	337, 611
CdO <sub>2</sub> <sup>-</sup>	<sup>2</sup> Π <sub>g</sub>	linear		483.6		487.9	612
LaO <sub>2</sub> <sup>-</sup>	<sup>1</sup> A <sub>1</sub>	bent		569.7 <sup>b</sup>	651.9	559.2	109
HfO <sub>2</sub> <sup>-</sup>	<sup>2</sup> A <sub>1</sub>	bent		770.3 <sup>b</sup>		747.9	132, 146
TaO <sub>2</sub> <sup>-</sup>	<sup>1</sup> A <sub>1</sub>	bent	938.7 <sup>b</sup>	876.6 <sup>b</sup>		836.9	183
WO <sub>2</sub> <sup>-</sup>	<sup>2</sup> B <sub>1</sub>	bent	952.3	887.8	946.3	880.0	201
ReO <sub>2</sub> <sup>-</sup>	<sup>3</sup> B <sub>1</sub>	bent	950.8 <sup>b</sup>	893.8		885.5	261
OsO <sub>2</sub> <sup>-</sup>	<sup>2</sup> B <sub>1</sub>	near linear		897.5			261
IrO <sub>2</sub> <sup>-</sup>	<sup>1</sup> Σ <sub>g</sub> <sup>+</sup>	linear		919.9		915.7	340, 611
PtO <sub>2</sub> <sup>-</sup>	<sup>2</sup> Π <sub>g</sub>	linear		839.9 <sup>b</sup>	<sup>d</sup>	836.2	611
AuO <sub>2</sub> <sup>-</sup>	<sup>3</sup> Σ <sub>g</sub> <sup>-</sup>	linear		740.8 <sup>b</sup>	<sup>d</sup>	738.2	611

<sup>a</sup> Only the values for the most abundant metal isotope and major site are listed. <sup>b</sup> Unpublished results. <sup>c</sup> A linear geometry was proposed for the NiO<sub>2</sub><sup>-</sup> anion (ref 347). DFT/BPW91 calculations predicted a <sup>2</sup>A<sub>2</sub> ground state with a bond angle of 170.4° (ref 77), while a <sup>4</sup>B<sub>1</sub> state with a bond angle of 179.9° was found to be lowest in energy at the DFT/B1LYP level of theory (ref 76). <sup>d</sup> The symmetric OMO stretching vibrations were observed in the gas phase from anion photoelectron spectroscopy: NiO<sub>2</sub><sup>-</sup> (715 ± 30, ref 342); CuO<sub>2</sub><sup>-</sup> (600 ± 80, ref 382); PtO<sub>2</sub><sup>-</sup> (760 ± 35, ref 342); AuO<sub>2</sub><sup>-</sup> (640 ± 40, ref 440).

suggests that the CuO bond is strengthened upon electron attachment to the neutral diatomic molecule. The electronic structures of the 3d transition metal monoxide anions have been the subject of a series of theoretical studies.<sup>28,63,65</sup> Anions for the second and third row transition metal monoxides are less investigated.<sup>71,73,74,89,93,136,174,204,333,342,360,432,440,441,489</sup>

The M=O vibrations for the YO<sup>-</sup> and MoO<sup>-</sup> anions exhibit large shifts upon electron detachment,<sup>89,204</sup> while the rhodium and silver monoxide anions have similar vibrational frequencies as their neutral molecules.<sup>333,432</sup>

Nine lanthanide monoxide anions have been characterized in solid argon, and their vibrational frequencies are about 40 cm<sup>-1</sup> red-shifted from those of the neutral molecules.<sup>504,505</sup> The early lanthanide monoxide anions absorb around 770 cm<sup>-1</sup>, while the infrared absorptions for the late lanthanide monoxide anions are about 10 cm<sup>-1</sup> higher. The general trend for the change of vibrational frequencies from Ce to Er is similar to that of the neutral and cationic lanthanide monoxides as shown in Figure 16. The ground-state properties of all the lanthanide monoxide anions have been systematically studied recently using the DFT/B3LYP method.<sup>74</sup>

#### 4.2.2. Dioxide Anions

Most transition metal dioxide anions have been experimentally observed. It was found that the early transition metal dioxide anions from the Sc group to the Mn group possess bent geometry<sup>105,109,132,182,183,201,261,609</sup> while the late transition metal dioxide anions are linear or near linear.<sup>57,261,347,382,402,610–612</sup> The geometric structures and vibrational frequencies of transition metal as well as lanthanide and actinide metal dioxide anions are listed in Tables 10 and 11. The antisymmetric stretching

**Table 11. Ground Spin States, Experimental Bond Angles (deg), and Vibrational Frequencies (cm<sup>-1</sup>) for Lanthanide and Uranium Dioxide Anions (cm<sup>-1</sup>) in Solid Neon and Argon Matrices<sup>a</sup>**

molecule	bond angle <sup>b</sup>	Ne		Ar	
		$\nu_1$	$\nu_3$	$\nu_1$	$\nu_3$
CeO <sub>2</sub> <sup>-</sup>	140			712.0	662.0
PrO <sub>2</sub> <sup>-</sup>	157		667.6	665.0	658.3
NdO <sub>2</sub> <sup>-</sup>	121				660.6
SmO <sub>2</sub> <sup>-</sup>	121			676.4	575.5
EuO <sub>2</sub> <sup>-</sup>	129			661.0	560.8
GdO <sub>2</sub> <sup>-</sup>	120			685.9	589.4
TbO <sub>2</sub> <sup>-</sup>	137			711.2	669.0
DyO <sub>2</sub> <sup>-</sup>			591.2	693.9	574.6
HoO <sub>2</sub> <sup>-</sup>				696.2	547
ErO <sub>2</sub> <sup>-</sup>	127			702.3	613.4
TmO <sub>2</sub> <sup>-</sup>	133				613.1
YbO <sub>2</sub> <sup>-</sup>	142			701.2	604.2
LuO <sub>2</sub> <sup>-</sup>	124				626.9
UO <sub>2</sub> <sup>-</sup>	180		857.2		

<sup>a</sup> The values for all the lanthanide dioxide anions are taken from refs 504 and 505, and the values for UO<sub>2</sub><sup>-</sup> anion are taken from ref 549. <sup>b</sup> For lanthanide dioxide anions, angles are upper limits estimated from oxygen 16/18 isotopic ratio for  $\nu_3$ ; the true bond angle for bent species is probably 5° lower.

vibrational frequencies ( $\nu_3$ ) for the first row transition metal dioxide anions increase from Sc to Cr and from Mn to Co. The value of manganese dioxide anion is about 50 cm<sup>-1</sup> lower than that of the CrO<sub>2</sub><sup>-</sup> anion. In general, the  $\nu_3$  frequencies of the dioxide anions are lower than those of the corresponding neutrals. However, the cobalt dioxide anion is an exception since its  $\nu_3$  mode is blue-shifted with respect to that of neutral. Our recent matrix isolation infrared spectroscopic study reveals that the antisymmetric stretching

vibration of cobalt dioxide anion at  $972.5\text{ cm}^{-1}$  is about  $30\text{ cm}^{-1}$  higher than that of the neutral dioxide molecule, suggesting that the CoO bonds are strengthened upon electron attachment to the neutral molecule.<sup>610</sup> For the second row transition metal dioxide anions, the antisymmetric stretching vibrational frequencies generally increase from left to right although the values for Nb, Mo, and Ru are close to each other. The  $\nu_3$  frequencies of the third row transition metal dioxide anions increase from La to Ir and then decrease from Ir to Au.

All the lanthanide metal dioxide anions were characterized to be bent. The  $\nu_3$  vibrational frequencies of the anions are lower than those of the corresponding neutrals. But the neutral-to-anion frequency shifts are quite small for the late lanthanide metals from Dy to Yb. The  $\text{UO}_2^-$  anion is the only actinide metal dioxide anion experimentally observed. It is characterized to be linear with a  $^2\Phi_u$  ground state.<sup>549</sup>

The frequency shift upon electron attachment to the neutral molecules strongly depends on the nature of the frontier orbitals. Take the  $\text{PtO}_2^-$  and  $\text{IrO}_2^-$  anions as an example, the frequency difference for platinum ( $106.1\text{ cm}^{-1}$ ) is much larger than that for iridium ( $13.3\text{ cm}^{-1}$ ).<sup>611</sup> The  $\text{PtO}_2$  neutral has a linear singlet ground state. The LUMO of neutral  $\text{PtO}_2$  is an antibonding  $\pi$  orbital, which mainly consists of the O 2p orbital and Pt 5d orbital. Addition of an electron to this orbital of neutral  $\text{PtO}_2$  results in the  $^2\Pi_g$  ground-state  $\text{PtO}_2^-$  anion, in which the Pt–O bond is elongated with the stretching vibrational frequency lowered. For the  $\text{IrO}_2^-$  anion, the additional electron occupies the SOMO of neutral  $\text{IrO}_2$  which is mainly a nonbonding orbital derived from the 5s atomic orbital of iridium. Apparently, the bond strength of  $\text{IrO}_2$  does not change significantly upon electron attachment to this orbital, which leads to a slight decrease of the antisymmetric stretching vibrational frequency for the anion due to the increase in electrostatic interactions.

The properties of most ground-state transition metal dioxide anions have been obtained from the theoretical point of view although they are not as extensively studied as the neutrals.<sup>76,77,105,109,132,183,197,201,240,261,440,549,609–612</sup> In some cases, it is very difficult to determine the electronic ground state of the anions based solely upon theoretical calculations, and comparison between the experimental observations and the calculated values is essential in determining the true ground-state structure. The  $\text{FeO}_2^-$  anion provides as a good example demonstrating that theoretical calculations on such linear species require sophisticated treatment.<sup>57</sup> Recent studies in our laboratory indicate that calculations with single-reference methods, including various DFT and post-HF methods are unreliable for the  $\text{FeO}_2^-$  anion, which is experimentally determined to be linear. However, the state-averaged multireference MRCI method, which incorporates both the dynamic and nondynamic correlations predicts that the anion has a linear doublet ground state, consistent with the experimental observations.

#### 4.2.3. Oxygen-Rich Anions

Trioxide anions have been observed for several systems including the V group metals, chromium, rhenium, and some rare earth metals in matrix infrared spectroscopic studies.<sup>183,201,261,504,505</sup> The vanadium, niobium, and tantalum trioxide anions are determined to have  $C_{3v}$  or  $D_{3h}$  structures with a closed-shell singlet ground state, in which the metal centers are in the highest +5 oxidation state.<sup>183</sup> The doubly degenerate M=O stretching modes are observed at 916.2,

817.1, and  $807.0\text{ cm}^{-1}$  in solid argon. The  $\text{YO}_3^-$ ,  $\text{PrO}_3^-$ , and  $\text{TbO}_3^-$  anions were suggested to have planar  $D_{3h}$  symmetry, while the  $\text{GdO}_3^-$  anion seemed to have a pyramidal structure due to the strong intermediate absorptions observed in the experiments using mixed and scrambled oxygen isotopic samples.<sup>109,504,505</sup> The M=O stretching vibrational frequencies for these four rare earth metal trioxide anions are more than  $250\text{ cm}^{-1}$  lower than those of the V group trioxide anions due to the lack of enough valence electrons to afford three formal M=O double bonds. A recent vibrationally resolved photoelectron spectroscopic study revealed that the  $\text{WO}_3^-$  anion possesses a trioxide structure with three oxygen atoms atomically bound to the tungsten center, while a dioxygen–dioxide complex structure was proposed for the  $\text{WO}_4^-$  anion.<sup>236</sup> However, based upon a more recent PES study, the ground state of  $\text{WO}_4^-$  is found to be a tetroxide structure with  $C_{2v}$  symmetry, which comprises two W=O double bonds with the extra charge delocalized on the other two W–O units.<sup>228</sup>

The Mn group transition metals are known to form stable tetroxide anions with the metal centers in the highest +7 oxidation state.<sup>316</sup> The  $\text{MnO}_4^-$  anion has been well studied in salts and solutions. It has a tetrahedron geometry with a bond length of  $1.629 \pm 0.008\text{ \AA}$ .<sup>613</sup> The triply degenerate antisymmetric OMnO stretching vibration is observed at  $910\text{ cm}^{-1}$  in salts,<sup>614</sup> which is slightly higher than the argon matrix value of  $896.9\text{ cm}^{-1}$ .<sup>609</sup> The  $\text{MnO}_4^-$  anion is unusually stable. Photoelectron spectroscopic study shows that the  $\text{MnO}_4$  neutral has an electron affinity of  $4.80 \pm 0.10\text{ eV}$ ,<sup>249</sup> which is significantly larger than that of atomic chlorine.<sup>578</sup> The  $\text{ReO}_4^-$  anion is isoelectronic with  $\text{OsO}_4$ . The triply degenerate ReO stretching vibration is observed around  $907\text{ cm}^{-1}$ .<sup>261</sup>

### 5. Multinuclear Transition Metal Oxide Clusters

Multinuclear transition metal oxide clusters serve as building blocks for nanostructured materials and also as representative models for gas-phase studies, which can provide an understanding of the function of transition metal oxide catalysts at the molecular level. The composition of cluster ions can be determined by mass spectrometric methods, and their geometric structures can, in principle, be predicted by quantum chemical calculations. However, reliable structural assignments for transition metal oxide clusters, particularly for larger clusters are quite difficult due to the existence of many low-energy isomers and low-lying electronic states. The identification of the transition metal oxide cluster structure generally requires the confirmation by experimental data from structurally sensitive methods such as vibrational spectroscopy. Vibrational spectroscopy combined with the state-of-the-art quantum chemical calculations offers one of the most direct and generally applicable experimental approaches to structural investigation of neutral and charged transition metal oxide clusters. With the development of tunable free electron lasers, IR photodissociation spectroscopy has been successfully used to measure indirectly the vibrational absorptions of mass-selected transition metal oxide cluster ions in the gas phase. Recent progress on vibrational spectroscopic investigations of transition metal oxide cluster ions has been outlined in recent reviews<sup>615</sup> and will not be repeated here. But some more recent progress will be discussed. For transition metal oxide neutral clusters, anion photoelectron spectroscopy has been used to measure the electron detachment energies of anions, which can provide vibrational information on the neutral clusters in the

gas phase. Due to the limited spectral resolution, vibrational frequencies can in general be resolved only for small sized clusters. Structural assignments for larger clusters are usually accomplished by combining experimental PES data with theoretical calculations. Infrared absorption spectroscopy offers another direct experimental method to investigate the vibrational frequencies of neutral multinuclear transition metal oxide clusters in solid matrices. However, matrix infrared spectroscopic experiments also face difficulties for larger multinuclear clusters owing to low concentrations and spectral congestion. It is quite difficult to determine the number of transition metal atoms involved in the clusters because the metal–metal vibrations generally lie in the far-infrared region with very low IR intensities. Nevertheless, some multinuclear transition metal oxide clusters (mainly dinuclear clusters) have been studied using matrix infrared spectroscopy. In this section, spectroscopic studies on multinuclear transition metal oxide clusters will be summarized. We will focus on small clusters with their spectral and structural information being clearly determined, in particular, dinuclear oxide clusters. The experimental vibrational frequencies of some multinuclear transition metal oxide clusters are listed in Table 12. There are a large number of studies on the reactivity of transition metal oxide clusters. These studies go beyond the scope of this review and will not be discussed here.

## 5.1. Sc Group

There is no experimental report on the spectroscopic study of multinuclear scandium oxide clusters except a photoionization study of scandium cluster monoxides. The photoionization efficiency spectra and ionization energies of  $\text{Sc}_n\text{O}$  ( $n = 5\text{--}36$ ) are reported.<sup>616</sup> Density functional theory calculations on dinuclear scandium oxide clusters indicate that  $\text{Sc}_2\text{O}_2$  has a  ${}^3\text{B}_{1u}$  ground state with planar  $D_{2h}$  symmetry (Figure 18A).<sup>85</sup> Minor structural changes in the cluster are seen upon adding or removing electrons, since this involves the weakly bonding half-filled valence orbitals. Infrared absorptions at 699.1 and 647.8  $\text{cm}^{-1}$  have been tentatively assigned to the cyclic  $\text{Sc}_2\text{O}_2$  cluster in solid argon.<sup>104</sup> The  $\text{Sc}_2\text{O}_3$  cluster has a trigonal bipyramid structure with  $D_{3h}$  symmetry (Figure 19A).<sup>85</sup> Mass-selected  $\text{Y}_n\text{O}_m^-$  cluster anions with  $n = 2\text{--}10$  have been investigated by photoelectron spectroscopy using 355 and 266 nm for the detachment wavelengths.<sup>617</sup> Electron affinities and vertical detachment energies were measured. A general trend in the observed photoelectron spectra is a shifting of threshold energies to higher binding energies with increasing cluster size  $n$ . At low electron binding energies, main spectral features are contributed from metal d-band orbitals, whereas the O 2p contribution becomes apparent with increasing oxygen content due to a higher degree of hybridization of yttrium s and d and oxygen 2p orbitals. In addition, theoretical calculations on the oxygen-deficient metal cluster monoxides of scandium and yttrium have also been reported.<sup>618,619</sup>

## 5.2. Ti Group

The dinuclear  $\text{Ti}_2\text{O}_2$  cluster has been observed in solid matrices and was characterized to have a four-membered ring structure. It was calculated to have a closed-shell singlet ground state having a nonplanar  $C_{2v}$  geometry with a strong Ti–Ti bond (Figure 18B).<sup>620,621</sup> The zirconium and hafnium analogs also have a closed-shell singlet ground state but were

predicted to have planar  $D_{2h}$  symmetry (Figure 18A).<sup>620</sup> All three  $\text{M}_2\text{O}_4$  clusters of group IV metals have been observed in solid argon matrix.<sup>620</sup> These clusters are formed by the dimerization reactions between two metal dioxide molecules, which requires negligible activation energy. All these  $\text{M}_2\text{O}_4$  clusters are characterized to have a  ${}^1\text{A}_g$  ground state with nonplanar  $C_{2h}$  symmetry (Figure 20A). The clusters involve a rhombus  $\text{M}(\mu\text{-O})_2\text{M}$  subunit and two terminal O atoms bending out of the  $\text{M}(\mu\text{-O})\text{M}$  plane in opposite directions.<sup>140–144,620,622–626</sup> A comparison between the experimental PES data and theoretical calculations verifies unequivocally that the  $\text{Ti}_2\text{O}_4^-$  anion has a  $C_{3v}$  structure.<sup>135,149</sup> The electronic structures of larger  $(\text{TiO}_2)_n$  clusters have been the subject of several theoretical calculations.<sup>141,142,627–629</sup> The recently reported photoelectron spectra of  $(\text{TiO}_2)_n^-$  ( $n = 3\text{--}10$ ) clusters reveal that the band gap is strongly size-dependent for  $n < 7$ , but it rapidly approaches the bulk limit at  $n = 7$  and remains constant up to  $n = 10$ . All PES features are observed to be very broad, suggesting large geometry changes between the anions and the neutral clusters due to the localized nature of the extra electron in the anions. The extra electron in the  $(\text{TiO}_2)_n^-$  clusters appears to be localized in a tricoordinated Ti atom, creating a single  $\text{Ti}^{3+}$  site and making these clusters ideal molecular models for mechanistic understanding of  $\text{TiO}_2$  surface defects and photocatalytic properties.<sup>135</sup>

Titanium and zirconium oxide clusters with the  $\text{M}_n\text{O}_{2n-1}$  stoichiometry have been studied using infrared photodissociation spectroscopy. Most of these clusters exhibited similar broad features in the bridged M–O–M stretching frequency region, which are assigned to the M–O stretching vibrations of the four-membered  $\text{M}_2\text{O}_2$  rings.<sup>46,626</sup>

## 5.3. V Group

Infrared photodissociation spectroscopic investigation in the gas phase indicates that the  $\text{V}_2\text{O}_2^+$  cation has a four-membered ring structure.<sup>630</sup> It is calculated to have a planar  ${}^2\text{A}'$  ground state.<sup>160b</sup> The  $\text{V}_2\text{O}_2$  neutral has a  ${}^3\text{A}_1$  ground state, in which the two vanadium atoms are slightly inequivalent in forming a planar  $C_{2v}$  geometry.<sup>631</sup> The  $\text{V}_2\text{O}_3^+$  cation and  $\text{V}_2\text{O}_3$  neutral have nonplanar  $C_s$  symmetry (a four-membered  $\text{V}_2\text{O}_2$  ring with an extra O atom terminally attached to a vanadium atom, Figure 19B).<sup>630,631</sup> The  $\text{V}_2\text{O}_4$  cluster has been observed as the photodetachment product of the  $\text{V}_2\text{O}_4^-$  anion. It is calculated to have a triplet ground state with nonplanar  $C_{2v}$  symmetry, in which no direct V–V bond is formed (Figure 20B).<sup>160,161,631,632</sup> The  $\text{V}_2\text{O}_4^-$  anion is calculated to have a high-spin  ${}^4\text{B}_{2g}$  ground state with planar  $D_{2h}$  symmetry (Figure 20C).<sup>161</sup> The IR photodissociation spectrum indicates that the  $\text{V}_2\text{O}_4^+$  cation is nonplanar with the two vanadyl groups in trans positions with respect to the ring plane (Figure 20A).<sup>630</sup> The ground state of  $\text{V}_2\text{O}_5$  is found to be a doubly bridged structure ( ${}^1\text{A}_1$ ), where one vanadium atom has a tetrahedral coordination and the other has a trigonal-pyramidal coordination (Figure 21A).<sup>161,631</sup> The  $\text{V}_2\text{O}_5^-$  anion is found to possess a similar doubly bridged structure with a  ${}^2\text{A}'$  ground state. A nonplanar  $D_{2h}$  structure (Figure 21 F) is suggested to be the structure observed in anion photoelectron spectroscopic investigation of the  $\text{V}_2\text{O}_6^-$  anion in the gas phase.<sup>633</sup> The terminal VO vibration is measured around 800  $\text{cm}^{-1}$ , which is lower than the value of  $\text{V}_2\text{O}_4$  cluster with two terminal VO double bonds but higher than that of cyclic  $\text{V}_2\text{O}_2$  cluster with VO single bonds. Since each vanadium atom in the  $\text{V}_2\text{O}_6$  cluster cannot afford two VO

**Table 12. Vibrational Frequencies (cm<sup>-1</sup>) for Selected Multinuclear Transition Metal Oxide Clusters**

molecule	symmetry	vibrational frequency	experimental method <sup>a</sup>	ref
Sc <sub>2</sub> O <sub>2</sub>	<i>D</i> <sub>2h</sub>	699.1, 647.8	MI-IR	104
Y <sub>2</sub> O <sub>2</sub>	<i>D</i> <sub>2h</sub>	546.2	MI-IR	109
Ti <sub>2</sub> O <sub>2</sub>	<i>C</i> <sub>2v</sub>	746.1, 736.2	MI-IR	620
Ti <sub>2</sub> O <sub>4</sub>	<i>C</i> <sub>2h</sub>	956.8, 704.1, 679.9	MI-IR	620
Zr <sub>2</sub> O <sub>2</sub>	<i>D</i> <sub>2h</sub>	701.5	MI-IR	620
Zr <sub>2</sub> O <sub>4</sub>	<i>C</i> <sub>2h</sub>	870.6, 652.0, 593.4	MI-IR	620
Hf <sub>2</sub> O <sub>2</sub>	<i>D</i> <sub>2h</sub>	684.2	MI-IR	620
Hf <sub>2</sub> O <sub>4</sub>	<i>C</i> <sub>2h</sub>	866.4, 649.4, 591.3	MI-IR	620
V <sub>2</sub> O <sub>2</sub> <sup>+</sup>	<i>C</i> <sub>s</sub>	833, 724	IR-PD	630
V <sub>2</sub> O <sub>3</sub> <sup>+</sup>	<i>C</i> <sub>s</sub>	1044, 803, 765, 666	IR-PD	630
V <sub>2</sub> O <sub>4</sub> <sup>+</sup>	<i>C</i> <sub>s</sub>	1049, 1029, 794, 776, 594	IR-PD	630
V <sub>2</sub> O <sub>4</sub>	<i>C</i> <sub>2v</sub>	1090 ± 30	PES	633
V <sub>2</sub> O <sub>5</sub> <sup>+</sup>	<i>C</i> <sub>s</sub>	1034, 911, 815, 738, 657	IR-PD	630
V <sub>2</sub> O <sub>6</sub> <sup>+</sup>	<i>C</i> <sub>1</sub>	1160, 1060, 1028, 836, 751, 673	IR-PD	630
V <sub>2</sub> O <sub>6</sub>	<i>D</i> <sub>2h</sub>	800 ± 40	PES	633
V <sub>2</sub> O <sub>6</sub> <sup>-</sup>	<i>C</i> <sub>2v</sub>	975, 959, 930, 911, 888, 800, 775, 738, 620	IR-MPD	636b
V <sub>2</sub> O <sub>7</sub> <sup>-</sup>	<i>C</i> <sub>s</sub>	1112, 987, 965, 952, 775, 705, 627	IR-MPD	636b
Nb <sub>2</sub> O <sub>6</sub> <sup>+</sup>	<i>C</i> <sub>1</sub>	990, 790, 675, 625	IR-MPD	637
Cr <sub>2</sub> O <sub>2</sub>	<i>C</i> <sub>s</sub> (chain)	934.4, 844.6	MI-IR	652
	<i>D</i> <sub>2h</sub> (cyclic)	628.2	MI-IR	202
Cr <sub>2</sub> O <sub>3</sub>	<i>C</i> <sub>s</sub>	620 ± 30, 280 ± 30	PES	650
Cr <sub>2</sub> O <sub>4</sub>	<i>D</i> <sub>2h</sub>	630 ± 50	PES	650
	<i>D</i> <sub>2h</sub>	984.1, 716.1, 642.9	MI-IR	652
Cr <sub>2</sub> O <sub>5</sub>	<i>C</i> <sub>s</sub>	710 ± 50	PES	650
Cr <sub>2</sub> O <sub>6</sub>	<i>D</i> <sub>2h</sub>	780 ± 50	PES	650
	<i>D</i> <sub>2h</sub>	1014.8, 975.4, 704.1, 690.5	MI-IR	652
Mo <sub>2</sub> O <sub>2</sub>	<i>C</i> <sub>s</sub>	880 ± 100, 320 ± 50	PES	653
Mo <sub>2</sub> O <sub>3</sub>	<i>C</i> <sub>2</sub>	560 ± 30	PES	653
Mo <sub>2</sub> O <sub>4</sub>	<i>C</i> <sub>s</sub>	970 ± 40	PES	653
W <sub>2</sub> O	<i>C</i> <sub>s</sub>	810 ± 40	PES	654
W <sub>2</sub> O <sub>3</sub>	<i>C</i> <sub>2v</sub>	920 ± 50	PES	654
W <sub>2</sub> O <sub>4</sub>	<i>C</i> <sub>1</sub>	920 ± 40	PES	654
W <sub>2</sub> O <sub>5</sub>	<i>C</i> <sub>s</sub>	920 ± 40	PES	654
W <sub>2</sub> O <sub>6</sub>	<i>D</i> <sub>2h</sub>	920 ± 40	PES	654
Mn <sub>2</sub> O	<i>C</i> <sub>2v</sub>	808.3	MI-IR	246
Mn <sub>2</sub> O <sub>2</sub>	<i>D</i> <sub>2h</sub>	601.0, 506.8	MI-IR	246
Mn <sub>2</sub> O <sub>6</sub>	<i>D</i> <sub>2h</sub>	1092.0, 683.6	MI-IR	247
Fe <sub>2</sub> O	<i>C</i> <sub>2v</sub>	868.6	MI-IR	270
Fe <sub>2</sub> O <sub>2</sub>	<i>D</i> <sub>2h</sub>	670 ± 70	PES	268
	<i>D</i> <sub>2h</sub>	660.6, 517.4	MI-IR	270, 320
Fe <sub>2</sub> O <sub>3</sub>		810 ± 100	PES	268
Fe <sub>2</sub> O <sub>4</sub>	<i>D</i> <sub>2h</sub>	710 ± 60	PES	268
		861.5, 705.1	MI-IR	270
Fe <sub>2</sub> O <sub>5</sub>		750 ± 50	PES	268
Co <sub>2</sub> O <sub>2</sub>	<i>D</i> <sub>2h</sub>	685.2, 469.5, 304.1	MI-IR	672
Co <sub>2</sub> O <sub>4</sub>		859.6, 540.0	MI-IR	320
Ni <sub>2</sub> O <sub>2</sub>	<i>D</i> <sub>2h</sub>	650.2, 481.6	MI-IR	347
Pd <sub>2</sub> O <sub>2</sub>	<i>C</i> <sub>2v</sub>	875.6	MI-IR	380
Pd <sub>2</sub> O <sub>4</sub>	<i>D</i> <sub>2h</sub>	937.8	MI-IR	380
Cu <sub>2</sub> O	<i>C</i> <sub>2v</sub>	<200	PES	679
Cu <sub>2</sub> O <sub>2</sub>	<i>D</i> <sub>2h</sub>	630 ± 30	PES	679
	<i>C</i> <sub>2v</sub>	1096.5	MI-IR	682
	<i>C</i> <sub>∞v</sub>	955.0	MI-IR	682
Cu <sub>2</sub> O <sub>3</sub>	<i>D</i> <sub>3h</sub>	640	PES	679
Cu <sub>2</sub> O <sub>4</sub>	<i>D</i> <sub>2h</sub>	985.9	MI-IR	682
V <sub>3</sub> O	<i>C</i> <sub>2v</sub>	750 ± 20, 415 ± 15, 340 ± 15	PES	641
V <sub>3</sub> O <sup>-</sup>	<i>C</i> <sub>2v</sub>	355 ± 20, 770 ± 20	PES	641
V <sub>3</sub> O <sub>8</sub> <sup>-</sup>	<i>C</i> <sub>2v</sub>	965, 922, 834, 680, 656	IR-MPD	636b
Nb <sub>3</sub> O <sup>+</sup>	<i>C</i> <sub>2v</sub>	312 ± 1	ZEKE	639
Nb <sub>3</sub> O	<i>C</i> <sub>2v</sub>	710 ± 15, 320 ± 15	PES	641
Nb <sub>3</sub> O <sup>-</sup>	<i>C</i> <sub>2v</sub>	300 ± 20	PES	641
Nb <sub>3</sub> O <sub>8</sub> <sup>+</sup>	<i>C</i> <sub>s</sub>	1000, 700	IR-MPD	637
Ta <sub>3</sub> O	<i>C</i> <sub>2v</sub>	710 ± 15, 225 ± 15	PES	641
Ta <sub>3</sub> O <sup>-</sup>	<i>C</i> <sub>2v</sub>	215 ± 20	PES	641
V <sub>4</sub> O <sub>10</sub> <sup>+</sup>	<i>C</i> <sub>s</sub>	1032, 842	IR-MPD	638
V <sub>4</sub> O <sub>10</sub> <sup>-</sup>	<i>T</i> <sub>d</sub>	1028.4, 826.8, 623	MI-IR	635
V <sub>4</sub> O <sub>10</sub> <sup>-</sup>	<i>D</i> <sub>2d</sub>	990, 670, 637, 602	IR-MPD	636
V <sub>4</sub> O <sub>11</sub> <sup>-</sup>	<i>C</i> <sub>s</sub>	999, 990, 976, 899, 874, 824, 785, 721, 721, 684	IR-MPD	636b

<sup>a</sup> Abbreviations: MI-IR, matrix-isolation infrared spectroscopy; PES, photoelectron spectroscopy; IR-(M)PD, infrared (multiple) photon dissociation spectroscopy; ZEKE, zero-electron kinetic energy photoelectron spectroscopy. All the vibrational frequencies from MI-IR spectroscopy are obtained in solid argon.

double bonds due to the five valence electrons of vanadium, it is reasonable for the two terminal VO bonds in the V<sub>2</sub>O<sub>6</sub>

cluster to exhibit some intermediate properties with bond order roughly viewed as 1.5.<sup>633</sup> The observation of an O—O

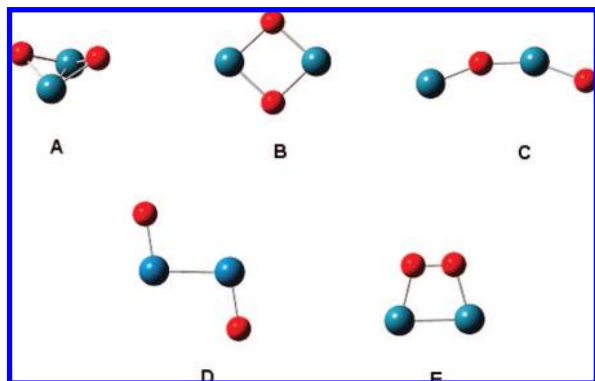


**Figure 18.** Experimentally observed structures for the  $M_2O_2$  clusters.

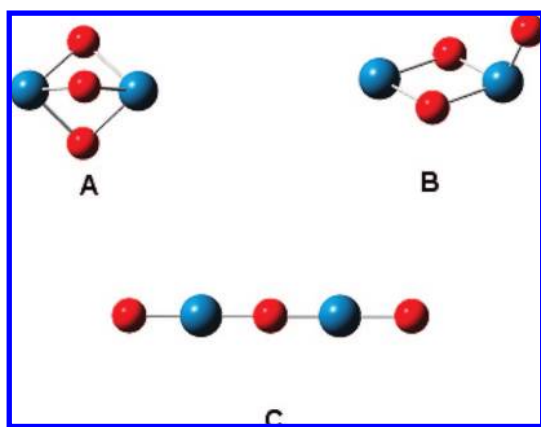


**Figure 19.** Experimentally observed structures for the  $M_2O_3$  clusters.

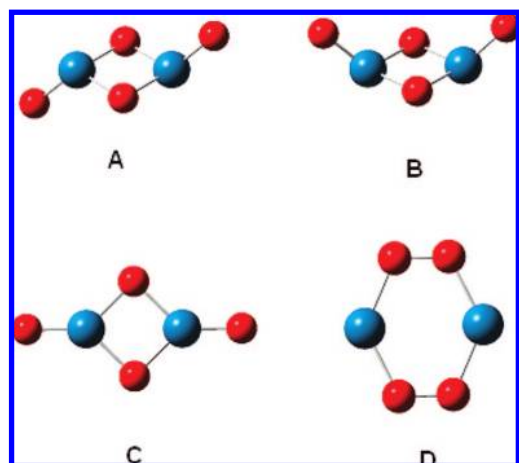


**Figure 20.** Experimentally observed structures for the  $M_2O_4$  clusters.

stretching vibration at  $1160\text{ cm}^{-1}$  in the IR photodissociation spectrum of  $V_2O_6^+$  (Figure 22) indicates that  $V_2O_6^+$  involves a superoxo group. In the ground state of  $V_2O_6^+$ , the two vanadyl groups occupy the trans position and the  $\eta^2$ -superoxo unit forms a three-membered ring with one of the two vanadium atoms (Figure 21E).<sup>630</sup> The  $V_2O_7$  and  $V_2O_7^-$  clusters are oxygen-rich species, and their ground-state structures are found to be similar to those of  $V_2O_6$  and  $V_2O_6^-$  except that one terminal oxygen atom is replaced by a peroxo  $O_2$  unit (Figure 23A,B).<sup>631,633</sup>

Higher multinuclear vanadium oxide clusters have also been the subject of several gas-phase and matrix experimental studies. By condensation of the gas evaporating from a

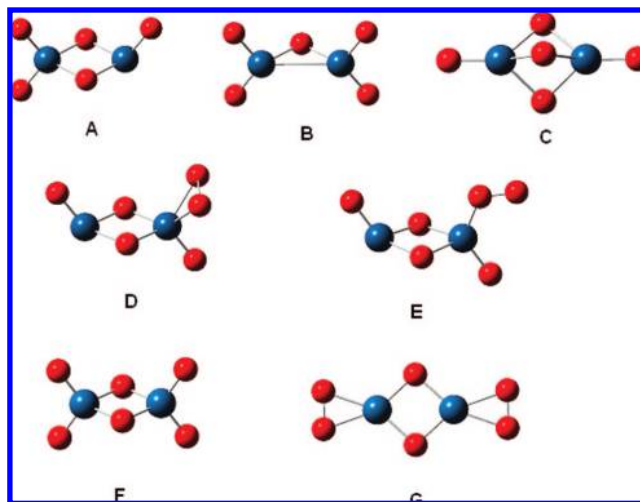


**Figure 21.** Experimentally observed structures for the  $M_2O_5$  and  $M_2O_6$  clusters.

Knudsen cell containing  $V_2O_5$ , two absorptions at  $1030$  and  $828\text{ cm}^{-1}$  in solid nitrogen are assigned to the terminal  $V=O$  and bridged  $V-O-V$  stretching vibrational modes of the neutral  $V_4O_{10}$  cluster, in analogy to  $P_4O_{10}$ .<sup>634</sup> Very recently, the  $V_4O_{10}$  cluster has been produced and trapped in solid argon and nitrogen matrices with high concentrations and comprehensively characterized by infrared, Raman, and UV/visible spectroscopy.<sup>635</sup> In addition, the  $V_4O_8$  and  $V_6O_{12}$  clusters were also suggested to be observed.

The infrared spectra of vanadium oxide anionic clusters have been studied by infrared multiple photodissociation spectroscopy.<sup>636</sup> Three types of anions including the open-shell  $(V_2O_5)_n^-$  anion, the fully oxidized closed-shell  $(V_2O_5)_nVO_3^-$  anions and the oxygen-rich  $V_4O_{11}^-$  cluster. Three types of vibrational modes in the range from  $600$  to  $1600\text{ cm}^{-1}$  are identified and assigned to (i) superoxo ( $\sim 1100\text{ cm}^{-1}$ ), (ii) vanadyl ( $1020\text{--}870\text{ cm}^{-1}$ ), and (iii)  $V-O-V$  and terminal  $V-O$  single bond vibrational modes ( $<950\text{ cm}^{-1}$ ). Comparison of the experimental and calculated spectra favors an assignment of the closed-shell  $V_3O_8^-$  anion to a  $C_{2v}$  structure consisting of a six-ring fused with a four-ring. For  $V_5O_{13}^-$ , two nearly isoenergetic isomers, a pyramidal  $C_{4v}$  structure and a bridged  $C_{2v}$  structure may be probed in the experiment. The spectra of the open-shell  $(V_2O_5)_n^-$  clusters are distinctly different from those of closed-shell clusters. The  $V_4O_{10}^-$  anion is characterized to have a tetragonal  $D_{2d}$  structure, which is minimally Jahn–Teller distorted from the  $T_d$  structure. It is found that the oxygen-rich  $V_4O_{11}^-$  anion does not exhibit a caged structure derived from the exceptionally stable  $V_4O_{10}$ , but an open structure is found. It is concluded that the dinuclear and trinuclear oxide anion clusters are characterized by open structures involving four-membered  $V_2O_2$  rings, but this motif is replaced by the less strained and more stable six- and eight-membered rings in the larger clusters.

The infrared spectra of vanadium and niobium oxide cationic clusters have been studied using mass-selected infrared photodissociation spectroscopy. The infrared spectra are obtained for the nearly stoichiometric  $(Nb_2O_5)_n^+$  and  $(Nb_2O_5)_nNbO_2^+$  ( $n = 2, 3$ ) clusters as well as for oxygen-rich clusters of typical compositions  $(Nb_2O_5)_nO^+$  and  $(Nb_2O_5)_nNbO_3^+$  ( $n = 1\text{--}3$ ).<sup>637</sup> The spectra of all examined oxide clusters exhibit two main absorption features that can be assigned to vibrations of terminal  $Nb=O$  and bridged

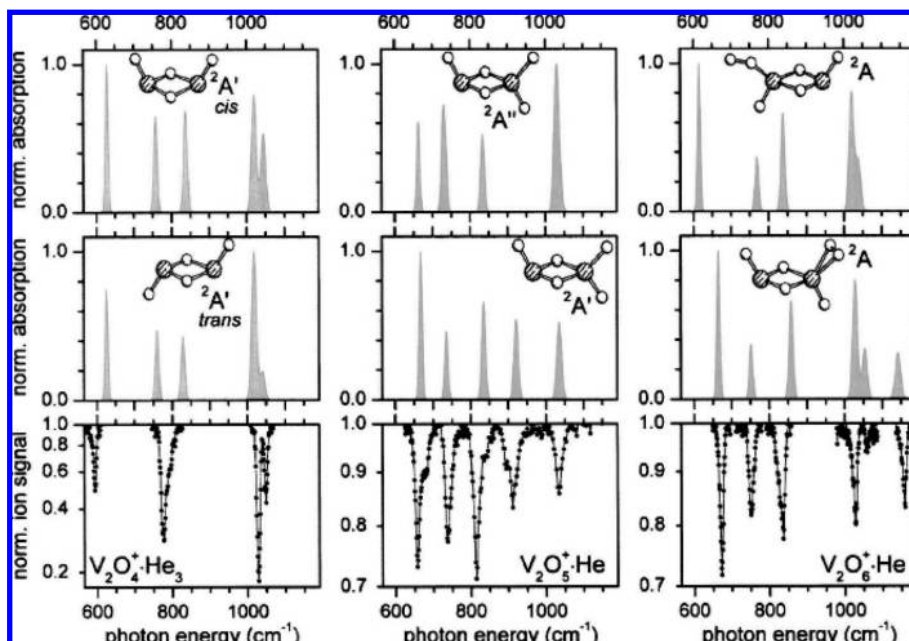


**Figure 22.** Experimental photodepletion spectra (solid black dots connected by black lines) of  $V_2O_4^+-He_3$  (left),  $V_2O_5^+-He$  (center), and  $V_2O_6^+-He$  (right) and simulated IR spectra (gray line and gray shaded area), based on scaled B3LYP/TZVP frequencies and relative intensities of the ground state (middle row) and an energetically low-lying isomer (top row) of  $V_2O_4^+$  (left),  $V_2O_5^+$  (center), and  $V_2O_6^+$  (right) in the region from 565 to 1190  $cm^{-1}$ . Reprinted with permission from ref 630. Copyright 2004 American Institute of Physics.

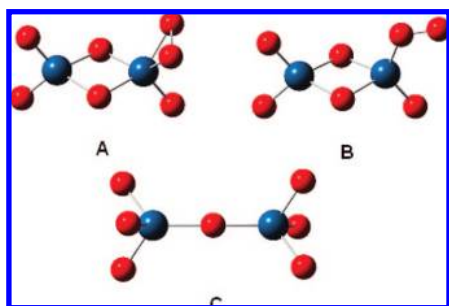


**Figure 23.** Experimentally observed structures for the  $M_2O_7$  clusters.

Nb–O–Nb oxide groups. The stretching vibrations of isolated Nb=O units absorb at about 990–1000  $cm^{-1}$ . The stretching vibrations of Nb–O–Nb bridges are found in the 700–900  $cm^{-1}$  range, varying with cluster size and stoichiometry. Comparisons between the experimental IR spectra and calculated spectra for possible structures help to identify the gas-phase structures of the clusters. The most stable structure of  $Nb_3O_8^+$  contains a peroxo  $\eta^2-O_2^{2-}$  unit. Fragmentation channels indicate that similar units are present in the larger  $(Nb_2O_5)_nO^+$  and  $(Nb_2O_5)_nNbO_3^+$  clusters. The  $Nb_4O_{10}^+$  cation is assumed to have a similar structure to that of neutral  $V_4O_{10}$ , which has  $T_d$  symmetry. Theoretical calculations give a minimum structure with  $C_1$  symmetry; however the distortion relative to  $T_d$  is small and mainly caused by the presence of one terminal single-bonded Nb–O unit, where the unpaired electron is located at the O atom. The photodissociation spectrum of  $V_4O_{10}^+$  recorded by monitoring the  $V_4O_8^+$  yield as a function of the excitation wavelength is very similar to that of the neutral  $V_4O_{10}$  cluster.<sup>638</sup> Two absorption bands at 842 and 1032  $cm^{-1}$  are observed, which are assigned to the antisymmetric V–O–V stretching and V=O stretching vibrations of the  $V_4O_{10}^+$  cation. In contrast to  $Nb_4O_{10}^+$ , the  $V_4O_{10}^+$  cation is determined to have a structure involving a  $V_4O_8^+$  ionic core weakly bound to an oxygen molecule.<sup>638</sup>

Multinuclear oxide clusters have also been the subject of gas-phase photoelectron spectroscopic studies. A high-resolution zero-electron kinetic energy (ZEKE) photoelectron spectroscopic study on the  $Nb_3O$  and  $Nb_3O^+$  monoxides observed a vibrational progression in a mode with frequencies of 312  $cm^{-1}$  in the cation and 320  $cm^{-1}$  in the neutral.<sup>639</sup> Density functional theory calculations and Franck–Condon spectral simulations indicate that  $Nb_3O$  and  $Nb_3O^+$  have low-spin, planar  $C_{2v}$  ground states with the O atom doubly bridging across the elongated bond of an isosceles Nb<sub>3</sub> cluster.<sup>639,640</sup> Vibrationally resolved 488 nm anion photoelectron spectra of  $V_3O$ ,  $Nb_3O$ , and  $Ta_3O$  indicate that the neutral and anionic clusters all have planar structures with doubly bridging oxygen atoms and that the electrons in the anions occupy essentially nonbonding orbitals.<sup>641</sup> The metal–oxygen symmetric stretching fundamentals for both the neutral and anionic clusters are reported. The ground-state of  $Nb_3O_2^-$  is found surprisingly to be a low-symmetry  $C_1$  ( $^1A$ ) structure, which contains a bridging and a terminal O atoms.<sup>642</sup> Anion photoelectron spectroscopic study on the  $Ta_3O_3^-$  anion shows that the  $Ta_3O_3^-$  cluster has a planar  $D_{3h}$  triangular structure.<sup>643</sup> Chemical-bonding analyses reveal that among the five valence molecular orbitals involved in the multicenter metal–metal bonding, there is a completely bonding  $\delta$  and  $\pi$  orbital formed from the 5d atomic orbitals of Ta. The totally delocalized multicenter d bond renders d aromaticity for  $Ta_3O_3^-$  and represents a new mode of chemical bonding. Similar PES studies have also been reported for higher clusters, but the spectra are not well vibrationally resolved.<sup>644,645</sup> Very high electron affinities and large HOMO–LUMO gaps are observed for the  $(V_2O_5)_n$  ( $n = 2–4$ ) clusters. The HOMO–LUMO gaps of  $(V_2O_5)_n$  all exceed that of the band gap of the bulk oxide and are found to increase with cluster size from  $n = 2–4$ . These clusters are predicted to possess polyhedral cage structures.<sup>645,646</sup>



## 5.4. Cr Group

Combined PES and DFT studies on  $\text{Cr}_2\text{O}^-$  imply that  $\text{Cr}_2\text{O}^-$  has a high-spin ground state ( $S = 9/2$ ) with  $C_{2v}$  symmetry.<sup>647–651</sup> However, the  $\text{Cr}_2\text{O}$  neutral is predicted to have a low-spin triplet ground state.<sup>194</sup> Two structural isomers with  $\text{Cr}_2\text{O}_2$  stoichiometry have been characterized in solid matrices. Besides the cyclic structure, which is predicted to have a nonet ground state, a chainlike  $\text{CrOCrO}$  isomer has also been identified in a recent matrix infrared spectroscopic study.<sup>652</sup> The  $\text{CrOCrO}$  cluster is predicted to have a  ${}^9\text{A}''$  ground state with bent geometry (Figure 18C). The cyclic structure is predicted to be more stable than the chainlike isomer from most theoretical studies.<sup>647–649</sup> The cyclic  $\text{Cr}_2\text{O}_2^-$  anion is calculated to have a high-spin ground state ( $S = 9/2$ ).<sup>651</sup> DFT calculations predict that  $\text{Cr}_2\text{O}_3^-$  possesses  $C_s$  symmetry and a puckered four-membered ring structure with an extra oxygen atom terminally bonded to one Cr atom (Figure 19B). A high-spin state ( $S = 7/2$ ) and a low-spin state ( $S = 1/2$ ) are nearly degenerate with the low-spin state only 0.04 eV higher in energy.<sup>649</sup> The PES data imply that the experimentally observed  $\text{Cr}_2\text{O}_3^-$  anion is due to a high-spin species.<sup>650</sup> The  $\text{Cr}_2\text{O}_4$  cluster is formed from the barrierless dimerization of the chromium dioxide molecules in solid argon, which is characterized to have a planar  $D_{2h}$  symmetry (Figure 20C).<sup>652</sup> The cluster is calculated to have a  ${}^5\text{A}_2$  ground state with the four unpaired electrons occupying the nonbonding molecular orbitals, which are largely chromium 3d in character.<sup>652</sup> A triplet state with nonplanar  $C_{2v}$  symmetry is proposed to be the ground state of  $\text{Cr}_2\text{O}_4$  by earlier theoretical calculations,<sup>647,648</sup> but this state is predicted to be much less stable than the  ${}^5\text{A}_2$  state planar  $D_{2h}$  structure based on recent DFT calculations.<sup>652</sup> The structure of  $\text{Cr}_2\text{O}_5$  is predicted to be similar to that of  $\text{Cr}_2\text{O}_4$  with the extra O atom bonded to one Cr atom (Figure 21A). The ground state of  $\text{Cr}_2\text{O}_5$  is predicted to be a singlet.<sup>647</sup> A vibrational progression of  $710\text{ cm}^{-1}$  in the PES spectrum is observed for the ground-state transition, which is likely due to a Cr–O stretching mode.<sup>650</sup> The  $\text{Cr}_2\text{O}_6$  cluster is also formed in our recent matrix infrared spectroscopic study on the reaction of chromium atom with dioxygen.<sup>652</sup> The observed vibrational frequencies indicate that the  $\text{Cr}_2\text{O}_6$  cluster involves a four-membered ring and two terminal oxygen atoms on each chromium centers. Theoretical calculations indicate that the  $\text{Cr}_2\text{O}_6$  cluster has a closed-shell singlet ground state with nonplanar  $D_{2h}$  symmetry (Figure 21F).<sup>232,647,652</sup> This structure is also suggested to be the structure observed in anion photoelectron spectroscopic investigation of the  $\text{Cr}_2\text{O}_6^-$  anion in gas phase.<sup>650</sup>

Dinuclear oxide clusters,  $\text{Mo}_2\text{O}_n^-$  ( $n = 2–4$ ) and  $\text{W}_2\text{O}_n^-$  ( $n = 1–6$ ), have also been studied by PES.<sup>653,654</sup> The  $\text{Mo}_2\text{O}_n$  clusters are in general similar to  $\text{W}_2\text{O}_n$ . The geometric and electronic structures of  $\text{W}_2\text{O}_n$  clusters are quite different from those of  $\text{Cr}_2\text{O}_n$  clusters for the very O-deficient systems from  $n = 1–3$ . The  $\text{Cr}_2\text{O}_n$  ( $n = 1–3$ ) clusters are ferromagnetic. Although the ground state of  $\text{W}_2\text{O}$  is a triplet state, the ground states of both  $\text{W}_2\text{O}_2$  and  $\text{W}_2\text{O}_3$  are singlets and nonmagnetic. The structures of the two systems are also very different. Whereas in  $\text{Cr}_2\text{O}_n$ , the first two O atoms bond to both Cr atoms in a bridging manner, in  $\text{W}_2\text{O}_n$  the first two O atoms each bond only to one W atom because of the strong W–O bond strength (Figure 18D). This leaves strong W–W bonding in the O-deficient  $\text{W}_2\text{O}_n$  clusters, resulting in nonmagnetic or very weak magnetic systems. For  $n = 4$  and higher, the  $\text{Cr}_2\text{O}_n$  and  $\text{W}_2\text{O}_n$  systems become similar as the

magnetic coupling in the Cr systems becomes weakened due to the loss of 3d electrons to oxygen. Density functional calculations establish that the  $\text{W}_2\text{O}_7^{2-}$ ,  $\text{W}_2\text{O}_7^-$ , and  $\text{W}_2\text{O}_7$  clusters possess different global minimum structures. The dianion is predicted to have a highly symmetric structure ( $D_{3d}$ , Figure 23C), in which the two  $\text{WO}_3$  moieties are connected by a single oxygen atom. Both the monoanion and neutral clusters are calculated to have lower symmetry ( $C_1$ ) with a cyclic  $\text{W}_2\text{O}_2$  four-membered ring. A terminal peroxo ligand bound to one tungsten center is predicted to be most stable for the neutral cluster (Figure 23A), while the isomer with a terminal oxo ligand ( $-\text{O}^\bullet$ ) is lowest in energy in the monoanion case. The calculated electron affinities are in good agreement with the experimental values.<sup>655</sup> Based on photoelectron spectroscopy and density functional theory calculations,<sup>656</sup> the  $\text{W}_2\text{O}_8^-$  anionic cluster is characterized as  $[\text{W}_2\text{O}_6(\text{O}_2^-)]$ , that is, a superoxide species interacting with the neutral  $\text{W}_2\text{O}_6$  cluster. In contrast, the neutral  $\text{W}_2\text{O}_8$  cluster is found to contain an  $\text{O}_2$  molecule weakly interacting with the  $\text{W}_2\text{O}_6$  cluster.

Well-resolved photoelectron spectra have been obtained for  $(\text{CrO}_3)_n^-$  ( $n = 3–5$ ) and compared with DFT calculations.<sup>227</sup> Unique nonplanar cyclic ring structures are firmly established for  $(\text{CrO}_3)_n$  and  $(\text{CrO}_3)_n^-$ . The structures can be described as formed from corner-sharing tetrahedral  $\text{CrO}_4$  units with two Cr=O  $\mu$ -oxo bonds and two Cr–O bridge bonds. The structural parameters of the  $(\text{CrO}_3)_n$  clusters are shown to converge rapidly to those of the  $\text{CrO}_3$  bulk crystal. The extra electron in the  $(\text{CrO}_3)_n^-$  anions is shown to be largely delocalized over all Cr centers. The  $(\text{MoO}_3)_n$  and  $(\text{WO}_3)_n$  clusters are predicted to have similar ring structures.<sup>232b</sup>

Electronic and structural properties of tritungsten oxide clusters:  $\text{W}_3\text{O}_n^-$  and  $\text{W}_3\text{O}_n$  ( $n = 7–11$ ) have been investigated using PES and density functional theory calculations.<sup>656,657</sup> Detachment features due to W 5d and O 2p features are observed in  $\text{W}_3\text{O}_7^-$  and  $\text{W}_3\text{O}_8^-$  with the 5d feature at lower electron binding energies and the O 2p features at very high electron binding energies.<sup>657</sup> A large energy gap is observed in the PES spectrum of the stoichiometric  $\text{W}_3\text{O}_9$  cluster. High electron binding energies ( $>7.0\text{ eV}$ ) are observed for  $\text{W}_3\text{O}_{10}^-$ , suggesting that the  $\text{W}_3\text{O}_{10}$  neutral cluster is an unusually strong oxidizing agent. The calculation results show that  $\text{W}_3\text{O}_9$  is a  $D_{3h}$  cluster with a  $\text{W}_3\text{O}_3$  six-membered ring and two terminal W=O units on each W site. The structure of  $\text{W}_3\text{O}_8$  can be viewed as removing a terminal O atom from  $\text{W}_3\text{O}_9$ , whereas that of  $\text{W}_3\text{O}_7$  can be viewed as removing two terminal O atoms from  $\text{W}_3\text{O}_9$ . The O-rich cluster  $\text{W}_3\text{O}_{10}$  can be viewed with replacing a terminal O atom in  $\text{W}_3\text{O}_9$  by an  $\text{O}_2$  unit. The  $\text{W}_3\text{O}_{11}^-$  anionic cluster is characterized as  $[\text{W}_3\text{O}_9(\text{O}_2^-)]$ , a superoxide species interacting with the neutral  $\text{W}_3\text{O}_9$  cluster. The neutral  $\text{W}_3\text{O}_{11}$  cluster is found to contain an  $\text{O}_2$  molecule weakly interacting with the  $\text{W}_3\text{O}_9$  cluster.<sup>656</sup> The  $\text{M}_3\text{O}_9^-$  and  $\text{M}_3\text{O}_9^{2-}$  clusters ( $\text{M} = \text{Mo}$  and  $\text{W}$ ) are characterized to involve a single, fully delocalized metal–metal bond and may be considered as a new class of d-orbital aromatic molecules.<sup>658</sup>

Recent photoelectron spectroscopic and theoretical studies on the  $\text{W}_4\text{O}_x^-$  ( $x \leq 6$ ) clusters reveal that tungsten oxide clusters undergo a transition from metal-like to semiconductor-like behavior with oxygen uptake at  $x = 5$ . The oxygen atoms are bound to the  $\text{W}_4$  cluster in either terminal or bridged fashions for both neutral and anionic  $\text{W}_4\text{O}_x^-$  ( $x = 1–4$ ) clusters, while the tetrahedral  $\text{W}_4$  core is changed to

ringlike structure with fewer metal–metal bonds in the  $W_4O_5$  case.<sup>659</sup> The structural and spectral properties of some multinuclear clusters have also been theoretically reported.<sup>660</sup>

## 5.5. Mn Group

The  $Mn_2O$  cluster is identified to possess high-spin state with ferromagnetic feature.<sup>661</sup> The  $Mn_2O_2$  cluster is regarded as a building block for bulk manganese oxide.<sup>241</sup> The  $Mn_2O_2$  cluster can be formed via the reaction of manganese dimer with dioxygen in solid argon and is characterized to have a rhombic structure.<sup>246,247</sup> It is predicted to have a high-spin ferromagnetic ground state with the unpaired electrons mainly distributed on the manganese atoms. Unlike the bare  $Mn_2$  dimer, which is considered as a weakly bound van der Waals system, the Mn–Mn interaction is enhanced in the rhombus  $Mn_2O_2$  cluster.<sup>241</sup> The distance between two manganese centers is predicted to be 2.56 Å, about 0.9 Å shorter than that of the manganese dimer.<sup>662</sup> The  $Mn_2O_6$  cluster has been spectroscopically characterized in solid argon matrix, which is determined to be a bisdioxygen complex of cyclic  $Mn_2O_2$  cluster.<sup>247</sup> The cluster is predicted to have a  $^1B_{1u}$  ground state with planar  $D_{2h}$  symmetry, in which the  $Mn_2O_2$  core is coordinated by two equivalent  $O_2$  molecules in a side-on fashion (Figure 21G). Based on the observed O–O stretching frequency and predicted O–O bond length, the two  $O_2$  subunits are due to superoxide ligands. Hence, the  $Mn_2O_6$  cluster can be described as  $[(O_2^-)_2(Mn_2O_2)^{2-}]$ , a disuperoxide complex.

There is no experimental report on spectroscopic study of multinuclear manganese oxide clusters except a photoelectron spectroscopic study on the  $Mn_5O$  and  $Mn_6O$  clusters. The results show that while the O atom occupies either a bridge or hollow site in  $Mn_5$ , it prefers a hollow site in  $Mn_6$  clusters.<sup>663</sup>

## 5.6. Fe Group

It is found that the ground-state iron dimer reacts with dioxygen directly to form the cyclic  $Fe_2O_2$  cluster without activation energy.<sup>270,320</sup> A slightly distorted rhombus structure with triplet state is found to be lowest in energy using density functional methods.<sup>320</sup> However, subsequent B3LYP calculations indicate that the cyclic  $Fe_2O_2$  cluster has a planar  $D_{2h}$  structure with a  $^7B_{2u}$  ground state, which is also confirmed by single-point CCSD(T) calculations. The existence of an effective Fe–Fe bonding is confirmed by NBO and Bader analyses.<sup>664</sup> The  $Fe_2O_4$  cluster has also been observed in solid argon from the dimerization reaction of the corresponding metal dioxide molecules.<sup>270</sup> Spectroscopically, only some small iron oxide clusters have been studied by PES in the gas phase.<sup>665,666</sup> The PES spectra for the  $Fe_2O_x$  ( $x = 1–5$ ) series are quite similar. Isomers are observed for the  $Fe_2O_x^-$  series when  $x > 1$ . These isomers are proposed to be complexes involving  $O_2$  or  $O_3$  units.<sup>268a</sup> The  $Fe_2O$  cluster is determined to have  $C_{2v}$  triangle structure. But the ground-state geometry of the  $Fe_2O^-$  anion changes drastically from that of the neutral. The anion is predicted to have a linear Fe–O–Fe structure.<sup>667</sup> The ground state of  $Fe_2O_3^-$  anion has a four-membered ring structure with an extra oxygen atom terminally bonded to one Fe atom (Figure 19B). The  $Fe_2O_4^-$  anion has a planar structure (Figure 20C), while in the neutral the two terminal O atoms are placed in a trans position with respect to the  $Fe_2O_2$  ring (Figure 20A).<sup>667</sup> The structural and magnetic properties of tri- and tetranuclear

anionic clusters,  $Fe_3O_m^-$  ( $m = 1–5$ ) and  $Fe_4O_m^-$  ( $m = 1–6$ ) are theoretically predicted by means of the first-principles molecular dynamics based on the density functional theory.<sup>668</sup> The structural and electronic structures of some neutral multinuclear iron oxide clusters have also been theoretically predicted.<sup>669–671</sup> First-principles electronic structure calculations show that small  $Fe_nO_n$  ( $n = 2–5$ ) clusters form single highly stable rings; starting at  $Fe_6O_6$ , these elementary rings begin to assemble into nano columnar structures to form stable  $Fe_nO_n$  ( $n = 6–12$ ) towers. The rings and the empty towers can be further stabilized by capping O atoms at the ends, leading to  $Fe_nO_{n+1}$  and  $Fe_nO_{n+2}$  sequences.<sup>669</sup> A very recent DFT calculation on both cage and noncage structures of  $(Fe_2O_3)_n$  ( $n = 2–6$  and 10) clusters shows that all the cage structures are stable, but the global minima are the noncage clusters for most cases.<sup>670</sup>

## 5.7. Co Group

The cyclic  $Co_2O_2$  cluster has been identified using matrix infrared spectroscopy.<sup>320</sup> Recent thermal evaporation experiments suggest that photoexcitation is required for the formation of the  $Co_2O_2$  cluster.<sup>672</sup> DFT calculations reveal that a  $^5B_{1g}$  state is less stable than a  $^7A_u$  state by 27 kcal/mol although the calculated frequencies for the former state seem to be more similar to the experimental values.<sup>320</sup> In a recent combined DFT and high-level ab initio theoretical study, a  $^1A_g$  state was predicted to be the ground state for the planar  $D_{2h}$   $Co_2O_2$  cluster. Its properties are better described by meta-GGA functional TPSS. Wave functional based ab initio calculations result in a number of closely spaced electronic states for this rhombus cluster, but the closed-shell singlet state is still a bit more stable.<sup>673</sup> The  $Co_2O_4$  cluster has also been observed in solid argon from the dimerization of the cobalt dioxide molecules.<sup>320</sup> It is suggested to have a similar structure to the other  $M_2O_4$  clusters, but detailed information on the electronic and geometric structure requires further theoretical study.

Anion photoelectron spectroscopy of mass-selected  $Co_n^-$   $O_m^-$  clusters ( $n = 4–20$ ;  $m = 0–2$ ) was performed at photon energies of 3.49 and 4.66 eV.<sup>674</sup> Main PES spectral features are contributed from Co 3d-derived orbitals throughout the complete series. The additional oxygen atoms indicate a minor influence toward the electronic structure. With increasing oxygen content, electron affinities shift to higher values. The experimental values are well reproduced by the DFT/B3LYP calculations.<sup>675</sup> There are no experimental reports on spectroscopic study of rhodium and iridium oxide clusters. The infrared vibrational spectra of low-lying isomers of rhodium oxide clusters have been predicted using density functional theory.<sup>676</sup>

## 5.8. Ni Group

The cyclic  $Ni_2O_2$  cluster has been identified in solid matrices.<sup>347,677</sup> Based on the unrestricted hybrid DFT calculations with a broken symmetry approach, an open shell singlet state, the vibrational frequencies of which were in good agreement with the experimental values, was predicted to be lowest in energy. Although a short Ni–Ni bond length was predicted for the  $D_{2h}$   $Ni_2O_2$  cluster, no direct bonding interactions were found between the two nickel centers.<sup>677</sup> The most recent MRCI calculations gave a  $^1A_g$  ground state for this cluster species, which correlates with the density functional results.<sup>678</sup>

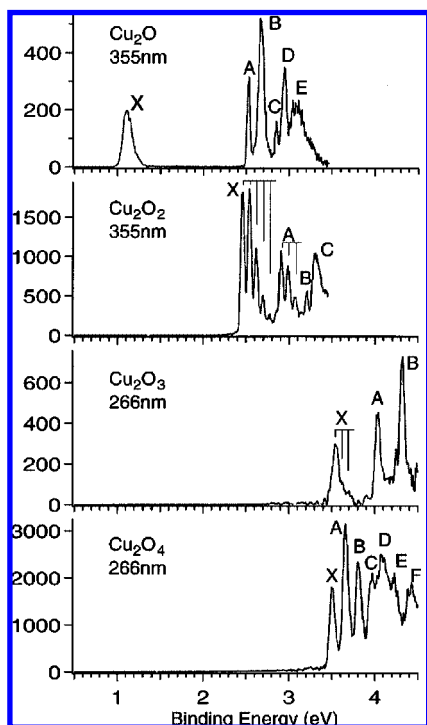


**Figure 24.** Photoelectron spectra of  $\text{Cu}_2\text{O}_x^-$  ( $x = 1-4$ ). The ground states of the neutral clusters are labeled “X”, and their low-lying electronic excited states are labeled with the alphabet. The vertical lines indicate the resolved vibrational structures. Reprinted with permission from ref 679. Copyright 1996 American Physical Society.

It was found that the palladium dimer interacts with dioxygen to form the  $\text{Pd}_2(\text{O}_2)$  complex under visible light excitation, in which the dioxygen molecule is predicted to be side-on bonded to the metal dimer with a planar  $C_{2v}$  symmetry (Figure 18E).<sup>380</sup> The  $\text{Pd}_2\text{O}_4$  cluster, which was characterized to be a bisdioxygen complex, has also been experimentally observed. It was predicted to have a singlet ground state with planar  $D_{2h}$  symmetry (Figure 20D).<sup>380</sup>

The structures of platinum oxide clusters have been studied using density functional methods. Clusters with  $\text{Pt}_x\text{O}_x$  ( $x > 2$ ) stoichiometry prefer to form closed ring-like structures with a bridged oxygen atom bound to two platinum atoms, which roughly form two-dimensional structures. The  $\text{Pt}_x\text{O}_{2x}$  clusters are found to possess nearly one-dimensional structures with periodical cyclic  $\text{Pt}_2\text{O}_2$  subunits. All of these structures are quite different from that of bulk platinum oxide.<sup>368</sup>

## 5.9. Cu Group

A PES study indicated that the  $\text{Cu}_2\text{O}$  cluster exhibits a large HOMO–LUMO gap (Figure 24), suggesting a closed-shell nature for this simple triatomic cluster.<sup>679</sup> Theoretical calculations revealed that the  $\text{Cu}_2\text{O}$  cluster possesses a bent  $C_{2v}$  geometry with the central oxygen atom bound to two copper atoms,<sup>679,680</sup> which can serve as the building block for the formation of larger copper oxide clusters via the active oxygen site.<sup>681</sup> The cationic cluster is predicted to be more bent than the anionic and neutral ones.<sup>680</sup>

Three structural isomers with  $\text{Cu}_2\text{O}_2$  stoichiometry have been experimentally characterized. Matrix isolation experiments show that the copper dimer is able to react with dioxygen in forming a  $\text{Cu}_2(\text{O}_2)$  complex, which is characterized to be a side-on bonded superoxide complex with a

$\text{Cu}-\text{Cu}$  bond (Figure 18E).<sup>682</sup> Upon near-infrared excitation, the  $\text{Cu}_2(\text{O}_2)$  complex isomerizes to a  $\text{CuOCuO}$  cluster, in which both oxygen atoms are atomically bound to the copper centers.<sup>682</sup> An anion photoelectron spectroscopic study revealed that the cyclic  $\text{Cu}_2\text{O}_2$  cluster is experimentally observed (Figure 18A).<sup>679</sup> Recent theoretical studies predicted that the linear or near linear  $\text{CuOCuO}$  structure is the most stable isomer with  $\text{Cu}_2\text{O}_2$  stoichiometry.<sup>680</sup> For  $\text{Cu}_2\text{O}_3$ , two isomers with close energies are predicted: a  $D_{3h}$  bipyramid (Figure 19A) and a  $C_{2v}$  bent structure with an  $\text{O}-\text{Cu}-\text{O}-\text{Cu}-\text{O}$  atomic arrangement. The  $D_{3h}$  isomer was proposed to be the observed structure in the gas-phase PES experiment.<sup>679</sup> However, recent DFT calculations suggested that the calculated electron affinity of a linear isomer (Figure 19C) is in better agreement with the experimental value.<sup>680</sup> A matrix-isolation infrared study indicated that the  $\text{Cu}_2\text{O}_4$  cluster is a side-on bonded dicopper bis-superoxide complex, which was predicted to have a  ${}^3\text{B}_{3u}$  ground state with a planar  $D_{2h}$  symmetry (Figure 20D). The  $\text{Cu}-\text{Cu}$  distance in the  $\text{Cu}_2\text{O}_4$  complex was computed to be quite long, indicating no direct bonding interaction between the two copper atoms.<sup>682</sup> The dicopper bis-superoxide structure is also proposed as the photodetachment product of the corresponding anion in the gas phase.<sup>679</sup> Vibrationally resolved PES studies on larger  $\text{Cu}_x\text{O}_2^-$  clusters ( $x = 6-11$ ) indicate that  $\text{O}_2$  molecularly adsorbs on the  $\text{Cu}_x^-$  anionic clusters.<sup>683</sup>

The  $\text{Au}_2\text{O}^-$  anion is characterized to have a near linear doublet ground state with direct  $\text{Au}-\text{Au}$  bond.<sup>684</sup> Recent time-resolved photoelectron spectroscopic study on  $\text{Au}_2\text{O}^-$  suggests the existence of a long-lived excited state with the lifetime being more than 100 ps.<sup>685</sup> The PES spectrum of the  $\text{Au}_4\text{O}^-$  anionic cluster was also recorded.<sup>684</sup> The calculation results showed that the geometric structure of  $\text{Au}_4^-$  is significantly modified upon the chemisorption of atomic oxygen.<sup>684</sup>

Dioxygen adsorption on silver and gold anionic clusters has been studied using vibrationally resolved photoelectron spectroscopy. The results have been summarized in a recent review.<sup>686</sup> In general, the odd-numbered silver and gold anionic clusters were unreactive toward dioxygen, while the even-numbered clusters interacted with dioxygen to form  $\text{M}_x\text{O}_2^-$  clusters ( $\text{M} = \text{Ag}, \text{Au}$ ). PES investigations on these  $\text{M}_x\text{O}_2^-$  anionic clusters showed that  $\text{O}_2$  molecularly adsorbs on the metal clusters,<sup>684,687</sup> in agreement with theoretical predictions.<sup>449,452,688-690</sup> Besides the molecularly adsorbed clusters, dissociative adsorption species were also reported. For  $\text{Au}_4\text{O}_2^-$  anionic cluster, the dissociative oxide isomer can be prepared by using atomic oxygen reagent.<sup>691</sup> The formation of dissociative oxide clusters was predicted to be thermodynamically favored but kinetically hindered due to the existence of a high energy barrier.<sup>692,693</sup>

Most theoretical calculations indicate that  $\text{O}_2$  adsorbs molecularly on small gold clusters such as  $\text{Au}_3$  and  $\text{Au}_5$ .<sup>452,689,692</sup> But dissociative adsorption is predicted to be more favorable for larger  $\text{Au}_x$  clusters with  $x > 3$  in a recent theoretical study, and the geometric structures of gold clusters are strongly distorted upon  $\text{O}_2$  adsorption.<sup>693</sup> For both the neutral and anionic  $\text{Au}_{24}$  clusters, density functional calculations indicated that  $\text{O}_2$  prefers to adsorb on the tubelike gold clusters molecularly in the side-on fashion. The binding energy between neutral  $\text{Au}_{24}$  and  $\text{O}_2$  is comparable to that of small neutral odd-numbered gold clusters.<sup>694</sup> The oxide products from  $\text{O}_2$  dissociative adsorption on both  $\text{Au}_{32}$  ( $I_h$ ) and  $\text{Au}_{32}$  ( $C_1$ ) clusters are predicted to be more stable than

the molecularly adsorbed isomers, although the Au<sub>32</sub> (*I<sub>h</sub>*) cluster is found to be highly inert chemically.<sup>695</sup>

## 6. Summary

Transition metal oxides and dioxygen complexes are potential intermediates or products during the oxidation of metal atoms or clusters and are of major importance in a wide range of catalytic and biological processes. Spectroscopic and theoretical investigations of these species are therefore of considerable interest and are reviewed and summarized.

Matrix infrared spectroscopy has provided a powerful technique for the investigation of transition metal oxide molecules and their cations and anions. The formation of subject species can be integrated over time to accumulate a sufficient number density in the matrix to afford the measurement of a suitable vibrational spectrum. Isotopic substitution is straightforward and important for the identification of subject species. Laser ablation provides a convenient source of transition metal atoms, cations, and electrons for the synthetic preparation of the subject species, and a source of excitation when such activation is needed to promote the reaction with oxygen molecules. The forming matrix is unique in that it quenches reaction energies and allows triatomic molecules such as MO<sub>2</sub> to be stabilized where the gas-phase reaction provides only MO diatomic molecules. Doping of the sample with an electron-trapping molecule such as CCl<sub>4</sub> aids in the identification of cations and anions. The condensing matrix allows for the formation of further oxygen-rich MO<sub>*x*</sub> (*x* ≥ 3) complexes between initial products and additional reagent molecules, which reveal rich structure and bonding properties.

Molecular spectroscopies such as laser-induced fluorescence (LIF), resonance-enhanced multiple photon ionization spectroscopy (REMPI), pulsed-field ionization zero kinetic energy (PFI-ZEKE) photoelectron spectroscopy, and rotational spectroscopy offer precise and detailed measurements of vibrational or rotational transitions of simple transition metal oxide molecules in the gas phase. Photoelectron spectroscopy is another quite powerful method, which provides direct information on the electron affinities, low-lying electronic states, and vibrational frequencies of size-selected transition metal–oxygen molecules and small clusters in the gas phase. Although the vibrational assignment is less accurate due to limited resolution compared with other spectroscopic methods, PES is a versatile and convenient method in gas phase studies, which complements the extensively used matrix-isolation infrared spectroscopic investigations.

Spectral and structural assignments for sized transition metal oxide clusters are quite difficult due to the existence of many low-energy isomers and low-lying electronic states. With the development of tunable IR lasers, infrared photon dissociation spectroscopy has recently been successfully used to measure the vibrational spectra of some mass-selected transition metal oxide clusters in the gas phase, which can provide reliable structural assignments for these cluster species. The well-resolved vibrational spectroscopic data combined with the state-of-the-art quantum chemical calculations may provide a very powerful and applicable approach to motivate further detailed understanding of the geometric and electronic structures and bonding and reactivity of more complicated oxygen-rich transition metal oxygen complexes as well as transition metal oxide clusters.

## 7. Acknowledgments

The authors gratefully acknowledge financial support from the National Basic Research Program of China (Grant Nos. 2004CB719501 and 2007CB815203) and the National Natural Science Foundation of China (Grant No. 20773030).

## 8. References

- (1) (a) Rao, C. N. R.; Raveau, B. *Transition Metal Oxides*; VCH: New York, 1995. (b) Rao, C. N. R. *Annu. Rev. Phys. Chem.* **1989**, *40*, 291. (c) Cox, P. A. *Transition Metal Oxides: An Introduction to their Electronic Structure and Properties*; Clarendon: Oxford, U.K., 1992.
- (2) (a) Kieber-Emmons, M. T.; Riordan, C. G. *Acc. Chem. Res.* **2007**, *40*, 618. (b) Cramer, C. J.; Tolman, W. B. *Acc. Chem. Res.* **2007**, *40*, 601. (c) Chufán, E. E.; Puiui, S. C.; Karlin, K. D. *Acc. Chem. Res.* **2007**, *40*, 563. (d) Korendovych, I. V.; Kryatov, S. V.; Rybak-Akimova, E. V. *Acc. Chem. Res.* **2007**, *40*, 510.
- (3) (a) Mirica, L. M.; Ottenwaelder, X.; Stack, T. D. P. *Chem. Rev.* **2004**, *104*, 1013. (b) Costas, M.; Mehn, M. P.; Jensen, M. P.; Que, L., Jr. *Chem. Rev.* **2004**, *104*, 939. (c) Crans, D. C.; Smee, J. J.; Gaidamauskas, E.; Yang, L. Q. *Chem. Rev.* **2004**, *104*, 849. (d) Lewis, E. A.; Tolman, W. B. *Chem. Rev.* **2004**, *104*, 1047.
- (4) (a) Solomon, E. I.; Tuzcek, F.; Root, D. E.; Brown, C. A. *Chem. Rev.* **1994**, *94*, 827. (b) Pecoraro, V. L.; Baldwin, M. J.; Gelasco, A. *Chem. Rev.* **1994**, *94*, 807. (c) Kitajima, N.; Moro-oka, Y. *Chem. Rev.* **1994**, *94*, 737. (d) Momenteau, M.; Reed, C. A. *Chem. Rev.* **1994**, *94*, 659. (e) Bytheway, I.; Hall, M. B. *Chem. Rev.* **1994**, *94*, 639. (f) Butler, A.; Clague, M. J.; Meister, E. *Chem. Rev.* **1994**, *94*, 625. (g) Dickman, M. H.; Pope, M. T. *Chem. Rev.* **1994**, *94*, 569.
- (5) (a) Lanci, M. P.; Brinkley, D. W.; Stone, K. L.; Smirnov, V. V.; Roth, J. P. *Angew. Chem., Int. Ed.* **2005**, *44*, 7273. (b) Smirnov, V. V.; Brinkley, D. W.; Lanci, M. P.; Karlin, K. D.; Roth, J. P. *J. Mol. Catal. A* **2006**, *251*, 100. (c) Karlin, K. D.; Tolman, W. B.; Kaderli, S.; Zuberbühler, A. D. *J. Mol. Catal. A* **1997**, *117*, 215.
- (6) Jena, P.; Castleman, A. W., Jr. *Proc. Natl. Acad. Sci. U.S.A.* **2006**, *103*, 10560.
- (7) Lai, X.; Goodman, D. W. *J. Mol. Catal. A* **2000**, *162*, 1647.
- (8) (a) Pramann, A.; Rademann, K. *Int. J. Mass Spectrom.* **2001**, *209*, 1. (b) Optiz-Coutureau, J.; Fielicke, A.; Kaiser, B.; Rademann, K. *Phys. Chem. Chem. Phys.* **2001**, *3*, 3034. (c) Justes, D. R.; Mitrić, R.; Moore, N. A.; Bonačić-Koutecký, V.; Castleman, A. W., Jr. *J. Am. Chem. Soc.* **2003**, *125*, 6289. (d) Kimble, M. L.; Castleman, A. W., Jr.; Mitrić, R.; Bürgel, C.; Bonačić-Koutecký, V. *J. Am. Chem. Soc.* **2004**, *126*, 2526. (e) Fialko, E. F.; Kikhtenko, A. V.; Goncharov, V. B.; Zamaraev, K. I. *J. Phys. Chem. B* **1997**, *101*, 5772.
- (9) (a) Zemski, K. A.; Justes, D. R.; Castleman, A. W., Jr. *J. Phys. Chem. B* **2002**, *106*, 6136. (b) Bell, R. C.; Zemski, K. A.; Castleman, A. W., Jr. *J. Cluster Sci.* **1999**, *10*, 509. (c) Johnson, G. E.; Mitrić, R.; Bonačić-Koutecký, V.; Castleman, A. W., Jr. *Chem. Phys. Lett.* **2009**, *475*, 1.
- (10) (a) Feyel, S.; Schröder, D.; Schwarz, H. *Eur. J. Inorg. Chem.* **2008**, 4961. (b) Feyel, S.; Scharfenberg, L.; Daniel, C.; Hartl, H.; Schröder, D.; Schwarz, H. *J. Phys. Chem. A* **2007**, *111*, 3278. (c) Feyel, S.; Schröder, D.; Schwarz, H. *J. Phys. Chem. A* **2006**, *110*, 2647. (d) Schröder, D.; Schwarz, H. *Top. Organomet. Chem.* **2007**, *22*, 1. (e) Zhang, X. G.; Armentrout, P. B. *J. Phys. Chem. A* **2003**, *107*, 8915. (f) Sievers, M. R.; Armentrout, P. B. *Int. J. Mass Spectrom.* **1999**, *185/186/187*, 117. (g) Sievers, M. R.; Armentrout, P. B. *Inorg. Chem.* **1999**, *38*, 397. (h) Sievers, M. R.; Armentrout, P. B. *Int. J. Mass Spectrom.* **1998**, *179/180*, 103. (i) Sievers, M. R.; Armentrout, P. B. *J. Phys. Chem. A* **1998**, *102*, 10754. (j) Schröder, D.; Schwarz, H.; Clemmer, D. E.; Chen, Y.; Armentrout, P. B.; Baranov, V.; Bohme, D. K. *Int. J. Mass Spectrom. Ion Processes* **1997**, *161*, 175. (k) Chen, Y. M.; Clemmer, D. E.; Armentrout, P. B. *J. Am. Chem. Soc.* **1994**, *116*, 7815.
- (11) (a) Reed, Z. D.; Duncan, M. A. *J. Phys. Chem. A* **2008**, *112*, 5354. (b) Molek, K. S.; Anfusio-Cleary, C.; Duncan, M. A. *J. Phys. Chem. A* **2008**, *112*, 9238. (c) Molek, K. S.; Reed, Z. D.; Ricks, A. M.; Duncan, M. A. *J. Phys. Chem. A* **2007**, *111*, 8080. (d) Molek, K. S.; Jaeger, T. D.; Duncan, M. A. *J. Chem. Phys.* **2005**, *123*, 144313.
- (12) (a) Xie, Y.; Dong, F.; Heinbuch, S.; Rocca, J. J.; Bernstein, E. R. *J. Chem. Phys.* **2009**, *130*, 114306. (b) Dong, F.; Heinbuch, S.; Xie, Y.; Rocca, J. J.; Bernstein, E. R. *J. Phys. Chem. A* **2009**, *113*, 3029. (c) Dong, F.; Heinbuch, S.; Xie, Y.; Bernstein, E. R.; Rocca, J. J.; Wang, Z. C.; Ding, X. L.; He, S. G. *J. Am. Chem. Soc.* **2009**, *131*, 1057. (d) Xue, W.; Wang, Z. C.; He, S. G.; Xie, Y.; Bernstein, E. R. *J. Am. Chem. Soc.* **2008**, *130*, 15879. (e) He, S. G.; Xie, Y.; Dong, F.; Heinbuch, S.; Jakubikova, E.; Rocca, J. J.; Bernstein, E. R. *J. Phys. Chem. A* **2008**, *112*, 11067. (f) Dong, F.; Heinbuch, S.; Xie, Y.; Rocca, J. J.; Bernstein, E. R.; Wang, Z. C.; Deng, K.; He, S. G. *J. Am. Chem. Soc.* **2008**, *130*, 1932.

- (13) Andrews, L.; Moskovits, M. *Chemistry and Physics of Matrix-Isolated Species*; North-Holland: Amsterdam, The Netherlands, 1989.
- (14) Moskovits, M.; Ozin, G. A. *Matrix Cryochemistry Using Transition Metal Atoms. Cryochemistry*; Wiley: New York, 1976.
- (15) (a) Zhou, M. F.; Andrews, L.; Bauschlicher, C. W., Jr. *Chem. Rev.* **2001**, *101*, 1931. (b) Andrews, L.; Citra, A. *Chem. Rev.* **2002**, *102*, 885.
- (16) (a) Wang, G. J.; Zhou, M. F. *Int. Rev. Phys. Chem.* **2008**, *27*, 1. (b) Andrews, L. *Chem. Soc. Rev.* **2004**, *33*, 123. (c) Andrews, L.; Cho, H. G. *Organometallics* **2006**, *25*, 4040.
- (17) (a) Himmel, H. J.; Downs, A. J.; Greene, T. M. *Chem. Rev.* **2002**, *102*, 4191. (b) Himmel, H. J.; Reiher, M. *Angew. Chem., Int. Ed.* **2006**, *45*, 6264.
- (18) (a) Khriachtchev, L.; Räsänen, M.; Gerber, R. B. *Acc. Chem. Res.* **2009**, *42*, 183. (b) Gerber, R. B. *Annu. Rev. Phys. Chem.* **2004**, *55*, 55.
- (19) Mascetti, J.; Galan, F.; Pápai, I. *Coord. Chem. Rev.* **1999**, *190–192*, 557.
- (20) (a) Perutz, R. N. *Chem. Rev.* **1985**, *85*, 77. (b) Perutz, R. N. *Chem. Rev.* **1985**, *85*, 97.
- (21) (a) Jacox, M. E. *Chem. Phys.* **1994**, *189*, 149. (b) Jacox, M. E. *J. Phys. Chem. Ref. Data* **1998**, *27*, 115. (c) Jacox, M. E. *J. Phys. Chem. Ref. Data* **2003**, *32*, 1.
- (22) (a) Jacox, M. E. *Chem. Soc. Rev.* **2002**, *31*, 108. (b) Jacox, M. E. *Acc. Chem. Res.* **2004**, *37*, 727. (c) Jacox, M. E. *Int. J. Mass Spectrom.* **2007**, *267*, 268.
- (23) Beattie, I. R. *Angew. Chem., Int. Ed.* **1999**, *38*, 3294.
- (24) Merer, A. J. *Annu. Rev. Phys. Chem.* **1989**, *40*, 407.
- (25) Huber, K. P.; Herzberg, G. *Constants of Diatomic Molecules*; Van Nostrand-Reinhold: New York, 1979.
- (26) Wang, L. S. Photodetachment Photoelectron Spectroscopy of Transition Metal Oxide Species. In *Photoionization and Photodetachment*; Ng, C. Y., Ed.; Advanced Series in Physical Chemistry, Vol. 10. World Scientific: Singapore, 2000; Chapter 16.
- (27) Harrison, J. F. *Chem. Rev.* **2000**, *100*, 679.
- (28) (a) Gutsev, G. L.; Andrews, L.; Bauschlicher, C. W., Jr. Structure and chemical bonding of 3d-metal anions. In *Theoretical Prospects of Negative Ions*; Kalcher, J., Ed.; Research Signpost: Trivandrum, India, 2002, pp 43–60. (b) Langhoff, S. R.; Bauschlicher, C. W., Jr. *Annu. Rev. Phys. Chem.* **1988**, *39*, 181.
- (29) Kretzschmar, I.; Schröder, D.; Schwarz, H.; Armentrout, P. B. The binding in neutral and cationic 3d and 4d transition-metal monoxides and sulfides. In *Advances in Metal and Semiconductor Clusters*; Elsevier Science: Amsterdam, 2001; Vol. 5, pp 347–395.
- (30) (a) Ozin, G. A. *Acc. Chem. Res.* **1977**, *10*, 21. (b) Ozin, G. A.; Vander Voet, A. *Acc. Chem. Res.* **1973**, *6*, 313.
- (31) Bondybey, V. E.; Smith, A. M.; Agreiter, J. *Chem. Rev.* **1996**, *96*, 2113.
- (32) Cramer, C. J.; Tolman, W. B.; Theopold, K. H.; Rheingold, A. L. *Proc. Natl. Acad. Sci. U.S.A.* **2003**, *100*, 3635.
- (33) Akita, M.; Moro-oka, Y. *Catal. Today* **1998**, *44*, 183.
- (34) Gubelmann, M. H.; Williams, A. F. *Struct. Bonding (Berlin)* **1983**, *55*, 1.
- (35) Vaska, L. *Acc. Chem. Res.* **1976**, *9*, 175.
- (36) Valentine, J. S. *Chem. Rev.* **1973**, *73*, 235.
- (37) (a) Andrews, L.; Liang, B. Y.; Li, J.; Bursten, B. E. *J. Am. Chem. Soc.* **2003**, *125*, 3126. (b) Liang, B. Y.; Andrews, L.; Li, J.; Bursten, B. E. *J. Am. Chem. Soc.* **2002**, *124*, 9016.
- (38) Zhao, Y. Y.; Gong, Y.; Zhou, M. F. *J. Phys. Chem. A* **2006**, *110*, 10777.
- (39) (a) Andrews, L.; Liang, B. Y.; Li, J.; Bursten, B. E. *New J. Chem.* **2004**, *28*, 289. (b) Liang, B. Y.; Andrews, L.; Li, J.; Bursten, B. E. *Inorg. Chem.* **2004**, *43*, 882. (c) Liang, B. Y.; Andrews, L.; Li, J.; Bursten, B. E. *Chem.—Eur. J.* **2003**, *9*, 4781.
- (40) (a) Engelking, P. C.; Lineberger, W. C. *J. Chem. Phys.* **1977**, *66*, 5054. (b) Andersen, T.; Lykke, K. R.; Neumark, D. M.; Lineberger, W. C. *J. Chem. Phys.* **1987**, *86*, 1858.
- (41) (a) Hotop, H.; Lineberger, W. C. *J. Chem. Phys.* **1973**, *58*, 2379. (b) Stevens, A. E.; Feigerle, C. S.; Lineberger, W. C. *J. Chem. Phys.* **1983**, *78*, 5420. (c) Leopold, D. G.; Lineberger, W. C. *J. Chem. Phys.* **1986**, *85*, 51.
- (42) Wang, L. S.; Chen, H. S.; Fan, J. *J. Chem. Phys.* **1995**, *102*, 9480.
- (43) (a) Weltner, W., Jr. *Magnetic Atoms and Molecules*; Scientific and Academic Edition: New York, 1983. (b) Van Zee, R. J.; Li, S. J. *Phys. Chem.* **1995**, *99*, 6277.
- (44) Van Zee, R. J.; Brown, C. M.; Zeringue, K. J.; Weltner, W., Jr. *Acc. Chem. Res.* **1980**, *13*, 237.
- (45) Duncan, M. A. *Int. Rev. Phys. Chem.* **2003**, *22*, 407.
- (46) (a) Oomens, J.; Sartakov, B. G.; Meijer, G.; von Helden, G. *Int. J. Mass Spectrom.* **2006**, *254*, 1. (b) von Helden, G.; van Heijnsbergen, D.; Meijer, G. *J. Phys. Chem. A* **2003**, *107*, 1671.
- (47) Hirota, E. *Annu. Rep. Prog. Chem., Sect. C* **2000**, *96*, 95.
- (48) Bernath, P. F. *Annu. Rep. Prog. Chem., Sect. C* **2000**, *96*, 177.
- (49) Demtroder, W. *Laser Spectroscopy*; Springer-Verlag: Berlin, 2002.
- (50) (a) Schlag, E. W. *ZEKE Spectroscopy*; Cambridge University Press: Cambridge, U.K., 1998. (b) Cockett, M. C. R. *Chem. Soc. Rev.* **2005**, *34*, 935.
- (51) (a) Head-Gordon, M.; Pople, J. A.; Frisch, M. J. *Chem. Phys. Lett.* **1988**, *153*, 503. (b) Frisch, M. J.; Head-Gordon, M.; Pople, J. A. *Chem. Phys. Lett.* **1990**, *166*, 275. (c) Pople, J. A.; Seeger, R.; Krishnan, R. *Int. J. Quantum Chem. Symp.* **1976**, *10*, 1. (d) Pople, J. A.; Seeger, R.; Krishnan, R. *Int. J. Quantum Chem. Symp.* **1977**, *11*, 149. (e) Krishnan, R.; Pople, J. A. *Int. J. Quantum Chem.* **1978**, *14*, 91.
- (52) Pople, J. A.; Gordon, M. H.; Raghavachari, K. *J. Chem. Phys.* **1987**, *87*, 5968.
- (53) Sousa, S. F.; Fernandes, P. A.; Ramos, M. J. *J. Phys. Chem. A* **2007**, *111*, 10439.
- (54) Zhao, Y.; Truhlar, D. G. *Acc. Chem. Res.* **2008**, *41*, 157.
- (55) (a) Hegarty, D.; Robb, M. A. *Mol. Phys.* **1979**, *38*, 1795. (b) Eade, R. H. E.; Robb, M. A. *Chem. Phys. Lett.* **1981**, *83*, 362. (c) Schlegel, H. B.; Robb, M. A. *Chem. Phys. Lett.* **1982**, *93*, 43. (d) Bernardi, F.; Bottini, A.; McDougall, J. J. W.; Robb, M. A.; Schlegel, H. B. *Faraday Symp. Chem. Soc.* **1984**, *19*, 137.
- (56) (a) Burton, P. G.; Buenker, R. J.; Bruna, P. J.; Peyerimhoff, S. D. *Chem. Phys. Lett.* **1983**, *95*, 379. (b) Bauschlicher, C. W., Jr.; Taylor, P. R. *J. Chem. Phys.* **1987**, *86*, 858. (c) Shavitt, I.; Brown, F. B.; Burton, P. G. *Int. J. Quantum Chem.* **1987**, *31*, 507.
- (57) Li, Z. H.; Gong, Y.; Fan, K. N.; Zhou, M. F. *J. Phys. Chem. A* **2008**, *112*, 13641.
- (58) Pyykkö, P. *Chem. Rev.* **1988**, *88*, 563.
- (59) Pepper, M.; Bursten, B. E. *Chem. Rev.* **1991**, *91*, 719.
- (60) Piechota, J.; Suffczynski, M. Z. *Phys. Chem.* **1997**, *200*, 39.
- (61) Baranowska, A.; Siedlecka, M.; Sadlej, A. J. *Theor. Chem. Acc.* **2007**, *118*, 959.
- (62) Jensen, K. P.; Roos, B. O.; Ryde, U. *J. Chem. Phys.* **2007**, *126*, 14103.
- (63) Dai, B.; Deng, K. M.; Yang, J. L.; Zhu, Q. S. *J. Chem. Phys.* **2003**, *118*, 9608.
- (64) (a) Gutsev, G. L.; Andrews, L.; Bauschlicher, C. W., Jr. *Theor. Chem. Acc.* **2003**, *109*, 298. (b) Bauschlicher, C. W., Jr.; Maitre, P. *Theor. Chim. Acta* **1995**, *90*, 189.
- (65) Gutsev, G. L.; Rao, B. K.; Jena, P. *J. Phys. Chem. A* **2000**, *104*, 5374.
- (66) Bridgeman, A. J.; Rothery, J. *J. Chem. Soc., Dalton Trans.* **2000**, 211.
- (67) Bakalbassis, E. G.; Stiakaki, M. A. D.; Tsipis, A. C.; Tsipis, C. A. *Chem. Phys.* **1996**, *205*, 389.
- (68) (a) Anderson, A. B.; Hong, S. Y.; Smialek, J. L. *J. Phys. Chem.* **1987**, *91*, 4250. (b) Anderson, A. B.; Grimes, R. W.; Hong, S. Y. *J. Phys. Chem.* **1987**, *91*, 4245.
- (69) Dolg, M.; Wedig, U.; Stoll, H.; Preuss, H. *J. Chem. Phys.* **1987**, *86*, 2123.
- (70) Siegbahn, P. E. M. *Chem. Phys. Lett.* **1993**, *201*, 15.
- (71) Song, P.; Guan, W.; Yao, C.; Su, Z. M.; Wu, Z. J.; Feng, J. D.; Yan, L. K. *Theor. Chem. Acc.* **2007**, *117*, 407.
- (72) Kharat, B.; Deshmukh, S. B.; Chaudhari, A. *Int. J. Quantum Chem.* **2009**, *109*, 1103.
- (73) Yao, C.; Guan, W.; Song, P.; Su, Z. M.; Feng, J. D.; Yan, L. K.; Wu, Z. J. *Theor. Chem. Acc.* **2007**, *117*, 115.
- (74) Wu, Z. J.; Guan, W.; Meng, J.; Su, Z. M. *J. Cluster Sci.* **2007**, *18*, 444.
- (75) Dolg, M.; Stoll, H. *Theor. Chim. Acta* **1989**, *75*, 369.
- (76) Uzunova, E. L.; Mikosch, H.; Nikolov, G. St. *J. Chem. Phys.* **2008**, *128*, 094307.
- (77) Gutsev, G. L.; Rao, B. K.; Jena, P. *J. Phys. Chem. A* **2000**, *104*, 11961.
- (78) Siegbahn, P. E. M. *J. Phys. Chem.* **1993**, *97*, 9096.
- (79) (a) Wilson, E. B., Jr.; Decius, J. C.; Cross, P. C. *Molecular Vibrations*; McGraw-Hill: New York, 1955. (b) Herzberg, G. *Molecular Spectra and Molecular Structure. II. Infrared and Raman Spectra of Polyatomic Molecules*; Van Nostrand: Princeton, NJ, 1945.
- (80) Allavena, M.; Rysnik, R.; White, D.; Calder, V.; Mann, D. E. *J. Chem. Phys.* **1969**, *50*, 3399.
- (81) (a) Brabson, G. D.; Mielke, Z.; Andrews, L. *J. Phys. Chem.* **1991**, *95*, 79. (b) Thorwirth, S.; McCarthy, M. C.; Gottlieb, C. A.; Thaddeus, P.; Gupta, H.; Stanton, J. F. *J. Chem. Phys.* **2005**, *123*, 054326.
- (82) (a) Weltner, W., Jr.; McLeod, D., Jr.; Kasai, P. H. *J. Chem. Phys.* **1967**, *46*, 3172. (b) Kasai, P. H.; Weltner, W., Jr. *J. Chem. Phys.* **1965**, *43*, 2553.
- (83) Knight, L. B.; Kaup, J. G.; Petzoldt, B.; Ayyad, R.; Ghanty, T. K.; Davidson, E. R. *J. Chem. Phys.* **1999**, *110*, 5658.
- (84) Gonzales, J. M.; King, R. A.; Schaefer, H. F., III. *J. Chem. Phys.* **2000**, *113*, 567.
- (85) Johnson, J. R. T.; Panas, I. *Chem. Phys.* **1999**, *248*, 161.
- (86) Mattar, S. M. *J. Phys. Chem.* **1993**, *97*, 3171.
- (87) Jeung, G. H.; Koutecký, J. *J. Chem. Phys.* **1988**, *88*, 3747.

- (88) Bauschlicher, C. W., Jr.; Langhoff, S. R. *J. Chem. Phys.* **1986**, *85*, 5936.
- (89) Wu, H. B.; Wang, L. S. *J. Phys. Chem. A* **1998**, *102*, 9129.
- (90) Howard, J. A.; Histed, M.; Mile, B.; Hampson, C. A.; Morris, H. *J. Chem. Soc., Faraday Trans.* **1991**, *87*, 3189.
- (91) Hoefl, J.; Törring, T. *Chem. Phys. Lett.* **1993**, *215*, 367.
- (92) Suenram, R. D.; Lovas, F. J.; Fraser, G. T.; Matsumura, K. *J. Chem. Phys.* **1990**, *92*, 4724.
- (93) Klingeler, R.; Lüttgers, G.; Pontius, N.; Rochow, R.; Bechthold, P. S.; Neeb, M.; Eberhardt, W. *Eur. Phys. J., D* **1999**, *9*, 263.
- (94) Törring, T.; Zimmermann, K.; Hoefl, J. *Chem. Phys. Lett.* **1988**, *151*, 520.
- (95) Langhoff, S. R.; Bauschlicher, C. W., Jr. *J. Chem. Phys.* **1988**, *89*, 2160.
- (96) (a) Cao, X.; Dolg, M. *THEOCHEM* **2002**, *581*, 139. (b) Cao, X.; Dolg, M. *J. Chem. Phys.* **2001**, *115*, 7348. (c) Kühle, W.; Dolg, M.; Stoll, H. *J. Phys. Chem. A* **1997**, *101*, 7128.
- (97) Wang, S. G.; Schwarz, W. H. E. *J. Phys. Chem.* **1995**, *99*, 11687.
- (98) (a) Wang, S. G.; Pan, D. K.; Schwarz, W. H. E. *J. Chem. Phys.* **1995**, *102*, 9296. (b) Cao, X.; Liu, W.; Dolg, M. *Sci. Chin., Ser. B* **2002**, *45*, 91.
- (99) Kotzian, M.; Rösch, N.; Zerner, M. C. *Theor. Chim. Acta* **1992**, *81*, 201.
- (100) Todorova, T. K.; Infante, I.; Gagliardi, L.; Dyke, J. M. *J. Phys. Chem. A* **2008**, *112*, 7825.
- (101) Schamps, J.; Bencheikh, M.; Barthelat, J.-C.; Field, R. W. *J. Chem. Phys.* **1995**, *103*, 8004.
- (102) Márquez, A.; Capitán, M. J.; Odriozola, J. A.; Sanz, J. F. *Int. J. Quantum Chem.* **1994**, *52*, 1329.
- (103) Clemmer, D. E.; Dalleska, N. F.; Armentrout, P. B. *Chem. Phys. Lett.* **1992**, *190*, 259.
- (104) Chertihin, G. V.; Andrews, L.; Rosi, M.; Bauschlicher, C. W., Jr. *J. Phys. Chem. A* **1997**, *101*, 9085.
- (105) Bauschlicher, C. W., Jr.; Zhou, M. F.; Andrews, L.; Johnson, J. R. T.; Panas, I.; Snis, A.; Roos, B. O. *J. Phys. Chem. A* **1999**, *103*, 5463.
- (106) Lee, E. P. F.; Mok, D. K. W.; Chau, F. T.; Dyke, J. M. *J. Comput. Chem.* **2008**, *30*, 337.
- (107) Rosi, M.; Bauschlicher, C. W.; Chertihin, G. V.; Andrews, L. *Theor. Chem. Acc.* **1998**, *99*, 106.
- (108) Kim, S. J.; Crawford, T. D. *J. Phys. Chem. A* **2004**, *108*, 3097.
- (109) Andrews, L.; Zhou, M. F.; Chertihin, G. V.; Bauschlicher, C. W., Jr. *J. Phys. Chem. A* **1999**, *103*, 6525.
- (110) Lee, E. P. F.; Dyke, J. M.; Mok, D. K. W.; Chau, F. T. *J. Phys. Chem. A* **2008**, *112*, 4511.
- (111) Gong, Y.; Ding, C. F.; Zhou, M. F. *J. Phys. Chem. A* **2007**, *111*, 11572.
- (112) Gong, Y.; Ding, C. F.; Zhou, M. F. *J. Phys. Chem. A* **2009**, *113*, 8569.
- (113) Stösser, G.; Schnöckel, H. *Angew. Chem., Int. Ed.* **2005**, *44*, 4261.
- (114) (a) Flemmig, B.; Wolczanski, P. T.; Hoffmann, R. *J. Am. Chem. Soc.* **2005**, *127*, 1278. (b) Venter, G. A.; Raubenheimer, H. G.; Dillen, J. *J. Phys. Chem. A* **2007**, *111*, 8193.
- (115) Wu, H. B.; Wang, L. S. *J. Chem. Phys.* **1997**, *107*, 8221.
- (116) Looch, H.; Simard, B.; Wallin, S.; Linton, C. *J. Chem. Phys.* **1998**, *109*, 8980.
- (117) Gustavson, T.; Amiot, C.; Vergès, J. *J. Mol. Spectrosc.* **1991**, *145*, 56.
- (118) (a) Namiki, K. I.; Saito, S.; Robinson, J. S.; Steimle, T. C. *J. Mol. Spectrosc.* **1998**, *191*, 176. (b) Steimle, T. C.; Shirley, J. E.; Jung, K. Y.; Russon, L. R.; Scurlock, C. T. *J. Mol. Spectrosc.* **1990**, *144*, 27. (c) Steimle, T. C.; Shirley, J. E. *J. Chem. Phys.* **1989**, *91*, 8000.
- (119) Dyke, J. M.; Gravenor, B. W.; Josland, G. D.; Lewis, R. A.; Morris, A. *Mol. Phys.* **1984**, *53*, 465.
- (120) Powell, D.; Brittain, R.; Vala, M. *Chem. Phys.* **1981**, *58*, 355.
- (121) Gallaher, T. N.; DeVore, T. C. *High Temp. Sci.* **1979**, *11*, 123.
- (122) Walsh, M. B.; King, R. A.; Schaefer, H. F., III. *J. Chem. Phys.* **1999**, *110*, 5224.
- (123) Bauschlicher, C. W., Jr.; Langhoff, S. R.; Komornicki, A. *Theor. Chim. Acta* **1990**, *77*, 263.
- (124) Bauschlicher, C. W.; Bagus, P. S.; Nelin, C. J. *Chem. Phys. Lett.* **1983**, *101*, 229.
- (125) Beaton, S. A.; Gerry, M. C. L. *J. Chem. Phys.* **1999**, *110*, 10715.
- (126) Simard, B.; Mitchell, S. A.; Humphries, M. R.; Umphries, M. R.; Hackett, P. A. *J. Mol. Spectrosc.* **1988**, *129*, 186.
- (127) Lauchlan, L. J.; Brom, J. M., Jr.; Broida, H. P. *J. Chem. Phys.* **1976**, *65*, 2672.
- (128) Weltner, W., Jr.; McLeod, D., Jr. *Nature* **1965**, *206*, 87.
- (129) (a) Edvinsson, G.; Nylén, Ch. *Phys. Scr.* **1971**, *3*, 261. (b) Jonsson, J.; Edvinsson, G.; Taklif, A. G. *J. Mol. Spectrosc.* **1995**, *172*, 299.
- (130) Hammer, P. D.; Davis, S. P. *Astrophys. J.* **1980**, *237*, L51.
- (131) Weltner, W., Jr.; McLeod, D., Jr. *J. Phys. Chem.* **1965**, *69*, 3488.
- (132) Chertihin, G. V.; Andrews, L. *J. Phys. Chem.* **1995**, *99*, 6356.
- (133) McIntyre, N. S.; Thompson, K. R.; Weltner, W., Jr. *J. Phys. Chem.* **1971**, *75*, 3243.
- (134) Brünken, S.; Müller, H. S. P.; Menten, K. M.; McCarthy, M. C.; Thaddeus, P. *Astrophys. J.* **2008**, *676*, 1367.
- (135) Zhai, H. J.; Wang, L. S. *Am. Chem. Soc.* **2007**, *129*, 3022.
- (136) Thomas, O. C.; Xu, S.; Lippa, T. P.; Bowen, K. H. *J. Cluster Sci.* **1999**, *10*, 525.
- (137) Zheng, W.; Bowen, K. H., Jr.; Li, J.; Dabkowska, I.; Gutowski, M. *J. Phys. Chem. A* **2005**, *109*, 11521.
- (138) (a) Lesarri, A.; Suenram, R. D.; Brugh, D. *J. Chem. Phys.* **2002**, *117*, 9651. (b) Brugh, D. J.; Suenram, R. D.; Stevens, W. J. *J. Chem. Phys.* **1999**, *111*, 3526.
- (139) Grein, F. *J. Chem. Phys.* **2007**, *126*, 034313.
- (140) Li, S.; Dixon, D. A. *J. Phys. Chem. C* **2008**, *112*, 6646.
- (141) Woodley, S. M.; Hamad, S.; Mejias, J. A.; Catlow, C. R. A. *J. Mater. Chem.* **2006**, *16*, 1927.
- (142) Qu, Z. W.; Kroes, G. J. *J. Phys. Chem. B* **2006**, *110*, 8998.
- (143) Albaret, T.; Finocchi, F.; Noguera, C. *Appl. Surf. Sci.* **1999**, *144*, 672.
- (144) (a) Hagfeldt, A.; Bergström, R.; Siegbahn, H. O. G.; Lunell, S. *J. Phys. Chem.* **1993**, *97*, 12725. (b) Bergström, R.; Lunell, S.; Eriksson, L. A. *Int. J. Quantum Chem.* **1996**, *59*, 427.
- (145) Ramana, M. V.; Phillips, D. H. *J. Chem. Phys.* **1988**, *88*, 2637.
- (146) (a) Mok, D. K. W.; Chau, F. T.; Dyke, J. M.; Lee, E. P. F. *Chem. Phys. Lett.* **2008**, *458*, 11. (b) Mok, D. K. W.; Lee, E. P. F.; Chau, F. T.; Dyke, J. M. *Phys. Chem. Chem. Phys.* **2008**, *10*, 7270.
- (147) Gong, Y.; Zhou, M. F. *J. Phys. Chem. A* **2008**, *112*, 9758.
- (148) Gong, Y.; Zhou, M. F. *Chin. J. Chem. Phys.* **2009**, *22*, 113.
- (149) Albaret, T.; Finocchi, F.; Noguera, C. *J. Chem. Phys.* **2000**, *113*, 2238.
- (150) Jeong, K. S.; Chang, Ch.; Sedlmayr, E.; Sülzle, D. *J. Phys. B* **2000**, *33*, 3417.
- (151) (a) Zhou, M. F.; Andrews, L. *J. Phys. Chem. A* **1999**, *103*, 5259. (b) Zhou, M. F.; Andrews, L. *J. Am. Chem. Soc.* **2000**, *122*, 1531.
- (152) Gong, Y.; Zhou, M. F.; Tian, S. X.; Yang, J. L. *J. Phys. Chem. A* **2007**, *111*, 6127.
- (153) Gong, Y.; Zhou, M. F. *J. Phys. Chem. A* **2007**, *111*, 8973.
- (154) (a) Wight, C. A.; Ault, B. S.; Andrews, L. *J. Chem. Phys.* **1976**, *65*, 1244. (b) Andrews, L.; Ault, B. S.; Grzybowski, J. M.; Allen, R. O. *J. Chem. Phys.* **1975**, *62*, 2461.
- (155) (a) Bayot, D.; Devillers, M. *Coord. Chem. Rev.* **2006**, *250*, 2610. (b) Bortolini, O.; Conte, V. *J. Inorg. Biochem.* **2005**, *99*, 1549.
- (156) Miliordos, E.; Mavridis, A. *J. Phys. Chem. A* **2007**, *111*, 1953.
- (157) (a) Broclawik, E.; Borowski, T. *Chem. Phys. Lett.* **2001**, *339*, 433. (b) Broclawik, E. *Catal. Today* **1995**, *23*, 379. (c) Broclawik, E. *Theor. Comput. Chem.* **1995**, *2*, 349. (d) Broclawik, E.; Salahub, D. R. *J. Mol. Catal.* **1993**, *82*, 117.
- (158) Pykavy, M.; Van Wüllen, C. *J. Phys. Chem. A* **2003**, *107*, 5566.
- (159) Rakowitz, F.; Marian, C. M.; Seijo, L.; Wahlgren, U. *J. Chem. Phys.* **1999**, *110*, 3678.
- (160) (a) Calatayud, M.; Berski, S.; Beltran, A.; Andres, J. *Theor. Chem. Acc.* **2002**, *108*, 12. (b) Calatayud, M.; Silvi, B.; Andres, J.; Beltran, A. *Chem. Phys. Lett.* **2001**, *333*, 493. (c) Calatayud, M.; Andres, J.; Beltran, A.; Silvi, B. *Theor. Chem. Acc.* **2001**, *105*, 299.
- (161) Vyboishchikov, S. F.; Sauer, J. *J. Phys. Chem. A* **2000**, *104*, 10913.
- (162) Jakubikova, E.; Rappé, A. K.; Bernstein, E. R. *J. Phys. Chem. A* **2007**, *111*, 12938.
- (163) Bände, A.; Lühchow, A. *Phys. Chem. Chem. Phys.* **2008**, *10*, 3371.
- (164) Knight, L. B., Jr.; Babb, R.; Ray, M.; Banisaukas, T. J., III; Russon, L.; Dailey, R. S.; Davidson, E. R. *J. Chem. Phys.* **1996**, *105*, 10237.
- (165) Wu, H. B.; Wang, L. S. *J. Chem. Phys.* **1998**, *108*, 5310.
- (166) Dyke, J. M.; Gravenor, B. W. J.; Hastings, M. P.; Morris, A. *J. Phys. Chem.* **1985**, *89*, 4613.
- (167) Kasai, P. H. *J. Chem. Phys.* **1968**, *49*, 4979.
- (168) Dolg, M.; Stoll, H.; Preuss, H.; Pitzer, R. M. *J. Phys. Chem.* **1993**, *97*, 5852.
- (169) Osanai, Y.; Sekiya, M.; Noro, T.; Koga, T. *Mol. Phys.* **2003**, *101*, 65.
- (170) Vala, M.; Brittain, R. D.; Powell, D. *Chem. Phys.* **1985**, *93*, 147.
- (171) Dyke, J. M.; Ellis, A. M.; Feher, M.; Morris, A.; Paul, A. J.; Stevens, J. C. *J. Chem. Soc., Faraday Trans. 2* **1987**, *83*, 1555.
- (172) Wu, Z. J.; Kawazoe, Y.; Meng, J. *THEOCHEM* **2006**, *764*, 123.
- (173) Manke, K. J.; Vervoort, T. R.; Kuwata, K. T.; Varberg, T. D. *J. Chem. Phys.* **2008**, *128*, 104302.
- (174) Zheng, W.; Li, X.; Eustis, S.; Bowen, K. *Chem. Phys. Lett.* **2008**, *460*, 68.
- (175) Al-Khalili, A.; Hallsten, U.; Launila, O. *J. Mol. Spectrosc.* **1999**, *198*, 230.
- (176) Brittain, R.; Powell, D.; Kreglewski, M.; Vala, M. *Chem. Phys.* **1980**, *54*, 71.
- (177) Weltner, W., Jr.; McLeod, D., Jr. *J. Chem. Phys.* **1965**, *42*, 882.
- (178) Cheetham, C. J.; Barrow, R. F. *Trans. Faraday Soc.* **1967**, *63*, 1835.
- (179) Matsuda, Y.; Bernstein, E. R. *J. Phys. Chem. A* **2005**, *109*, 3803.

- (180) Sambrano, J. R.; Andrés, J.; Beltrán, A.; Sensato, F.; Longo, E. *Chem. Phys. Lett.* **1998**, *287*, 620.
- (181) Gershikov, A. G.; Spiridonov, V. P.; Prikhod'ko, A. Ya.; Erokhin, E. V. *High Temp. Sci.* **1981**, *14*, 17.
- (182) Chertihin, G. V.; Bare, W. D.; Andrews, L. J. *Phys. Chem. A* **1997**, *101*, 5090.
- (183) Zhou, M. F.; Andrews, L. J. *Phys. Chem. A* **1998**, *102*, 8251.
- (184) Chen, M. H.; Wang, X. F.; Qin, Q. Z. *Appl. Surf. Sci.* **2000**, *156*, 16.
- (185) Brom, J. M., Jr.; Durham, C. H., Jr.; Weltner, W., Jr. *J. Chem. Phys.* **1974**, *61*, 970.
- (186) Green, D. W.; Korfmacher, W.; Gruen, D. M. *J. Chem. Phys.* **1973**, *58*, 404.
- (187) Chen, M. H.; Wang, X. F.; Zhang, L. N.; Yu, M.; Qin, Q. Z. *Chem. Phys.* **1999**, *242*, 81.
- (188) Zhao, Y. Y.; Gong, Y.; Chen, M. H.; Zhou, M. F. *J. Phys. Chem. A* **2006**, *110*, 1845.
- (189) Zhao, Y. Y.; Zheng, X. M.; Zhou, M. F. *Chem. Phys.* **2008**, *351*, 13.
- (190) Almond, M. J.; Atkins, R. W. *J. Chem. Soc., Dalton Trans.* **1994**, 835.
- (191) (a) Wells, J. R.; Weitz, E. *J. Am. Chem. Soc.* **1992**, *114*, 2783. (b) Sun, X. Z.; George, M. W.; Kazarian, S. G.; Nikiforov, S. M.; Poliakov, M. *J. Am. Chem. Soc.* **1996**, *118*, 10525. (c) Ball, G. E.; Darwish, T. A.; Geftakis, S.; George, M. W.; Lawes, D. J.; Portius, P.; Rourke, J. P.; Bergman, R. G. *Proc. Natl. Acad. Sci. U.S.A.* **2005**, *102*, 1853.
- (192) Stevens, F.; Carmichael, I.; Callens, F.; Waroquier, M. *J. Phys. Chem. A* **2006**, *110*, 4846.
- (193) Bauschlicher, C. W., Jr.; Gutsev, G. L. *J. Chem. Phys.* **2002**, *116*, 3659.
- (194) Veliah, S.; Xiang, K. H.; Pandey, R.; Recio, J. M.; Newsam, J. M. *J. Phys. Chem. B* **1998**, *102*, 1126.
- (195) Jasien, P. G.; Stevens, W. J. *Chem. Phys. Lett.* **1988**, *147*, 72.
- (196) Bauschlicher, C. W., Jr.; Nelin, C. J.; Bagus, P. S. *J. Chem. Phys.* **1985**, *82*, 3265.
- (197) Gutsev, G. L.; Jena, P.; Zhai, H. J.; Wang, L. S. *J. Chem. Phys.* **2001**, *115*, 7935.
- (198) Wenthold, P. G.; Gunion, R. F.; Lineberger, W. C. *Chem. Phys. Lett.* **1996**, *258*, 101.
- (199) Steimle, T. C.; Nachman, D. F.; Shirley, J. E.; Bauschlicher, C. W., Jr.; Langhoff, S. R. *J. Chem. Phys.* **1989**, *91*, 2049.
- (200) (a) Cheung, A. S. C.; Zyrnicki, W.; Merer, A. J. *J. Mol. Spectrosc.* **1984**, *104*, 315. (b) Hocking, W. H.; Merer, A. J.; Milton, D. J.; Jones, W. E.; Krishnamurthy, G. *Can. J. Phys.* **1980**, *58*, 516. (c) Barnes, M.; Hajigeorgiou, P. G.; Merer, A. J. *J. Mol. Spectrosc.* **1993**, *160*, 289.
- (201) Zhou, M. F.; Andrews, L. J. *J. Chem. Phys.* **1999**, *111*, 4230.
- (202) Chertihin, G. V.; Bare, W. D.; Andrews, L. J. *J. Chem. Phys.* **1997**, *107*, 2798.
- (203) Kuzyakov, Y. Y.; Moskvitina, E. N.; Filippova, E. N. *Spectrosc. Lett.* **1997**, *30*, 1057.
- (204) Gunion, R. F.; Dixon-Warren, St. J.; Lineberger, W. C. *J. Chem. Phys.* **1996**, *104*, 1765.
- (205) Hamrick, Y. M.; Taylor, S.; Morse, M. D. *J. Mol. Spectrosc.* **1991**, *146*, 274.
- (206) Broclawik, E.; Salahub, D. R. *Int. J. Quantum Chem.* **1994**, *52*, 1017.
- (207) Langhoff, S. R.; Bauschlicher, C. W., Jr.; Pettersson, L. G. M.; Siegbahn, P. E. M. *Chem. Phys.* **1989**, *132*, 49.
- (208) Bates, J. K.; Gruen, D. M. *J. Mol. Spectrosc.* **1979**, *78*, 284.
- (209) Ram, R. S.; Liévin, J.; Li, G.; Hirao, T.; Bernath, P. F. *Chem. Phys. Lett.* **2001**, *343*, 437.
- (210) Bare, W. D.; Souter, P. F.; Andrews, L. J. *Phys. Chem. A* **1998**, *102*, 8279.
- (211) Samoilova, A. N.; Efremov, Yu. M.; Gurvich, L. V. *J. Mol. Spectrosc.* **1981**, *86*, 1.
- (212) Weltner, W., Jr.; McLeod, D., Jr. *J. Mol. Spectrosc.* **1965**, *17*, 276.
- (213) Nelin, C. J.; Bauschlicher, C. W., Jr. *Chem. Phys. Lett.* **1985**, *118*, 221.
- (214) Lorenz, M.; Bondybey, V. E. *Chem. Phys.* **1999**, *241*, 127.
- (215) (a) Almond, M. J.; Hahne, M. *J. Chem. Soc., Dalton Trans.* **1988**, 2255. (b) Darling, J. H.; Garton Sprenger, M. B.; Ogden, J. S. *Symp. Faraday Soc.* **1974**, *8*, 74.
- (216) (a) Almond, M. J.; Crayston, J. A.; Downs, A. J.; Poliakov, M.; Turner, J. J. *Inorg. Chem.* **1986**, *25*, 19. (b) Almond, M. J.; Downs, A. J. *J. Chem. Soc., Dalton Trans.* **1988**, 809.
- (217) Wenthold, P. G.; Jonas, K.-L.; Lineberger, W. C. *J. Chem. Phys.* **1997**, *106*, 9961.
- (218) Grein, F. *Chem. Phys.* **2008**, *343*, 231.
- (219) Sniatynsky, R.; Cedeño, D. L. *THEOCHEM* **2004**, *711*, 123.
- (220) Li, G. L.; Xu, W. G.; Li, Q. S. *THEOCHEM* **2000**, *498*, 61.
- (221) Martínez, A. J. *Phys. Chem. A* **1998**, *102*, 1381.
- (222) Murugan, P.; Kumar, V.; Kawazoe, Y.; Ota, N. *Chem. Phys. Lett.* **2006**, *423*, 202.
- (223) Oliveira, J. A.; De Almeida, W. B.; Duarte, H. A. *Chem. Phys. Lett.* **2003**, *372*, 650.
- (224) Hewett, W. D., Jr.; Newton, J. H.; Weltner, W., Jr. *J. Phys. Chem.* **1975**, *79*, 2640.
- (225) Davico, G. E.; Schwartz, R. L.; Ramond, T. M.; Lineberger, W. C. *J. Phys. Chem. A* **1999**, *103*, 6167.
- (226) Green, D. W.; Ervin, K. M. *J. Mol. Spectrosc.* **1981**, *89*, 145.
- (227) Zhai, H. J.; Li, S.; Dixon, D. A.; Wang, L. S. *J. Am. Chem. Soc.* **2008**, *130*, 5167.
- (228) Zhai, H. J.; Kiran, B.; Cui, L. F.; Li, X.; Dixon, D. A.; Wang, L. S. *J. Am. Chem. Soc.* **2004**, *126*, 16134.
- (229) Walter, C. W.; Hertzler, C. F.; Devynck, P.; Smith, G. P.; Peterson, J. R. *J. Chem. Phys.* **1991**, *95*, 824.
- (230) Neikirk, D. L.; Fagerli, J. C.; Smith, M. L.; Mosman, D.; Devore, T. C. *J. Mol. Struct.* **1991**, *244*, 165.
- (231) Iorns, T. V.; Stafford, F. E. *J. Am. Chem. Soc.* **1966**, *88*, 4819.
- (232) (a) Li, S.; Dixon, D. A. *J. Phys. Chem. A* **2007**, *111*, 11908. (b) Li, S.; Dixon, D. A. *J. Phys. Chem. A* **2006**, *110*, 6231.
- (233) Sun, Q.; Rao, B. K.; Jena, P.; Stolcic, D.; Kim, Y. D.; Ganteför, G.; Castleman, A. W., Jr. *J. Chem. Phys.* **2004**, *121*, 9417.
- (234) Tsipis, A. C. *Phys. Chem. Chem. Phys.* **2000**, *2*, 1357.
- (235) Tsipis, A. C.; Tsipis, C. A. *J. Phys. Chem. A* **2000**, *104*, 859.
- (236) Stolcic, D.; Kim, Y. D.; Ganteför, G. *J. Chem. Phys.* **2004**, *120*, 5.
- (237) Chen, Z. Y.; Yang, J. L. *Chin. J. Chem. Phys.* **2007**, *20*, 78.
- (238) Zhao, Y. Y.; Su, J.; Gong, Y.; Li, J.; Zhou, M. F. *J. Phys. Chem. A* **2008**, *112*, 8606.
- (239) Uzunova, E. L.; Nikolov, G. St.; Mikosch, H. *ChemPhysChem* **2004**, *5*, 192.
- (240) Gutsev, G. L.; Rao, B. K.; Jena, P.; Li, X.; Wang, L. S. *J. Chem. Phys.* **2000**, *113*, 1473.
- (241) (a) Nayak, S. K.; Jena, P. *J. Am. Chem. Soc.* **1999**, *121*, 644. (b) Nayak, S. K.; Jena, P. *Phys. Rev. Lett.* **1998**, *81*, 2970.
- (242) Namiki, K.; Saito, S. *J. Chem. Phys.* **1997**, *107*, 8848.
- (243) Ferrante, R. F.; Wilkerson, J. L.; Graham, W. R. M.; Weltner, W., Jr. *J. Chem. Phys.* **1977**, *67*, 5904.
- (244) Gordon, R. M.; Merer, A. J. *Can. J. Phys.* **1980**, *58*, 642.
- (245) (a) Pinchemel, B.; Schamps, J. *Chem. Phys.* **1976**, *18*, 481. (b) Pinchemel, B.; Schamps, J. *Can. J. Phys.* **1975**, *53*, 431.
- (246) Chertihin, G. V.; Andrews, L. J. *Phys. Chem. A* **1997**, *101*, 8547.
- (247) Gong, Y.; Wang, G. J.; Zhou, M. F. *J. Phys. Chem. A* **2008**, *112*, 4936.
- (248) Brown, C. E.; Mitchell, S. A.; Hackett, P. A. *J. Phys. Chem.* **1991**, *95*, 1062.
- (249) Gutsev, G. L.; Rao, B. K.; Jena, P.; Wang, X. B.; Wang, L. S. *Chem. Phys. Lett.* **1999**, *312*, 598.
- (250) Gutsev, G. L.; Rao, B. K.; Jena, P. *J. Phys. Chem. A* **1999**, *103*, 10819.
- (251) Zhou, M. F.; Zeng, A. H.; Wang, Y.; Kong, Q. Y.; Wang, Z. X.; Schleyer, P. V. R. *J. Am. Chem. Soc.* **2003**, *125*, 11512.
- (252) (a) Griffiths, J. E.; Sunder, W. A.; Falconer, W. E. *Spectrochim. Acta* **1975**, *31A*, 1207. (b) Edwards, A. J.; Falconer, W. E.; Griffiths, J. E.; Sunder, W. A.; Vasile, M. J. *J. Chem. Soc., Dalton Trans.* **1974**, 1129.
- (253) Zhou, M. F.; Zhao, Y. Y.; Gong, Y.; Li, J. *J. Am. Chem. Soc.* **2006**, *128*, 2504.
- (254) Beckers, H.; Garcia, P.; Willner, H.; Argüello, G. A.; Cobos, C. J.; Francisco, J. S. *Angew. Chem., Int. Ed.* **2007**, *46*, 3754.
- (255) Viggiano, A. A.; Henschman, M. J.; Dale, F.; Deakyne, C. A.; Paulson, J. F. *J. Am. Chem. Soc.* **1992**, *114*, 4299.
- (256) Kuznetsov, S. V.; Korobov, M. V.; Sidorov, L. N.; Shipachev, V. A.; Mitkin, V. N. *Int. J. Mass Spectrom. Ion Processes* **1989**, *87*, 13.
- (257) Bartlett, N. *Proc. Chem. Soc.* **1962**, 218.
- (258) Gancheff, J.; Kremer, C.; Kremer, E.; Ventura, O. N. *THEOCHEM* **2002**, *580*, 107.
- (259) (a) Balfour, W. J.; Ram, R. S. *J. Mol. Spectrosc.* **1983**, *100*, 164. (b) Balfour, W. J.; Orth, F. B. *J. Mol. Spectrosc.* **1980**, *84*, 424.
- (260) Roberts, M. A.; Alfonso, C. G.; Manke, K. J.; Ames, W. M.; Ron, D. B.; Varberg, T. D. *Mol. Phys.* **2007**, *105*, 917.
- (261) Zhou, M. F.; Citra, A.; Liang, B. Y.; Andrews, L. J. *Phys. Chem. A* **2000**, *104*, 3457.
- (262) Pramann, A.; Rademann, K. *Chem. Phys. Lett.* **2001**, *343*, 99.
- (263) Metz, R. B.; Nicolas, C.; Ahmed, M.; Leone, S. R. *J. Chem. Phys.* **2005**, *123*, 114313.
- (264) Chestakov, D. A.; Parker, D. H.; Baklanov, A. V. *J. Chem. Phys.* **2005**, *122*, 084302.
- (265) Son, H. S.; Lee, K.; Shin, S. K.; Ku, J. K. *Chem. Phys. Lett.* **2000**, *320*, 658.
- (266) Drechsler, G.; Boesl, U.; Bässmann, C.; Schlag, E. W. *J. Chem. Phys.* **1997**, *107*, 2284.
- (267) Allen, M. D.; Ziurys, L. M.; Brown, J. M. *Chem. Phys. Lett.* **1996**, *257*, 130.

- (268) (a) Wu, H. B.; Desai, S. R.; Wang, L. S. *J. Am. Chem. Soc.* **1996**, *118*, 5296. (b) Wu, H. B.; Desai, S. R.; Wang, L. S. *J. Am. Chem. Soc.* **1996**, *118*, 7434.
- (269) Fan, J.; Wang, L. S. *J. Chem. Phys.* **1995**, *102*, 8714.
- (270) Chertihin, G. V.; Saffel, W.; Yustein, J. T.; Andrews, L.; Neurock, M.; Ricca, A.; Bauschlicher, C. W., Jr. *J. Phys. Chem.* **1996**, *100*, 5261.
- (271) Kröckertskothén, T.; Knöckel, H.; Tiemann, E. *Mol. Phys.* **1987**, *62*, 1031.
- (272) (a) Cheung, A. S. C.; Gordon, R. M.; Merer, A. J. *J. Mol. Spectrosc.* **1981**, *87*, 289. (b) Cheung, A. S.-C.; Lee, N.; Lyyra, A. M.; Merer, A. J.; Taylor, A. W. *J. Mol. Spectrosc.* **1982**, *95*, 213. (c) Taylor, A. W.; Cheung, A. S.-C.; Merer, A. J. *J. Mol. Spectrosc.* **1985**, *113*, 487. (d) Barnes, M.; Fraser, M. M.; Hajigeorgiou, P. G.; Merer, A. J.; Rosner, S. D. *J. Mol. Spectrosc.* **1995**, *170*, 449. (e) Steimle, T. C.; Nachman, D. F.; Shirley, J. E.; Merer, A. J. *J. Chem. Phys.* **1989**, *90*, 5360.
- (273) Harris, S. M.; Barrow, R. F. *J. Mol. Spectrosc.* **1980**, *84*, 334.
- (274) Green, D. W.; Reedy, G. T.; Kay, J. G. *J. Mol. Spectrosc.* **1979**, *78*, 257.
- (275) West, J. B.; Broida, H. P. *J. Chem. Phys.* **1975**, *62*, 2566.
- (276) (a) Hendrickx, M. F. A.; Anam, K. R. *J. Phys. Chem. A* **2009**, *113*, 8746. (b) Neumark, D. M.; Lineberger, W. C. *J. Phys. Chem. A*, published online August 28, 2009, doi:10.1021/jp906974n.
- (277) Shiroishi, H.; Oda, T.; Hamada, I.; Fujima, N. *Eur. Phys. J., D* **2003**, *24*, 85.
- (278) Gutsev, G. L.; Khanna, S. N.; Rao, B. K.; Jena, P. *J. Phys. Chem. A* **1999**, *103*, 5812.
- (279) Glukhovtser, M. N.; Bach, R. D.; Nagel, C. J. *J. Phys. Chem. A* **1997**, *101*, 316.
- (280) Krauss, M.; Stevens, W. J. *J. Chem. Phys.* **1985**, *82*, 5584.
- (281) Blyholder, G.; Head, J.; Ruetter, F. *Inorg. Chem.* **1982**, *21*, 1539.
- (282) Bagus, P. S.; Preston, H. J. T. *J. Chem. Phys.* **1973**, *59*, 2986.
- (283) Abramowitz, S.; Acquista, N.; Levin, I. W. *Chem. Phys. Lett.* **1977**, *50*, 423.
- (284) Chang, S.; Blyholder, G.; Fernandez, J. *Inorg. Chem.* **1981**, *20*, 2813.
- (285) Fanfarillo, M.; Downs, A. J.; Green, T. M.; Almond, M. J. *Inorg. Chem.* **1992**, *31*, 2973.
- (286) Andrews, L.; Chertihin, G. V.; Ricca, A.; Bauschlicher, C. W., Jr. *J. Am. Chem. Soc.* **1996**, *118*, 467.
- (287) Yamada, Y.; Sumino, H.; Okamura, Y.; Shimasaki, H.; Tominaga, T. *Appl. Radiat. Isot.* **2000**, *52*, 157.
- (288) Gong, Y.; Zhou, M. F.; Andrews, L. *J. Phys. Chem. A* **2007**, *111*, 12001.
- (289) Grein, F. *Int. J. Quantum Chem.* **2009**, *109*, 549.
- (290) Cao, Z.; Duran, M.; Solà, M. *Chem. Phys. Lett.* **1997**, *274*, 411.
- (291) Lyne, P. D.; Mingos, D. M. P.; Ziegler, T.; Downs, A. J. *Inorg. Chem.* **1993**, *32*, 4785.
- (292) García-Sosa, A. T.; Castro, M. *Int. J. Quantum Chem.* **2000**, *80*, 307.
- (293) Kellogg, C. B.; Irikura, K. K. *J. Phys. Chem. A* **1999**, *103*, 1150.
- (294) Plane, J. M. C.; Rollason, R. J. *J. Phys. Chem. Chem. Phys.* **1999**, *1*, 1843.
- (295) Gong, Y.; Zhou, M. F. *J. Phys. Chem. A* **2008**, *112*, 10838.
- (296) Rollason, R. J.; Plane, J. M. C. *J. Phys. Chem. Chem. Phys.* **2000**, *2*, 2335.
- (297) Atanasov, M. *Inorg. Chem.* **1999**, *38*, 4942.
- (298) Gutsev, G. L.; Khanna, S. N.; Rao, B. K.; Jena, P. *Phys. Rev. A* **1999**, *59*, 3681.
- (299) Cao, Z.; Wu, W.; Zhang, Q. *THEOCHEM* **1999**, *489*, 165.
- (300) Carbonniere, P.; Ciofini, I.; Adamo, C.; Pouchan, C. *Chem. Phys. Lett.* **2006**, *429*, 52.
- (301) Hohm, U.; Maroulis, G. *J. Chem. Phys.* **2004**, *121*, 10411.
- (302) Pershina, V.; Bastug, T.; Fricke, B.; Varga, S. *J. Chem. Phys.* **2001**, *115*, 792.
- (303) Nakajima, T.; Koga, K.; Hirao, K. *J. Chem. Phys.* **2000**, *112*, 10142.
- (304) Bridgeman, A. J.; Cavigliasso, G. *Polyhedron* **2001**, *20*, 2269.
- (305) Ujaque, G.; Maseras, F.; Lledós, A. *Int. J. Quantum Chem.* **2000**, *77*, 544.
- (306) Stückl, A. C.; Daul, C. A.; Güdel, H. U. *J. Chem. Phys.* **1997**, *107*, 4606.
- (307) Pyykkö, P.; Li, J.; Bastug, T.; Fricke, B.; Kolb, D. *Inorg. Chem.* **1993**, *32*, 1525.
- (308) (a) Bursten, B. E.; Green, J. C.; Kaltsoyannis, N. *Inorg. Chem.* **1994**, *33*, 2315. (b) Green, J. C.; Guest, M. F.; Hillier, I. H.; Jarrett-Sprague, S. A.; Kaltsoyannis, N.; MacDonald, M. A.; Sze, K. H. *Inorg. Chem.* **1992**, *31*, 1588. (c) Green, J. C.; Kaltsoyannis, N.; Sze, K. H.; MacDonald, M. A. *Chem. Phys. Lett.* **1990**, *175*, 359.
- (309) Gulliver, D. J.; Levason, W. *Coord. Chem. Rev.* **1982**, *46*, 1.
- (310) Green, D. W.; Kay, J. G.; Zimmerman, G. L.; Balko, B. *J. Mol. Spectrosc.* **1989**, *138*, 62.
- (311) Grinter, R.; Zimmerman, R. L.; Dunn, T. M. *J. Mol. Spectrosc.* **1984**, *107*, 12.
- (312) Beattie, I. R.; Blayden, H. E.; Crocombe, R. A.; Jones, P. J.; Ogden, J. S. *J. Raman Spectrosc.* **1976**, *4*, 313.
- (313) Kay, J. G.; Green, D. W.; Duca, K.; Zimmerman, G. L. *J. Mol. Spectrosc.* **1989**, *138*, 49.
- (314) Scullman, R.; Thelin, B. *J. Mol. Spectrosc.* **1975**, *56*, 64.
- (315) Raziunas, V.; Macur, G.; Katz, S. *J. Chem. Phys.* **1965**, *43*, 1010.
- (316) Riedel, S.; Kaupp, M. *Coord. Chem. Rev.* **2009**, *253*, 606.
- (317) McLamarrah, S. K.; Sheridan, P. M.; Ziurys, L. M. *Chem. Phys. Lett.* **2005**, *414*, 301.
- (318) Danset, D.; Manceron, L. *J. Phys. Chem. A* **2003**, *107*, 11324.
- (319) Namiki, K. C.; Saito, S. *J. Chem. Phys.* **2001**, *114*, 9390.
- (320) Chertihin, G. V.; Citra, A.; Andrews, L.; Bauschlicher, C. W., Jr. *J. Phys. Chem. A* **1997**, *101*, 8793.
- (321) (a) Clouthier, D. J.; Huang, G.; Merer, A. J.; Friedman-Hill, E. J. *J. Chem. Phys.* **1993**, *99*, 6336. (b) Adam, A. G.; Azuma, Y.; Barry, J. A.; Huang, G.; Lyne, M. P. J.; Merer, A. J.; Schröder, J. O. *J. Chem. Phys.* **1987**, *86*, 5231.
- (322) Uzunova, E. L.; Nikolov, G. St.; Mikosch, H. *J. Phys. Chem. A* **2002**, *106*, 4104.
- (323) Piechota, J.; Suffczynski, M. *Phys. Rev. A* **1993**, *48*, 2679.
- (324) DeVore, T. C.; Gallaher, T. N. *J. Chem. Phys.* **1979**, *71*, 474.
- (325) Van Zee, R. J.; Hamrick, Y. M.; Li, S.; Weltner, W., Jr. *J. Phys. Chem.* **1992**, *96*, 7247.
- (326) Danset, D.; Alikhani, M. E.; Manceron, L. *J. Phys. Chem. A* **2005**, *109*, 97.
- (327) Danset, D.; Alikhani, M. E.; Manceron, L. *J. Phys. Chem. A* **2005**, *109*, 105.
- (328) Suo, B.; Han, H.; Lei, Y.; Zhai, G.; Wang, Y.; Wen, Z. *J. Chem. Phys.* **2009**, *130*, 094304.
- (329) Stevens, F.; Van Speybroeck, V.; Carmichael, I.; Callens, F.; Waroquier, M. *Chem. Phys. Lett.* **2006**, *421*, 281.
- (330) Mains, G. J.; White, J. M. *J. Phys. Chem.* **1991**, *95*, 112.
- (331) Gengler, J.; Ma, T.; Adam, A. G.; Steimle, T. C. *J. Chem. Phys.* **2007**, *126*, 134304.
- (332) (a) Heuff, R. F.; Fougere, S. G.; Balfour, W. J. *J. Mol. Spectrosc.* **2005**, *231*, 99. (b) Jensen, R. H.; Fougere, S. G.; Balfour, W. J. *Chem. Phys. Lett.* **2003**, *370*, 106.
- (333) Li, X.; Wang, L. S. *J. Chem. Phys.* **1998**, *109*, 5264.
- (334) Citra, A.; Andrews, L. *J. Phys. Chem. A* **1999**, *103*, 4845.
- (335) (a) Hanlan, A. J. L.; Ozin, G. A. *Inorg. Chem.* **1977**, *16*, 2848. (b) Hanlan, A. J. L.; Ozin, G. A. *Inorg. Chem.* **1977**, *16*, 2857.
- (336) Yang, R.; Gong, Y.; Zhou, H.; Zhou, M. F. *J. Phys. Chem. A* **2007**, *111*, 64.
- (337) Riedel, S.; Gong, Y.; Zhou, M. F.; Kaupp, M. Unpublished results.
- (338) Jansson, K.; Scullman, R. *J. Mol. Spectrosc.* **1972**, *43*, 208.
- (339) Campbell, M. L. *J. Phys. Chem. A* **1997**, *101*, 9377.
- (340) Gong, Y.; Zhou, M. F.; Kaupp, M.; Riedel, S. *Angew. Chem., Int. Ed.* **2009**, doi: 10.1002/anie.200902733.
- (341) Citra, A.; Andrews, L. *J. Phys. Chem. A* **1999**, *103*, 4182.
- (342) Ramond, T. M.; Davico, G. E.; Hellberg, F.; Svedberg, F.; Salen, P.; Söderqvist, P.; Lineberger, W. C. *J. Mol. Spectrosc.* **2002**, *216*, 1.
- (343) Moravec, V. D.; Jarrold, C. C. *J. Chem. Phys.* **1998**, *108*, 1804.
- (344) Wu, H.; Wang, L. S. *J. Chem. Phys.* **1997**, *107*, 16.
- (345) Namiki, K.; Saito, S. *Chem. Phys. Lett.* **1996**, *252*, 347.
- (346) Srdanov, V. I.; Harris, D. O. *J. Chem. Phys.* **1988**, *89*, 2748.
- (347) Citra, A.; Chertihin, G. V.; Andrews, L.; Neurock, M. *J. Phys. Chem. A* **1997**, *101*, 3109.
- (348) Hwang, D. Y.; Mebel, A. M. *J. Phys. Chem. A* **2002**, *106*, 520.
- (349) Doll, K.; Dolg, M.; Fulde, P.; Stoll, H. *Phys. Rev. B* **1997**, *55*, 10282.
- (350) Chung, S. C.; Krüger, S.; Pacchioni, G.; Röscher, N. *J. Chem. Phys.* **1995**, *102*, 3695.
- (351) Bridgeman, A. J. *J. Chem. Soc., Dalton Trans.* **1996**, 4555.
- (352) Bauschlicher, C. W., Jr. *Chem. Phys.* **1985**, *93*, 399.
- (353) Walch, S. P.; Goddard, W. A., III. *J. Am. Chem. Soc.* **1978**, *100*, 1338.
- (354) Hwang, D. Y.; Mebel, A. M. *J. Phys. Chem. A* **2002**, *106*, 12072.
- (355) Wang, X. F.; Andrews, L. *J. Phys. Chem. A* **2001**, *105*, 5812.
- (356) Dedieu, A. *Chem. Rev.* **2000**, *100*, 543.
- (357) Bare, W. D.; Citra, A.; Chertihin, G. V.; Andrews, L. *J. Phys. Chem. A* **1999**, *103*, 5456.
- (358) (a) Broclawik, E.; Yamauchi, R.; Endou, A.; Kubo, M.; Miyamoto, A. *Int. J. Quantum Chem.* **1997**, *61*, 673. (b) Broclawik, E.; Yamauchi, R.; Eudou, A.; Kubo, M.; Miyamoto, A. *J. Chem. Phys.* **1996**, *104*, 4098.
- (359) Schwerdtfeger, P.; McFeaters, J. S.; Moore, J. J.; McPherson, D. M.; Cooney, R. P.; Bowmaker, G. A.; Dolg, M.; Andrae, D. *Langmuir* **1991**, *7*, 116.
- (360) Klopčič, S. A.; Moravec, V. D.; Jarrold, C. C. *J. Chem. Phys.* **1999**, *110*, 10216.
- (361) Liu, H.; O'Brien, L. C.; Shaji, S.; O'Brien, J. J. *J. Mol. Spectrosc.* **2009**, *253*, 73.



- (362) Citir, M.; Metz, R. B.; Belau, L.; Ahmed, M. *J. Phys. Chem. A* **2008**, *112*, 9584.
- (363) Cooke, S. A.; Gerry, M. C. L. *Phys. Chem. Chem. Phys.* **2005**, *7*, 2453.
- (364) Okabayashi, T.; Yamazaki, E.; Tanimoto, M. *J. Mol. Spectrosc.* **2005**, *229*, 283.
- (365) Steimle, T. C.; Jung, K. Y.; Li, B. Z. *J. Chem. Phys.* **1995**, *103*, 1767.
- (366) Jansson, K.; Scullman, R. *Ber. Bunsen-Ges.* **1978**, *82*, 92.
- (367) (a) Sassenberg, U.; Scullman, R. *Phys. Scr.* **1983**, *28*, 139. (b) Sassenberg, U.; Scullman, R. *J. Mol. Spectrosc.* **1977**, *68*, 331.
- (368) (a) Xu, Y.; Shelton, W. A.; Schneider, W. F. *J. Phys. Chem. B* **2006**, *110*, 16591. (b) Xu, Y.; Shelton, W. A.; Schneider, W. F. *J. Phys. Chem. A* **2006**, *110*, 5839.
- (369) Hwang, D. Y.; Mebel, A. M. *Chem. Phys. Lett.* **2002**, *365*, 140.
- (370) Kirchner, E. J. J.; Baerends, E. J.; van Slooten, U.; Kleyn, A. W. *J. Chem. Phys.* **1992**, *97*, 3821.
- (371) Allouti, F.; Manceron, L.; Alikhani, M. E. *Phys. Chem. Chem. Phys.* **2006**, *8*, 448.
- (372) Danset, D.; Manceron, L.; Andrews, L. *J. Phys. Chem. A* **2001**, *105*, 7205.
- (373) Huber, H.; Ozin, G. A. *Can. J. Chem.* **1972**, *50*, 3746.
- (374) Huber, H.; Klotzbücher, W.; Ozin, G. A.; Vander Voet, A. *Can. J. Chem.* **1973**, *51*, 2722.
- (375) Song, J.; Aprá, E.; Khait, Y. G.; Hoffmann, M. R.; Kowalski, K. *Chem. Phys. Lett.* **2006**, *428*, 277.
- (376) Bauschlicher, C. W., Jr. *J. Phys. Chem. A* **2004**, *108*, 2871.
- (377) Bauschlicher, C. W., Jr.; Langhoff, S. R.; Partridge, H.; Sodupe, M. *J. Phys. Chem.* **1993**, *97*, 856.
- (378) Blomberg, M. R. A.; Siegbahn, P. E. M.; Strich, A. *Chem. Phys.* **1985**, *97*, 287.
- (379) Deng, K.; Yang, J. L.; Zhu, Q. S. *J. Chem. Phys.* **2003**, *118*, 6868.
- (380) Yang, R.; Gong, Y.; Zhou, M. F. *Chem. Phys.* **2007**, *340*, 134.
- (381) Campbell, M. L.; Plane, J. M. C. *J. Phys. Chem. A* **2003**, *107*, 3747.
- (382) Wu, H. B.; Desai, S. R.; Wang, L. S. *J. Phys. Chem. A* **1997**, *101*, 2103.
- (383) Chertihin, G. V.; Andrews, L.; Bauschlicher, C. W., Jr. *J. Phys. Chem. A* **1997**, *101*, 4026.
- (384) Polak, M. L.; Gilles, M. K.; Ho, J.; Lineberger, W. C. *J. Phys. Chem.* **1991**, *95*, 3460.
- (385) O'Brien, L. C.; Kubicek, R. L.; Wall, S. J.; Koch, D. E.; Friend, R. J.; Brazier, C. R. *J. Mol. Spectrosc.* **1996**, *180*, 365.
- (386) (a) Steimle, T.; Namiki, K.; Saito, S. *J. Chem. Phys.* **1997**, *107*, 6109. (b) Steimle, T. C.; Chang, W. L.; Nachman, D. F. *Chem. Phys. Lett.* **1988**, *153*, 534. (c) Gerry, M. C. L.; Merer, A. J.; Sassenberg, U.; Steimle, T. C. *J. Chem. Phys.* **1987**, *86*, 4754.
- (387) (a) Appelblad, O.; Lagerqvist, A.; Renhorn, I.; Field, R. W. *Phys. Scr.* **1980**, *22*, 603. (b) Appelblad, O.; Lagerqvist, A. *Phys. Scr.* **1974**, *10*, 307.
- (388) Griffiths, M. J.; Barrow, R. F. *J. Chem. Soc., Faraday Trans. 2* **1977**, *73*, 943.
- (389) (a) Thompson, K. R.; Easley, W. C.; Knight, L. B. *J. Phys. Chem.* **1973**, *77*, 49.
- (390) Shirk, J. S.; Bass, A. M. *J. Chem. Phys.* **1970**, *52*, 1894.
- (391) Tevault, D. E.; Mowery, R. L.; De Marco, R. A.; Smardzewski, R. R. *J. Chem. Phys.* **1981**, *74*, 4342.
- (392) Ferrão, L. F. A.; Roberto-Neto, O.; Machado, F. B. C. *Int. J. Quantum Chem.* **2008**, *108*, 2512.
- (393) Midda, S.; Bera, N. C.; Bhattacharyya, I.; Das, A. K. *THEOCHEM* **2006**, *761*, 17.
- (394) Xian, H.; Cao, Z. X.; Xu, X.; Lu, X.; Zhang, Q. E. *Chem. Phys. Lett.* **2000**, *326*, 485.
- (395) Daoudi, A.; Touimi, B. A.; Flament, J. P.; Berthier, G. *J. Mol. Spectrosc.* **1999**, *194*, 8.
- (396) (a) Hippe, D.; Peyerimhoff, S. D. *Mol. Phys.* **1992**, *76*, 293. (b) Hippe, D.; Peyerimhoff, S. D. *J. Chem. Phys.* **1992**, *96*, 3503.
- (397) (a) Langhoff, S. R.; Bauschlicher, C. W., Jr. *Chem. Phys. Lett.* **1986**, *124*, 241. (b) Bagus, P. S.; Nelin, C. J.; Bauschlicher, C. W., Jr. *J. Chem. Phys.* **1983**, *79*, 2975.
- (398) Madhavan, P. V.; Newton, M. D. *J. Chem. Phys.* **1985**, *83*, 2337.
- (399) Basch, H.; Osman, R. *Chem. Phys. Lett.* **1982**, *93*, 51.
- (400) Igel, G.; Wedig, U.; Dolg, M.; Fuentealba, P.; Preuss, H.; Stoll, H.; Frey, R. *J. Chem. Phys.* **1984**, *81*, 2737.
- (401) Schamps, J.; Pinchemel, B.; Lefebvre, Y.; Raseev, G. *J. Mol. Spectrosc.* **1983**, *101*, 344.
- (402) Den Boer, D. H. W.; Kaleveld, E. W. *Chem. Phys. Lett.* **1980**, *69*, 389.
- (403) Wu, H. B.; Desai, S. R.; Wang, L. S. *J. Chem. Phys.* **1995**, *103*, 4363.
- (404) (a) Caspary, N.; Savchenko, E. V.; Thoma, A.; Lammers, A.; Bondybey, V. E. *Low Temp. Phys.* **2000**, *26*, 744. (b) Bondybey, V. E.; English, J. H. *J. Phys. Chem.* **1984**, *88*, 2247.
- (405) Kasai, P. H.; Jones, P. M. *J. Phys. Chem.* **1986**, *90*, 4239.
- (406) Howard, J. A.; Sutcliffe, R.; Mile, B. *J. Phys. Chem.* **1984**, *88*, 4351.
- (407) Ozin, G. A.; Mitchell, S. A.; García-Prieto, J. *J. Am. Chem. Soc.* **1983**, *105*, 6399.
- (408) Tevault, D. E. *J. Chem. Phys.* **1982**, *76*, 2859.
- (409) Mattar, S. M.; Ozin, G. A. *J. Phys. Chem.* **1988**, *92*, 3511.
- (410) Güell, M.; Luis, J. M.; Rodríguez-Santiago, L.; Sodupe, M.; Solà, M. *J. Phys. Chem. A* **2009**, *113*, 1308.
- (411) Mochizuki, Y.; Nagashima, U.; Yamamoto, S.; Kashiwagi, H. *Chem. Phys. Lett.* **1989**, *164*, 225.
- (412) (a) Pouillon, Y.; Massobrio, C.; Celino, M. *Comput. Mater. Sci.* **2000**, *17*, 539. (b) Pouillon, Y.; Massobrio, C. *Chem. Phys. Lett.* **2000**, *331*, 290.
- (413) Hrušák, J.; Koch, W.; Schwarz, H. *J. Chem. Phys.* **1994**, *101*, 3898.
- (414) Hasegawa, J.; Pierloot, K.; Roos, B. O. *Chem. Phys. Lett.* **2001**, *335*, 503.
- (415) Deng, K.; Yang, J. L.; Yuan, L. F.; Zhu, Q. S. *J. Chem. Phys.* **1999**, *111*, 1477.
- (416) Mochizuki, Y.; Tanaka, K.; Kashiwagi, H. *Chem. Phys.* **1991**, *151*, 11.
- (417) Ha, T. K.; Nguyen, M. T. *J. Phys. Chem.* **1985**, *89*, 5569.
- (418) (a) Andrews, L.; Prochaska, E. S.; Ault, B. S. *J. Chem. Phys.* **1978**, *69*, 556. (b) Spiker, R. C., Jr.; Andrews, L. *J. Chem. Phys.* **1973**, *59*, 1851. (c) Andrews, L. *J. Am. Chem. Soc.* **1973**, *95*, 4487.
- (419) Bates, J. B.; Brooker, M. H.; Boyd, G. E. *Chem. Phys. Lett.* **1972**, *16*, 391.
- (420) Pouillon, Y.; Massobrio, C. *Appl. Surf. Sci.* **2004**, *226*, 306.
- (421) Baruah, T.; Zope, R. R.; Pederson, M. R. *Phys. Rev. A* **2004**, *69*, 023201.
- (422) Cao, Z. X.; Solà, M.; Xian, H.; Duran, M.; Zhang, Q. E. *Int. J. Quantum Chem.* **2001**, *81*, 162.
- (423) Deng, K.; Yang, J. L.; Zhu, Q. S. *J. Chem. Phys.* **2000**, *113*, 7867.
- (424) Darling, J. H.; Garton-Sprenger, M. B.; Ogden, J. S. *Faraday Symp. Chem. Soc.* **1973**, *7*, 75.
- (425) Gong, Y.; Zhou, M. F. *Phys. Chem. Chem. Phys.* **2009**, *11*, doi: 10.1039/b909999a.
- (426) Massobrio, C.; Pouillon, Y. *J. Chem. Phys.* **2003**, *119*, 8305.
- (427) Pouillon, Y.; Massobrio, C. *Chem. Phys. Lett.* **2002**, *356*, 469.
- (428) Gong, Y.; Wang, G. J.; Zhou, M. F. *J. Phys. Chem. A* **2009**, *113*, 5355.
- (429) (a) Reynolds, A. M.; Gherman, B. F.; Cramer, C. J.; Tolman, W. B. *Inorg. Chem.* **2005**, *44*, 6989. (b) Aboelella, N. W.; Kryatov, S. V.; Gherman, B. F.; Brennessel, W. W.; Young, V. G., Jr.; Sarangi, R.; Rybak-Akimova, E. V.; Hodgson, K. O.; Hedman, B.; Solomon, E. I.; Cramer, C. J.; Tolman, W. B. *J. Am. Chem. Soc.* **2004**, *126*, 16896.
- (430) Citra, A.; Andrews, L. *THEOCHEM* **1999**, *489*, 95.
- (431) Tevault, D. E.; DeMarco, R. A.; Smardzewski, R. R. *J. Chem. Phys.* **1981**, *75*, 4168.
- (432) Andrews, D. H.; Gianola, A. J.; Lineberger, W. C. *J. Chem. Phys.* **2002**, *117*, 4074.
- (433) Steimle, T.; Tanimoto, M.; Namiki, K.; Saito, S. *J. Chem. Phys.* **1998**, *108*, 7616.
- (434) (a) O'Brien, L. C.; Wall, S. J.; Henry, G. L. *J. Mol. Spectrosc.* **1998**, *191*, 218. (b) O'Brien, L. C.; Wall, S. J.; Sieber, M. K. *J. Mol. Spectrosc.* **1997**, *183*, 57.
- (435) (a) Bojović, V.; Antić-Jovanović, A.; Stoiljković, M. M.; Miletić, M.; Pečić, D. S. *Spectrosc. Lett.* **1999**, *32*, 875. (b) Vujisić, B. R.; Savović, J. J.; Bojović, V.; Pešić, D. S. *Spectrosc. Lett.* **1993**, *26*, 1529.
- (436) Griffiths, M. J.; Barrow, R. F. *J. Phys. B* **1977**, *10*, 925.
- (437) Bauschlicher, C. W., Jr.; Partridge, H.; Langhoff, S. R. *Chem. Phys.* **1990**, *148*, 57.
- (438) Hay, P. J.; Martin, R. L. *J. Chem. Phys.* **1985**, *83*, 5174.
- (439) Andzelm, J.; Radzio, E.; Salahub, D. R. *J. Chem. Phys.* **1985**, *83*, 4573.
- (440) Zhai, H. J.; Bürgel, C.; Bonacic-Koutecky, V.; Wang, L. S. *J. Am. Chem. Soc.* **2008**, *130*, 9156.
- (441) Ichino, T.; Gianola, A. J.; Andrews, D. H.; Lineberger, W. C. *J. Phys. Chem. A* **2004**, *108*, 11307.
- (442) (a) O'Brien, L. C.; Oberlink, A. E.; Roos, B. O. *J. Phys. Chem. A* **2006**, *110*, 11954. (b) O'Brien, L. C.; Hardimon, S. C.; O'Brien, J. J. *J. Phys. Chem. A* **2004**, *108*, 11302.
- (443) Okabayashi, T.; Koto, F.; Tsukamoto, K.; Yamazaki, E.; Tanimoto, M. *Chem. Phys. Lett.* **2005**, *403*, 223.
- (444) Wu, Z. J. *J. Phys. Chem. A* **2005**, *109*, 5951.
- (445) Okumura, M.; Kitagawa, Y.; Haruta, M.; Yamaguchi, K. *Chem. Phys. Lett.* **2001**, *346*, 163.
- (446) Schwerdtfeger, P.; Dolg, M.; Schwarz, W. H. E.; Bowmaker, G. A.; Boyd, P. D. W. *J. Chem. Phys.* **1989**, *91*, 1762.
- (447) Tevault, D. E.; Smardzewski, R. R.; Urban, M. W.; Nakamoto, K. *J. Chem. Phys.* **1982**, *77*, 577.
- (448) McIntosh, D.; Ozin, G. A. *Inorg. Chem.* **1977**, *16*, 59.
- (449) Zhou, J.; Li, Z. H.; Wang, W. N.; Fan, K. N. *Chem. Phys. Lett.* **2006**, *421*, 448.

- (450) Kasai, P. H. *J. Phys. Chem.* **1990**, *94*, 3539.
- (451) McIntosh, D.; Ozin, G. A. *Inorg. Chem.* **1976**, *15*, 2869.
- (452) Ding, X. L.; Li, Z. Y.; Yang, J. L.; Hou, J. G.; Zhu, Q. S. *J. Chem. Phys.* **2004**, *120*, 9594.
- (453) Tielens, F.; Gracia, L.; Polo, V.; Andrés, J. *J. Phys. Chem. A* **2007**, *111*, 13255.
- (454) Andrews, L.; Hwang, J. T.; Trindle, C. *J. Phys. Chem.* **1973**, *77*, 1065.
- (455) Wang, X. F.; Andrews, L.; Riedel, S.; Kaupp, M. *Angew. Chem., Int. Ed.* **2007**, *46*, 8371.
- (456) Zack, L. N.; Pulliam, R. L.; Ziurys, L. M. *J. Mol. Spectrosc.* **2009**, *256*, 186.
- (457) Cannavo, D.; Knopp, G.; Radi, P.; Beaud, P.; Tulej, M.; Bodek, P.; Gerber, T.; Wokaun, A. *J. Mol. Struct.* **2006**, *782*, 67.
- (458) Clemmer, D. E.; Dalleska, N. F.; Armentrout, P. B. *J. Chem. Phys.* **1991**, *95*, 7263.
- (459) Wikde, B. G. *J. Chem. Phys.* **1983**, *78*, 6036.
- (460) Kim, J. H.; Li, X.; Wang, L. S.; de Clercq, H. L.; Fancher, C. A.; Thomas, O. C.; Bowen, K. H. *J. Phys. Chem. A* **2001**, *105*, 5709.
- (461) Moravec, V. D.; Klopcic, S. A.; Chatterjee, B.; Jarrold, C. C. *Chem. Phys. Lett.* **2001**, *341*, 313.
- (462) Fancher, C. A.; de Clercq, H. L.; Thomas, O. C.; Robinson, D. W.; Bowen, K. H. *J. Chem. Phys.* **1998**, *109*, 8426.
- (463) Prochaska, E. S.; Andrews, L. *J. Chem. Phys.* **1980**, *72*, 6782.
- (464) Chertihin, G. V.; Andrews, L. *J. Chem. Phys.* **1997**, *106*, 3457.
- (465) Boughdiri, S.; Tangour, B.; Teichteil, C.; Barthelat, J. C.; Leininger, T. *Chem. Phys. Lett.* **2008**, *462*, 18.
- (466) Chambaud, G.; Guitou, M.; Hayashi, S. *Chem. Phys.* **2008**, *352*, 147.
- (467) von Szentpály, L. *J. Phys. Chem. A* **2008**, *112*, 12695.
- (468) Peterson, K. A.; Shepler, B. C.; Singleton, J. M. *Mol. Phys.* **2007**, *105*, 1139.
- (469) Kullie, O.; Zhang, H.; Kolb, J.; Kolb, D. *J. Chem. Phys.* **2006**, *125*, 244303.
- (470) Erhart, P.; Juslin, N.; Goy, O.; Nordlund, K.; Müller, R.; Albe, K. *J. Phys. (Paris)* **2006**, *18*, 6585.
- (471) Gusarov, A. V.; Iorish, V. S. *Russ. J. Phys. Chem.* **2006**, *80*, 1864.
- (472) Bauschlicher, C. W., Jr.; Partridge, H. *J. Chem. Phys.* **1998**, *109*, 8430.
- (473) Bauschlicher, C. W., Jr.; Langhoff, S. R. *Chem. Phys. Lett.* **1986**, *126*, 163.
- (474) Boldyrev, A. I.; Simons, J. *Mol. Phys.* **1997**, *92*, 365.
- (475) Butler, R.; Katz, S.; Snelson, A.; Stephens, J. B. *J. Phys. Chem.* **1979**, *83*, 2578.
- (476) Cremer, D.; Kraka, E.; Filatov, M. *ChemPhysChem* **2008**, *9*, 2510.
- (477) Shepler, B. C.; Peterson, K. A. *J. Phys. Chem. A* **2003**, *107*, 1783.
- (478) Hu, A.; Otto, P.; Ladik, J. *THEOCHEM* **1999**, *468*, 163.
- (479) Kaledin, L. A.; McCord, J. E.; Heaven, M. C. *J. Mol. Spectrosc.* **1995**, *170*, 166.
- (480) (a) Linton, C.; Dulick, M.; Field, R. W.; Carette, P.; Leyland, P. C.; Barrow, R. F. *J. Mol. Spectrosc.* **1983**, *102*, 441. (b) Linton, C.; Dulick, M.; Field, R. W.; Carette, P.; Barrow, R. F. *J. Chem. Phys.* **1981**, *74*, 189. (c) Linton, C.; Dulick, M.; Field, R. W. *J. Mol. Spectrosc.* **1979**, *78*, 428.
- (481) Childs, W. J.; Azuma, Y.; Goodman, G. L. *J. Mol. Spectrosc.* **1990**, *144*, 70.
- (482) (a) Shenyavskaya, E. A.; Kaledin, L. A. *J. Mol. Spectrosc.* **1982**, *91*, 22. (b) Shenyavskaya, E. A.; Egorova, I. V.; Lupanov, V. N. *J. Mol. Spectrosc.* **1973**, *47*, 355.
- (483) (a) Dulick, M.; Field, R. W.; Beaufils, J. C.; Schamps, J. *J. Mol. Spectrosc.* **1981**, *87*, 278. (b) Dulick, M.; Field, R. W.; Beaufils, J. C. *J. Mol. Spectrosc.* **1981**, *87*, 268. (c) Dulick, M.; Field, R. W. *J. Mol. Spectrosc.* **1985**, *113*, 105.
- (484) Linton, C.; Ma, T.; Wang, H.; Steimle, T. C. *J. Chem. Phys.* **2008**, *129*, 124310.
- (485) (a) Effantin, C.; Bernard, A.; Crozet, P.; Ross, A. J.; d'Incan, J. *J. Mol. Spectrosc.* **2005**, *231*, 154. (b) Linton, C.; Effantin, C.; Crozet, P.; Ross, A. J.; Shenyavskaya, E. A.; d'Incan, J. *J. Mol. Spectrosc.* **2004**, *225*, 132. (c) Shenyavskaya, E. A.; Bernard, A.; Verges, J. *J. Mol. Spectrosc.* **2003**, *222*, 240.
- (486) (a) Kaledin, L. A.; Shenyavskaya, E. A.; Kovacs, I. *Acta Phys. Hung.* **1983**, *54*, 189. (b) Kaledin, L. A.; Shenyavskaya, E. A. *Opt. Spekt.* **1979**, *47*, 1015.
- (487) (a) Bujin, G.; Linton, C. *J. Mol. Spectrosc.* **1991**, *147*, 120. (b) Bujin, G.; Linton, C. *J. Mol. Spectrosc.* **1989**, *137*, 114. (c) Linton, C.; Bujin, G.; Rana, R. S.; Gray, J. A. *J. Mol. Spectrosc.* **1987**, *126*, 370.
- (488) Linton, C.; James, A. M.; Simard, B. *J. Chem. Phys.* **1993**, *99*, 9420.
- (489) Klingeler, R.; Pontius, N.; Lüttgens, G.; Bechthold, P. S.; Neeb, M.; Eberhardt, W. *Phys. Rev. A* **2002**, *65*, 032502.
- (490) Kaledin, L. A.; Erickson, M. G.; Heaven, M. C. *J. Mol. Spectrosc.* **1994**, *165*, 323.
- (491) Carette, P.; Hocquet, A.; Douay, M.; Pinchemel, B. *J. Mol. Spectrosc.* **1987**, *124*, 243.
- (492) Yadav, B. R.; Rai, S. B.; Rai, D. K. *J. Mol. Spectrosc.* **1981**, *89*, 1.
- (493) Van Zee, R. J.; Ferrante, R. F.; Zeringue, K. J.; Weltner, W., Jr. *J. Chem. Phys.* **1981**, *75*, 5297.
- (494) Kulikov, A. N.; Kaledin, L. A.; Kobylanski, A. I.; Gurvich, L. V. *Can. J. Phys.* **1984**, *62*, 1855.
- (495) Kaledin, L. A.; Shenyavskaya, E. A. *J. Mol. Spectrosc.* **1981**, *90*, 590.
- (496) (a) Linton, C.; Simard, B. *J. Chem. Phys.* **1992**, *96*, 1698. (b) Linton, C.; Gaudet, D. M.; Schall, H. *J. Mol. Spectrosc.* **1986**, *115*, 58.
- (497) (a) Chen, J.; Steimle, T. C.; Linton, C. *J. Mol. Spectrosc.* **2005**, *232*, 105. (b) Linton, C.; Liu, Y. C. *J. Mol. Spectrosc.* **1988**, *131*, 367. (c) Liu, Y. C.; Linton, C.; Schall, H.; Field, R. W. *J. Mol. Spectrosc.* **1984**, *104*, 72.
- (498) Kaledin, L. A.; Shenyavskaya, E. A. *J. Mol. Spectrosc.* **1989**, *133*, 469.
- (499) Melville, T. C.; Gordon, I.; Tereszchuk, K. A.; Coxon, J. A.; Bernath, P. F. *J. Mol. Spectrosc.* **2003**, *218*, 235.
- (500) Steimle, T. C.; Goodridge, D. M.; Linton, C. *J. Chem. Phys.* **1997**, *107*, 3723.
- (501) (a) McDonald, S. A.; Rice, S. F.; Field, R. W.; Linton, C. *J. Chem. Phys.* **1990**, *93*, 7676. (b) Linton, C.; McDonald, S.; Rice, S.; Dulick, M.; Liu, Y. C.; Field, R. W. *J. Mol. Spectrosc.* **1983**, *101*, 332.
- (502) Bernard, A.; Effantin, C. *Can. J. Phys.* **1986**, *64*, 246.
- (503) Weltner, W., Jr.; DeKock, R. L. *J. Phys. Chem.* **1971**, *75*, 514.
- (504) Willson, S. P.; Andrews, L. *J. Phys. Chem. A* **1999**, *103*, 3171.
- (505) Willson, S. P.; Andrews, L. *J. Phys. Chem. A* **1999**, *103*, 6972.
- (506) Field, R. W. *Ber. Bunsen-Ges. Phys. Chem.* **1982**, *86*, 771.
- (507) Sekiya, M.; Noro, T.; Miyoshi, E.; Osanai, Y.; Koga, T. *J. Comput. Chem.* **2006**, *27*, 463.
- (508) Dolg, M.; Stoll, H.; Preuss, H. *J. Chem. Phys.* **1989**, *90*, 1730.
- (509) Dai, D.; Li, L.; Ren, J.; Whangbo, M. H. *J. Chem. Phys.* **1998**, *108*, 3479.
- (510) Todorova, T. K.; Infante, I.; Gagliardi, L.; Dyke, J. M. *Int. J. Quantum Chem.* **2009**, *109*, 2068.
- (511) Kotzian, M.; Rösch, N. *J. Mol. Spectrosc.* **1991**, *147*, 346.
- (512) (a) Liu, W. J.; Hong, G. Y.; Dai, D. D.; Li, L. M.; Dolg, M. *Theor. Chem. Acc.* **1997**, *96*, 75. (b) Dolg, M.; Stoll, H.; Preuss, H. *Chem. Phys.* **1990**, *148*, 219.
- (513) Sakai, Y.; Nakai, T.; Mogi, K.; Miyoshi, E. *Mol. Phys.* **2003**, *101*, 117.
- (514) (a) Dolg, M.; Liu, W.; Kalvoda, S. *Int. J. Quantum Chem.* **2000**, *76*, 359. (b) Dolg, M.; Stoll, H.; Preuss, H. *Chem. Phys. Lett.* **1990**, *174*, 208.
- (515) (a) Dolg, M.; Stoll, H.; Flad, H. J.; Preuss, H. *J. Chem. Phys.* **1992**, *97*, 1162. (b) Liu, W.; Dolg, M.; Li, L. *J. Chem. Phys.* **1998**, *108*, 2886.
- (516) Allouche, A. R.; Aubert-Frécon, M.; Umanskiy, S. Ya. *J. Chem. Phys.* **2006**, *124*, 184317.
- (517) Boudreaux, E. A.; Baxter, E. *Int. J. Quantum Chem.* **2002**, *90*, 629.
- (518) Paulovič, J.; Gagliardi, L.; Dyke, J. M.; Hirao, K. *J. Chem. Phys.* **2004**, *120*, 9998.
- (519) Dulick, M.; Murad, E.; Barrow, R. F. *J. Chem. Phys.* **1986**, *85*, 385.
- (520) Gibson, J. K. *J. Phys. Chem. A* **2003**, *107*, 7891.
- (521) Gabelnick, S. D.; Reedy, G. T.; Chasanov, M. G. *J. Chem. Phys.* **1974**, *60*, 1167.
- (522) Hu, Z.; Kaindl, G.; Müller, B. G. *J. Alloys Compd.* **1997**, *246*, 177.
- (523) Goncharov, V.; Han, J.; Kaledin, L. A.; Heaven, M. C. *J. Chem. Phys.* **2005**, *122*, 204311.
- (524) (a) Edvinsson, G.; Lagerqvist, A. *Phys. Scr.* **1984**, *30*, 309. (b) von Bornstedt, A.; Edvinsson, G.; Lagerqvist, A.; Renhorn, I. *Phys. Scr.* **1979**, *20*, 599.
- (525) Han, J.; Kaledin, L. A.; Goncharov, V.; Komissarov, A. V.; Heaven, M. C. *J. Am. Chem. Soc.* **2003**, *125*, 7176.
- (526) (a) Kaledin, L. A.; Heaven, M. C. *J. Mol. Spectrosc.* **1997**, *185*, 1. (b) Kaledin, L. A.; McCord, J. E.; Heaven, M. C. *J. Mol. Spectrosc.* **1994**, *164*, 27. (c) Heaven, M. C.; Nicolai, J. P.; Riley, S. J.; Parks, E. K. *Chem. Phys. Lett.* **1985**, *119*, 229.
- (527) Allen, G. C.; Baerends, E. J.; Vernooijs, P.; Dyke, J. M.; Ellis, A. M.; Feher, M.; Morris, A. *J. Chem. Phys.* **1988**, *89*, 5363.
- (528) Han, J.; Goncharov, V.; Kaledin, L. A.; Komissarov, A. V.; Heaven, M. C. *J. Chem. Phys.* **2004**, *120*, 5155.
- (529) Lue, C. J.; Jin, J.; Ortiz, M. J.; Rienstra-Kiracofe, J. C.; Heaven, M. C. *J. Am. Chem. Soc.* **2004**, *126*, 1812.
- (530) Abramowitz, S.; Acquista, N. *J. Phys. Chem.* **1972**, *76*, 648.
- (531) Abramowitz, S.; Acquista, N.; Thompson, K. R. *J. Phys. Chem.* **1971**, *75*, 2283.
- (532) Heaven, M. C. *Phys. Chem. Chem. Phys.* **2006**, *8*, 4497.
- (533) (a) Kushto, G. P.; Andrews, L. *J. Phys. Chem. A* **1999**, *103*, 4836. (b) Souter, P. F.; Kushto, G. P.; Andrews, L.; Neurock, M. *J. Phys. Chem. A* **1997**, *101*, 1287.
- (534) Paulovič, J.; Nakajima, T.; Hirao, K.; Lindh, R.; Malmqvist, P. A. *J. Chem. Phys.* **2003**, *119*, 798.
- (535) Seijo, L.; Barandiarán, Z.; Harguindey, E. *J. Chem. Phys.* **2001**, *114*, 118.

- (536) Watanabe, Y.; Matsuoka, O. *J. Chem. Phys.* **1997**, *107*, 3738.
- (537) Marian, C. M.; Wahlgren, U.; Gropen, O.; Pykkö, P. *THEOCHEM* **1988**, *46*, 339.
- (538) Zhou, M. F.; Andrews, L. *J. Chem. Phys.* **1999**, *111*, 11044.
- (539) Jackson, V. E.; Craciun, R.; Dixon, D. A.; Peterson, K. A.; de Jong, W. A. *J. Phys. Chem. A* **2008**, *112*, 4095.
- (540) Straka, M.; Dyal, K. G.; Pykkö, P. *Theor. Chem. Acc.* **2001**, *106*, 393.
- (541) Dyal, K. G. *Mol. Phys.* **1999**, *96*, 511.
- (542) Pykkö, P.; Laakkonen, L. J.; Tatsumi, K. *Inorg. Chem.* **1989**, *28*, 1801.
- (543) Wadt, W. R. *J. Am. Chem. Soc.* **1981**, *103*, 6053.
- (544) Gabelnick, S. D.; Reedy, G. T.; Chasanov, M. G. *J. Chem. Phys.* **1973**, *58*, 4468.
- (545) Carstens, D. H. W.; Gruen, D. M.; Kozłowski, J. F. *High Temp. Sci.* **1972**, *4*, 436.
- (546) Hunt, R. D.; Andrews, L. *J. Chem. Phys.* **1993**, *98*, 3690.
- (547) Sankaran, K.; Sundararajan, K.; Viswanathan, K. S. *Bull. Mater. Sci.* **1999**, *22*, 785.
- (548) Paulović, J.; Gagliardi, L.; Dyke, J. M.; Hirao, K. *J. Chem. Phys.* **2005**, *122*, 144317.
- (549) Zhou, M. F.; Andrews, L.; Ismail, N.; Marsden, C. J. *Phys. Chem. A* **2000**, *104*, 5495.
- (550) Wang, H. Y.; Zhu, Z. H.; Gao, T.; Fu, Y. B.; Wang, X. L.; Sun, Y. *Mol. Phys.* **2000**, *98*, 875.
- (551) Majumdar, D.; Balasubramanian, K.; Nitsche, H. *Chem. Phys. Lett.* **2002**, *361*, 143.
- (552) Van Wezenbeek, E. M.; Baerends, E. J.; Snijders, J. G. *Theor. Chim. Acta* **1991**, *81*, 139.
- (553) Fleig, T.; Jensen, H. J. A.; Olsen, J.; Visscher, L. *J. Chem. Phys.* **2006**, *124*, 104106.
- (554) Infante, I.; Eliav, E.; Vilkas, M. J.; Ishikawa, Y.; Kaldor, U.; Visscher, L. *J. Chem. Phys.* **2007**, *127*, 124308.
- (555) Gagliardi, L.; Roos, B. O.; Malmqvist, P.; Dyke, J. M. *J. Phys. Chem. A* **2001**, *105*, 10602.
- (556) Li, J.; Bursten, B. E.; Andrews, L.; Marsden, C. J. *J. Am. Chem. Soc.* **2004**, *126*, 3424.
- (557) (a) Li, J.; Bursten, B. E.; Liang, B. Y.; Andrews, L. *Science* **2002**, *295*, 2242. (b) Andrews, L.; Liang, B. Y.; Li, J.; Bursten, B. E. *Angew. Chem., Int. Ed.* **2000**, *39*, 4565.
- (558) Gagliardi, L.; Heaven, M. C.; Krogh, J. W.; Roos, B. O. *J. Am. Chem. Soc.* **2005**, *127*, 86.
- (559) Gabelnick, S. D.; Reedy, G. T.; Chasanov, M. G. *J. Chem. Phys.* **1973**, *59*, 6397.
- (560) Green, D. W.; Reedy, G. T.; Gabelnick, S. D. *J. Chem. Phys.* **1980**, *73*, 4207.
- (561) Privalov, T.; Schimmelpennig, B.; Wahlgren, U.; Grenthe, I. *J. Phys. Chem. A* **2002**, *106*, 11277.
- (562) Pykkö, P.; Li, J.; Runeberg, N. J. *J. Phys. Chem.* **1994**, *98*, 4809.
- (563) Green, D. W.; Reedy, G. T. *J. Chem. Phys.* **1978**, *69*, 544.
- (564) La Macchia, G.; Infante, I.; Raab, J.; Gibson, J. K.; Gagliardi, L. *Phys. Chem. Chem. Phys.* **2008**, *10*, 7278.
- (565) Archibong, E. F.; Ray, A. K. *THEOCHEM* **2000**, *530*, 165.
- (566) (a) Ritter, D.; Weisshaar, J. C. *J. Phys. Chem.* **1990**, *94*, 4907. (b) Ritter, D.; Weisshaar, J. C. *J. Phys. Chem.* **1989**, *93*, 1576.
- (567) (a) Campbell, M. L.; Hooper, K. L.; Kölsch, E. *J. Chem. Phys. Lett.* **1997**, *274*, 7. (b) Campbell, M. L. *Chem. Phys. Lett.* **1998**, *294*, 339. (c) Campbell, M. L.; McClean, R. E. *J. Phys. Chem.* **1993**, *97*, 7942. (d) Campbell, M. L. *J. Chem. Soc., Faraday Trans.* **1998**, *94*, 1687. (e) McClean, R. E.; Campbell, M. L.; Kölsch, E. *J. Phys. Chem. A* **1997**, *101*, 3348. (f) Campbell, M. L.; Hooper, K. L. *J. Chem. Soc., Faraday Trans.* **1997**, *93*, 2139. (g) Campbell, M. L.; McClean, R. E.; Harter, J. S. *S. Chem. Phys. Lett.* **1995**, *235*, 497. (h) Campbell, M. L.; McClean, R. E. *J. Chem. Soc., Faraday Trans.* **1995**, *91*, 3787.
- (568) Higashiyama, T.; Ishida, M.; Matsumoto, Y.; Honma, K. *Phys. Chem. Chem. Phys.* **2005**, *7*, 2418.
- (569) Sakurai, H.; Kato, S. *J. Phys. Chem. A* **2002**, *106*, 4350.
- (570) Campbell, M. L. *J. Chem. Soc., Faraday Trans.* **1996**, *92*, 4377.
- (571) Campbell, M. L. *J. Phys. Chem.* **1996**, *100*, 19430.
- (572) Whetten, R. L.; Cox, D. M.; Trevor, D. J.; Kaldor, A. *J. Phys. Chem.* **1984**, *89*, 566.
- (573) Mitchell, S. A.; Hackett, P. A. *J. Chem. Phys.* **1990**, *93*, 7822.
- (574) Matsui, R.; Senba, K.; Honma, K. *J. Phys. Chem. A* **1997**, *101*, 179.
- (575) Campbell, M. L. *J. Phys. Chem. A* **1998**, *102*, 892.
- (576) Simons, J. *J. Phys. Chem. A* **2008**, *112*, 6401.
- (577) (a) Knight, L. B., Jr. *Acc. Chem. Res.* **1996**, *19*, 313. (b) Knight, L. B., Jr.; Kerr, K.; Villanueva, M.; McKinley, A. J.; Feller, D. *J. Chem. Phys.* **1992**, *97*, 5363.
- (578) *CRC Handbook of Chemistry and Physics*; CRC Press: Boca Raton, FL, 1985.
- (579) Merritt, J. M.; Bondybey, V. E.; Heaven, M. C. *J. Chem. Phys.* **2009**, *130*, 144503.
- (580) Goncharov, V.; Heaven, M. C. *J. Chem. Phys.* **2006**, *124*, 064312.
- (581) Goncharov, V.; Kaledin, L. A.; Heaven, M. C. *J. Chem. Phys.* **2006**, *125*, 133202.
- (582) (a) Aguirre, F.; Husband, J.; Thompson, C. J.; Stringer, K. L.; Metz, R. B. *J. Chem. Phys.* **2003**, *119*, 10194. (b) Husband, J.; Aguirre, F.; Ferguson, P.; Metz, R. B. *J. Chem. Phys.* **1999**, *111*, 1433.
- (583) Thompson, C. J.; Stringer, K. L.; McWilliams, M.; Metz, R. B. *Chem. Phys. Lett.* **2003**, *376*, 588.
- (584) Kamariotis, A.; Hayes, T.; Bellert, D.; Brucat, P. J. *Chem. Phys. Lett.* **2000**, *316*, 60.
- (585) Linton, C.; Simard, B.; Looch, H. P.; Wallin, S.; Rothschof, G. K.; Gunion, R. F.; Morse, M. D.; Armentrout, P. B. *J. Chem. Phys.* **1999**, *111*, 5017.
- (586) Harrington, J.; Weisshaar, J. C. *J. Chem. Phys.* **1992**, *97*, 2809.
- (587) Sappey, A. D.; Eiden, G.; Harrington, J. E.; Weisshaar, J. C. *J. Chem. Phys.* **1989**, *90*, 1415.
- (588) Merer, A. J.; Cheung, A. S. C.; Taylor, A. W. *J. Mol. Spectrosc.* **1984**, *108*, 343.
- (589) Dyke, J. M.; Gravenor, B. W. J.; Lewis, R. A.; Morris, A. *J. Chem. Soc., Faraday Trans. 2* **1983**, *79*, 1083.
- (590) (a) Balfour, W. J.; Lindgren, B. *Phys. Scr.* **1980**, *22*, 36. (b) Phillips, J. G.; Davis, S. P. *Astrophys. J.* **1979**, *234*, 393.
- (591) Stoll, H.; Peterson, K. A.; Merritt, J. M.; Heaven, M. C. *J. Phys. Chem. A* published online July 14, **2009**, doi: 10.1021/jp904936x.
- (592) Nakao, Y.; Hirao, K.; Taketsugu, T. *J. Chem. Phys.* **2001**, *114*, 7935.
- (593) Schröder, D.; Schwarz, H.; Shaik, S. *Struct. Bonding (Berlin)* **2000**, *97*, 91.
- (594) Bauschlicher, C. W., Jr.; Gutsev, G. L. *Theor. Chem. Acc.* **2002**, *107*, 309.
- (595) Carter, E. A.; Goddard, W. A., III. *J. Phys. Chem.* **1988**, *92*, 2109.
- (596) Broclawik, E. *Int. J. Quantum Chem.* **1995**, *56*, 779.
- (597) Schofield, K. *J. Phys. Chem. A* **2006**, *110*, 6938.
- (598) (a) Zhao, Y. Y.; Wang, G. J.; Chen, M. H.; Zhou, M. F. *J. Phys. Chem. A* **2005**, *109*, 6621. (b) Zhao, Y. Y.; Gong, Y.; Chen, M. H.; Ding, C. F.; Zhou, M. F. *J. Phys. Chem. A* **2005**, *109*, 11765.
- (599) Van Zee, R. J.; Li, S.; Weltner, W., Jr. *Chem. Phys. Lett.* **1994**, *217*, 381.
- (600) Denning, R. G. *J. Phys. Chem. A* **2007**, *111*, 4125.
- (601) Green, D. W.; Gabelnick, S. D.; Reedy, G. T. *J. Chem. Phys.* **1976**, *64*, 1697.
- (602) Merritt, J. M.; Han, J.; Heaven, M. C. *J. Chem. Phys.* **2008**, *128*, 084304.
- (603) Wang, X. F.; Andrews, L.; Li, J.; Bursten, B. E. *Angew. Chem., Int. Ed.* **2004**, *43*, 2554.
- (604) Gagliardi, L.; Roos, B. O. *Chem. Phys. Lett.* **2000**, *331*, 229.
- (605) Gál, M.; Groggin, P. L.; Mink, J. *Spectrochim. Acta A* **1992**, *48*, 121.
- (606) Brümmer, M.; Kaposta, C.; Santambrogio, G.; Asmis, K. R. *J. Chem. Phys.* **2003**, *119*, 12700.
- (607) Koyanagi, G. K.; Bohme, D. K.; Kretschmar, I.; Schröder, D.; Schwarz, H. *J. Phys. Chem. A* **2001**, *105*, 4259.
- (608) Zhou, M. F.; Wang, G. J.; Zhao, Y. Y.; Chen, M. H.; Ding, C. F. *J. Phys. Chem. A* **2005**, *109*, 5079.
- (609) Dong, J.; Wang, Y.; Zhou, M. F. *Chem. Phys. Lett.* **2002**, *364*, 511.
- (610) Li, Z. H.; Gong, Y.; Fan, K. N.; Zhou, M. F. Unpublished results.
- (611) Gong, Y.; Zhou, M. F. *J. Phys. Chem. A* **2009**, *113*, 4990.
- (612) Gong, Y.; Zhou, M. F., manuscript in preparation (ZnO<sub>2</sub><sup>-</sup>, CdO<sub>2</sub><sup>-</sup>).
- (613) Palenik, G. J. *Inorg. Chem.* **1967**, *6*, 503.
- (614) Weinstock, N.; Schulze, H.; Müller, A. *J. Chem. Phys.* **1973**, *59*, 5063.
- (615) (a) Asmis, K. R.; Sauer, J. *Mass Spectrom. Rev.* **2007**, *26*, 542. (b) Asmis, K. R.; Fielicke, A.; von Helden, G.; Meijer, G. *Chem. Phys. Solid Surf.* **2007**, *12*, 327.
- (616) Yang, S.; Knickelbein, M. B. *Z. Phys. D* **1994**, *31*, 199.
- (617) Pramann, A.; Nakamura, Y.; Nakajima, A.; Kaya, K. *J. Phys. Chem. A* **2001**, *105*, 7534.
- (618) (a) Wang, J.; Wang, Y.; Wu, G.; Zhang, X.; Zhao, X.; Yang, M. *Phys. Chem. Chem. Phys.* **2009**, *11*, 5980. (b) Yang, Z.; Xiong, S. *J. J. Chem. Phys.* **2008**, *129*, 124308.
- (619) (a) Gu, G.; Dai, B.; Ding, X.; Yang, J. L. *Eur. Phys. J., D* **2004**, *29*, 27. (b) Dai, B.; Deng, K.; Yang, J. L. *Chem. Phys. Lett.* **2002**, *364*, 188.
- (620) Gong, Y.; Zhang, Q. Q.; Zhou, M. F. *J. Phys. Chem. A* **2007**, *111*, 3534.
- (621) Xiang, J.; Yan, X. H.; Xiao, Y.; Mao, Y. L.; Wei, S. H. *Chem. Phys. Lett.* **2004**, *387*, 66.
- (622) Calatayud, M.; Maldonado, L.; Minot, C. *J. Phys. Chem. C* **2008**, *112*, 16087.
- (623) Zhang, D.; Liu, P.; Liu, C. *J. Phys. Chem. C* **2008**, *112*, 16729.
- (624) Hagfeldt, A.; Lunell, S.; Siegbahn, H. O. G. *Int. J. Quantum Chem.* **1994**, *49*, 97.
- (625) Chen, S.; Yin, Y.; Wang, D.; Liu, Y.; Wang, X. *J. Cryst. Growth* **2005**, *282*, 498.

- (626) von Helden, G.; Kirilyuk, A.; Heijnsbergen, D. van.; Sartakov, B.; Duncan, M. A.; Meijer, G. *Chem. Phys.* **2000**, *262*, 31.
- (627) Qu, Z. W.; Kroes, G. J. *J. Phys. Chem. C* **2007**, *111*, 16808.
- (628) Hamad, S.; Catlow, C. R. A.; Woodley, S. M.; Lago, S.; Mejías, J. A. *J. Phys. Chem. B* **2005**, *109*, 15741.
- (629) Persson, P.; Gebhardt, J. C. M.; Lunell, S. *J. Phys. Chem. B* **2003**, *107*, 3336.
- (630) Asmis, K. R.; Meijer, G.; Brümmer, M.; Kaposta, C.; Santambrogio, G.; Wöste, L.; Sauer, J. *J. Chem. Phys.* **2004**, *120*, 6461.
- (631) Calatayud, M.; Andrés, J.; Beltran, A. *J. Phys. Chem. A* **2001**, *105*, 9760.
- (632) Pykavy, M.; van Wullen, C.; Sauer, J. *J. Chem. Phys.* **2004**, *120*, 4207.
- (633) Zhai, H. J.; Wang, L. S. *J. Chem. Phys.* **2002**, *117*, 7882.
- (634) Beattie, I. R.; Ogden, J. S.; Price, D. D. *Inorg. Chem.* **1978**, *17*, 3296.
- (635) Herwig, C.; Limberg, C. *Inorg. Chem.* **2008**, *47*, 2937.
- (636) (a) Asmis, K. R.; Santambrogio, G.; Brümmer, M.; Sauer, J. *Angew. Chem., Int. Ed.* **2005**, *44*, 3122. (b) Santambrogio, G.; Brümmer, M.; Wöste, L.; Döbler, J.; Sierka, M.; Sauer, J.; Meijer, G.; Asmis, K. R. *Phys. Chem. Chem. Phys.* **2008**, *10*, 3992.
- (637) Fielicke, A.; Meijer, G.; von Helden, G. *J. Am. Chem. Soc.* **2003**, *125*, 3659.
- (638) Asmis, K. R.; Brümmer, M.; Kaposta, C.; Santambrogio, G.; von Helden, G.; Meijer, G.; Rademann, K.; Wöste, L. *Phys. Chem. Chem. Phys.* **2002**, *4*, 1101.
- (639) Yang, D. S.; Zgierski, M. Z.; Rayner, D. M.; Hackett, P. A.; Martinez, A.; Salahub, D. R.; Roy, P. N.; Carrington, T., Jr. *J. Chem. Phys.* **1995**, *103*, 5335.
- (640) (a) Martinez, A.; Calaminici, P.; Köster, A. M.; Salahub, D. R. *J. Chem. Phys.* **2001**, *114*, 819. (b) Calaminici, P.; Flores-Moreno, R.; Köster, A. M. *J. Chem. Phys.* **2004**, *121*, 3558.
- (641) Green, S. M. E.; Alex, S.; Fleischer, N. L.; Millam, E. L.; Marcy, T. P.; Leopold, D. G. *J. Chem. Phys.* **2001**, *114*, 2653.
- (642) Zhai, H. J.; Wang, B.; Huang, X.; Wang, L. S. *J. Phys. Chem. A* **2009**, *113*, 3866.
- (643) Zhai, H. J.; Averkiev, B. B.; Zubarev, D. Y.; Wang, L. S.; Boldyrev, A. I. *Angew. Chem., Int. Ed.* **2007**, *46*, 4277.
- (644) Pramann, A.; Koyasu, K.; Nakajima, A. *J. Chem. Phys.* **2002**, *116*, 6521.
- (645) Zhai, H. J.; Döbler, J.; Sauer, J.; Wang, L. S. *J. Am. Chem. Soc.* **2007**, *129*, 13270.
- (646) Vyboishchikov, S. F.; Sauer, J. *J. Phys. Chem. A* **2001**, *105*, 8588.
- (647) (a) Reddy, B. V.; Khanna, S. N. *Phys. Rev. Lett.* **1999**, *83*, 3170. (b) Reddy, B. V.; Khanna, S. N.; Ashman, C. *Phys. Rev. B* **2000**, *61*, 5797.
- (648) Xiang, K. H.; Pandey, R.; Recio, J. M.; Francisco, E.; Newsam, J. M. *J. Phys. Chem. A* **2000**, *104*, 990.
- (649) (a) Tono, K.; Terasaki, A.; Ohta, T.; Kondow, T. *Phys. Rev. Lett.* **2003**, *90*, 133402. (b) Tono, K.; Terasaki, A.; Ohta, T.; Kondow, T. *J. Chem. Phys.* **2003**, *119*, 11221.
- (650) Zhai, H. J.; Wang, L. S. *J. Chem. Phys.* **2006**, *125*, 164315.
- (651) Paul, S.; Misra, A. *THEOCHEM* **2009**, 895, 156.
- (652) Zhang, Q. Q.; Zhao, Y. Y.; Gong, Y.; Zhou, M. F. *J. Phys. Chem. A* **2007**, *111*, 9775.
- (653) Yoder, B. L.; Maze, J. T.; Raghavachari, K.; Jarrold, C. C. *J. Chem. Phys.* **2005**, *122*, 094313.
- (654) Zhai, H. J.; Huang, X.; Cui, L. F.; Li, X.; Li, J.; Wang, L. S. *J. Phys. Chem. A* **2005**, *109*, 6019.
- (655) Zhai, H. J.; Huang, X.; Waters, T.; Wang, X. B.; O'Hair, R. A. J.; Wedd, A. G.; Wang, L. S. *J. Phys. Chem. A* **2005**, *109*, 10512.
- (656) Huang, X.; Zhai, H. J.; Waters, T.; Li, J.; Wang, L. S. *Angew. Chem., Int. Ed.* **2006**, *45*, 657.
- (657) Huang, X.; Zhai, H. J.; Li, J.; Wang, L. S. *J. Phys. Chem. A* **2006**, *110*, 85.
- (658) Huang, X.; Zhai, H. J.; Kiran, B.; Wang, L. S. *Angew. Chem., Int. Ed.* **2005**, *44*, 7251.
- (659) (a) Sun, Q.; Rao, B. K.; Jena, P.; Stolcic, D.; Ganteför, G.; Kawazoe, Y. *Chem. Phys. Lett.* **2004**, *387*, 29. (b) Bertram, N.; Kim, Y. D.; Ganteför, G.; Sun, Q.; Jena, P.; Tamuliene, J.; Seifert, G. *Chem. Phys. Lett.* **2004**, *396*, 341.
- (660) (a) Janssens, E.; Hou, X. J.; Neukermans, S.; Wang, X.; Silverans, R. E.; Lievens, P.; Nguyen, M. T. *J. Phys. Chem. A* **2007**, *111*, 4150. (b) Wang, B.; Zhang, X. H.; Huang, X.; Zhang, Y. F. *Jiegou Huaxue* **2008**, *27*, 990. (c) Li, J. *J. Cluster Sci.* **2002**, *13*, 137.
- (661) Tono, K.; Terasaki, A.; Ohta, T.; Kondow, T. *Chem. Phys. Lett.* **2004**, *388*, 374.
- (662) Lombardi, J. R.; Davis, B. *Chem. Rev.* **2002**, *102*, 2431.
- (663) Jones, N. O.; Khanna, S. N.; Baruah, T.; Pederson, M. R.; Zheng, W. J.; Nilles, J. M.; Bowen, K. H. *Phys. Rev. B* **2004**, *70*, 134422.
- (664) Cao, Z.; Duran, M.; Solà, M. *J. Chem. Soc., Faraday Trans.* **1998**, *94*, 2877.
- (665) Wang, L. S.; Wu, H. B.; Desai, S. R. *Phys. Rev. Lett.* **1996**, *76*, 4853.
- (666) Gutsev, G. L.; Bauschlicher, C. W., Jr.; Zhai, H. J.; Wang, L. S. *J. Chem. Phys.* **2003**, *119*, 11135.
- (667) Shiroishi, H.; Oda, T.; Hamada, I.; Fujima, N. *Mol. Simul.* **2004**, *30*, 911.
- (668) Shiroishi, H.; Oda, T.; Hamada, I.; Fujima, N. *Polyhedron* **2005**, *24*, 2472.
- (669) Jones, N. O.; Reddy, B. V.; Rasouli, F.; Khanna, S. N. *Phys. Rev. B* **2005**, *72*, 165411.
- (670) Ding, X. L.; Xue, W.; Ma, Y. P.; Wang, Z. C.; He, S. G. *J. Chem. Phys.* **2009**, *130*, 014303.
- (671) Sun, Q.; Wang, Q.; Parlinski, K.; Yu, J. Z.; Hashi, Y.; Gong, X. G.; Kawazoe, Y. *Phys. Rev. B* **2000**, *61*, 5781.
- (672) Danset, D.; Manceron, L. *Phys. Chem. Chem. Phys.* **2005**, *7*, 583.
- (673) Staemmler, V.; Reinhardt, P.; Allouti, F.; Alikhani, M. E. *Chem. Phys.* **2008**, *349*, 83.
- (674) Pramann, A.; Koyasu, K.; Nakajima, A.; Kaya, K. *J. Phys. Chem. A* **2002**, *106*, 4891.
- (675) Liu, L.; Zhao, R. N.; Han, J. G.; Liu, F. Y.; Pan, G. Q.; Sheng, L. S. *J. Phys. Chem. A* **2009**, *113*, 360.
- (676) (a) Harding, D. J.; Mackenzie, S. R.; Walsh, T. R. *Chem. Phys. Lett.* **2009**, *469*, 31. (b) Harding, D. J.; Davies, R. D. L.; Mackenzie, S. R.; Walsh, T. R. *J. Chem. Phys.* **2008**, *129*, 124304.
- (677) Allouti, F.; Manceron, L.; Alikhani, M. E. *Phys. Chem. Chem. Phys.* **2006**, *8*, 3715.
- (678) Hübner, O.; Himmel, H.-J. *Phys. Chem. Chem. Phys.* **2009**, *11*, 2241.
- (679) Wang, L. S.; Wu, H.; Desai, S. R.; Lou, L. *Phys. Rev. B* **1996**, *53*, 8028.
- (680) Dai, B.; Tian, L.; Yang, J. L. *J. Chem. Phys.* **2004**, *120*, 2746.
- (681) Jadraque, M.; Martín, M. *Chem. Phys. Lett.* **2008**, *456*, 51.
- (682) Gong, Y. Su, J.; Li, J.; Zhou, M. F. manuscript in preparation.
- (683) (a) von Gynz-Rekowski, F.; Bertram, N.; Ganteför, G.; Kim, Y. D. *J. Phys. Chem. B* **2004**, *108*, 18916. (b) von Gynz-Rekowski, F.; Bertram, N.; Ganteför, G.; Kim, Y. D. *Eur. Phys. J., D* **2005**, *36*, 187.
- (684) (a) Stolcic, D.; Fischer, M.; Ganteför, G.; Kim, Y. D.; Sun, Q.; Jena, P. *J. Am. Chem. Soc.* **2003**, *125*, 2848. (b) Sun, Q.; Jena, P.; Kim, Y. D.; Fischer, M.; Ganteför, G. *J. Chem. Phys.* **2004**, *120*, 6510.
- (685) Koyasu, K.; Niemietz, M.; Götz, M.; Ganteför, G. *Chem. Phys. Lett.* **2007**, *450*, 96.
- (686) Kim, Y. D. *Int. J. Mass Spectrom.* **2004**, *238*, 17.
- (687) (a) Kim, Y. D.; Ganteför, G. *Chem. Phys. Lett.* **2004**, *383*, 80. (b) Kim, Y. D.; Ganteför, G. *J. Mol. Struct.* **2004**, *692*, 139.
- (688) Ding, X.; Dai, B.; Yang, J. L.; Hou, J. G.; Zhu, Q. S. *J. Chem. Phys.* **2004**, *121*, 621.
- (689) (a) Mills, G.; Gordon, M. S.; Metiu, H. *J. Chem. Phys.* **2003**, *118*, 4198. (b) Mills, G.; Gordon, M. S.; Metiu, H. *Chem. Phys. Lett.* **2002**, *359*, 493.
- (690) Wells, D. H., Jr.; Delgass, W. N.; Thomson, K. T. *J. Chem. Phys.* **2002**, *117*, 10597.
- (691) Kim, Y. D.; Ganteför, G.; Sun, Q.; Jena, P. *Chem. Phys. Lett.* **2004**, *396*, 69.
- (692) Franceschetti, A.; Pennycook, S. J.; Pantelides, S. T. *Chem. Phys. Lett.* **2003**, *374*, 471.
- (693) Yoon, B.; Häkkinen, H.; Landman, U. *J. Phys. Chem. A* **2003**, *107*, 4066.
- (694) Luo, C.; Fa, W.; Dong, J. *J. Chem. Phys.* **2006**, *125*, 084707.
- (695) Wang, Y.; Gong, X. G. *J. Chem. Phys.* **2006**, *125*, 124703.